

BORON CLUSTERS AS THE CENTERPIECE OF ADVANCED LIQUID
CRYSTALS: FUNDAMENTAL CHEMISTRY AND PROPERTIES

BRYAN RINGSTRAND

Dissertation under the direction of Professor Piotr Kaszynski

Liquid crystals incorporating boron clusters are of interest for electro-optics, ion-transport, and fundamental structure-property relationship studies. A liquid crystal is a fluid possessing orientational and positional order between that of the lattice of a solid (long-range orientational and long-range positional order) and the random disorder (no orientational or positional order) of a liquid. Balance between the rigidity of the molecular core and flexible periphery dictates the type of liquid crystalline phase and its stability. Anisometric molecules, typically rods or discs, form liquid crystalline phases. *closo*-Boron clusters are inorganic structures characterized by highly delocalized bonding and high chemical, oxidative, and thermal stability. These clusters can exist as highly symmetrical molecules that are either neutral or negatively charged.

Within this framework, a negatively charged boron cluster, [*closo*-1-CB₉H₁₀]⁻, was exploited as the centerpiece of both zwitterionic and ionic liquid crystalline

materials. Access to these materials was limited by the lack of synthetic methodology and understanding of reactive intermediates of the [*closo*-1-CB₉H₁₀]⁻ anion. Therefore, a systematic approach was taken to advance the synthetic and physical-organic chemistry of the [*closo*-1-CB₉H₁₀]⁻ anion within the context of incorporating it into liquid crystalline structures. Once this stepwise approach was completed, the newly discovered methodology was employed in the preparation of advanced liquid crystalline materials containing the [*closo*-1-CB₉H₁₀]⁻ anion.

Both the zwitterionic and ionic materials were studied for liquid crystalline properties using thermal, optical, and in some cases dielectric and XRD methods. The zwitterionic materials possess large longitudinal dipole moments and were utilized as additives to other liquid crystals, which caused large increases in the dielectric properties of the bulk material. These findings are promising for electro-optical applications. The ionic materials displayed typical liquid crystalline behavior expected for ionic architectures. However, the design of such materials is unique in that the anisometric anion is the driving force behind the organization of the molecules in the fluid phase. These types of materials are promising for photo-physical effects and the potential transport of ions for energy storage or delivery.

BORON CLUSTERS AS THE CENTERPIECE OF ADVANCED LIQUID
CRYSTALS: FUNDAMENTAL CHEMISTRY AND PROPERTIES

By

Bryan Ringstrand

Dissertation

Submitted to the Faculty of the
Graduate School of Vanderbilt University
in partial fulfillment of the requirements

for the degree of

DOCTOR OF PHILOSOPHY

in

Chemistry

May, 2011

Nashville, Tennessee

Approved:

Professor Piotr Kaszynski

Professor Timothy Hanusa

Professor Jeffrey Johnston

Professor Kane Jennings

Table of Contents

	Page
Acknowledgements	x
Dissertation Synopsis and Guide	xii
 <i>Part I. Introduction to Boron Clusters and Liquid Crystals</i>	
Chapter 1: Boron Clusters and Liquid Crystals	1
Boron Clusters.....	1
Liquid Crystals	5
Boron Clusters and Liquid Crystals	10
References.....	13
 Chapter 2: The Chemistry and Properties of the [closo-1-CB₉H₁₀]⁻ Anion.....	 17
Abstract.....	17
Introduction.....	17
The First Isomerically Pure 1,10-Disubstituted [closo-1-CB ₉] Cluster	22
Transformations of [closo-1-CB ₉ H ₈ -1-COOH-10-I] ⁻	23
N ₂ ⁺ Derivatives of the [closo-1-CB ₉] Cluster	26
Liquid Crystals Derived from the [closo-1-CB ₉] Cluster	37
Summary and Conclusions	40
References.....	40

Part II. Fundamental Chemistry and Properties of the [closo-1-CB₉H₁₀]⁻ Cluster

Chapter 1: A Practical Synthesis of Isomerically Pure 1,10-Difunctionalized Derivatives of the [closo-1-CB₉H₁₀]⁻ Anion. (Ringstrand, B.; Balinski, A.; Franken, A.; Kaszynski, P. *Inorg. Chem.* **2005**, *44*, 9561-9566)..... 46

Abstract.....	46
Introduction.....	47
Results.....	49
Discussion.....	56
Summary and Conclusions	59
Computational Details	60
Experimental Section.....	61
Acknowledgements	66
References.....	66

Chapter 2: Synthesis and Reactivity of [closo-1-CB₉H₉-1-N₂]: Functional Group Interconversion at the Carbon Vertex of the {closo-1-CB₉} Cluster. (Ringstrand, B.; Kaszynski, P.; Franken, A. *Inorg. Chem.* **2009**, *48*, 7313-7329)..... 70

Abstract.....	71
Introduction.....	72
Results.....	74
Discussion.....	106
Summary and Conclusions	118
Computational Details	120
Experimental Section.....	136
Acknowledgements	136
References.....	136

Chapter 3: The Anionic Amino Acid [*closo*-1-CB₉H₈-1-COOH-10-NH₃] and Dinitrogen Acid [*closo*-1-CB₉H₈-1-COOH-10-N₂] as Key Precursors to Advanced Materials: Synthesis and Reactivity. (Ringstrand, B.; Kaszynski, P.; Young, V.G. Jr.; Janousek, Z. *Inorg. Chem.* **2010**, *49*, 1166-1179)..... 145

Abstract.....	146
Introduction.....	147
Results.....	151
Discussion.....	172
Summary and Conclusions	181
Computational Details	182
Experimental Section.....	183
Acknowledgements	197
References.....	197

*Part III. Liquid Crystals Incorporating the [*closo*-1-CB₉H₁₀]⁻ Cluster as a Structural Element*

Chapter 1: Polar Derivatives of the [*closo*-1-CB₉H₁₀]⁻ Cluster as Positive $\Delta\epsilon$ Additives to Nematic Hosts. (Ringstrand, B.; Kaszynski, P.; Januszko, A.; Young, V. G. Jr. *J. Mater. Chem.* **2009**, *19*, 9204-9212)..... 208

Abstract.....	209
Introduction.....	210
Results.....	213
Discussion.....	231
Summary and Conclusions	236
Computational Details	237
Experimental Section.....	237

Acknowledgements	244
References.....	245
Chapter 2: How Much Can an Electric Dipole Stabilize a Nematic Phase? Polar and Non-Polar Isosteric Derivatives of [closo-1-CB₉H₁₀]⁻ and [closo-1,10-C₂B₈H₁₀]. (Ringstrand, B.; Kaszynski, P. <i>J. Mater. Chem.</i> 2010, <i>20</i>, 9613-9615).....	252
Abstract.....	253
Introduction.....	253
Results and Discussion	254
Summary and Conclusions	260
Experimental Section.....	261
Acknowledgements	279
References.....	279
Chapter 3: High Δε Nematic Liquid Crystals: Fluxional Zwitterions of the [closo-1-CB₉H₁₀]⁻ Cluster. (Ringstrand, B.; Kaszynski, P. <i>J. Mater. Chem.</i> 2011, <i>21</i>, 90-95).....	283
Abstract.....	284
Introduction.....	285
Results and Discussion	287
Summary and Conclusions	299
Computational Details	300
Experimental Section.....	301
Acknowledgements	305
References.....	305

Chapter 4: Anion-Driven Mesogenicity: Ionic Liquid Crystals Based on the [closo-1-CB₉H₁₀]⁻ Cluster. (Ringstrand, B.; Kaszynski, P.; Monobe, H. <i>J. Mater. Chem.</i> 2009 , <i>19</i> , 4805-4812).....	308
Abstract.....	309
Introduction.....	309
Results and Discussion	313
Summary and Conclusions	327
Experimental Section.....	328
Acknowledgements	346
References.....	346
Chapter 5: Anion-Driven Mesogenicity: A Comparative Study of Ionic Liquid Crystals Based on the [closo-1-CB₉H₁₀]⁻ and [closo-1-CB₁₁H₁₂]⁻ Clusters.	353
Abstract.....	354
Introduction.....	354
Results and Discussion	357
Summary and Conclusions	364
Experimental Section.....	365
Acknowledgements	375
References.....	376
<i>Part IV. Other Projects Involving the [closo-1-CB₉H₁₀]⁻ Anion</i>	
Chapter 1: Improved Synthesis of [closo-1-CB₉H₁₀]⁻ Anion and New C-Substituted Derivatives. (Ringstrand, B.; Bateman, D.; Shoemaker, R.K.; Janousek, Z. <i>Collect. Czech. Chem. Commun.</i> 2009 , <i>74</i> , 419-431).....	380

Chapter 2: Diazotization of the Amino Acid [*closo*-1-CB₉H₈-1-COOH-6-NH₃] and Reactivity of the [*closo*-1-CB₉H₈-1-COO-6-N₂]⁻ Anion. (Ringstrand, B.; Kaszynski, P.; Young, V. G. Jr. *Inorg. Chem.*, **2011**, *50*, 2654-2660)..... 381

Chapter 3: The Preparation of [*closo*-1-CB₉H₈-1-COOH-10-(4-C₃H₇C₅H₉S)] as an Intermediate to Polar Liquid Crystals. (Pecyna, J.; Denicola, R.P.; Ringstrand, B.; Jankowiak, A.; Kaszynski, P. *Polyhedron*, submitted) 383

Chapter 4: Transmission of Electronic Effect through the [*closo*-1-CB₉H₁₀] Cage: Dissociation Constants for a Series of [*closo*-1-CB₉H₈-1-COOH-10-X]⁻ Acids..... 384

Chapter 5: The Preparation of 3-Substituted-1,5-Dibromopentanes as Precursors to Heteracyclohexanes. (Ringstrand, B.; Oltmanns, M.; Batt, J.; Kaszynski, P. *Beils. J. Org. Chem.* **2011**, *7*, in press) 386

*Part V. Projects Not Involving the [*closo*-1-CB₉H₁₀]⁻ Anion*

Chapter 1: Comparative Studies of Three- and Four-ring Mesogenic Esters Containing *p*-Carborane, Bicyclo[2.2.2]octane, Cyclohexane, and Benzene. (Ringstrand, B.; Vroman, J.; Jensen, D.; Januszko, A.; Kaszynski, P.; Dziaduszek, J.; Drzewinski W. *Liq. Cryst.*, **2005**, *32*, 1061-1070) 388

Chapter 2: A Convenient Preparation of Long Chain 4-(4-*n*-Alkylphenylazo)phenols and their 4-Pentylbenzoate Esters. (Johnson, L.; Ringstrand, B.; Kaszynski, P. *Liq. Cryst.* **2009**, *36*, 179-185) 389

Acknowledgements

My dissertation could not have been possible without the financial support of the National Science Foundation and the Vanderbilt Graduate School. I am grateful for their support during my time spent at Vanderbilt. In addition, the Vanderbilt Graduate School awarded me numerous Travel Grants to present my research at conferences both domestically and abroad. I was also the recipient of a Dissertation Enhancement Grant through the Vanderbilt Graduate School, which gave me the opportunity to spend time in Warsaw, Poland conducting research and learning about instrumentation that is not available here at Vanderbilt.

I am thankful to all those I have worked with during my dissertation research and other related projects. I would like to acknowledge my undergraduate advisor, Dr. Dell Jensen, for providing me the opportunity to have experienced undergraduate research. This was the springboard that convinced me to pursue graduate school in chemistry. I am especially indebted to my graduate advisor, Dr. Piotr Kaszynski, as his mentoring has molded me into the scientist that I have become. I believe Dr. Kaszynski's most valuable asset is his ability to provide instruction but also the freedom for his students to become scientists capable of independent thought. I would also like to thank the members of my PhD committee, Dr. Jeffrey Johnston, Dr. Timothy Hanusa, and Dr. Kane Jennings, for their willingness to sit on my committee, and their guidance and support through this process.

I cannot forget to mention Dr. Zbynek Janousek as my advisor away from

Vanderbilt. Dr. Janousek hosted me in Prague, Czech Republic where I spent 18 weeks continuing research initiated at Vanderbilt. In the same breath, I am grateful to Dr. Ewa Gorecka for hosting me during a 4-week stay in Warsaw, Poland.

I would like to acknowledge my family members for their support, love, and inspiration during this time. I do not think I would be here without my parents who always pushed me to strive for excellence. Lastly, I cannot stress how important the love of my life, Katherine, has been during my this process. Her support, dedication, and understanding have remained strong since day one and for this I am very grateful. The conclusion of my dissertation marks the moment that we can now start our lives together. This moment has been something we have both been looking forward to for some time.

Dissertation Synopsis and Guide

The main scope of my dissertation focuses on developing the fundamental chemistry of the $[closo-1-CB_9H_{10}]^-$ anion from both synthetic and physical-organic perspectives and exploring its use as a structural element of polar (**I** and **II**) and ionic (**III**) liquid crystals geared towards electro-optical, photo-physical, and ion-transport applications (Figure 1).

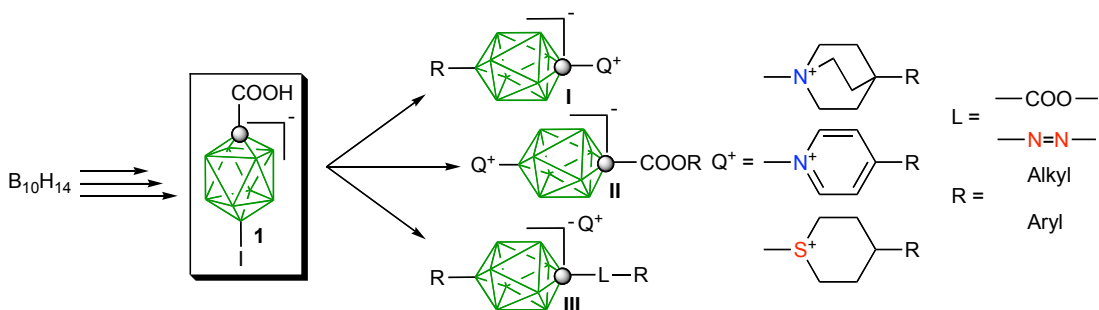


Figure 1. Polar (**I** and **II**) and ionic (**III**) liquid crystals derived from iodo acid $[closo-1-CB_9H_8-1-COOH-10-I]^-$ anion (**1**).

The research began from the preparation of iodo acid, $[closo-1-CB_9H_8-1-COOH-10-I]^-$ (**1**) as the first reported isomerically pure 1,10-disubstituted derivative of the $[closo-1-CB_9H_{10}]^-$ anion,^{1a} which can be obtained in up to 12 g at a time.^{1b} Iodo acid **1** serves as the key starting material for both polar (**I** and **II**) and ionic materials (**III**). The transformations of the C(1) carboxylic acid group² and B(10) iodine³ into the corresponding C(1) and B(10) amino groups, **2** and **3**, respectively, were developed. Diazotization of these amino derivatives provided isolable and stable zwitterionic diazonium species, **4** and **5**, respectively, as valuable synthetic intermediates. The

reactivity and properties of zwitterionic diazonium species **4** and **5** were investigated within the context of introducing onium fragments at both the C(1) and B(10) vertices.^{2,3} It was also demonstrated that the iodine can be replaced with an alkyl group using palladium-catalyzed coupling reactions with organozinc reagents, and the C(1) carboxylic acid can be converted into an ester^{4,5} (Figure 2).

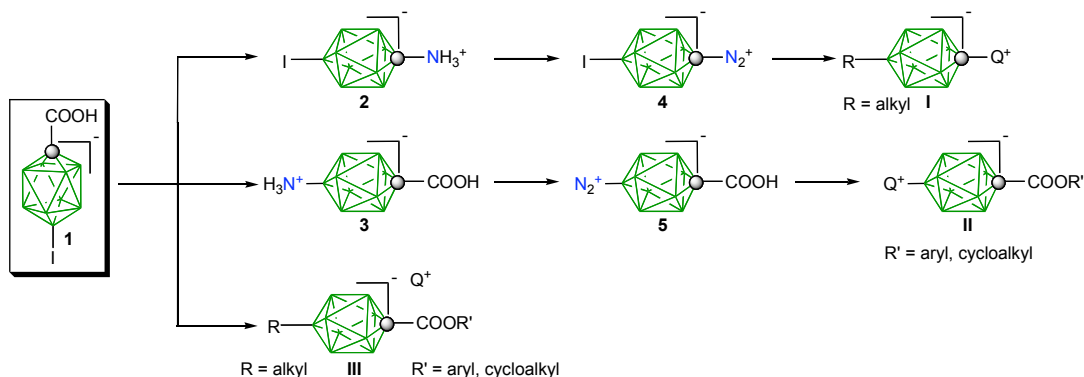


Figure 2. The transformations of the C(1) carboxylic acid group and B(10) iodine providing access to polar (**I** and **II**) and ionic (**III**) liquid crystalline derivatives.

These advancements in the fundamental chemistry of the $[closo-1-CB_9H_{10}]^-$ anion were performed in a systematic and goal-orientated fashion in the context of accessing polar (**I** and **II**) and ionic (**III**) materials. In addition, the diazonium species, **4** and **5**, and all relevant intermediates were comprehensively studied using standard physical-organic methods.^{2,3}

With developed methodology and understanding of reactivity and properties of intermediates, the first examples of polar (**I** and **II**) and ionic (**III**) liquid crystals derived from the $[closo-1-CB_9H_{10}]^-$ anion were prepared and their properties examined by thermal and optical and in some cases dielectric and XRD methods (Figure 3).

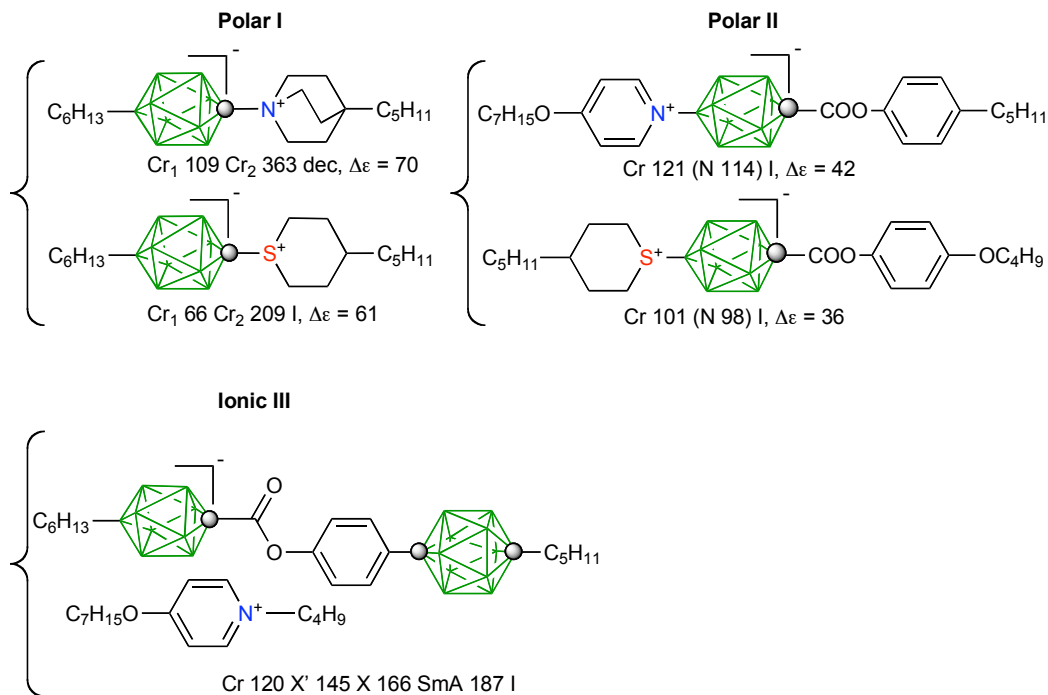


Figure 3. Examples of polar (**I** and **II**) and ionic (**III**) liquid crystals with transition temperatures and dielectric anisotropy.

The polar materials (**I** and **II**) were investigated as neat materials as well as additives to nematic hosts. Materials **I** exhibited high virtual T_{NI} and large extrapolated dielectric anisotropy, $\Delta\epsilon$, above 60 for dilute solutions.⁵ Analysis of polar materials **II** demonstrated that they display nematic properties, lower melting points, and greater compatibility with liquid crystalline hosts.^{6,7} In addition, polar materials **II** permitted for the effect of an electric dipole moment on the stability of the nematic phase to be investigated. This was accomplished by comparing polar and non-polar isosteric derivatives of the [*closo*-1- CB_9H_{10}]⁻ anion and carborane, [*closo*-1,10- $\text{C}_2\text{B}_8\text{H}_{10}$]⁺.⁷ A patent application⁸ protecting materials (**I** and **II**) has been filed.

The phase structures of the first examples of anion-driven ionic liquid crystals of the [*closo*-1-CB₉H₁₀]⁻ anion (**III**) were investigated using powder XRD to help elucidate the organization of the ion-pairs in the liquid crystalline and soft crystalline phases.⁴ Ionic liquid crystals of the [*closo*-1-CB₁₁H₁₂]⁻ anion were also prepared and their properties compared to those of the [*closo*-1-CB₉H₁₀]⁻ anion.⁹

Besides the main scope of my dissertation thesis, I was involved in other projects during my graduate career. For one, the preparation and thermal, optical, and dielectric characterization of other liquid crystalline materials, that did not involve the [*closo*-1-CB₉H₁₀]⁻ anion, were completed.^{10,11}

The fundamental chemistry of the [*closo*-1-CB₉H₁₀]⁻ anion was enhanced further by investigating substitution reactions at the C(1) vertex¹² as well as the reactivity of the amino group¹³ at the 6-position in amino acid [*closo*-1-CB₉H₈-1-COOH-6-NH₃]. These two developments in the fundamental chemistry of the [*closo*-1-CB₉H₁₀]⁻ anion were not pursued in the context of developing access to polar (**I** and **II**) or ionic liquid crystalline materials **III**, and therefore are not considered part of the main scope of the dissertation work. Access to amino acid [*closo*-1-CB₉H₈-1-COOH-6-NH₃] and hence diazonium species [*closo*-1-CB₉H₈-1-COOH-6-N₂] did provide an opportunity to compare its reactivity and stability to diazonium species **4** and **5**.

With access to a variety of 1,10-disubstituted [*closo*-1-CB₉H₈-1-COOH-10-X]⁻ acids, the potency of the [*closo*-1-CB₉H₁₀]⁻ anion as a conduit of electronic effects was compared to that of 4-substituted benzoic acid and 4-substituted bicyclo[2.2.2]octane-1-carboxylic acid derivatives. This was accomplished by measuring the

dissociation constant of each 1,10-disubstituted [*closo*-1-CB₉H₈-1-COOH-10-X]⁻ acid and plotting the results versus the Hammett parameter (σ) of substituent X.¹⁴

Lastly, the preparation of various 3-substituted-1,5-dibromopentanes containing both simple alkyl chains as well as more complex fragments was investigated.¹⁵ These dibromopentanes are of interest because they are used as building blocks in the preparation of polar derivatives **I** and **II**.

Overall, I was involved in the publication of twelve peer-reviewed articles (References 1a, 2, 3, 4, 5, 6, 7, 10, 11, 12, 13, and 15), eleven of which were first author works. Another three manuscripts are currently in various stages of preparation (References 1b, 9, and 14). In the interest of space, only publications that are related to the main scope of my dissertation work, which is liquid crystalline derivatives **I-III** of the [*closo*-1-CB₉H₁₀]⁻ anion, are included in full (References 1a, 2, 3, 4, 5, 6, and 7). In most cases, these publications contained electronic supporting information; however, for length considerations, only experimental details related to preparation of compounds are included. Other manuscripts that are outside the main emphasis of the dissertation (References 1b, 9, 10, 11, 12, 13, 14, and 15) are only summarized

The dissertation consists of five parts (Parts I, II, III, IV, and V). Part I consists of an introduction to boron clusters and liquid crystals and a review of the fundamental chemistry and properties of the [*closo*-1-CB₉H₁₀]⁻ anion. Parts II and III represent the main scope of my dissertation studies. Part II includes publications related to the advancements of the fundamental chemistry of the [*closo*-1-CB₉H₁₀]⁻ anion. Part III

contains publications describing the synthesis and characterization of liquid crystals derived from the [*closo*-1-CB₉H₁₀]⁻ anion. Part IV contains summaries of publications that are outside the main scope of my dissertation studies that involve the [*closo*-1-CB₉H₁₀]⁻ anion, while Part V contains summaries of publications not related to the main scope that do not involve the [*closo*-1-CB₉H₁₀]⁻ anion.

Each chapter begins with a statement of bibliographic information, the purpose of the research, the accomplishments, and the responsibilities of each author.

In addition to the work I have accomplished in this dissertation, there are other achievements that I wish to highlight that may not be apparent from the document. Besides publishing many peer-reviewed articles, I also took part in the submission of a patent disclosure that dealt with the liquid crystalline materials that were prepared as a result of my dissertation studies.⁸ I also had the opportunity to participate in several conferences and present my work at these events both in oral and poster formats. I have included a list of these conferences below and the formats of the presentations.

- 23rd International Liquid Crystals Conference, 2010 – Kraków, Poland (oral and poster)
- Liquid Crystal Gordon Conference – 2009, New London, NH (poster)
- Boron in Americas XI, 2008 – St. Louis, MO (oral and poster)
- IMEBORON XIII, 2008 – Platja d' Oro, Spain (poster)

- 60th SERMACS, 2008 – Nashville, TN (oral)
- 223rd ACS National Meeting, 2007 – Chicago, IL (oral and poster)
- 21st International Liquid Crystals Conference, 2006 – Keystone, CO (poster)

In addition to these sponsored events, I was an invited speaker at the University of Łódź located in Łódź, Poland in 2010, Augustana College in Rock Island, IL in 2009, University of Wrocław in Wrocław, Poland in 2008, and the Institute of Inorganic Chemistry of the Czech Academy of Sciences located in Rez, Czech Republic both in 2007 and 2008.

During my time as a graduate student, I was awarded a teaching fellowship for general chemistry, which permitted me to lead discussion sections for undergraduate students. I received several travel grants through the Vanderbilt University Graduate School that permitted me to travel to the conferences that I participated in. In addition, I had the opportunity to participate in the 2009 meeting of Nobel Laureates in Lindau, Germany. Lastly, I received a Dissertation Enhancement Grant, which allowed me to travel to Warsaw, Poland to conduct powder XRD measurements on ionic liquid crystals that were prepared as a result of my dissertation studies. The results of this DEG are included in this document (Part III, Chapter 5).

References:

- 1) (a) Ringstrand, B.; Balinski, A.; Franken, A.; Kaszynski, P. "A Practical Synthesis of Isomerically Pure 1,10-Difunctionalized Derivatives of the [*closo*-1-CB₉H₁₀] Anion", *Inorg. Chem.* **2005**, *44*, 9561-9566; (b) Pecyna, J.; Denicola, R.P.; Ringstrand, B.; Jankowiak, A.; Kaszynski, P. "The Preparation of [*closo*-1-CB₉H₈-1-COOH-10-(4-C₃H₇C₅H₉S)] as an Intermediate to Polar Liquid Crystals", *Polyhedron*, submitted.
- 2) Ringstrand, B.; Kaszynski, P.; Franken, A. "Synthesis and Reactivity of [*closo*-1-CB₉H₉-1-N₂]: Functional Group Interconversion at the Carbon Vertex of the {*closo*-1-CB₉} Cluster", *Inorg. Chem.* **2009**, *48*, 7313-7329.
- 3) Ringstrand, B.; Kaszynski, P.; Young, V. G. Jr.; Janousek, Z. "The Anionic Amino Acid [*closo*-1-CB₉H₈-1-COOH-10-NH₃] and Dinitrogen Acid [*closo*-1-CB₉H₈-1-COOH-10-N₂] as Key Precursors to Advanced Materials: Synthesis and Reactivity", *Inorg. Chem.* **2010**, *49*, 1166-1179.
- 4) Ringstrand, B.; Kaszynski, P.; Monobe, H. "Anion-Driven Mesogenicity: Ionic Liquid Crystals based on the [*closo*-1-CB₉H₁₀] Cluster", *J. Mater. Chem.* **2009**, *19*, 4805-4812.
- 5) Ringstrand, B.; Kaszynski, P.; Januszko, A.; Young, V. G. Jr. "Polar Derivatives of the [*closo*-1-CB₉H₁₀] Cluster as Positive $\Delta\epsilon$ Additives to Nematic Hosts", *J. Mater. Chem.* **2009**, *19*, 9204-9212.
- 6) Ringstrand, B.; Kaszynski, P. "High $\Delta\epsilon$ Nematic Liquid Crystals: Fluxional Zwitterions of the [*closo*-1-CB₉H₁₀] Cluster", *J. Mater. Chem.* **2011**, *21*, 90-95.
- 7) Ringstrand, B.; Kaszynski, P. "How Much Can an Electric Dipole Stabilize a Nematic Phase? Polar and Non-Polar Isosteric Derivatives of [*closo*-1-CB₉H₁₀] and [*closo*-1,10-C₂B₈H₁₀]", *J. Mater. Chem.* **2010**, *20*, 9613-9615.
- 8) Ringstrand, B.; Kaszynski, P. "Polar Nematic Compounds". U.S. Patent Application Number 61287863, December 18, 2009.

- 9) Ringstrand, B.; Johnson, L.; Kaszynski, P. "Anion-Driven Mesogenicity: A Comparative Study of Ionic Liquid Crystals Based on the [*closo*-1-CB₉H₁₀]⁻ and [*closo*-1-CB₁₁H₁₂]⁻ Clusters", *Inorg. Chem.*, in preparation.
- 10) Ringstrand, B.; Vroman, J.; Jensen, D.; Januszko, A.; Kaszynski, P.; Dziaduszek, J.; Drzewinski W. "Comparative Studies of Three- and Four-ring Mesogenic Esters Containing *p*-Carborane, Bicyclo[2.2.2]octane, Cyclohexane, and Benzene", *Liq. Cryst.*, **2005**, *32*, 1061-1070.
- 11) Johnson, L.; Ringstrand, B.; Kaszynski, P. "A Convenient Preparation of Long Chain 4-(4-*n*-Alkylphenylazo)phenols and their 4-Pentylbenzoate Esters", *Liq. Cryst.* **2009**, *36*, 179-185.
- 12) Ringstrand, B.; Bateman, D.; Shoemaker, R. K.; Janousek, Z. "Improved Synthesis of [*closo*-1-CB₉H₁₀]⁻ Anion and New C-Substituted Derivatives", *Collect. Czech. Chem. Commun.* **2009**, *74*, 419-431.
- 13) Ringstrand, B.; Kaszynski, P.; Young, V. G. Jr. "Diazotization of the Amino Acid [*closo*-1-CB₉H₈-1-COOH-6-NH₃] and Reactivity of the [*closo*-1-CB₉H₈-1-COO-6-N₂]⁻ Anion", *Inorg. Chem.* **2011**, *50*, 2654-2660.
- 14) Ringstrand, B.; Kaszynski, P.; Pecyna, J. "Transmission of Electronic Effect through the {*closo*-1-CB₉} Cage: Dissociation Constants for a Series of [*closo*-1-CB₉H₈-1-COOH-10-X]⁻ Acids", *Inorg. Chem.*, in preparation.
- 15) Ringstrand, B.; Oltmanns, M.; Batt, J.; Kaszynski, P. "The Preparation of 3-Substituted-1,5-Dibromopentanes as Precursors to Heteracyclohexanes", *Beils. J. Org. Chem.* **2011**, *7*, in press.

Boron Clusters and Liquid Crystals

Boron Clusters

Boron is the only other element besides carbon that can build molecules of unlimited size by covalently bonding to itself. Instead of chains and rings, boron, having only three valence electrons, prefers to adopt cluster motifs. This is apparent in boron's elemental form, icosahedra B₁₂. In 1900, Alfred Stock and coworkers opened up the doorway to an era of new structural chemistry with the discovery of these polyhedral boranes.¹ The effects of this breakthrough on the understanding of covalent bonding are still unfolding. The existence of both neutral and anionic structures some of which contain heteroatoms have influenced both organic and inorganic chemistry.^{2,3} The prototypical borane is borate [*closo*-B₁₂H₁₂]⁻² anion **1[12]**, which possesses ideal icosahedral symmetry. Replacement of one BH vertex with an isoelectronic CH⁺ unit gives monocarbaborate [*closo*-1-CB₁₁H₁₂]⁻ anion **2[12]**. A second CH⁺ replacement gives neutral carborane, [*closo*-C₂B₁₀H₁₂] (**3[12]**). Besides the twelve-vertex family, there also exists the ten-vertex family, which contains borate [*closo*-B₁₀H₁₀]⁻² anion **1[10]**, monocarbaborate [*closo*-1-CB₉H₁₀]⁻ anion **2[10]**, and neutral carborane, [*closo*-C₂B₈H₁₀]. The two neutral carboranes are routinely found as three regioisomers (*ortho*, **3-o[12]** and **3-o[10]**, *meta*, **3-m[12]** and **3-m[10]**, and *para*, **3-p[12]** and **3-p[10]**) (Figure 1).

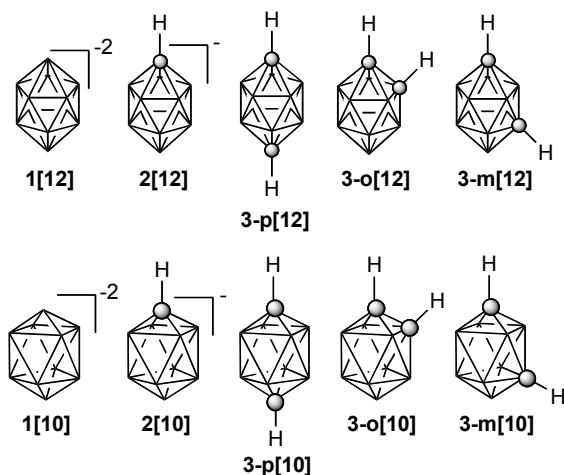


Figure 1. Structures of ten and twelve-vertex *closo*-boranes. The dark oval circles represent carbon atoms. All other vertices are B-H bonds.

Other sized clusters exist ranging from as small as 5-vertices to as big as 22 vertices, but the ten and twelve vertex clusters are the most commonly encountered in the literature due to availability.² The *closo* prefix distinguishes a cluster by only having triangular faces or no missing vertices.

These *closo*-boranes are characterized by high thermal and oxidative stability due in part to their highly delocalized bonding within a σ -framework, which is considered bonding similar to that of a three-dimensional aromatic benzene (π -framework). This type of bonding is possible since boron, being electron deficient, prefers to form three-center two-electron bonds. This bonding concept, described by Higgins and Lipscomb, deviates from the standard Lewis model and is labeled as “non-classical” by inorganic and organic chemists.^{4,5}

Even if these unique structures had no practical use, their existence would still be worthwhile for challenging the way chemists understand covalent bonding. Fortunately, this is not the case as these polyhedral boranes have found uses in a variety of applications.

Since polyhedral boranes have low chemical reactivity (due to their extensive bonding networks) and resistance to breakdown in biological systems making them relatively non-toxic, they can be tailored for specific purposes. For one, the ^{10}B isotope, accounting for 20 % of boron in nature, has a very large neutron cross-section (ability to absorb neutrons). The collision of thermal neutrons with the ^{10}B isotope produces high-energy α -particles.⁶ This led to the development of boron neutron capture therapy (BNCT). If this reaction was conducted in tissue, the immediate cells would be damaged, but their neighbors left unharmed. Therefore, if a significant amount of ^{10}B could be absorbed by a tumor, irradiation of these cells with relatively harmless thermal neutrons would constitute a noninvasive means of treating cancer.⁷ Some earlier pitfalls of implementing BNCT were availability of proper boron compounds which were non-toxic and possessed good solubility in the biological matrix and selectivity for tumor tissue. Today, most efforts of BNCT focus on linking boron clusters, both neutral and anionic, to biologically active molecules that permit better absorption of the material by the tumor tissue.

The neutral carboranes are readily soluble in organic solvents but insoluble in water. On the other hand, the anionic boron clusters are both soluble in water and

organic solvents. Therefore, there are efforts aimed at using anionic boron cluster as metal ion extraction agents. This is important for other applications such as the removal of radioactive ions from nuclear waste.⁸

In order to stabilize highly reactive cationic species such as R_3Si^+ or arenium ions, it is important to have a non-coordinating or non-nucleophilic anion to compensate the reactive cationic species. In fact, this is one such use of the anionic monocarbaborates. Since their negative charge is highly delocalized, the anion is weakly nucleophilic, and this provides a suitable environment for the stabilization of reactive cationic species. The $[closo-1-CB_{11}H_{12}]^-$ anion and its perhalogenated derivatives have been thoroughly studied in such systems.⁹ Such derivatives show very little affinity for electrophiles such as silylium, hydrated protons, benzenium, and other protonated arenes permitting for their isolation.

An area of study that takes advantage of both the three-dimensional cage geometry and the special electronic properties of boron clusters is the field of liquid crystals. Incorporation of boron clusters into liquid crystalline structural motifs is particularly attractive because of the clusters thermal stability, delocalized bonding, and ease of functionalization.^{10,11} In most, if not all cases, the introduction of a boron cluster can significantly change the electronic structure of the liquid crystal, and hence the response of the bulk material to external stimuli such as an applied electric or magnetic field. However, before going into any further in detail on this topic, it would be prudent

to first introduce the concept of liquid crystals.

Liquid Crystals

Solids, liquids, and gases are routinely considered the three states of matter. However, in the nineteenth century a new state of matter classified as liquid crystal was discovered. The term implies molecular order of a substance between that of the three-dimensional lattice of a solid (long-range orientational and positional order) and the complete random disorder (no orientational and positional order) of a liquid.^{12,13} Since their discovery, liquid crystals have found application in liquid crystal displays (LCDs) used commonly in today's digital watches, laptop screens, and televisions.^{12,14,15}

Molecules that are capable of forming liquid crystal phases are called mesogens and have mesogenic properties. The term mesophase can also be used in place of liquid crystal phase. Mesogens can be divided into two categories one being thermotropic and the other lyotropic. Thermotropic liquid crystal phases are formed by pure mesogens in a specific temperature range. On the other hand, lyotropic liquid crystal phases form in solution and the phase structure depends on concentration.^{12,13}

Thermotropic mesophases are formed by anisometric molecules with long-range orientational order and in some cases a degree of positional order. The term anisotropy means having properties that vary depending on the direction of measurement. This means that liquid crystals have a specific. The two most common shapes of liquid

crystalline molecules found are rod-like (calamitic) and disc-like (discotic). For a better understanding, one might think of a matchstick representing a calamitic liquid crystal and a quarter a discotic. The key feature of calamitic liquid crystals is typically a rigid core consisting of one or more 1,4-benzene, *trans*-1,4-cyclohexane, or 1,4-bicyclo[2.2.2]octane rings having alkyl or alkoxy chains attached at the periphery (Figure 2).^{12,13}

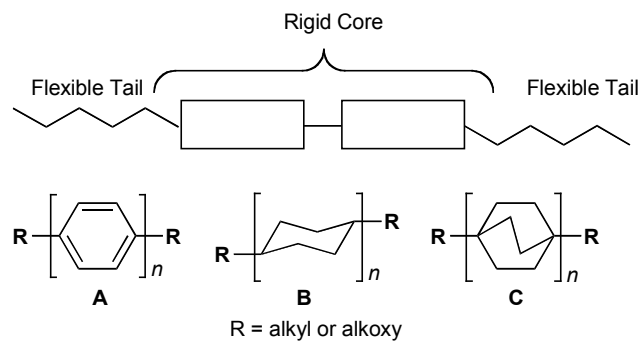


Figure 2. A general schematic of a calamitic liquid crystal and typical examples of liquid crystalline rigid core molecules with “*n*” repeating units.

The rigid core elements may be connected directly or linked through functional groups such as esters, imines, azo, or ethylene spacers. The alkyl or alkoxy chains provide flexibility and help lower the melting point of the material. Altering this balance between the rigid core and the flexible periphery permits one to fine tune liquid crystalline properties within a homologous series. Other terminal groups such as a cyano group can enhance the formation of the liquid crystalline phase due to dipole-dipole interactions between pairs of molecules. Lateral substituents attached to the core, such as fluorine atoms, can modify molecular packing and can increase molecular polarizability,

but may have a negative effect on the liquid crystal phase stability.^{12,13}

The two main types of calamitic liquid crystal phases are classified as nematic and smectic. The nematic phase is the simplest liquid crystal phase that possesses no long-range positional order but possess weak long-range orientational order. The notation for the nematic phase is “N”, and the direction of the average molecular orientation is called the director. Referring back to the matchstick analogy, the nematic phase would be best represented by matches in a matchbox. There are domains of molecular order, but over long ranges the matches do not follow any specific organizational pattern as one would see in a crystal three-dimensional lattice.^{12,13}

On the other hand, the smectic phase more closely resembles a crystal lattice where the molecules organize in diffuse layers and show both orientational and in some cases short-range positional order within the plane of the layers. The most common smectic phases are classified as smectic A, SmA, and smectic C, SmC, In SmA, the molecules are on average normal to the planes whereas in SmC, the molecules on average are tilted (Figure 3).

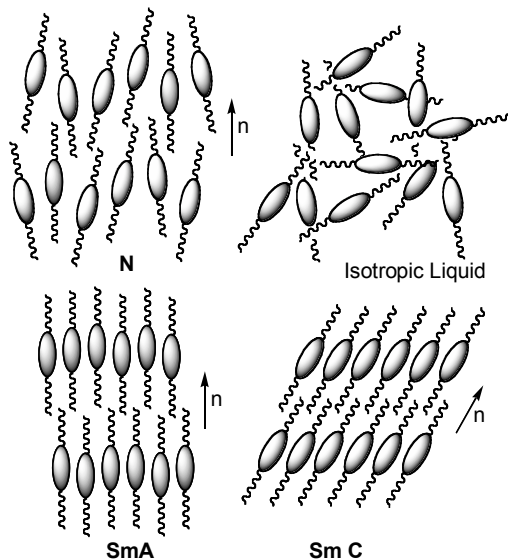


Figure 3. Schematics of nematic (N), smectic A (SmA), smectic C (SmC), and an isotropic liquid. The dark ovals represent the rigid core of a calamitic liquid crystals and the squiggly lines the alkyl or alkoxy chains. The arrow represents the director “n”.

More ordered phases are classified as soft crystal phases such as crystal B, crystal I, and crystal F. Unlike SmA and SmC, these phases do possess long-range positional order in three dimensions, but the layers are weakly attached to each other.^{12,13}

Liquid crystals phases are typically characterized by textures one observes under polarized light. Since liquid crystals are anisotropic fluids, they demonstrate double refraction (birefringence) meaning that polarized light parallel to the director has a different refractive index (i.e. velocity) than one normal to the director. In effect, when a birefringent material is placed between crossed polarizers, the velocity and phase of polarized light is changed and some light can now pass through the second polarizer, and this is what is observed as an optical effect. Without the birefringent material, one would only observe darkness. Depending on the thickness of the sample of liquid crystal,

one will see lighter and darker areas, which is a measure of the degree that the polarization direction was altered. Colors are sometimes observed due to the fact that the liquid crystal molecules are ordered in domains. These domains act as prisms that can split light into different wavelengths. The thickness of the liquid crystal layer plays a role in which colors are observed.¹²

The common method to quantify the liquid crystal phase transition temperatures is differential scanning calorimetry (DSC). DSC measures the endothermic enthalpy associated with the phase transition. Typically liquid crystal-liquid crystal or liquid crystal-isotropic liquid transitions exhibit much lower enthalpies than the melting enthalpy. This is due to the fact that there are much smaller changes in molecular organization as one approaches the isotropic liquid transition. The size of the enthalpy of transition aids in the identification of liquid crystal phases.^{12,13}

Since liquid crystalline molecules are anisometric, they will be differentiated in electric and magnetic fields. In other words, applying an electric field across a thin film of liquid crystal can change the orientation of the liquid crystalline molecules and therefore the intensity and direction of transmitted light.¹⁴ This is the basic operating principle for a liquid crystal display (LCD). In a typical LCD, a nematic liquid crystal is sandwiched between two pieces of glass. The two plates of glass are treated with a polymer in such a way to facilitate parallel alignment of molecules with the sandwiched glass. The polymer provides microscopic grooves for some molecules to interact with which then acts as a seed for the rest of the bulk material to follow as a guide.¹²

Application of a voltage across a thin film of liquid crystal will cause the molecules to reorientate in such a way to align the net molecular dipole in the direction of the electric field. This phenomenon is called the Fréedericksz transition, and the reorganization of molecules occurs above a critical voltage (threshold voltage, V_{th}) (Figure 4).¹⁶

$$V_{th} = \pi \sqrt{\frac{K}{\Delta\epsilon\epsilon_0}}$$

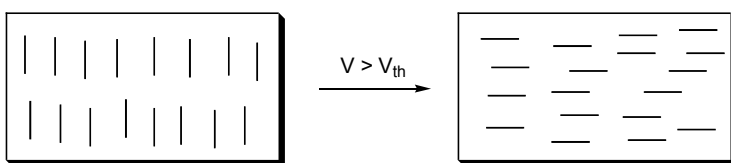


Figure 4. The threshold voltage (V_{th}) for the Fréedericksz transition

The threshold voltage (V_{th}) for the reorientation of the LC molecules is inversely proportional to the square root of dielectric anisotropy, $\Delta\epsilon$, which in turn is proportional to the molecular dipole moment and its orientation. Therefore, the larger the dipole moment, the lower the threshold voltage ($V_{th} \sim 1/\mu$).^{17,18} There is much interest in designing liquid crystalline molecules with large positive $\Delta\epsilon$ values for this reason.

Boron Clusters and Liquid Crystals

As was previously stated, an area of study that takes advantage of both the three-dimensional cage geometry and the special properties of boron clusters is the field of liquid crystals. One such property of boron clusters that the field of liquid crystals can

take advantage of is the clusters' lack of UV absorption above 200 nm, and the clusters' ability to interact with substituents ranging from weak to strong. Another includes the clusters' high electronic polarizability and low anisotropy, which results in low birefringence and high isotropic refractive index^{19,20} for a liquid crystal containing a boron cluster.²¹ The clusters also have large molecular size²² and high symmetry axes (D_{5d} and D_{4d} for the twelve and ten-vertex clusters, respectively) when compared to benzene bicyclo[2.2.2]octane, and therefore have atypical distribution of their conformational minima.²³ The clusters are highly chemically,²⁴ electrochemically,²⁵ and thermally stable and are available from commercial sources or through synthesis. The chemistry of boron clusters is well understood and developed in most cases, and classical organic synthesis is typically applicable. The preparation and functionalization of many of the boron clusters (see Figure 1) has already been reviewed in the context of preparing liquid crystalline materials.²⁶

Depending on the choice of boron cluster, different types of liquid crystalline molecules can be envisioned. For example, the borates, [*closo*- $B_{12}H_{12}$]⁻² (**1[12]**) or [*closo*- $B_{10}H_{10}$]⁻² (**1[10]**), if properly substituted with onium fragments (Q^+) such as quinuclidinium, sulfonium, or pyridinium, may lead to quadrupolar liquid crystalline derivatives (**I**). Substitution of a monocarbaborate, [*closo*-1- $CB_{11}H_{12}$]⁻¹ (**2[12]**) or [*closo*-1- CB_9H_{10}]⁻¹ (**2[10]**), with a single onium fragment (Q^+) at either antipodal position (positions 1 and 12 or 1 and 10, respectively) may lead to zwitterionic and highly polar liquid crystals (**II**) in which the dipole moment is aligned parallel to the longitudinal axis

of the molecule. These types of materials may be useful in electro-optical devices such as LCDs in order to lower the V_{th} for Fréedericksz transition. On the other hand, if the onium fragment (Q^+) is only associated with the monocarbaborate, [*closo*-1-CB₁₁H₁₂]⁻¹ (**2[12]**) or [*closo*-1-CB₉H₁₀]⁻¹ (**2[10]**), as an ion-pair this may lead to ionic liquid crystals (**III**) that could be useful electrolytes for anisotropic ion transport or undergo photophysical phenomenon such as charge-transfer. Lastly, using the neutral carboranes, [*closo*-C₂B₁₀H₁₂] (**3[12]**) or [*closo*-C₂B₈H₁₀] (**3[10]**), leads to liquid crystals of low but varying polarity (**IV**) depending on which carborane regioisomer (*ortho*, *meta*, and *para*) is incorporate into the liquid crystalline molecule (Figure 5).

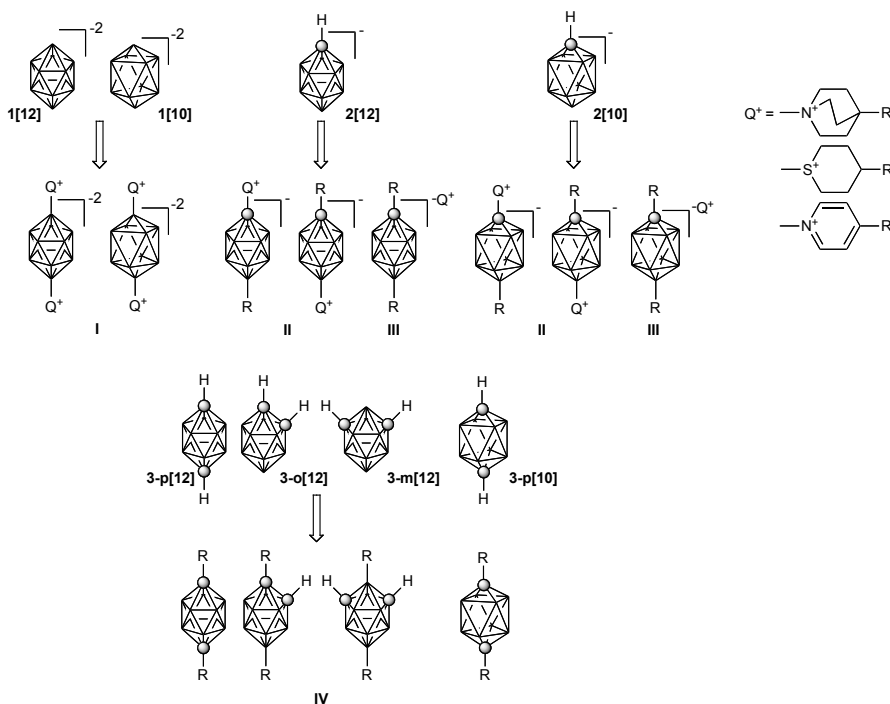


Figure 5. Boron clusters and their potential use in quadrupolar (**I**), highly polar (**II**), ionic (**III**), and low polarity (**IV**) liquid crystals. Q^+ represents an onium fragment such as quinuclidinium, sulfonium, or pyridinium. R can represent any organic fragment.

Many liquid crystalline materials containing boron clusters have been prepared to date. These studies have helped to further the fundamental chemistry of boron clusters and established that boron clusters are indeed effective building blocks for liquid crystals.²⁷⁻³⁰ Most of these materials have focused on the twelve and ten-vertex neutral *p*-carboranes due to the availability of the clusters and ease of their functionalization. The data suggests that boron clusters promote the nematic phase and destabilize the smectic phase. Within the family of boron clusters, twelve-vertex liquid crystalline derivatives generally have higher melting and clearing temperatures than their ten-vertex analogs. Fewer examples of the quadrupolar derivatives are known, and the polar and ionic derivatives have been completely unknown.

References

- (1) Stock, A. *Hydrides of Boron and Silicon*; Cornell Univ. Press: Ithaca, NY, 1933 and references therein.
- (2) *Contemporary Boron Chemistry*; Davidson, M.; Hughes, A. K.; Marder, T. B.; Wade, K., Eds.; Royal Society of Chemistry: Cambridge, United Kingdom, 2000.
- (3) *The Borane, Carborane, and Carbocation Continuum*; Casanova, J., Ed.; Wiley-Interscience: New York, 1998.
- (4) Lipscomb, W. N. *Boron Hydrides*; Benjamin: New York, 1963.

- (5) Longuet-Higgins, H. C. *J. Chim. Phys.* **1949**, *46*, 268-275.
- (6) Taylor, H. J.; Goldhaber, M. *Nature* **1935**, *135*, 341.
- (7) Locher, G. L. *Am. J. Roentgenol. Radium Ther.* **1936**, *36*, 1-13.
- (8) Rais, J.; Selucky, P.; Krys, M. *J. Inorg. Nucl. Chem.* **1976**, *38*, 1376-1378.
- (9) Reed, C. A. *Acc. Chem. Res.* **1998**, *31*, 133-139.
- (10) Kaszynski, P. *Collect. Czech. Chem. Commun.* **1999**, *64*, 895-926.
- (11) Kaszynski, P.; Douglass, A. G. *J. Organomet. Chem.* **1999**, *581*, 28-38.
- (12) Hamley, I. W. *Introduction to Soft Matter: Polymers, Colloids, Amphiphiles and Liquid Crystals*; John Wiley & Sons, Inc.: West Sussex, England, 2000.
- (13) Demus, D. In *Handbook of Liquid Crystals*; Goodby, J. W., Gray, G. W., Spiess, H.-W., Vill, V., Eds.; Wiley-VCH: New York, 1998; Vol. 1, p 133-187.
- (14) Blinov, L. M.; Chigrinov, V. G. *Electrooptic Effects in Liquid Crystal Materials*; Springer-Verlag: New York, 1994.
- (15) Sage, I. C. In *Handbook of Liquid Crystals*; Demus, D., Goodby, J. W., Gray, G. W., Spiess, H.-W., Vill, V., Eds.; Wiley-VCH: New York, 1998; Vol. 1, p 731-762.
- (16) Fréedericksz, V.; Zolina, V. *Trans. Faraday. Soc.* **1933**, *29*, 919-930.

- (17) Blinov, L. M. In *Handbook of Liquid Crystals*; Demus, D., Goodby, J. W., Gray, G. W., Spiess, H.-W., Vill, V., Eds.; Wiley-VCH: New York, 1998; Vol. 1, p 477-534.
- (18) Kirsch, P.; Bremer, M. *Angew. Chem., Int. Ed.* **2000**, *39*, 4216-4235.
- (19) Kaczmarczyk, A.; Kolski, G. B. *Inorg. Chem.* **1965**, *4*, 665-671.
- (20) Kaczmarczyk, A.; Kolski, G. B. *J. Phys. Chem.* **1964**, *68*, 1227-1229.
- (21) Douglass, A. G.; Czuprynski, K.; Mierzwa, M.; Kaszynski, P. *J. Mater. Chem.* **1998**, *8*, 2391-2398.
- (22) Kaszynski, P.; Lipiak, D. In *Materials for Optical Limiting*; Crane, R., Lewis, K., Stryland, E. V., Khoshvevisan, M., Eds.; MRS: Boston, 1995; Vol. 374, p 341-347.
- (23) Kaszynski, P.; Douglass, A. G. *J. Organomet. Chem.* **1999**, *581*, 28-38.
- (24) Todd, L. J. In *Progress in Boron Chemistry*; Brotherton, R. J., Steinberg, H., Eds.; Pergamon Press: New York, 1970; Vol. 2, p 1-35.
- (25) Muetterties, E. L.; Balthis, J. H.; Chia, Y. T.; Knoth, W. H.; Miller, H. C. *Inorg. Chem.* **1964**, *3*, 444-451.
- (26) (a) Kaszynski, P. *Collect. Czech. Chem. Commun.* **1999**, *64*, 895-926; (b) Kaszynski, P. "closo-Boranes as Structural Elements for Liquid Crystals" in *Boron Science: New Technologies & Applications*, Hosmane, N, Ed.; CRC Press, 2011.
- (27) Kaszynski, P.; Pakhomov, S.; Young, V. G. Jr. *Collect. Czech. Chem. Commun.* **2002**, *67*, 1061-1083; Pakhomov, S.; Kaszynski, P.; Young, V. G. Jr. *Inorg. Chem.* **2000**,

39, 2243-2245; Balinski, A.; Januszko, A.; Harvey, E. J.; Brady, E.; Kaszynski, P.; Young, V. G. Jr. unpublished results; Kaszynski, P. In *Anisotropic Organic Materials*; Glaser, R. and Kaszynski, P. Eds.; ACS Symposia: Washington D.C., 2001; Vol. 798, p 68-82.

(28) Januszko, A.; Kaszynski, P.; Wand, M. D.; More, K. M.; Pakhomov, S.; O'Neill, M. J. *Mater. Chem.* **2004**, *14*, 1544-1553; Jasinski, M.; Jankowiak, A.; Januszko, A.; Bremer, M.; Pauluth, D.; Kaszynski, P. *Liq. Cryst.* **2008**, *35*, 343-350.

(29) Ohta, K.; Januszko, A.; Kaszynski, P.; Nagamine, T.; Sasnouski, G.; Endo, Y. *Liq. Cryst.* **2004**, *31*, 671-682; Januszko, A.; Kaszynski, P. *Liq. Cryst.* **2008**, *35*, 705-710.

(30) Ringstrand, B.; Vroman, J.; Jensen, D.; Januszko, A.; Kaszynski, P.; Dziaduszek, J.; Drzewinski, W. *Liq. Cryst.* **2005**, *32*, 1061-1070; Januszko, A.; Glab, K. L.; Kaszynski, P. *Liq. Cryst.* **2008**, *35*, 549-553; Nagamine, T.; Januszko, A.; Ohta, K.; Kaszynski, P.; Endo, Y. *Liq. Cryst.* **2008**, *35*, 865-884.

The Chemistry and Properties of the [*closo*-1-CB₉H₁₀]⁻ Anion.

Abstract

The [*closo*-1-CB₉H₁₀]⁻ anion is one member of an extensive family of *closo*-boranes that possess impressive stability and functionalization characteristics. These *closo*-boranes are considered some of the least coordinating anions known since the negative charge is highly delocalized. Despite these properties, the [*closo*-1-CB₉H₁₀]⁻ anion has received little attention relative to the [*closo*-1-CB₁₁H₁₂]⁻ anion. This was in part due to the lack of availability of the [*closo*-1-CB₉H₁₀]⁻ anion and understanding of its fundamental chemistry. This review details progress made in the fundamental chemistry of the [*closo*-1-CB₉H₁₀]⁻ anion and comments briefly on how these advancements have been applied towards modern technologies.

Introduction

The discovery of polyhedral boron clusters was one of the most exciting and important developments in inorganic chemistry of the last century. These boron clusters are characterized by electron-deficient bonding and formation of unusual three-center two-electron bonds, which were described by William Lipscomb. Lipscomb's discovery,

for which he eventually was awarded the Nobel Prize in 1976, revolutionized the way chemists understood chemical bonding.¹ As a result of this unique bonding characteristic, these boron clusters were shown to be exceptionally stable chemically, electrochemically, and thermally.² These properties opened up possibilities for the practical use of boron clusters in a variety of fields such as treatment of nuclear waste, catalysis, material science, and the treatment of cancer.³

Of the structures known experimentally, the carboranes and the *closo*-borates have dominated the literature due to their availability and relative ease of functionalization.⁴⁻⁷ On the other hand, the *closo*-monocarbaborates have garnered less attention. Two such structures include the [*closo*-1-CB₉H₁₀]⁻ and [*closo*-1-CB₁₁H₁₂]⁻ anions, **1** and **2**, respectively (Figure 1).

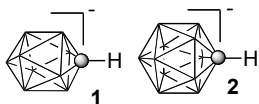


Figure 1. The [*closo*-1-CB₉H₁₀]⁻ anion **1** and [*closo*-1-CB₁₁H₁₂]⁻ anion **2**. The dark sphere represents a carbon atom and all other vertices, BH bonds.

The negative charge in anions **1** and **2** is completely delocalized making them weakly coordinating anions for strong electrophiles, oxidants, and superacids.⁸ Critical for exploiting the unique properties of **1** and **2** is the chemistry that is well established both for the carboranes and boranes. Substitution at the C-H vertex is accomplished via deprotonation with strong bases such as alkyllithiums affording a carboranyl anion capable of reacting with a wide range of electrophiles.⁹ Conversely, the B-H

vertices permit functionalization by reactive electrophiles, leading to, for example, B-iodo derivatives. Such B-iodo derivatives have been shown to be useful substrates in Pd-catalyzed coupling reactions such as Kumada,¹⁰ Suzuki,¹¹ Negishi,¹² Sonogashira,¹³ Heck,¹⁴ and Buchwald-Hartwig¹⁵ to facilitate syntheses of a diverse range of B-derivatives.¹⁶

Of the *closo*-monocarbaborates **1** and **2**, the [*closo*-1-CB₁₁H₁₂]⁻ anion (**2**) has been the most studied, and as a result, its chemistry most developed.¹⁷ On the other hand, the [*closo*-1-CB₉H₁₀]⁻ anion (**1**) was until recently unexplored mostly due to its poor accessibility. Anion **1** was originally discovered in 1971 by Knoth as a product of thermal comproportionation of the [*nido*-7-CB₁₀H₁₃]⁻ anion, which also gives, as a by-product, anion **2**.¹⁸ Other methods expanded on Knoth's original work, but none of them permitted for the preparation of 1,10-difunctionalized species of the [*closo*-1-CB₉H₁₀]⁻ anion (**1**).^{18,19} Reports of C-substituted derivatives were rare with only a couple works occurring before the year 2000.^{20,21} Results also showed that electrophilic halogenation of anion **1** occurred selectively at the 6-position with less than 2% of 10-isomer being observed.²²

This situation changed with development of the Brellocks reaction, which permitted for the synthesis of a variety of C(1) substituted {*closo*-1-CB₉} derivatives and opened up new possibilities for studying the {*closo*-1-CB₉} framework.²³ According to Brellocks, the reaction of decaborane, B₁₀H₁₄, with aldehydes in alkaline solution results in the formation of either [*arachno*-6-CB₉H₁₃-6-R]⁻ (**I**) or [*nido*-6-CB₉H₁₁-6-R]⁻ (**II**)

derivatives.²⁴ These species undergo oxidation resulting in closure of the {CB₉} framework to [*closo*-2-CB₉H₉-2-R]⁻ (**III**) derivatives, and subsequent thermal rearrangement of **III** to the more thermodynamically stable [*closo*-1-CB₉H₉-1-R]⁻ (**IV**) isomer.²⁴ The aldehydes that have been studied in this reaction range from aryl to formaldehyde and glyoxylic acid (Figure 2).²⁴⁻²⁶

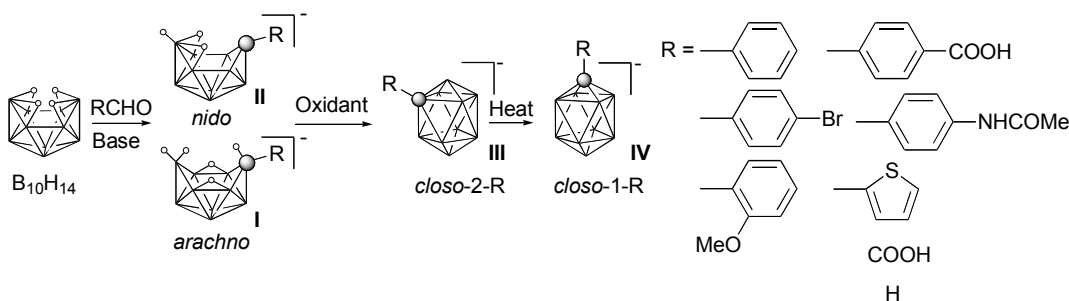


Figure 2. The Brellochs Reaction

Despite the explosion of the number of [*closo*-1-CB₉H₁₀]⁻ derivatives being reported due to the Brellochs reaction, 1,10-difunctionalized derivatives of the [*closo*-1-CB₉H₁₀]⁻ were still practically unknown. This was mostly due to electrophilic processes of the [*closo*-1-CB₉H₁₀]⁻ anion (**1**) occurring exclusively at the 6-position.²² This posed a serious challenge for efficient and direct substitution at the 10-position. However, it was demonstrated that the halogenation of [*closo*-2-CB₉H₈-2-(4-Br-C₆H₅)]⁻ occurred regioselectively at the 7-position. Thermal rearrangement of this compound gave a mixture of 1,10 and 1,6 substituted {*closo*-1-CB₉} derivatives in greater than or equal to 1:1 ratio. Attempts to separate the two isomers were not made.²⁴ Such isomerically pure 1,10-disubstituted derivatives are sought after in the synthesis of linear molecular

systems^{27,28} and our liquid crystals program in particular.²⁹

Since [*closo*-1-CB₉H₁₀]⁻ anion (**1**) possesses a highly delocalized negative charge, it offers solutions to obtaining both zwitterionic (**V** and **VI**) liquid crystals for electro-optical applications and anion-driven ionic liquid crystals capable of supporting ion transport (**VII**) (Figure 3).

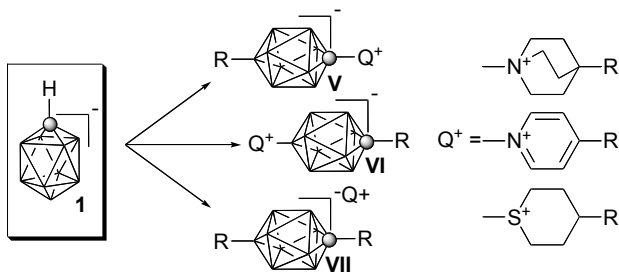


Figure 3. General structures of zwitterions (**V** and **VI**) and anion-driven ionic liquid crystals (**VII**). Q⁺ represents an onium fragment such as ammonium, sulfonium, or pyridinium or a metal cation only in the case of structures **VII**. R represents an organic fragment typically an alkyl chain.

Despite the potential of the [*closo*-1-CB₉H₁₀]⁻ anion (**1**) as a unique structural element of advanced liquid crystals, understanding of its fundamental chemistry was lacking and prevented such materials from being prepared. For one, structures **V**, **VI**, and **VII** require the proper isomerically pure 1,10-disubstitution pattern, which although reported, had only been observed as a mixture with a second isomer. Second, introduction of onium fragments at either the C(1) or B(10) vertices would best be accomplished using electrically neutral, zwitterionic dinitrogen derivatives (N₂⁺). Such apical derivatives of decaborate [*closo*-B₁₀H₁₀]⁻² were long known to be isolable and stable intermediates that

are useful in the preparation of a variety of nitrogen,³⁰⁻³³ sulfur,^{30,33} oxygen,³³ and even carbon³³ derivatives. The inherent stability of apical 10-vertex dinitrogen derivatives and hence synthetic usefulness originates from the electronic interaction between the cluster and the N₂ group.³⁴ Nonetheless, only scant evidence existed that suggested apical dinitrogen derivatives of the [*closo*-1-CB₉H₁₀]⁻ anion (**1**) were accessible and synthetically viable intermediates.²⁰

This review will highlight the progress made in these areas of the fundamental chemistry anion **1**, the fundamental properties of new derivatives of anion **1** and its reactive intermediates, as well as briefly comment on the exciting potential of the [*closo*-1-CB₉H₁₀]⁻ anion (**1**) as structural element of advanced liquid crystalline materials.

The First Isomerically Pure 1,10-Disubstituted [*closo*-1-CB₉] Cluster

Due to our interest in electrically neutral polar liquid crystals (**V** and **VI**) for electro-optical applications and anion-driven ionic liquid crystals (**VII**) capable of supporting ion transport (see Figure 3), we envisioned iodo acid [*closo*-1-CB₉H₈-1-COOH-10-I]⁻ (**3**) as a general precursor to these materials. The iodine at position B(10) provides means to introduce alkyl or amino functionality in Pd-catalyzed coupling reactions. The carboxylic acid group at the C(1) position offers a convenient synthetic handle that can be introduced using the Brellocks reaction with aldehyde, glyoxylic acid monohydrate. The carboxylic acid group can be converted to esters or transformed to an

amino group using classical organic synthetic methods. The amino group at position C(1) or B(10) can be transformed into a quinuclidine ring or diazotized producing dinitrogen derivatives.

The iodo acid **3** was prepared starting from the known [*closo*-2-CB₉H₉-2-COOH]⁻ (**4**) obtained according to the Brellocks method.³⁵ Iodination of **4** with N-iodosuccinimide gave the 2,7-iodo derivative **5**, which was thermolyzed in boiling MeCN giving iodo acids **3** and **6** as mixtures in ratios varying from 3:2 to 3:1. Pure iodo acid **3** was obtained by recrystallization from aqueous EtOH giving isomerically pure acid **3** in about 10% overall yield based on decaborane, B₁₀H₁₄ (Figure 4).³⁶

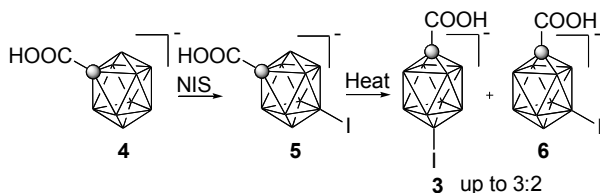


Figure 4. Preparation of Isomerically Pure Iodo Acid **3**

Transformations of [*closo*-1-CB₉H₈-1-COOH-10-I]⁻

With iodo acid **3** now available, we focused on synthetic transformations of the carboxylic acid and iodine at positions C(1) and B(10), respectively, to amino groups in the context of our liquid crystals program and structures **V**, **VI**, and **VII** (see Figure 3). For the transformation at the C(1) vertex, the carboxyl group was transformed into an amino group using a modified Curtius rearrangement, via acid chloride **10**, acyl azide **11**,

isocyanate **12**, and carbamate **9** providing amine [*closo*-1-CB₉H₈-1-NH₃-10-R] (**8**, R = H or I). The key step was formation of carbamate **9** as the isolable intermediate, which could be purified and serve as a convenient storage for amine **8** (Figure 5). Deprotection of carbamate **9** with HCl in CH₃OH solution followed by evaporation of the volatiles gave pure amine **8** in nearly quantitative yield.^{37,38}

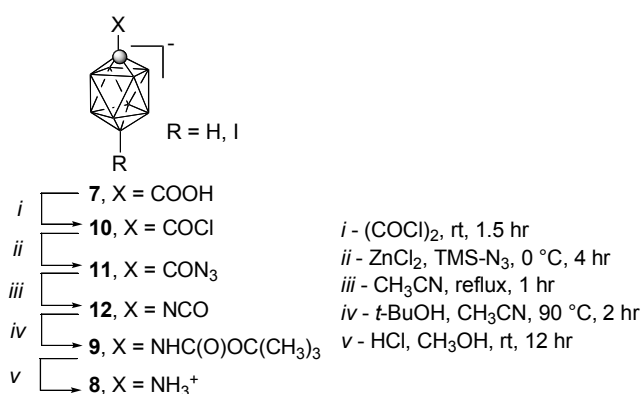


Figure 5. Preparation of Amine **8** using a Modified Curtius Rearrangement

For transformations at the B(10) position, we investigated a reaction of iodo acid **3** with LiHMDS as the best aminating reagent under Pd(0) catalysis. It was determined that using 15 equivalents of LiHMDS and 2-(dicyclohexylphosphine)biphenyl as the phosphine ligand, the ratio of amino acid **13** to parent acid **7** (R = H), obtained as a product of deiodination, could be as high as 5:1 (Figure 6). The parent acid **7** (R = H) was easily separated by selective precipitation from H₂O as a NEt₄⁺ salt. The amino acid **13** is routinely obtained in 40-50 % yield.³⁹

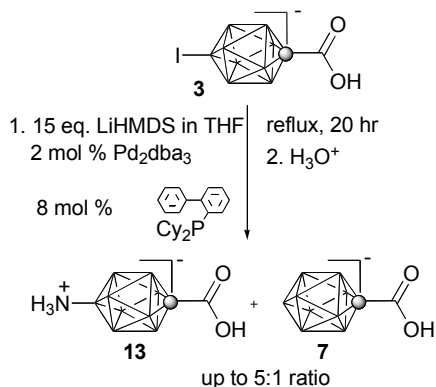


Figure 6. Preparation of Amino Acid **13** using the Buchwald-Hartwig Amination

We also investigated the amination of the 6-isomer iodo acid **6** as part of a mixture with iodo acid **3**. For example, a 4:1 mixture of iodo acid **6** to iodo acid **3** gave amino acids **14** and **13** up to a 12:1 ratio, respectively, and 35-45 % overall yield (Figure 7).⁴⁰

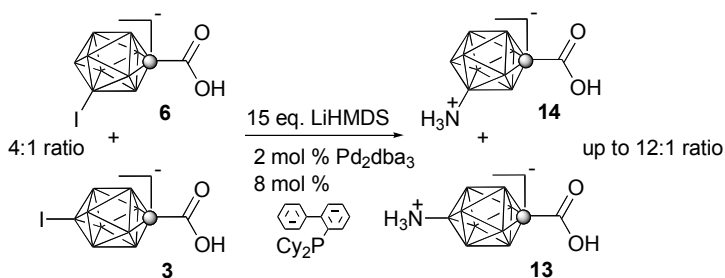


Figure 7. Preparation of Amino Acid **14** as a Mixture with Amino Acid **13** using the Buchwald-Hartwig Amination

The iodide in **3** was transformed to an alkyl group using the Negishi coupling. Thus, reaction of iodo acid **3** with 12-fold excess of hexylzinc chloride gave hexyl derivative **15** (Figure 8). The electron-rich tricyclohexylphosphine ligand, PCy₃, was

conveniently generated *in situ* from air-stable $[\text{HPCy}_3]^+[\text{BF}_4]^-$. The choice of the ligand was dictated by its reported efficiency in catalysis of coupling reactions of alkylzinc reagents with a broad range of unactivated iodides, bromides, and chlorides and excellent functional group tolerance.³⁸

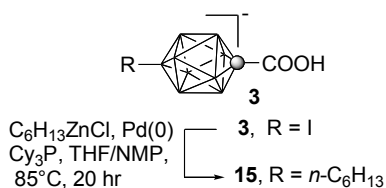


Figure 8. Negishi Coupling of Iodo Acid **3**

N_2^+ Derivatives of the {*closo*-1- CB_9 } Cluster

With access to amino groups at both the C(1) and B(10) positions, the next step in the progression of the fundamental chemistry of the $[\textit{closo}\text{-}1\text{-CB}_9\text{H}_{10}]^-$ (**1**) was the preparation of apical dinitrogen derivatives and their reaction with nucleophiles in order to introduce onium fragments such as pyridinium and sulfonium at positions C(1) and B(10). It was determined that the diazotization of $[\textit{closo}\text{-}1\text{-CB}_9\text{H}_8\text{-}1\text{-NH}_3\text{-}10\text{-R}]$ (**8**, $\text{R} = \text{H}$ or I) was best performed in a 50% aqueous AcOH with 1.1 eq of NaNO_2 giving $[\textit{closo}\text{-}1\text{-CB}_9\text{H}_8\text{-}1\text{-N}_2\text{-}10\text{-R}]$ (**16**, $\text{R} = \text{H}$ or I) as a white precipitate, which was isolated by filtration in yields greater than 80% (Figure 9).^{37,38}

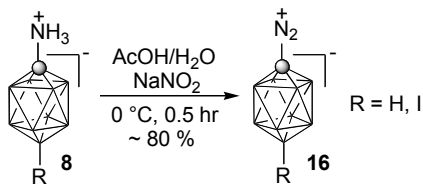


Figure 9. Preparation of Dinitrogen Derivative [*closo*-1-CB₉H₈-1-N₂-10-R] (**16**)

Diazotization of amino acid **13** was surprisingly difficult. Attempts to diazotize **13** in aqueous AcOH, conditions used for the parent amine [*closo*-1-CB₉H₈-1-NH₃-10-R] (**8**, R = H or I) were unsuccessful and only **13** was recovered. Amino-*closo*-borates were long known to be unusually basic. For instance, [*closo*-B₁₀H₉-1-NH₂]²⁻ and [*closo*-B₁₂H₁₁NH₂]²⁻ are highly basic and “the *N*-protonated forms of these amino compounds could be isolated directly from alkaline solutions.”⁴¹ This prompted us to explore the diazotization under basic conditions. In fact, complete diazotization of amino acid **13** was achieved with excess [NO]⁺[PF₆]⁻ in MeCN containing 5 equivalents of pyridine as the appropriate reaction medium. The yield of isolated dinitrogen acid [*closo*-1-CB₉H₈-1-COOH-10-N₂] (**17**) as a stable solid was 60 % after chromatographic separation (Figure 10).³⁹

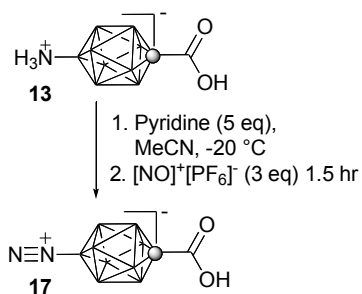


Figure 10. Preparation of Dinitrogen Acid [*closo*-1- CB_9H_8 -1-COOH-10- N_2] (**17**)

The reaction of $[\text{NO}]^+[\text{PF}_6]^-$ with **13** in the presence of pyridine is a complex process in which the base serves a dual role: it deprotonates the NH_3 group and presumably reacts with $[\text{NO}]^+[\text{PF}_6]^-$ to form an alternative diazotizing reagent, the *N*-nitrosopyridinium ion (**18**). It can be postulated that the formation of **17** involves initial deprotonation of the COOH group in **13** and subsequent proton-transfer equilibrium between the NH_3^+ group and pyridine. It can also be postulated that the equilibrium is significantly shifted to the left and the required dianion **13**²⁻ is present in low concentration (Figure 11).³⁹

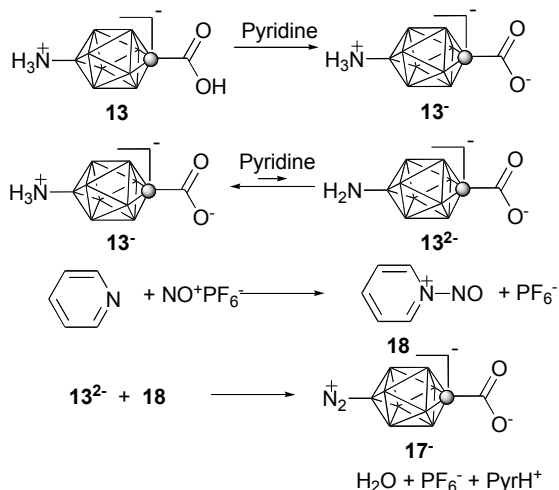


Figure 11. Proposed Mechanism for Diazotization of Amino Acid **13**

Dinitrogen derivative [*closo*-1-CB₉H₈-1-N₂-10-R] (**16**, R = H) was reacted with three types of nucleophiles: sulfur compounds, pyridine, and activated arenes. The reagents were chosen to demonstrate the formation of inner sulfonium through a masked mercaptan, to investigate the formation of 1-pyridinium derivatives at the C(1) position, and a classical organic transformation such as azo coupling.³⁷

Reaction of **16** with *N,N*-dimethylthioformamide at ambient temperature gave crude protected mercaptan **19** in 80% yield. Attempts to purify the zwitterion **19** further were unsuccessful due to its partial decomposition observed during recrystallization. Purification on silica gel was avoided, since **19** appeared to be hydrolytically unstable. Alkylation of crude **19** with 1,5-dibromopentane in the presence of a base followed by chromatographic separation and recrystallization gave pure sulfonium adduct **20** in 50% yield based on **16** (Figure 12).³⁷

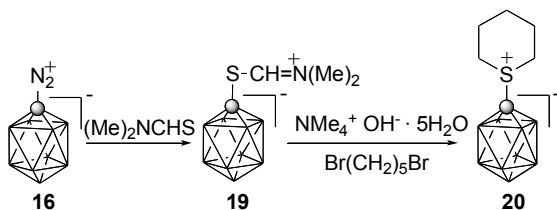


Figure 12. Preparation of Sulfonium Adduct **20**

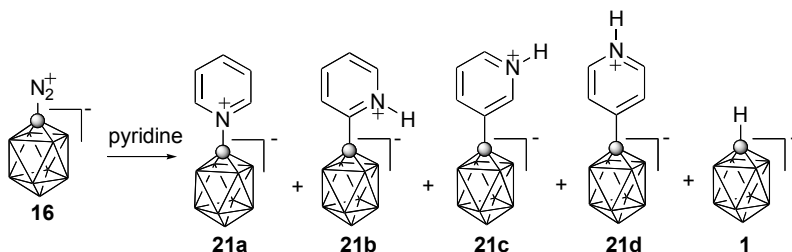
Reaction of **16** with pyridine was most interesting. When **16** was reacted in neat pyridine at ambient temperature for several hours, ^{11}B NMR analysis revealed a mixture of at least 4 products in the region of 25 ppm – 40 ppm (Table 1). Surprisingly, the major component of the reaction mixture, about 50%, was identified as the 2-isomer **21b**. The crude mixture was separated on silica gel giving the 2-isomer **21b** in 40% isolated yield as the first fraction. The most polar fraction contained a mixture of two other isomers, which were identified as **21c** and **21d**.³⁷

Addition of hot pyridine to the dinitrogen derivative **16** had a different outcome. ^{11}B NMR analysis of the crude reaction mixture revealed four products. Chromatographic separation gave **21a** in 17% isolated yield as the least polar fraction. The more polar fraction contained the remaining three isomers (**21b**, **21c**, **21d**) and also the parent anion **1** (Table 1).³⁷

To provide more information about the possible mechanism for the formation of these products, reactions of **16** were run in dilute solutions of pyridine at ambient temperature. Thus, a reaction of **16** with a 4% solution of pyridine in CH_2Cl_2 gave [*closo*-1- CB_9H_9 -1-Cl] as the major product along with **21a**, **21b**, and **1** (Table 1). A

similar reaction of **16** with a 4% solution of pyridine in benzene gave the [*closo*-1-CB₉H₉-1-Ph]⁻ as the major product. Isomers **21a** and **21b** were formed as minor products, and no signals belonging to **21c** or **21d** were detected (Table 1).³⁷

Table 1. Product Distributions in Reaction of **1** with Pyridine.



Conditions	Products				
	21a	21b	21c	21d	1
Neat pyridine					
25 °C ^a	Traces	40% ^b	17% ^c	10% ^c	6% ^c
90 °C ^c	17% ^b	20% ^c	18% ^c	9% ^c	5% ^c
Solutions of pyridine					
4% in CH ₂ Cl ₂ ^d	17% ^e	7% ^e	0% ^e	0% ^e	20% ^e
4% in Benzene ^f	13% ^e	17% ^e	0% ^e	0% ^e	5% ^e
¹¹ B NMR for B(10), δ ^g	33.1 ppm	37.2 ppm	33.9 ppm	35.9 ppm	29.6 ppm

^a About 75 % of total mass recovery after separation on SiO₂.

^b Yield of isolated product.

^c Yield based on ¹¹B NMR of the mixture corrected for its mass.

^d [*closo*-1-CB₉H₉-1-Cl]⁻ constituted 56% of the mixture.

^e Ratio of low field signals for the crude reaction mixture.

^f [*closo*-1-CB₉H₉-1-Ph]⁻ constituted 65% of the crude reaction mixture.

^g Chemical shifts of the isolated products or mixtures.

Reaction of **16** with pyridine was anticipated to give adduct **21a** as the only product. Support for this expectation is provided by the reported smooth transformations of similar dinitrogen derivatives of the [*closo*-B₁₀H₁₀]⁻² cluster with pyridine.^{32,33} Instead, the observed distribution of products in reaction of **16** with pyridine suggests a radical pathway, which is consistent with the known Gomberg-Bachmann free radical arylation reaction. A similar radical ion mechanism was postulated for the reaction of **16** with Me₂S and Me₂NCHS.⁴²

Lastly, reactions of **16** with tetraethylammonium phenolate and aniline showed that **16** was susceptible to diazocoupling providing azo phenol **22** and aniline **23** in yields of 50% and 80%, respectively, after chromatographic separation.³⁷

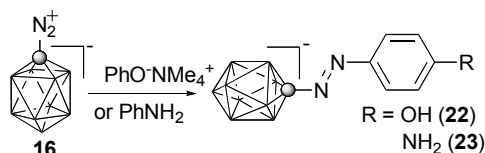


Figure 13. Diazocoupling of **16** with Phenolate and Aniline

Similar studies were conducted for dinitrogen acid **17**, which was reacted with two types of nucleophiles: sulfur compounds and pyridine. The reagents were again chosen to demonstrate the formation of inner sulfonium through a masked mercaptan and to investigate the formation of 1-pyridinium derivatives at the B(10) position.³⁹

Reactions of dinitrogen acid **17** in neat pyridine and *N,N*-dimethylthioformamide gave pyridinium acid **24** and masked mercaptan **25**, respectively, as the sole products. Masked mercaptan **25** was isolated as a crude product and used without further purification, whereas pyridinium acid **24** was isolated in 90% yield after chromatographic separation. In contrast to [*closo*-1-CB₉H₉-1-N₂] (**16**), reactions of dinitrogen acid **17** required heating to about 100 °C. The dinitrogen acid **17** also smoothly reacted with diazomethane to give methyl ester **26** in 78% yield demonstrating the robustness of B(10) dinitrogen derivatives (Figure 14).³⁹

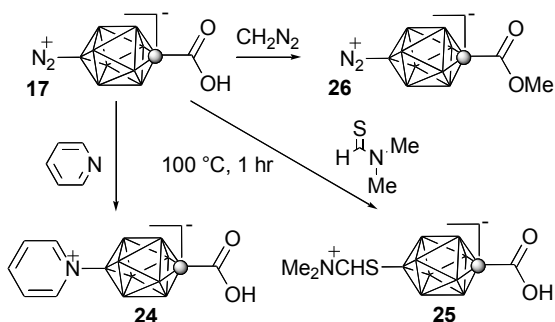


Figure 14. Transformations of Dinitrogen Acid **17**

The reaction of **17** with pyridine is in stark contrast to the similar reaction with dinitrogen derivative **16**. For one, the reaction requires heat. Second, in the case of **16**, a radical pathway identical to the Gomberg-Bachmann arylation of pyridine is operating. For dinitrogen acid **17**, only a heterolytic pathway is operating, and **24** is the sole product observed. This is consistent with precedence established with reactions of dinitrogen derivatives of the [*closo*-B₁₀H₁₀]⁻² cluster with pyridine.^{32,33} The difference in reaction mechanisms for treatment of **16** or **17** with pyridine is also confirmed by the reduction

potentials, where the potential of **17** is significantly more cathodic than **16** and therefore inhibits the radical pathway.³⁹

The synthetic utility of the protected mercaptan **25** was demonstrated by formation of sulfonium derivative **27** under hydrolytic conditions in the presence of a base and 3-substituted-1,5-dibromopentane (Figure 15).^{39,43}

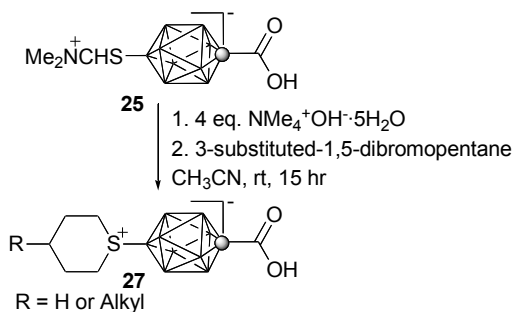


Figure 15. Preparation of Sulfonium Acid **27**

We previously demonstrated that for successful diazotization of **13** and formation of dinitrogen acid **17** the reaction mixture must contain pyridine. We applied the same protocol for the diazotization of a mixture of amino acids **13** and **14** (see Figure 7). Under these conditions (MeCN containing pyridine), dinitrogen derivative **17**, 6-pyridinium derivative **28a**, and another {1-CB₉} product derived presumably from MeCN were observed. To eliminate side reactions with MeCN, diazotization reactions were conducted in neat pyridine. Thus, a reaction of 6-amino acid **14** containing 10 % of amino acid **13** with $[\text{NO}]^+[\text{BF}_4]^-$ in pyridine at $-20\text{ }^\circ\text{C}$ gave 6-pyridinium acid **28a** as the sole product in 58% yield with only traces of dinitrogen acid **17**. The presumed reactive intermediate for

the generation of **28a** is dinitrogen derivative **29**⁻, which decomposes during the reaction and then is trapped by a solvent molecule (Figure 17). It should be emphasized that dinitrogen acid **17** remains intact and does not react with solvent molecules under these conditions. This demonstrates a dramatic difference in stability of apical versus equatorial N₂ derivatives of the [*closo*-1-CB₉H₁₀]⁻ anion (**1**).⁴⁰

The reaction was extended to other heterocyclic bases such as 4-methoxypyridine, 2-picoline, and quinoline, which gave the corresponding products **28b-28d** (Table 2).

Table 2. Results for Diazotization of Mixtures of [*closo*-1-CB₉H₈-1-COOH-6-NH₃] (**14**) and [*closo*-1-CB₉H₈-1-COOH-10-NH₃] (**13**)^a

Entry	Solvent	Conversion ^b	Yield (%) ^c
			28
1	Pyridine	100 %	a , 58 ^d
2	4-Methoxypyridine	100 %	b , 73 ^d
3	2-Picoline	50 %	c , 24 ^e
4	Quinoline	30 %	d , 3 ^e

^a Reaction conditions: 3 eq. of [NO]⁺[BF₄]⁻ added to a solution of 0.5 mmol of **1** in ~ 3 mL of amine at -20 °C (entry 1-3) or 0 °C (entry 4); reaction time 3 hr. Ratio of **14/13** in entry 1 is 12:1 and in entry 3-4 is 5:1.

^b Percent of reacted amino acid **14** by ¹¹B NMR.

^c After chromatographic separation and calculated based on the content of amino acid **14** in the mixture

^d Dinitrogen acid **17** was observed in the crude reaction mixture

^e Dinitrogen acid **17** was not observed in the crude reaction mixture

Reactions with 2-picoline and quinoline gave incomplete conversion of amino acids **13** and **14**. The incompleteness of the reaction with quinoline could be due to its lower basicity than that of pyridine. Poor results for diazotization in 2-picoline are presumably due to the methyl group, which hinders the NO^+ , transfer or promotes side reactions. Attempts to introduction other nucleophiles at the 6-position using this diazotization method were unsuccessful and still pose a challenge due to the solubility of the amines and compatibility of the solvent with the nitrosonium cation.⁴⁰

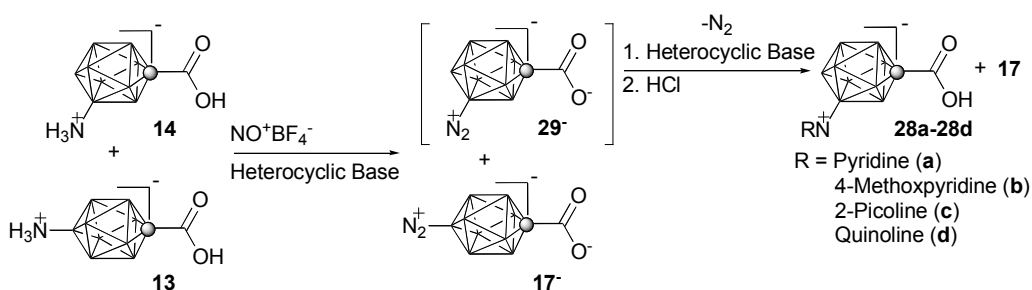


Figure 17. Competition Diazotization Reactions of Amino Acids **13** and **14** in Heterocyclic Bases

The difference in stability of the dinitrogen group in **29⁻** and **17⁻** originates in the efficiency of the MO overlap between the N_2 fragment and the $\{1\text{-CB}_9\}$ cage, and also electronegativity of the cage atoms. In the apical isomers such as **16** and **17** the double degenerate π -symmetry MO of the cage provides electronic communication with the N_2 π system, which is more effective than that between the non-degenerate π symmetry MO of the $\{1\text{-CB}_9\}$ cage and N_2 in the equatorial isomer.⁴⁰

Liquid Crystals Derived from the [*closo*-1-CB₉] Cluster

The developed chemistry and understanding of the reactivity and properties of the [*closo*-1-CB₉H₁₀]⁻ anion (**1**) and its functionalized derivatives permitted for the preparation of the first examples of polar (**V** and **VI**) and ionic liquid crystals (**VII**).

The polar materials **V** and **VI** were prepared following established protocols described in this review and were investigated as neat materials as well as additives to other liquid crystalline hosts. The compounds of type **V** such as **30** containing a quinuclidinium ring and **31** containing a sulfonium ring both at the C(1) position were not liquid crystalline materials and displayed high melting points (Figure 18). They exhibited limited solubility in other liquid crystalline materials, but examination of dilute solutions demonstrated that they possessed high virtual T_{NI} and large extrapolated dielectric anisotropy, Δε, above 60.⁴³

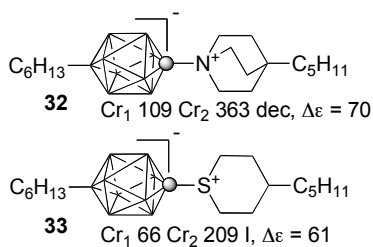


Figure 18. Polar Materials **30** and **31**

Analysis of polar materials **VI** such as **32** containing a pyridinium ring and **33** containing a sulfonium ring at the B(10) position were much more promising than

materials **V** (Figure 19). These materials displayed nematic properties, lower melting points, and greater compatibility with liquid crystalline hosts. Analysis of their dielectric properties in dilute solutions revealed extrapolated dielectric anisotropy, $\Delta\epsilon$, around 40, but this value is host dependent.^{44,45} Compound **33** containing the sulfonium ring at the B(10) position represents one example of a new class of shape-shifting nematic materials, where the molecule can exist in two different shapes (linear and bent) due to facile epimerization occurring at the sulfur center.⁴⁵

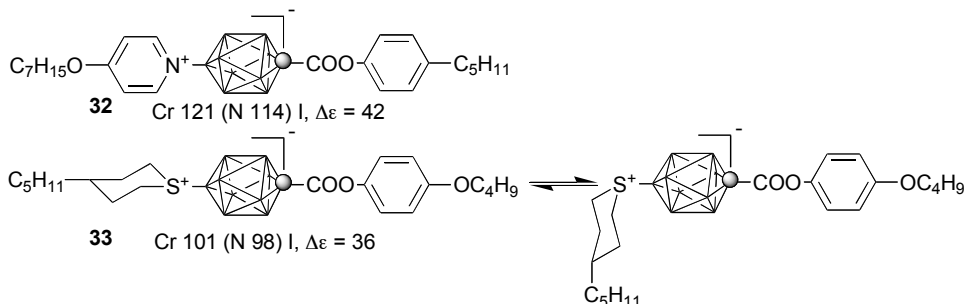


Figure 19. Polar Materials **32** and **33**

Polar materials such as **32** and **34** permitted for the first time the effect of a dipole moment on the stability of the nematic phase to be examined experimentally. This was accomplished by comparing polar and non-polar isosteric derivatives of the [*closo*-1-CB₉H₁₀][−] anion and *p*-carborane, [*closo*-1,10-C₂B₈H₁₀]. Replacement of a B-N bond with a C-C bond provided materials with drastically different dipole moments (calculated $\Delta\mu$ of 12 D) but with the identical geometrical and conformational properties (Figure 20).

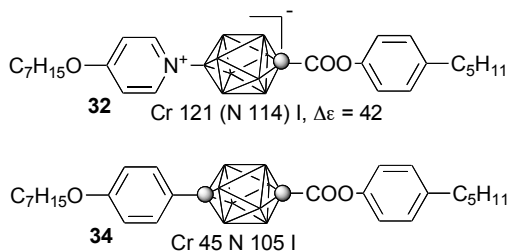
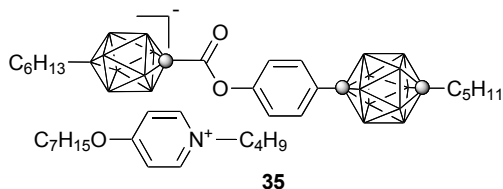


Figure 20. Polar and Non-Polar Isosteric Derivatives **32** and **34**

The results for pairs of compounds such as **32** and **34** demonstrated that a longitudinal dipole moment's effect on phase properties strongly depends on the nature of the substituent distant from the zwitterions, and it can either be substantiated or even moderately negative.⁴⁴

The phase structures of the first examples of anion-driven ionic liquid crystals (**VII**) such as **35** were investigated using powder XRD to help elucidate the organization of the ion-pairs in the liquid crystalline state. These materials possess the characteristic smectic A phase, commonly exhibited by ionic materials, and in some cases, phase X, which may be identified as a soft crystalline phase that adopts two mutually perpendicular layered molecular organization. In this particular molecular design, the elongated pyridinium cation was essentially to impart the liquid crystalline state (Figure 21).³⁸



Cr 120 X' 145 X 166 SmA 187 I

Figure 21. Ionic Liquid Crystal **35**

Summary and Conclusions

This review has provided a snapshot of the rapid development of the fundamental chemistry of [*closo*-1-CB₉H₁₀]⁻ (**1**). Three key advancements in the fundamental chemistry of **1** were commented on which include the preparation and isolation of the first isomerically pure 1,10-disubstituted derivative, iodo acid **3**, functional group transformations at the C(1) position, and functional group transformations at the B(10) position. The development of the fundamental chemistry of anion **1** permitted for the synthesis and characterization of polar (**I** and **II**) and ionic liquid crystals (**III**), and a brief synopsis of these exciting liquid crystalline molecules were presented.

References:

- (1) Lipscomb, W. N. *Boron Hydrides*; W.A. Benjamin: New York, 1963.
- (2) Todd, L. J. In *Progress in Boron Chemistry*; Brotherton, R. J., Steinberg, H., Eds.; Pergamon Press: New York, 1970; Vol. 2, p 1-35.

- (3) Plešek, J. *Chem. Rev.* **1992**, *92*, 269-278.
- (4) Stibr, B. *Chem. Rev.* **1992**, *92*, 225-250.
- (5) Onak, T. In *Boron Hydride Chemistry*; Muetterties, E. L., Ed.; Academic Press: New York, 1973, p 349-382.
- (6) Onak, T. In *Comprehensive Organometallic Chemistry*; Wilkinson, G., Abel, E. W., Stone, F. G. A., Eds.; Pergamon Press: New York, 1982; Vol. 5, p 411-458.
- (7) Bregadze, V. I. *Chem. Rev.* **1992**, *92*, 209-233.
- (8) Reed, C. A. *Acc. Chem. Res.* **1998**, *31*, 133-139.
- (9) Grimes, R. N. *Carboranes*; Academic Press: New York, 1970.
- (10) Zakharkin, L. I.; Kovredov, A. I.; Ol'shevskaya, V. A.; Shaugumbekova, Z. S. *J. Organomet. Chem.* **1982**, *226*, 217.
- (11) Eriksson, L.; Beletskaya, I. P.; Bregadze, V. I.; Sivaev, I. B.; Sjöberg, S. *J. Organomet. Chem.* **2002**, *657*, 267.
- (12) Beletskaya, I. P.; Bregadze, V. I.; Ivushkin, V. A.; Zhigareva, G. G.; Petrovskii, P. V.; Sivaev, I. B. *Russ. J. Org. Chem.* **2005**, *41*, 1359.
- (13) Jiang, W.; Knobler, C. B.; Curtis, C. E.; Mortimer, M. D.; Hawthorne, M. F. *Inorg. Chem.* **1995**, *36*, 3491.

- (14) Eriksson, L.; Winberg, K.-J.; Claro, R. T.; Sjoberg, S. *J. Org. Chem.* **2003**, *68*, 3569.
- (15) Sevryugina, Y.; Julius, R. L.; Hawthorne, M. F. *Inorg. Chem.* **2010**, *49*, 10627-10634.
- (16) Tsuji, J. *Palladium Reagents and Catalysts: Innovation in Organic Synthesis*; John Wiley & Sons: New York, 1994.
- (17) Korbe, S.; Schreiber, P. J.; Michl, J. *Chem. Rev.* **2006**, *106*, 5208-5249.
- (18) Knoth, W. H. *Inorg. Chem.* **1971**, *10*, 598-605.
- (19) Nestor, K.; Stibr, B.; Kennedy, J. D.; Thornton-Pett, M.; Jelinek, T. *Collect. Czech. Chem. Commun.* **1992**, *57*, 1262.
- (20) Jelinek, T.; Stibr, B.; Plesek, J.; Thornton-Pett, M.; Kennedy, J. D. *J. Chem. Soc., Dalton Trans.* **1997**, 4231-4236.
- (21) Tsnag, C.-W.; Yang, Q.; Sze, T.-P. E.; Mak, T. C. W.; Chan, D. T. W.; Xie, Z. *Inorg. Chem.* **2000**, *39*, 3582-3589.
- (22) Ivanov, S. V.; Rockwell, J. J.; Miller, S. M.; Anderson, O. P.; Solntsev, K. A.; Strauss, S. H. *Inorg. Chem.* **1996**, *35*, 7882-7891.
- (23) Brellocks, B. In *Contemporary Boron Chemistry*; Davidson, M.G.; Hughes, A. K.; Marder, T. B.; Wade, K., Eds.; Royal Society of Chemistry: Cambridge, England, 2000; pp 212-214.

- (24) Franken, A.; Kilner, C. A.; Thornton-Pett, M.; Kennedy, J. D. *Collect. Czech. Chem. Commun.* **2002**, *67*, 869-912.
- (25) Sivaev, I. B.; Starikova, Z. A.; Petrovskii, P. V.; Bregadze, V. I.; Sjoberg, S. J. *Organomet. Chem.* **2005**, *690*, 2790-2795.
- (26) Franken, A.; Carr, M. J.; Clegg, W.; Kilner, C. A.; Kennedy, J. D. *Dalton Trans.* **2004**, 3552-3561.
- (27) Schwab, P. F. H.; Levin, M. D.; Michl, J. *Chem. Rev.* **1999**, *99*, 1863-1933.
- (28) Grimes, R. N. *J. Chem. Ed.* **2004**, *81*, 657-672.
- (29) Kaszynski, P.; Lipiak, D. In *Materials for Optical Limiting*; Crane, R., Lewis, K., Stryland, E. V., Khoshnevisan, M., Eds.; MRS: Boston, 1995; Vol. 374, pp 341-347; Kaszynski, P.; Lipiak, D.; Bairamov, K. A.; Brady, E.; Patel, M. K.; Laska, J. In *Advances in Boron Chemistry*, W. Siebert, Ed.; Royal Society of Chemistry, Bodmin, Cornwall, UK 1997; pp 507-513; Kaszynski, P.; Douglass, A. G. *J. Organomet. Chem.* **1999**, *581*, 28-38.
- (30) Hertler, W. R.; Knoth, W. H.; Muetterties, E. L. *J. Am. Chem. Soc.* **1964**, *86*, 5434-5439.
- (31) Hertler, W. R.; Knoth, W. H.; Muetterties, E. L. *Inorg. Chem.* **1965**, *4*, 288-293.
- (32) Knoth, W. H.; Hertler, W. R.; Muetterties, E. L. *Inorg. Chem.* **1965**, *4*, 280-287.
- (33) Knoth, W. H. *J. Am. Chem. Soc.* **1966**, *88*, 935-939.

- (34) Kaszynski, P.; Pakhomov, S.; Young, V. G., Jr. *Collect. Czech. Chem. Commun.* **2002**, *67*, 1061-1083.
- (35) Franken, A.; Carr, M. J.; Clegg, W.; Kilner, C. A.; Kennedy, J. D. *J. Chem. Soc., Dalton Trans.* **2004**, 3552-3561.
- (36) Ringstrand, B.; Balinski, A.; Franken, A.; Kaszynski, P. *Inorg. Chem.* **2005**, *44*, 9561-9566.
- (37) Ringstrand, B.; Kaszynski, P.; Franken, A. *Inorg. Chem.* **2009**, *48*, 7313-7329.
- (38) Ringstrand, B.; Kaszynski, P.; Monobe, H. *J. Mater. Chem.* **2009**, *19*, 4805-4812.
- (39) Ringstrand, B.; Kaszynski, P.; Young, V. G. Jr.; Janousek, Z. *Inorg. Chem.* **2010**, *49*, 1166-1179.
- (40) Ringstrand, B.; Kaszynski, P.; Young, V. G. Jr. *Inorg. Chem.* **2011**, *50*, 2654-2660.
- (41) Hertler, W. R.; Raasch, M. S. *J. Am. Chem. Soc.* **1964**, *86*, 3661-3668.
- (42) Dermer, O. C.; Edmison, M. T. *Chem. Rev.* **1957**, *57*, 77-122; Bachmann, W. E., Hoffman, R. A. *Org. React.* **1944**, *2*, 224-261.
- (43) Ringstrand, B.; Kaszynski, P.; Januzsko, A.; Young, V. G. Jr. *J. Mater. Chem.* **2009**, *19*, 9204-9212.
- (44) Ringstrand, B.; Kaszynski, P. *J. Mater. Chem.* **2010**, *20*, 9613-9615.

(45) Ringstrand, B.; Kaszynski, P. *J. Mater. Chem.* **2011**, *21*, 90-95.

A Practical Synthesis of Isomerically Pure 1,10-Difunctionalized Derivatives of the [closo-1-CB₉H₁₀]⁻ Anion.

Reproduced with permission from Ringstrand, B.; Balinski, A.; Franken, A.; Kaszynski, P. *Inorg. Chem.* **2005**, *44*, 9561-9566. Copyright 2005 American Chemical Society. Available online: <http://pubs.acs.org/doi/abs/10.1021/ic051311j>

This work was performed while I was visiting as an undergraduate student from Augustana College in the summer of 2005. The goal was to develop the synthetic methodology for the preparation of the first isomerically pure 1,10-difunctionalized derivative of the [closo-1-CB₉H₁₀]⁻ anion. My role in this work was synthesis and characterization of all compounds.

Dr. Andreas Franken contributed preliminary results related to the preparation of iodo acid **4**, and the conversion of the carboxylic acid group to an amine. Mr. Andrzej Balinski assisted with purification of iodo acid **4**. Dr. Piotr Kaszynski performed quantum mechanical calculations.

Abstract

The isomer-free [closo-1-CB₉H₈-1-COOH-10-I]⁻ anion (**4**) was prepared in four

steps and 10% overall yield from B₁₀H₁₄. The key step is the skeletal isomerization of the [*closo*-2-CB₉H₈-2-COOH-7-I]⁻ anion (**3**) to a mixture of the 10- and 6-iodo derivatives of [*closo*-1-CB₉H₉-1-COOH]⁻ formed in up to a 3:1 ratio. The carboxylic acid **4** was converted to amine [*closo*-1-CB₉H₈-1-NH₂-10-I]⁻ (**1**) using the Curtius reaction. The relative thermodynamic stability of each product was calculated at the DFT and MP2 levels of theory. The regioselectivity of electrophilic substitution in [*closo*-CB₉H₁₀]⁻ derivatives was briefly investigated using the NBO population analysis of the MP2 wavefunction.

Introduction

Despite the relatively large number of [*closo*-1-CB₉H₁₀]⁻ derivatives prepared to date,^{1,2} 1,10-difunctionalized derivatives **I** are still practically unknown. Such derivatives are sought after³ in the context of synthesis of linear molecular systems^{4,5} and our liquid crystals program in particular.^{6,7}

One possible route to such derivatives **I** involves functionalization of the {*closo*-1-CB₉} cage (**II**, Figure 1). While C-functionalization proceeds rather smoothly,^{8,9} the selective and efficient direct substitution of the B(10) position poses a serious challenge. Previous results showed that electrophilic halogenation of the parent anion, [*closo*-1-CB₉H₁₀]⁻ (**II**, X = H), generally forms the 6-isomer **III**.¹⁰ The 10-isomer **I**, the expected thermodynamic product, is either absent (iodination and fluorination) or formed as a

minor product (< 9%). This observed kinetic control of regioselectivity appears to be common for 10-vertex *closo*-boranes.¹¹⁻¹³ In the case of the [*closo*-1-CB₉H₁₀]⁻ anion, the regioselectivity has been ascribed to the higher s-character of the B(10) exoskeletal orbital and consequently higher B-H bond strength as compared with the B(6) position.¹⁰

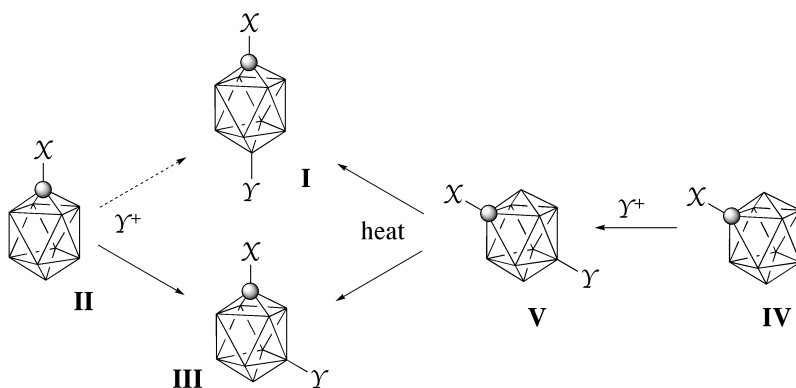


Figure 1. General pathways to disubstituted derivatives of the {*closo*-1-CB₉} cluster.

The recently discovered¹⁴ Brellocks' reaction was exploited¹ in synthesis of the {*closo*-1-CB₉} derivatives and opened new possibilities in practical preparation of 1,10-disubstituted derivatives **I**. It was demonstrated that halogenation of [*closo*-2-CB₉H₁₀] derivatives **IV** occurs selectively at the 7-position.¹ Subsequent thermal rearrangement of the resulting 2,7-disubstituted {*closo*-2-CB₉} **V** gives a mixture of 10- and 6-substituted {*closo*-1-CB₉} in a $\geq 1:1$ ratio.¹

In the context of our interest in electrically neutral highly polar liquid crystals for electro-optical applications,^{6,7} we envisioned 1-amino-10-iodo derivative **1** as a general precursor to this class of materials based on the 10-vertex cluster. The iodine provides a

means to introduce alkyl and aryl substituents in Pd-catalyzed coupling reactions reported for the $\{closo-1-CB_9\}^{1,9}$ and other *closo*-boranes.¹⁵ The amino group offers a convenient synthetic handle. It can be transformed to a quinuclidine ring^{16,17} or converted into an isolable stable diazo compound.¹⁸ The latter reacted with a range of nucleophiles^{18,19} in analogy to arenediazonium salts.

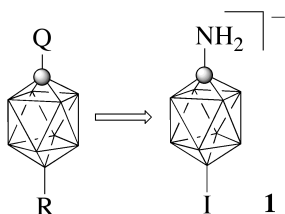


Figure 2. $[closo-1-CB_9H_8-1-NH_2-10-I]^-$ (**1**) as a precursor to electrically neutral derivatives. Q represents an onium fragment such as sulfonium, pyridinium or ammonium.

Here we describe a short and practical preparation of isomerically pure **1**. The thermodynamics and regioselectivity of the product formation are discussed with the aid of quantum-mechanical calculations.

Results

Synthesis

The preparation of amine **1** starts from the known²⁰ $[closo-2-CB_9H_9-2-COOH]^-$ anion **2** obtained according to the Brellocks method. The published²⁰ procedure using 30% excess I₂ and stirring for 3 hrs at ambient temperature gave only about 45% yield of

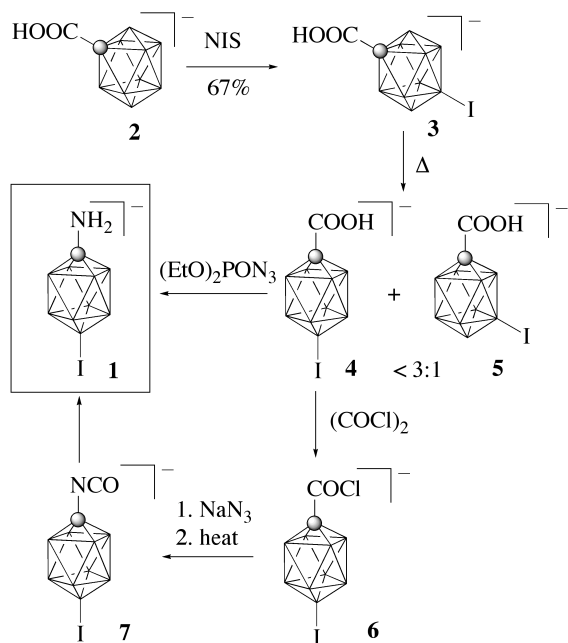
crude **2**, while with 90% excess I₂ and 6 hrs reaction time, the yield was increased to over 60%. In both cases, the anion **2** was obtained in about 70% purity with the main contaminant associated with a singlet at 7.0 ppm and a doublet at -10.9 ppm in the ¹¹B NMR spectrum.²¹ The crude product also contained up to 10% of [*closo*-1-CB₉H₉-1-COOH]⁻ anion. Iodination of crude **2**[NEt₄] with excess N-iodosuccinimide (NIS) gave the 7-iodo derivative **3** as a component of a mixture of products. Conducting the iodination of moist **2**[NEt₄] at ambient temperature leads to up to 40% rearrangement of the {*closo*-2-CB₉} skeleton, and the formation of 10-iodo and 6-iodo isomers (**4** and **5**, respectively) in approximately 1:1 ratio. Since a solution of isolated crude **3**[NEt₄] does not show any appreciable rearrangement over the period of 60 hrs at ambient temperature, the rearrangement observed during the reaction appears to be a chemically induced, rather than a thermally promoted process. The rearrangement was limited to < 15% of the product by carefully drying the starting **2**[NEt₄]. During the iodination process, the intensity of the signals at 7.0 and -10.9 ppm was significantly reduced.

Without separation, the mixture of the [NEt₄]⁺ salts was thermolyzed in boiling acetonitrile, and the resulting anions **4** and **5** were isolated as a mixture of their [NMe₄]⁺ salts in an overall yield of about 15-20% based on the starting B₁₀H₁₄. ¹¹B NMR analysis showed that the 10- and 6-iodo isomers, **4** and **5**, are the sole products formed in a ratio varying from about 3:2 to 3:1. Results of small scale thermolysis of the same crude salt **3**[NEt₄] show that the ratio of **4** to **5** is less favorable at 50 °C (~2:1) than at 80 °C (~5:2). The salt **4**[NMe₄] was separated by slow fractional crystallization of the mixture from

aqueous EtOH. In one instance, first recrystallization of a crude mixture of salts increased the ratio from about 3:1 to 15:1, and the second crystallization gave > 99 % pure [*closo*-1-CB₉H₈-1-COOH-10-I]⁻[NMe₄]⁺ salt (**4**[NMe₄]). The overall yield of the pure isomer was about 30% based on the crude **2**[NEt₄] or about 10 % based on B₁₀H₁₄. The combined mother liquors contained the two isomers in an approximately 1:1 ratio and could be used for isolation of further quantities of **4**[NMe₄].

The separation of the isomers by recrystallization varies from run to run and presumably depends on the amount of solvent used and the rate of EtOH evaporation. For instance, we observed that fast crystallization gives a much less satisfactory separation.

Scheme 1



The transformation of the carboxyl group of anion **4** to an amino group was accomplished using the Curtius reaction.²² Treatment of a suspension of acid salt **4**[NEt₄] in CH₂Cl₂ with oxalyl chloride gave the acid chloride **6**[NEt₄] as the sole product, fully soluble in CH₂Cl₂. Without purification, the isolated crude chloride was treated with sodium azide in boiling MeCN to give the isocyanate **7**. Upon hydrolysis, the isocyanate formed the amine **1** isolated as the **1**[NMe₄] or **1**[NHMe₃] salt in about 40%-60% of unoptimized yield. The purity of the amine varies somewhat from run to run and is possibly related to the quality of anhydrous MeCN. In contrast to **4**[NEt₄], the **4**[NMe₄] salt did not dissolve upon reaction with (COCl)₂, and the acid chloride **6**[NMe₄] presumably was not formed.

Alternatively, the amine was prepared using a modified Curtius reaction involving phosphoryl azide in the presence of Et₃N.^{23,24} Under these conditions, the acid **4**[NMe₄] undergoes deprotonation with NEt₃, as evident from about 4 ppm upfield shift of the B(10) signal in the ¹¹B NMR spectrum. Initial attempts using the commercial (PhO)₂OPN₃ demonstrated difficulties with separation of the amine from the phosphoric acid, since both are extracted from the acidic solution, rather than from alkaline as for a typical organic substrate. Therefore, we used the more hydrophilic (EtO)₂OPN₃, which was prepared from the corresponding chloride and NaN₃ in MeCN, and used as a crude solution in reaction with **4**[NMe₄]. The original conditions for the Curtius-Yamada reaction were modified, and the reaction was conducted in dry MeCN in the absence of alcohol. The resulting isocyanate **7** was hydrolyzed during aqueous workup directly to

amine **1** which was isolated either as oily acid **1**[**H**] or, more conveniently, as the crystalline salt **1**[**NMe**₄]. The purity of the product in this method was higher than that obtained in the classical Curtius reaction, and typical yields were >80%.

Attempts at conversion of carboxylic acid **4** to the amine **1** using the Schmidt reaction²⁵ were unsuccessful. Using either classical reaction conditions (CHCl₃/H₂SO₄) and **4**[**NBu**₄] salt, or **4**[**H**] in MeSO₃H, a complex reaction mixture was obtained that contained a precipitate insoluble in MeCN.

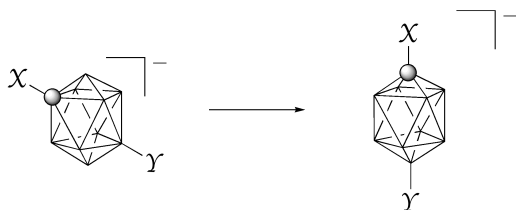
Theoretical Analysis

To better understand the thermodynamics and regioselectivity of the product formation, we conducted quantum mechanical calculations for ground state structures at the DFT and MP2 levels of theory. Transition structures and their energies were not considered at this point.

Calculations on both levels of theory show that the skeletal rearrangement of the {*closo*-2-CB₉} to the {*closo*-1-CB₉} cluster is exothermic by about 22 kcal/mol (Table 1). The exotherm appears to increase slightly with increasing substitution. Thus, introduction of a single substituent increases the exotherm by up to 1.5 kcal/mol for the iodide, while the presence of two substituents (COOH and I) increases the thermodynamic stability of the {*closo*-1-CB₉} isomer by nearly 3 kcal/mol, according to DFT calculations. Calculations at the MP2 level of theory show the same trend, but energy differences are smaller. The calculated energies for the parent anion are

consistent with those reported in literature.²⁶

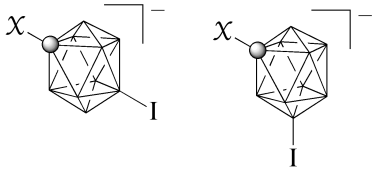
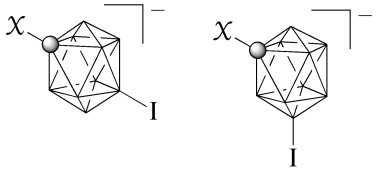
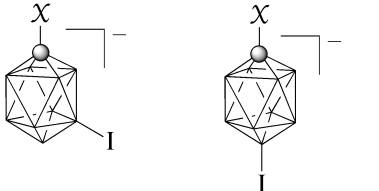
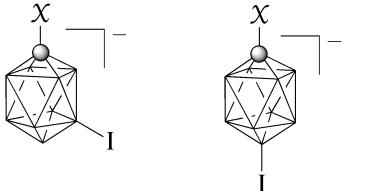
Table 1. Calculated exotherms for skeletal rearrangement of selected $\{closo-2-CB_9\}^-$ anions.



χ	γ	ΔH [kcal/mol]	
		DFT	MP2
H	H	-20.7	-20.7
COOH	H	-22.0	-21.1
H	I	-22.3	-21.8
COOH	I	-23.5	-22.0

Further analysis shows that the 10-iodo isomers are more thermodynamically stable than the 7- (for the $\{closo-2-CB_9\}$ skeleton) or 6-iodo (for the $\{closo-1-CB_9\}$ skeleton) derivatives by about 1 kcal/mol. Again, the difference is smaller by about 0.5 kcal/mol at the MP2 level.

Table 2. Difference in enthalpy of formation for selected $\{closo-CB_9\}$ regioisomers

Isomer A	Isomer B	$\Delta H = H_B - H_A$ [kcal/mol]	
		DFT	MP2
		X = H -1.2	X = H -0.4
		X = COOH -1.2	X = COOH -0.4
		X = H -1.0	X = H -0.7
		X = COOH -1.2	X = COOH -0.8

Limited conformational analysis for anions $[closo-2-CB_9H_9-2-COOH]^-$ (**2**) and $[closo-2-CB_9H_8-2-COOH-7-I]^-$ (**3**) shows that the structures with the COOH plane approximately orthogonal to the B(1)···B(10) axis (staggered orientation) represents the global minimum. This is consistent with the experimental molecular structure of the former anion²⁷ in which the O=C–C–B(1) dihedral angle is about 100 °, while the calculated angle is 93 °. The experimental interatomic distances in **2** are generally overestimated by both methods but are better reproduced by the MP2 method than by DFT calculations.

Calculations for the $[closo-1-CB_9H_8-1-COOH-6-I]^-$ anion (**5**) revealed that the C_1 -symmetric conformer with the B-I bond orthogonal to the COOH plane represents the global minimum (Figure 3). The C_s conformer with the C=O group *syn* to the I, is only

slightly higher in energy, while the conformer with the carbonyl group *anti* to the iodine is higher by 0.24 kcal/mol than that in the C_1 form.

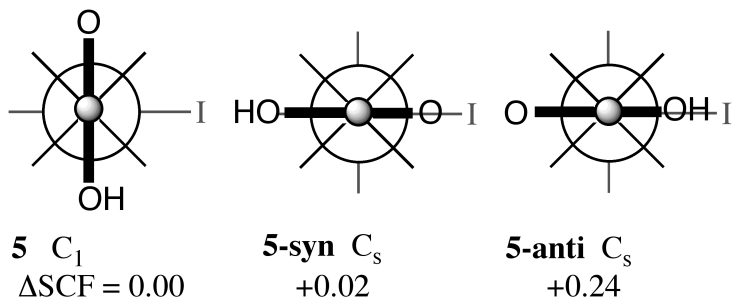


Figure 3. Newman projections and relative SCF energies (kcal/mol) for three conformers of $[closo-1-CB_9H_8-1-COOH-6-I]^-$ anion (**5**).

Discussion

Preparation of 1,10-disubstituted derivatives of the $[closo-1-CB_9H_{10}]^-$ anion relies on the regioselectivity of electrophilic substitution at the boron atom. Previous experiments have shown that halogenation gives the 6-halo derivatives as the sole product.^{1,10} Bromination¹ and iodination of the $\{closo-2-CB_9\}$ cluster are also kinetically controlled and occur preferentially at the equatorial position. The high selectivity for the 7 position in the $\{closo-2-CB_9\}$ cluster is evident from the isolation of $[closo-2-CB_9H_8-7-Br-2-Ph]^-$ in 92% yield.¹ Similarly, high regioselectivity for iodination of $[closo-2-CB_9H_9-2-COOH]^-$ is assumed, but the presence of small quantities of the thermodynamic 10-iodo isomer $[closo-2-CB_9H_8-2-COOH-10-I]^-$ in the reaction mixture cannot be excluded. If it were formed, it would give the undesired 6-substituted $[closo-1-CB_9H_{10}]^-$

derivative in the rearrangement. Thus, the same kinetic control, which prevents the substitution of the $\{closo-1-CB_9\}$ at the B(10) position, allows for the formation of the desired B(10)-substituted product through the $\{closo-2-CB_9\}$ anion.

The origin of the observed kinetic control in iodination of the $\{closo-CB_9\}$ clusters is not clear at the moment, and the preference for equatorial attack cannot be explained satisfactorily by using either charge distribution²⁸ or hybridization arguments. For instance, NBO analysis of the MP2 wavefunction for the parent $[closo-2-CB_9H_{10}]^-$ anion shows a significantly higher negative charge density at the B(10) (-0.23 e) than at the B(7) (-0.18 e) atoms (Figure 4). This charge distribution is little altered by the introduction of the carboxyl group in **2**. Most affected by the substitution is the carbon atom, which becomes less negative by 0.05 e, and the adjacent boron atoms, which are more positive by < 0.03 e. However, the same analysis for the parent $[closo-1-CB_9H_{10}]^-$ anion does show a slightly higher negative charge density at the equatorial position than at the apex. This could provide some rationale for the observed regioselectivity in this cluster.

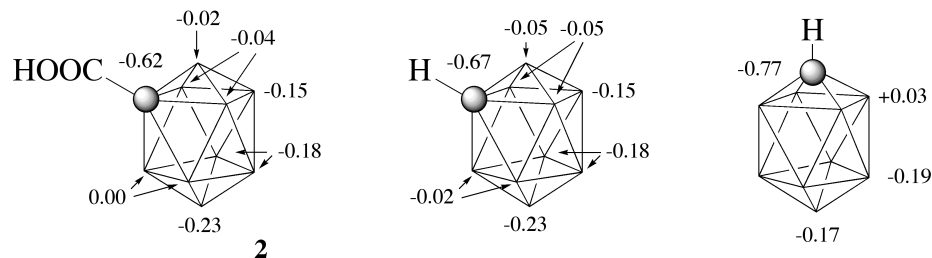


Figure 4. NBO-derived natural atomic charges (MP2/6-31G(d,p)-level calculations) in the carboxylic acid anion **2** and parent [*closo*-1-CB₉H₁₀]⁻.

Inspection of bonding orbitals shows that in all three anions the B(10) exocyclic orbital has slightly higher s-character ($sp^{2.9}$) than those of equatorial B(6) and B(7) atoms ($sp^{3.0}$). These differences seem too small to explain the observed regiochemistry of substitution. For comparison, the exocyclic orbital of B(1) in [*closo*-2-CB₉H₁₀]⁻ is $sp^{2.1}$ hybridized.

The {*closo*-2-CB₉} to {*closo*-1-CB₉} skeletal rearrangement is exothermic and requires relatively low activation energy. This is evident from a facile thermally-induced rearrangement, which is usually completed in <24 hr at 80 °C. At ambient temperature such a rearrangement practically does not occur thermally, but apparently it can be chemically-induced in the iodination reactions. Thus, in the oxidative ring closure and the preparation of anion **2**, small quantities of the [*closo*-1-CB₉H₉-1-COOH]⁻ anion are formed, which presumably undergoes iodination to the 6-iodo isomer **5**. A particularly large degree of rearrangement occurs during iodination of crude and moist **2**[NEt₄] with NIS, and the two isomers **4** and **5** are formed in a ~1:1 ratio. In the end, both processes

unfavorably affect the yield of the desired isomer **4** and give rise to the observed variable **4/5** ratio. Thus, limiting the extent of the rearrangement by drying starting **2**[NEt₄] and possibly lowering the temperature during the NIS iodination is critical for achieving a high ratio (up to 3:1) for anions **4** and **5**. If the activation energies for the rearrangement of [*closo*-2-CB₉H₈-2-COOH-7-I]⁻ and the formation of anions **4** and **5** were proportional to the relative thermodynamic stability of the products, the ratio of **4/5** could be as high as 4:1 at 80 °C, based on MP2 calculations.

The driving force for the rearrangement is the lowering of the coordination number for the more electronegative carbon atom and the simultaneous shift of negative charge density from the boron to the carbon atom.²⁶ This is illustrated by the charge distribution in the parent clusters [*closo*-2-CB₉H₁₀]⁻ and [*closo*-1-CB₉H₁₀]⁻. In the rearrangement, the carbon atom gains 0.1e at the expense of the boron atoms (Figure 4).

Summary and Conclusions

The isomerically pure 10-iodo acid [*closo*-1-CB₉H₈-1-COOH-10-I]⁻ **4** was prepared in four steps from B₁₀H₁₄ in about 10% overall yield. The critical step in the procedure exhibiting the greatest variability is the separation of the desired **4** from the 6-iodo isomer **5** by recrystallization. The preparation of the mixture of isomeric iodo acids **4** and **5** proceeds without purification of intermediates, and all impurities (up to 30%) are ultimately converted to the products **4** and **5** or are lost in the workup procedures. The

two isomers **4** and **5** are formed in a ratio < 3:1 in a thermal rearrangement of the {*closo*-2-CB₉} cage, and the overall ratio of the two isomers is controlled by the extent of rearrangement in the NIS iodination step. The current procedure utilizes 4.0 g of B₁₀H₁₄ and scaling it up will require optimization of extraction procedures, especially in the preparation of **2**[NEt₄].

Iodination and presumably other halogenation reactions of the {*closo*-2-CB₉} and {*closo*-1-CB₉} clusters are kinetically controlled and occur preferentially in the equatorial positions. The apical substituted products are more thermodynamically stable than equatorial isomers by about 1 kcal/mol. Population analysis shows that charge distribution and hybridization of the exocyclic bonding orbitals are not major factors in the regioselectivity of electrophilic substitution in the two {*closo*-2-CB₉} and {*closo*-1-CB₉} clusters.

Computational Details

Quantum-mechanical calculations were carried out with the B3LYP^{29,30} and MP2(fc) methods using the Linda-Gaussian 98 package³¹ on a Beowulf cluster of 16 processors. Calculations involving iodine used the LANL2DZdp effective core potential basis set (available from <http://www.emsl.pnl.gov/forms/basisform.html>) and 6-31G(d,p) for the remaining elements implemented with the GEN keyword.

Geometry optimizations were undertaken using appropriate symmetry constraints and tight convergence limits. Vibrational frequencies were calculated at the

B3LYP/6-31G(d,p) level of theory and were used to characterize the nature of the stationary points and to obtain thermodynamic parameters. Zero-point energy (ZPE) corrections were scaled by 0.9806.³² Population analysis was obtained using the NBO algorithm³³ supplied in the Gaussian package.

Experimental Section

Solvents were dried and deoxygenated before use, and reagents were used as supplied. Reactions were carried out under dry Ar, subsequent manipulations conducted in air. NMR spectra were obtained at 100 MHz (¹³C), 128.4 MHz (¹¹B) or 400 MHz (¹H) in CD₃CN unless otherwise specified. ¹H and ¹³C spectra were referenced to the solvent. ¹¹B NMR chemical shifts are relative to the resonance of BF₃•OEt₂ prerecorded in a sealed capillary in CDCl₃ and set to 0.0 ppm.

Preparation of [*closo*-1-CB₉H₈-1-NH₂-10-I]⁻ anion 1.

Method A. Dry salt 4[NEt₄] (0.80 g, 2.0 mmol) prepared in 80% yield from 4[NMe₄], was suspended in CH₂Cl₂ (10 mL), and a 2 M solution of (COCl)₂ (2 mL, 4 mmol) was added. The mixture was stirred protected from moisture until all solid dissolved (~ 1 hr). Volatiles were removed under reduced pressure, and the crude acid chloride 6[NEt₄] was dried in *vacuo* [¹¹B NMR δ 22.1 (s, 1B), -14.8 (d, *J* = 158 Hz, 4B), -20.6 (d, *J* = 144 Hz, 4B)].

The crude chloride was dissolved in dry MeCN (15 mL), solid NaN₃ (0.20 g, 3 mmol) was added, and the mixture was stirred and refluxed for 3 hrs. The mixture was cooled, dry CH₂Cl₂ (5 mL) was added, and the mixture was filtered through a glass frit. Solvents were evaporated and the resulting residue was dried in *vacuo* giving a 1:1 mixture of amine **1**[NEt₄] [¹¹B NMR δ 11.5 (1B), -17.9 (4B), -23.3 (4B)] and isocyanate **7**[NEt₄] [¹¹B NMR δ 12.6 (1B), -16.8 (4B), -23.3 (4B)] as the sole products.

The crude product was dissolved in THF (10 mL), 5% HCl (5 mL) was added and the mixture was stirred at 50 °C for 5 hrs. Solvents were evaporated, the resulting crude **1**[NEt₄] (~1.0 g) was treated with 5% HCl (25 mL), and the product was extracted with Et₂O (3 × 50 mL). The combined Et₂O extracts were evaporated, and the product was dried in *vacuo* to give 0.80 g of [*closo*-1-CB₉H₈-1-NH₃-10-I] (**1**[H]) hydrate as a colorless oil: ¹H NMR δ 4.1 (br s); ¹¹B NMR δ (MeCN) 15.0 (s, 1B), -17.5 (d, *J* = 153 Hz, 4B), -23.0 (d, *J* = 144 Hz, 4B). The amine was dissolved in water, neutralized with 5% NaOH and treated with NMe₃Cl solution to give 0.66 g of **1**[NMe₃] as a white solid.

Method B. Crude (EtO)₂OPN₃³⁴ was prepared from (EtO)₂OPCl (0.76 g, 4.4 mmol, 0.63 mL) which was added dropwise (10 min) to a stirred and gently refluxed mixture of NaN₃ (0.86 g, 13.0 mmol) and dry MeCN (10 mL) under Ar atmosphere. After 18 hrs of reflux, the aliquot containing the crude (EtO)₂OPN₃ was decanted from the inorganic salts and via syringe added to a stirred solution of the salt **4**[NMe₄] (0.80 g, 2.2 mmol) in MeCN (3 mL) followed by NEt₃ (4.8 mmol, 0.68 mL). The solution was

heated for 18 hrs under reflux, cooled, aqueous solution of KOH (2 g in 20 mL) was added, and MeCN was removed under reduced pressure. After adding HCl (5 %, 200 mL) the mixture was extracted with Et₂O (4 × 50 mL). H₂O (150 mL) was added to the combined Et₂O extracts, and the Et₂O was removed under reduce pressure. The aqueous solution was filtered, and the HCl (5 %, 100 mL) was added to the filtrate. The filtrate was extracted with Et₂O (4 × 50 mL) and 0.80 g of (**1[H]**) was isolated as in Method B.

An aqueous solution of the amine **1[H]** was neutralized with small excess of 5% NaOH and treated with excess NMe₄Cl. The precipitate was filtered and dried to give 0.58 g (80% yield) of salt **1[NMe₄]**: mp 180-182 °C; ¹H NMR δ 2.74 (s), ¹¹B NMR δ 11.8 (s, 1B), -17.8 (d, *J* = 150 Hz, 4B), -23.3 (d, *J* = 144 Hz, 4B); IR 3400 (N-H), 2552 and 2520 (B-H) cm⁻¹. Anal. Calcd for C₅H₂₂B₉IN₂: C, 17.96; H, 6.63; N, 8.38. Found: C, 19.01; H, 6.13; N, 7.93.

Preparation of [*closo*-2-CB₉H₈-2-COOH]⁻ anion **2.** Crude salt **2[NEt₄]** was prepared from B₁₀H₁₄ (4.0 g, mp 104-106 °C) following the literature procedure²⁰ with the exception of using 90% excess I₂ and 6 hr reaction time in the oxidation step. The resulting mixture containing ~70% (by NMR) of the main component was used for the preparation of **3[NEt₄]** without further purification. ¹¹B NMR: **3[NEt₄]** δ -0.3 (1B), -6.1 (1B), -22.9 (1B), -27.8 (2B), -30.5 (2B), -31.2 (2B) [lit.²⁰ (acetone-*d*₆) δ 0.8 (1B), -5.2 (1B), -21.7 (1B), -26.7 (2B), -29.2 (2B), -29.7 (2B)]; additional major signals: δ 7.2 (s, 1B), - 9.6 (d, 1B), -10.9 (d, 4B), -18.5 (d, 2B), 20.7 (d, 1B); minor signals ([*closo*-1-

CB₉H₈-1-COOH]⁻): δ 33.0 (d, 1B), -16.8 (d, 4B), -25.0 (d, 4B) [lit.²⁰ (acetone-*d*₆) δ 34.0 (1B), -15.7 (4B), -24.0 (4B)].

Preparation of [*closo*-1-CB₉H₈-1-COOH-10-I]⁻ anion 4 and [*closo*-1-CB₉H₈-1-COOH-6-I]⁻ anion 5. To a solution of rigorously dried over P₂O₅ crude salt **2**[NEt₄] (3.1 g, 10.5 mmol) in anhydrous CH₃CN (40 mL) was added N-iodosuccinimide (NIS, 3.51 g, 15.6 mmol), and the solution was stirred for 30-48 hrs at ice bath temperature. After adding Na₂SO₃ (0.4 g, 3.2 mmol) followed by HCl (5%, 200 mL), the CH₃CN was removed under reduced pressure. The aqueous solution was extracted with Et₂O (3 × 50 mL). Water (150 mL) was added to the combined extracts, and the Et₂O was removed under reduce pressure. The aqueous solution was filtered, and [NEt₄]⁺Br⁻ (3.1 g, 15 mmol) was added to the filtrate. After brief stirring, the white microcrystalline precipitate of the [NEt₄]⁺ salt mixture was filtered off, washed with H₂O (50 mL), and dried *in vacuo* to give 3.0 g (68% yield) of a white solid: ¹¹B NMR (MeCN-*d*₆) δ (signals characteristic for **3**[NEt₄] -0.1 (d, *J* = 162 Hz, 2B), -5.9 (d, *J* = 164 Hz, 2B), -33.9 (s, 1B).

Without further purification, the mixture of the [NEt₄]⁺ salts (3.0 g, 7.1 mmol) was dissolved in CH₃CN (20 mL) and heated for 20 hrs under reflux. After cooling, the solvent was removed *in vacuo*. After adding HCl (5%, 100 mL), the mixture was extracted with Et₂O (3 × 50 mL). H₂O (50 mL) was added to the combined Et₂O extracts, and the Et₂O was removed under reduce pressure. The aqueous solution was filtered, and [NMe₄]⁺Cl⁻ (1.64 g, 15 mmol) was added to the filtrate. The resulting white

precipitate was filtered off and dried in *vacuo* to give 2.51 g of a crude mixture of the $[\text{NMe}_4]^+$ salts of the $[\textit{closo-1-CB}_9\text{H}_8\text{-1-COOH-10-I}]^-$ anion **4** and $[\textit{closo-1-CB}_9\text{H}_8\text{-1-COOH-6-I}]^-$ anion **5** in a ratio ranging from about 3:2 to 3:1 (by integration of the signals at +18.8 and -29.1 ppm in the ^{11}B NMR spectrum). Anal Calcd for $\text{C}_6\text{H}_{21}\text{B}_9\text{INO}_2$: C, 19.83; H, 5.82; N, 3.85. Found: C 20.06, H 5.76, N 3.87.

The mixture of the $[\text{NMe}_4]^+$ salts (2.5 g) was dissolved in hot EtOH (80 mL), water (80 mL) was added and the solution was left to crystallize in a tall Petri dish yielding 1.90 g of about 92% pure **4** $[\text{NMe}_4]$. One more crystallization gave 1.30 g (11% yield based on $\text{B}_{10}\text{H}_{14}$) of >99% pure isomer: mp 244-245 °C; ^1H NMR (acetone $-d_6$) δ 0.5-2.5 (br m 8H), 3.43 (s, 12H), 10.9 (br s, 1H); ^{11}B NMR δ 18.8 (s, 1B), -16.6 (d, $J = 156$ Hz, 4B), -21.2 (d, $J = 143$ Hz, 4B); IR 2570 and 2524 (B-H), 1695 (C=O) cm^{-1} . Anal Calcd for $\text{C}_6\text{H}_{21}\text{B}_9\text{INO}_2$: C, 19.83; H, 5.82; N, 3.85. Found: C 20.06; H 5.76; N, 3.87.

$[\textit{closo-1-CB}_9\text{H}_8\text{-1-COOH-6-I}]^-[\text{NMe}_4]^+$ (5** $[\text{NMe}_4]$).** ^{11}B NMR (after subtracting signals due to the 1,10-isomer **4** $[\text{NMe}_4]$) δ 31.6 (d, $J = 174$ Hz, 1B), -14.5 (d, $J = 156$ Hz, 2B), -15.0 (d, 2B), -22.5 (d, $J = 169$ Hz, 2B), -25.1 (d, $J = 140$ Hz, 1B), -29.2 (s, 1B).

Deprotonation of $[\textit{closo-1-CB}_9\text{H}_8\text{-1-COOH-10-I}][\text{NMe}_4]$ with NEt_3 . A solution of **4** $[\text{NMe}_4]$ (10 mg) in CD_3CN was treated with NEt_3 (2.5 eq) and NMR spectrum was collected: ^{11}B NMR δ 15.1 (s, 1B), -17.4 (d, $J = 154$ Hz, 4B), -21.5 (d, $J = 141$ Hz, 4B).

Acknowledgments

This project was been supported by the NSF grant (DMR-0111657).

References

- (1) Franken, A.; Kilner, C. A.; Thornton-Pett, M.; Kennedy, J. D. *Collect. Czech. Chem. Comm.* **2002**, *67*, 869-912.
- (2) Sivaev, I. B.; Kayumov, A.; Yakushev, A. B.; Solntsev, K. A.; Kuznetsov, N. T. *Koord. Khim.* **1989**, *15*, 1466-1477.
- (3) Bullen, N. J.; Franken, A.; Kilner, C. A.; Kennedy, J. D. *Chem. Commun.* **2003**, 1684-1685.
- (4) Schwab, P. F. H.; Levin, M. D.; Michl, J. *Chem. Rev.* **1999**, *99*, 1863-1933.
- (5) Grimes, R. N. *J. Chem. Educ.* **2004**, *81*, 657-672.
- (6) Kaszynski, P.; Lipiak, D. In *Materials for Optical Limiting*; Crane, R., Lewis, K., Stryland, E. V., Khoshnevisan, M., Eds.; MRS: Boston, 1995; Vol. 374, p 341-347; Kaszynski, P.; Lipiak, D.; Bairamov, K. A.; Brady, E.; Patel, M. K.; Laska, J. in *Advances in Boron Chemistry*, W. Siebert, Ed.; Royal Society of Chemistry, Bodmin, Cornwall, UK (1997), pp 507-513.
- (7) Kaszynski, P.; Douglass, A. G. *J. Organomet. Chem.* **1999**, *581*, 28-38.
- (8) Knoth, W. H. *Inorg. Chem.* **1971**, *10*, 598-605.

- (9) Tsnag, C.-W.; Yang, Q.; Sze, T.-P. E.; Mak, T. C. W.; Chan, D. T. W.; Xie, Z. *Inorg. Chem.* **2000**, *39*, 3582-3589.
- (10) Ivanov, S. V.; Rockwell, J. J.; Miller, S. M.; Anderson, O. P.; Solntsev, K. A.; Strauss, S. H. *Inorg. Chem.* **1996**, *35*, 7882-7891.
- (11) Smith, W. L.; Meneghelli, B. J.; Thompson, D. A.; Klymko, P.; McClure, N.; Bower, M.; Rudolph, R. W. *Inorg. Chem.* **1977**, *16*, 3008-3012.
- (12) Meneghelli, B. J.; Rudolph, R. W. *J. Organomet. Chem.* **1977**, *133*, 139-145.
- (13) Knoth, W. H.; Hertler, W. R.; Muetterties, E. L. *Inorg. Chem.* **1965**, *4*, 280-287.
- (14) Brellocks, B. In *Contemporary Boron Chemistry*, M. G. Davidson, A. K. Hughes, T. B. Marder, and K. Wade Eds.; Royal Society of Chemistry, Cambridge, England (2000), pp. 212-214.
- (15) Kaszynski, P. *Collect. Czech. Chem. Commun.* **1999**, *64*, 895-926, and references cited therein.
- (16) Douglass, A. G.; Janousek, Z.; Kaszynski, P.; Young, V. G., Jr. *Inorg. Chem.* **1998**, *37*, 6361-6365.
- (17) Balinski, A.; Januszko, A.; Harvey, J. E.; Brady, E.; Kaszynski, P.; Young, V. G., Jr. unpublished results.
- (18) Ringstrand, B.; Kaszynski, P.; Franken, A.; Carr, M. J.; Kennedy, J. D. in preparation.

- (19) Jelínek, T.; Stibr, B.; Plešek, J.; Thornton-Pett, M.; Kennedy, J. D. *J. Chem. Soc., Dalton Trans.* **1997**, 4231-4236.
- (20) Franken, A.; Carr, M. J.; Clegg, W.; Kilner, C. A.; Kennedy, J. D. *J. Chem. Soc., Dalton Trans.* **2004**, 3552-3561.
- (21) This unidentified impurity does not interfere with the preparation of the [*closo*-1-CB₉H₉-1-COOH]⁻, and a complex ¹¹B NMR spectrum of the mixture yields clean spectrum of the product. Ref 18.
- (22) For a review see Banthorpe, D. V. in *The Chemistry of the Azido Group*, S. Patai Ed; Wiley, New York, 1971, p 397.
- (23) Shioiri, T.; Ninomiya, K.; Yamada, S. *J. Am. Chem. Soc.* **1972**, *94*, 6203-6205.
- (24) Ninomiya, K.; Shioiri, T.; Yamada, S. *Tetrahedron* **1974**, *30*, 2151-2157.
- (25) For a review see: Koldobskii, G. I.; Ostrovskii, V. A.; Gidasov, B. V. *Russ. Chem. Rev.* **1978**, *47*, 1084.
- (26) Schleyer, P. v. R.; Najafian, K. *Inorg. Chem.* **1998**, *37*, 3454-3470.
- (27) Franken, A.; Kilner, C. A.; Kennedy, J. D. *Chem. Commun.* **2004**, 328-329.
- (28) A similar conclusion was reached for the SB₉H₉ cluster. See ref 11 and 12.
- (29) Becke, A. D. *J. Chem. Phys.* **1993**, *98*, 5648-5652.

(30) Lee, C.; Yang, W.; Parr, R. G. *Phys. Rev. B*, **1988**, *37*, 785-789.

(31) Gaussian 98, Revision A.9, M. J. Frisch, G. W. Trucks, H. B. Schlegel, G. E. Scuseria, M. A. Robb, J. R. Cheeseman, V. G. Zakrzewski, J. A. Montgomery, Jr., R. E. Stratmann, J. C. Burant, S. Dapprich, J. M. Millam, A. D. Daniels, K. N. Kudin, M. C. Strain, O. Farkas, J. Tomasi, V. Barone, M. Cossi, R. Cammi, B. Mennucci, C. Pomelli, C. Adamo, S. Clifford, J. Ochterski, G. A. Petersson, P. Y. Ayala, Q. Cui, K. Morokuma, D. K. Malick, A. D. Rabuck, K. Raghavachari, J. B. Foresman, J. Cioslowski, J. V. Ortiz, A. G. Baboul, B. B. Stefanov, G. Liu, A. Liashenko, P. Piskorz, I. Komaromi, R. Gomperts, R. L. Martin, D. J. Fox, T. Keith, M. A. Al-Laham, C. Y. Peng, A. Nanayakkara, M. Challacombe, P. M. W. Gill, B. Johnson, W. Chen, M. W. Wong, J. L. Andres, C. Gonzalez, M. Head-Gordon, E. S. Replogle, and J. A. Pople, Gaussian, Inc., Pittsburgh PA, 1998.

(32) Scott, A. P.; Radom, L. *J. Phys. Chem.* **1996**, *100*, 16502-16513.

(33) Glendening, E. D.; Reed, A. E.; Carpenter, J. E.; Weinhold, F., NBO version 3.1.

(34) Scott, F. L.; Riordan, R.; Morton, P. D. *J. Org. Chem.* **1962**, *27*, 4255-4258.

Synthesis and Reactivity of [*closo*-1-CB₉H₉-1-N₂]: Functional Group Interconversion at the Carbon Vertex of the {*closo*-1-CB₉} Cluster.

Reproduced with permission from Ringstrand, B.; Kaszynski, P.; Franken, A. *Inorg. Chem.* **2009**, *48*, 7313-7329. Copyright 2009 American Chemical Society. Available online: <http://pubs.acs.org/doi/abs/10.1021/ic9007476>

The goal of this project was to investigate functional group transformations at the C(1) position of the [*closo*-1-CB₉H₁₀]⁻ anion with emphasis on the N₂⁺ group. The importance of this research was in opening up the C(1) vertex of the [*closo*-1-CB₉H₁₀]⁻ anion for substitution with onium fragments, which provides access to polar materials of type **I** (see Dissertation Synopsis and Guide).

My role in this work was to synthesize and characterize all compounds and to conduct all physical-organic studies, which included UV-vis spectroscopy, NMR temperature-dependent studies to determine the activation parameters of thermal decomposition of **1** in acetonitrile, and electrochemical measurements on **1** to determine its redox properties.

Dr. Andreas Franken contributed initial results related to the preparation of dinitrogen derivative **1**. Dr. Piotr Kaszynski performed quantum mechanical calculations

to support the experimental evidence for both the radical and closed-shell reaction pathways for **1**.

Abstract

The dinitrogen derivative [*closo*-1-CB₉H₉-1-N₂] (**1**) was prepared from amine [*closo*-1-CB₉H₉-1-NH₃] (**2**) and reacted with three types of nucleophiles: activated arenes (phenolate and aniline), divalent sulfur compounds (Me₂S and Me₂NCHS), and pyridine giving products of substitution at C(1). The reaction of **1** with pyridine gave all four isomers **11a-11d** indicating the Gomberg-Bachmann mechanism, which involves radical anion [*closo*-1-CB₉H₉]^{•-} (**25**). The radical and also closed-shell electrophilic aromatic substitution mechanisms were probed with the aid of DFT and MP2 computational methods and compared to those of phenylation of pyridine. Overall, experimental results supported by computational analysis suggest two mechanisms for the substitution of the N₂ group in **1**: *i*) thermal heterolytic cleavage of the C–N bond and the formation of electrophilic carbenium ylide [*closo*-1-CB₉H₉] (**19**), and *ii*) electron transfer induced homolytic cleavage of the C–N bond and the formation of **25**. Decomposition of **1** in MeCN is believed to proceed by the non-radical mechanism involving formation of the ylide **19** as the rate-determining step with experimental activation parameters $\Delta H^\ddagger = 38.4 \pm 0.8 \text{ kcal mol}^{-1}$ and $\Delta S^\ddagger = 44.5 \pm 2.5 \text{ cal mol}^{-1} \text{ K}^{-1}$. The ET-induced formation of **25** is consistent with the relatively high reduction potential of **1** ($E_{pc} = -0.54 \text{ V}$), which is more cathodic than that of PhN₂⁺ by 0.38 V.

Transformations of the phenol **8a** and the Me₂NCHS adduct **10** were demonstrated by *O*-methylation of the former and hydrolysis of **10** followed by *S*-alkylative cyclization. Direct products and their derivatives were investigated by UV-vis spectroscopy and analyzed with ZINDO computational method.

Introduction

Dinitrogen derivatives of the [*closo*-B₁₀H₁₀]⁻² cluster are isolable stable¹⁻⁶ and important intermediates in the preparation of a variety of nitrogen,^{1-4,6-8} sulfur,^{4,6,8,9} oxygen,^{4,10} and even carbon⁴ derivatives. Our calculations showed that the moderate stability and hence synthetic usefulness of these intermediates originates from the electronic interaction between the cluster and the N₂ group, which appears to be general for the apical position of 10-vertex *closo*-boranes.¹¹ Indeed, scant indirect evidence suggests that [*closo*-1-CB₉H₉-1-N₂] (**1**), formed by diazotization of amine [*closo*-1-CB₉H₉-1-NH₃] (**2**), is also reasonably stable and was implied as an intermediate in a reaction with Me₂S.¹² Therefore, in analogy to the dinitrogen derivatives of [*closo*-B₁₀H₁₀]⁻², compound **1** and its derivatives have the potential of becoming synthetically valuable intermediates in introduction of substituents at the C(1) position of the {*closo*-1-CB₉} cage.

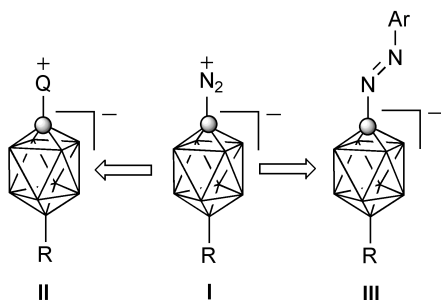


Figure 1. General structures for the polar and ionic derivatives **II** and **III**, and their precursor **I**. Q represents an onium fragment such as quinuclidinium, pyridinium, or sulfonium.

Our interest^{7,8,13-15} in highly polar and ionic molecular materials focused our attention on dinitrogen derivatives **I**, 10-substituted derivatives of **1**, as potential intermediates in the synthesis of zwitterionic and anionic azo compounds of the general structure **II** and **III**, respectively (Figure 1). In this context, we recently developed^{15,16} synthetic access to isomerically pure [*closo*-1-CB₉H₈-1-NH₂-10-I]⁻ as the key starting material for the preparation of **II** and **III**. In this precursor, the amino group is expected to serve as a synthetic handle for the introduction of a sulfonium fragment, a pyridin-1-yl group, and an azo group through the dinitrogen derivative **I**. Therefore, we desired to gain an understanding of the properties and reactivity of **1** as a model for **I** and a step towards the development of synthetic access to **II** and **III**.

Here we report a reliable method for the preparation of amine **2**, which upon diazotization gives [*closo*-1-CB₉H₉-1-N₂] (**1**). Then, we describe the thermal stability and reactivity of dinitrogen derivative **1** with several nucleophilic reagents. In particular, we explored reactions that lead to derivatives with the protected mercapto functionality,

diazocoupling to aromatic compounds, and reactions with pyridine. The mechanism of the reaction of **1** with pyridine was investigated experimentally and analyzed with the aid of DFT and MP2 computational methods. The dinitrogen derivative **1** and several products derived from it were investigated with UV-vis spectroscopic methods, and the experimental results were compared to the ZINDO computational data. Finally, the transmission of the C(1) substituent electronic effects through the {*closo*-1-CB₉} cage was briefly investigated and compared to that of {*closo*-1-CB₁₁} and the benzene ring.

Results

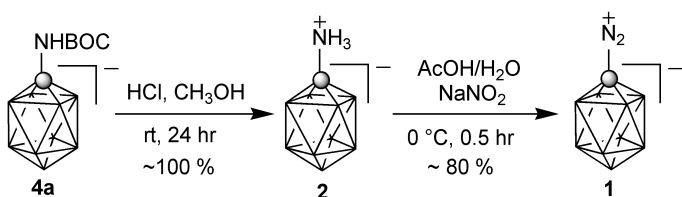
Synthesis of [closo-1-CB₉H₉-1-N₂] (1)

The preparation of [*closo*-1-CB₉H₉-1-N₂] (**1**) was accomplished by diazotization of [*closo*-1-CB₉H₉-1-NH₃] (**2**) in a 50% aqueous AcOH with 1.1 eq of NaNO₂ (Scheme 1). The dinitrogen derivative **1** was formed as a white precipitate and conveniently isolated by filtration in yields >80%. Diazotization of contaminated amine **2**, for example with carboxylic acid **3**, also was satisfactory albeit with lower yields of **1**, since the ionic impurity tends to stay in solution. The ratio and amounts of AcOH and H₂O were optimized to maximize the material recovery.

The dinitrogen derivative **1** is a white microcrystalline substance easily soluble in common organic solvents, except for alkanes. It is stable in the solid state at 0 °C for at

least 18 months without traces of decomposition. When heated, solid **1** rapidly decomposes at 87 °C. Its solutions in MeCN are stable for 24 hr at ambient temperature in the dark with little (about 10%) decomposition to a single product. In contrast, dinitrogen **1** completely decomposes in CH₂Cl₂ and benzene solutions into mostly intractable mixture of presumably polymeric and degradation products after 24 hr in the dark at ambient temperature. NMR spectra of **1** display a significant solvent dependence. Thus, the signals of ¹¹B(10) and ¹H(10) nuclei are shifted by about 6 ppm and 1.2 ppm, respectively, downfield in benzene-*d*₆ relative to those measured in CD₃CN solutions.

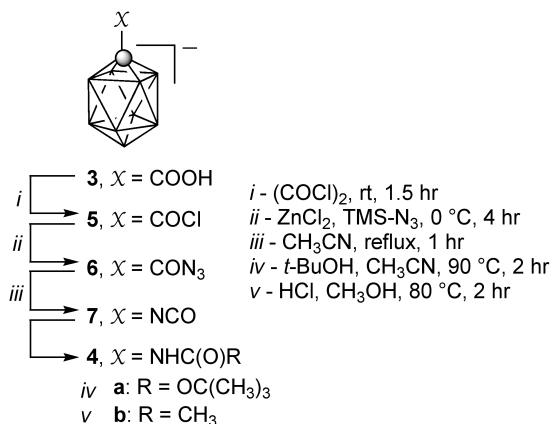
Scheme 1



Although amine **2** has been reported in the literature,¹² its previous preparation was complicated by the formation of the closely related [*closo*-1-CB₁₁H₁₁-1-NH₃] as a byproduct. Also, this method does not allow for introduction of a substituent at the B(10) position. Therefore, we decided to develop a reliable access to **2** starting from the readily accessible carboxylic acid **3**.¹⁶ Our initial attempts at direct conversion of carboxylic acid **3** to amine **2** using several methods such as the classical Schmidt¹⁷ and Curtius reactions,¹⁸ azidotrimethylsilane,¹⁹ azidotrimethylsilane and NaN₃,²⁰ diphenylphosphoryl azide,²¹ and hydroxylamine sulfonic acid²² were unsatisfactory and plagued by poor yields,

irreproducibility, low reactivity with acid **3**[NEt₄], and numerous unidentified side products as evident by ¹¹B NMR. Eventually, we focused on the Curtius reaction and carbamate **4** as the isolable intermediate, which could be purified and serve as a convenient storage for amine **2**. Conditions for each synthetic step were optimized and the reactions were followed by monitoring the chemical shifts of the B(10) nucleus in ¹¹B NMR spectra and the IR vibrations of the carbonyl group (see Supporting Information). Thus, the required carbamate **4a**[NEt₄] was prepared in four steps and about 50% overall yield based on carboxylic acid **3**[NEt₄] using a modified Curtius rearrangement (Scheme 2). The starting acid **3**[NEt₄] was obtained from B₁₀H₁₄ as described before.¹⁶

Scheme 2



The first step of the preparation of carbamate **4a**[NEt₄] was the typically quantitative transformation of carboxylic acid **3**[NEt₄] to carbonyl chloride **5**[NEt₄] using (COCl)₂. The crude chloride **5**[NEt₄] was then converted to acyl azide **6**[NEt₄] using Me₃SiN₃ in the presence of ZnCl₂ according to a general literature procedure.²³ ¹¹B NMR

spectra typically showed 85% conversion to the azide **6**[NEt₄] with the remaining chloride **5**[NEt₄] being hydrolyzed back to acid **3**[NEt₄]. A minor peak at 25.1 ppm in ¹¹B NMR spectra of the crude reaction mixture was also present, which was later attributed to isocyanate **7**[NEt₄]. The premature rearrangement of azide **6**[NEt₄] to **7**[NEt₄] was most likely promoted by the Lewis acid catalyst rather than thermal induction.²⁴

Attempts at improving this process through manipulation with reaction times, catalyst loading, and thorough drying the catalyst were unsuccessful. The IR spectrum of azide **6**[NEt₄] revealed vibrations characteristic for the azido and carbonyl groups and similar to those reported for benzoyl azide.²⁵

Crude azide **6**[NEt₄] was rearranged to isocyanate **7**[NEt₄] by refluxing in anhydrous CH₃CN. The completeness of the transformation was evident from ¹¹B NMR spectra in which the B(10) chemical shift of the former at 36.4 ppm was replaced with a peak at 25.1 ppm in the isocyanate. The product also showed an intense peak at 2262 cm⁻¹ in the IR spectrum, which is consistent with the ν_{NCO} vibration reported for phenyl isocyanate in the solid state (2255 cm⁻¹).²⁶ On the basis of the ¹¹B NMR spectrum the purity of the crude isocyanate **7**[NEt₄] was estimated as about 90%.

Initially, we envisioned conversion of isocyanate **7**[NEt₄] directly to amine **2**, but this approach was not fruitful. Isocyanate **7**[NEt₄] was insoluble in aqueous HCl even at elevated temperatures. Attempted hydrolysis of **7**[NEt₄] in a 1:1 mixture of 18% HCl and CH₃OH at 80 °C gave a mixture of amine **2** and methyl carbamate **4b**[H₃O] upon

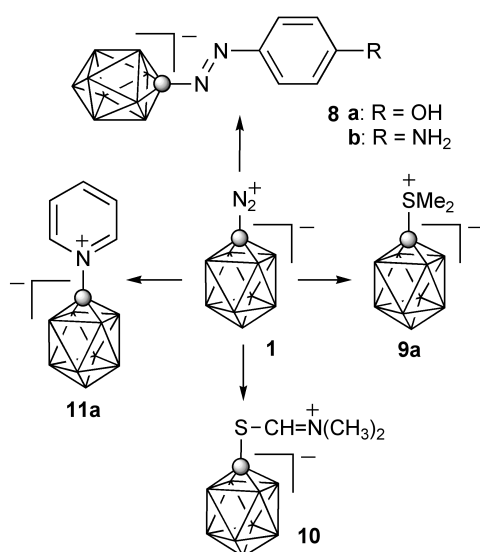
extraction from acidified aqueous solutions, according to ^{11}B NMR analysis. The carbamate **4b**[H_3O] was cleanly converted to amine **2** under basic conditions, which prompted us to investigate the carbamates as possible intermediates that could be isolated in their pure forms and converted to amine **2** in high yields. However, attempts to separate the methyl carbamate **4b**[NEt_4] from carboxylic acid **3**[NEt_4] by chromatography proved difficult due to its low solubility and also insufficient difference in mobility on silica gel. Therefore, we focused on *t*-Bu carbamate **4a**[NEt_4], which could be converted to the amine under mildly acidic conditions.

A reaction of isocyanate **7**[NEt_4] with anhydrous *t*-butanol gave *t*-Bu carbamate **4a**[NEt_4] in a high yield. Initial attempts at chromatographic separation on SiO_2 column using $\text{CH}_3\text{CN}/\text{CH}_2\text{Cl}_2$ (1:4) as the eluent showed that pure carbamate **4a**[NEt_4] could be isolated in low yields (~20%). Mass balance was achieved with more polar fractions, which contained mostly amine **2** apparently arising from deprotection of the BOC group on the SiO_2 support. The decomposition of **4a**[NEt_4] was minimized by buffering the solvent system with 1% NEt_3 . The yield of carbamate **4a**[NEt_4] rose to about 50%, but deprotection on the column was still observed. Treatment of carbamate **4a**[NEt_4] with HCl in CH_3OH solution followed by evaporation of the volatiles gave pure **2** in quantitative yield.

Reactivity of [closo-1-CB₉H₉-1-N₂]

Dinitrogen derivative **1** was reacted with three types of nucleophiles: activated arenes, divalent sulfur compounds, and pyridine. The reagents were chosen to demonstrate the formation of functionalizable azo derivatives **8**, the formation of inner sulfonium salts directly (**9a**) or through a masked mercaptan (**10**), and to investigate the formation of pyridin-1-yl derivative **11a** (Scheme 3).

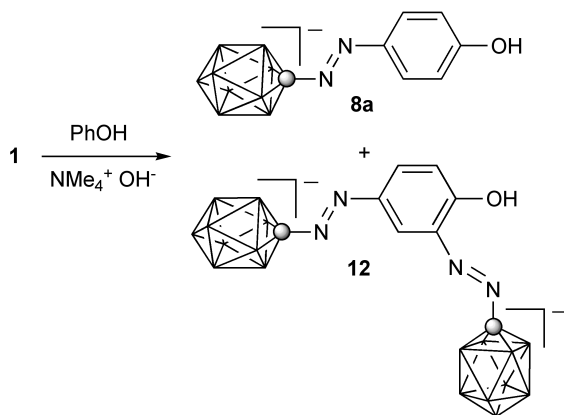
Scheme 3



A reaction of **1** with stoichiometric amounts of tetraethylammonium phenolate showed that both mono **8a** and double **12** diazocoupling products were formed in a ratio of up to 5:1 (Scheme 4). Attempts to separate **8a**[NEt₄] from **12**[2NEt₄] were unsuccessful both by recrystallization (EtOH/H₂O mixtures) and chromatography (CH₃CN/CH₂Cl₂ mixtures). The formation of the double substitution product **12** was

minimized by using a 5-fold excess of the phenolate. In contrast, no double diazocoupling was observed in reactions of **1** with stoichiometric amounts of aniline.

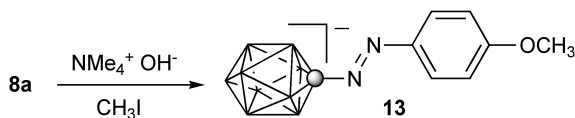
Scheme 4



Purification of azo derivatives **8a** and **8b** was cumbersome, however, chromatographic separation of the acid extract followed by precipitation as the NMe_4^+ salt gave reasonably pure compound in yields of 50% and 80%, respectively. The use of NMe_4^+ as the counterion gave more crystalline products compared to those with NEt_4^+ .

The azophenol **8a**[NMe_4] was easily methylated under basic conditions to give the methoxy derivative **13**[NMe_4] in 95% yield (Scheme 5).

Scheme 5

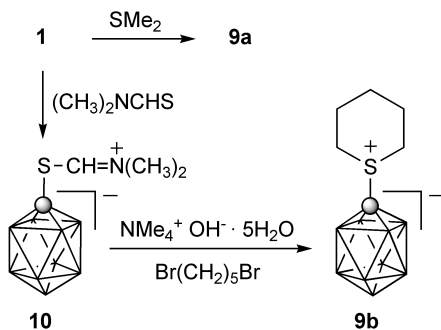


Dinitrogen derivative **1** was completely reacted with neat Me_2S at ambient

temperature over the period of 24 hrs giving adduct **9a**, which was isolated in 40% yield. ¹¹B NMR analysis of the crude reaction mixture revealed four signals; three doublets of product **9a** and an unrelated singlet at 20.1 ppm. The singlet appears to be associated with the film of white material, presumably boric acid, which was poorly soluble in CD₃CN and well soluble in CD₃OD (18.8 ppm). Previously, **9a** was prepared in 68% yield based on amine **2** without isolation of the intermediate **1**.¹²

A 24 hr reaction of **1** with *N,N*-dimethylthioformamide at ambient temperature gave 80% yield of crude **10** after washing with toluene. ¹¹B NMR analysis of the crude product revealed the presence of about 10% of the parent anion [*closo*-1-CB₉H₁₀]⁻ (**14**), and also a low intensity singlet at 20.1 ppm. Attempts to purify the zwitterion **10** further were unsuccessful due to its partial decomposition observed during recrystallization from CH₃CN/toluene mixtures or 1,2-dichloroethane. Purification on silica gel was avoided, since **10** appeared to be hydrolytically unstable. Alkylation of crude **10** with 1,5-dibromopentane in the presence of a base followed by chromatographic separation and recrystallization gave pure **9b** in 50% yield based on **1** (Scheme 6). This represents a slightly higher yield than that for a single step preparation of **9a** directly from **1**.

Scheme 6

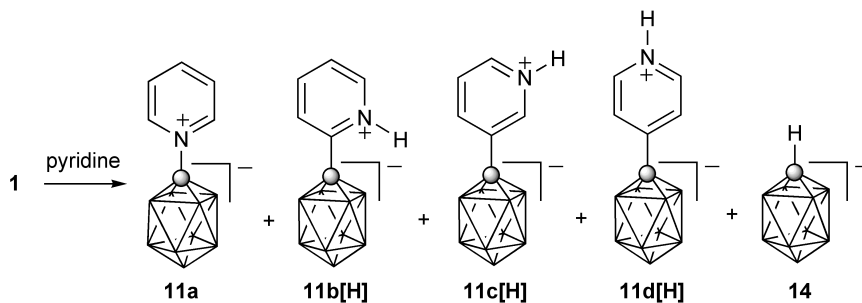


Reactions of **1** with pyridine were most interesting. When **1** was reacted in neat pyridine at ambient temperature for several hours, ^{11}B NMR analysis revealed a complex mixture of at least 4 products exhibiting characteristic doublets in the region of 25 ppm to 40 ppm (Table 1). Surprisingly, the major component of the reaction mixture, about 50%, was identified as the 2-isomer **11b[H]**. A doublet at δ 29.6 ppm with 20% intensity was assigned to the parent anion **14** on the basis of comparison with literature data.²⁷ This was further supported by a comparison with an authentic sample of **14** with pyridinium as the counterion (**14[PyrH]**) to maintain consistency with the reaction conditions.

The crude mixture was separated on silica gel giving the 2-isomer **11b[H]** in 40% isolated yield as the first fraction. The doublet at δ at 35.7 ppm observed in the crude mixture and originally assigned to the B(10) nucleus of **11b**, was shifted downfield by about 2 ppm in the isolated sample. This shift presumably results from transformation of pyridinium salt of **11b[-]** to the zwitterionic structure **11b[H]** of the isolated product. Such downfield shifts were observed for the other two isomers **11c** and **11d** but they were less significant. The more polar fraction contained a mixture of two other isomers, **11c[H]**

and **11d**[H], which were identified on the basis of 1D ^1H and 2D ^1H - ^1H COSY NMR analysis.

Table 1. Product Distributions in Reaction of **1** with Pyridine.



Conditions	Products				
	11a	11b [H]	11c [H]	11d [H]	14
Neat pyridine					
25 °C ^a	Traces	40% ^b	17% ^c	10% ^c	6% ^c
90 °C ^c	17% ^b	20% ^c	18% ^c	9% ^c	5% ^c
Solutions of pyridine					
4% in CH ₂ Cl ₂ ^d	17% ^e	7% ^e	0% ^e	0% ^e	20% ^e
4% in Benzene ^f	13% ^e	17% ^e	0% ^e	0% ^e	5% ^e
¹¹ B NMR for B(10), δ ^g	33.1 ppm	37.2 ppm	33.9 ppm	35.9 ppm	29.6 ppm

^a About 75 % of total mass recovery after separation on SiO₂.

^b Yield of isolated product.

^c Yield based on ¹¹B NMR of the mixture corrected for its mass.

^d [*closo*-1-CB₉H₉-1-Cl]⁻ (**15**) constituted 56% of the mixture.

^e Ratio of low field signals for the crude reaction mixture.

^f [*closo*-1-CB₉H₉-1-Ph]⁻ (**16**) constituted 65% of the crude reaction mixture.

^g Chemical shifts of the isolated products or mixtures.

Addition of hot pyridine to the dinitrogen derivative **1** had a different outcome. ¹¹B NMR analysis of the crude reaction mixture revealed four products [δ B(10): 35.0, 33.1, 31.9, 29.6]. Chromatographic separation gave **11a** in 17% isolated yield as the least polar fraction. The more polar fraction contained the remaining three isomers and also the parent anion **14** in about 4:4:2:1 ratio (Table 1).

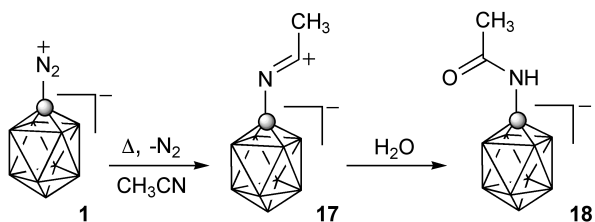
To provide more information about the possible mechanism for the formation of these products, reactions of **1** were run in dilute solutions of pyridine at ambient temperature for 18 hrs. Thus, a reaction of **1** with a 4% solution of pyridine in CH₂Cl₂ gave [*closo*-1-CB₉H₉-1-Cl]⁻ (**15**)²⁸ as the major product along with **11a**, **11b**, and **14** in an approximate ratio of 8:3:1:3, respectively, according to the ¹¹B NMR analysis of the crude reaction mixture (Table 1). A similar reaction of **1** with a 4% solution of pyridine in benzene gave the [*closo*-1-CB₉H₉-1-Ph]⁻ (**16**)²⁹ as the major product. Isomers **11a** and **11b** were formed as minor products, in 13% and 17% yields, respectively, and no signals belonging to **11c** or **11d** were found in the ¹¹B NMR spectrum of the crude mixture (Table 1). For comparison, decomposition of **1** in pure benzene-*d*₆ at ambient temperature gave a number of products among which **16-d**₅ was identified by MS. A solution of **1** in CD₂Cl₂ gave only a broad featureless absorption band in a range -10 ppm to -40 ppm and a broad band around 20 ppm in ¹¹B NMR after 24 hr at ambient temperature, which suggests complete destruction of the {*closo*-1-CB₉} cluster. Dinitrogen derivative **1** in 4% solution

of pyridine in CD₃CN was stable at 0 °C for 3 hrs, whereas at 45 °C, 45% of **1** reacted in 75 min giving about 30% of **17** (Scheme 7) and 4% of **11a** in addition to unidentified signals at 16.7, 25.3, and 10.0 ppm (in decreasing intensity order) in the ¹H-decoupled spectrum.

Reaction with MeCN and kinetic data for 1

Decomposition of dinitrogen derivative **1** in dried CH₃CN at elevated temperatures (~ 50 °C) gave a mixture of zwitterion **17** and acetamide **18** in about 1:1 ratio as the only products (Scheme 7). ¹H NMR revealed two partially overlapping quartets centered at 5.91 and 5.52 ppm and attributed to **17** and **18**, respectively. Adduct **17** appears to be the primary product, which partially undergoes hydration to the acetamide **18** with residual H₂O in the solvent. Exposure of the crude reaction mixture to moisture quickly and quantitatively converted **17** to the acetamide **18**, which was isolated and characterized by NMR and MS techniques. The clean transformation of **1** to the two related products and sufficient separation of the signals in the ¹H NMR spectrum made it possible to analyze kinetics of this reaction. It is believed that the rate determining step of the process is the heterolytic cleavage of the C–N bond in **1**.

Scheme 7



Kinetics of decomposition of the dinitrogen derivative **1** was investigated in dried CD₃CN as a function of temperature and was followed by ¹H NMR spectroscopy. Intensities of the disappearing B(10)-H signal at 7.21 ppm, which is part of a quartet centered at 6.72 ppm belonging to **1**, and the growing peak at 5.82 ppm, part of the pseudo quintet (partially overlapping quartets of **17-d₃** and **18-d₃**) were used to calculate the ratio of **1** to the sum of products **17-d₃** and **18-d₃**. Standard kinetic analysis using the Eyring equation found $\Delta H^\ddagger = 38.4 \pm 0.8 \text{ kcal mol}^{-1}$, $\Delta S^\ddagger = 44.5 \pm 2.5 \text{ cal mol}^{-1} \text{ K}^{-1}$, and $\Delta G^\ddagger = 25.1 \pm 0.8 \text{ kcal mol}^{-1}$ at 298 K.

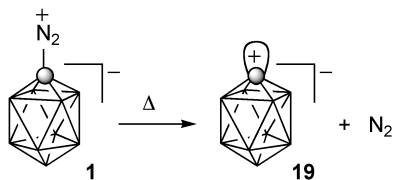
Mechanistic Studies. Computational Analysis.

To shed more light on properties of **1** and its reactions with nucleophiles, we conducted quantum-mechanical calculations initially at the B3LYP/6-31G(d,p) level of theory to establish conformational minima and to obtain thermodynamic corrections. The resulting structures were used to calculate the SCF energies at the MP2/6-31(d,p) level of theory. Since **1** and other molecules involved are highly polar or ionic, the SCRF solvation model was used to compute their SCF energies at the MP2/6-31G(d,p) or

MP2/6-31+G(d,p) level of theory in an appropriate dielectric medium (pyridine or MeCN). Computational results are shown in Figures 2-5 and Tables 2-5, and full numerical data is provided in Supporting Information.

Generation and structure of the carbenium ylide. The dinitrogen derivative **1** undergoes a heterolytic cleavage of the C–N bond and the process is calculated to be endothermic by 33.2 kcal/mol in gas phase at the MP2//DFT level of theory with the 6-31G(d,p) basis set. This value is practically the same as that obtained using the MP2//MP2 method with the same basis set (Table 2). Since the resulting carbenium ylide **19** ($\mu = 4.0$ D) is less polar than **1** ($\mu = 7.2$ D), the endotherm increases to 35.4 kcal/mol in pyridine ($\epsilon = 13.3$) and to 36.4 kcal/mol in MeCN ($\epsilon = 36.6$) dielectric medium. The MP2//DFT and MP2//MP2 calculations using diffused functions do not change the results significantly, although they give lower ΔH values up to 2 kcal/mol for the latter method. In contrast to the MP2 results, the enthalpy change in the reaction calculated by the DFT method was smaller by about 10 kcal/mol. This difference is related to the inadequate treatment of electron correlation by the DFT methods and demonstrates the importance of dispersive forces in stabilization of **1**.

Table 2. Enthalpy change in heterolytic dissociation of **1**.



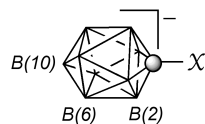
Method	ΔH /kcal/mol
<i>Gas Phase</i>	
B3LYP/6-31G(d,p)	24.6
MP2/6-31G(d,p)//B3LYP/6-31G(d,p) ^a	33.2
MP2/6-31G(d,p)	33.3
<i>ICPM model ($\epsilon = 36.6$)</i>	
MP2/6-31G(d,p)//B3LYP/6-31G(d,p) ^a	36.4
MP2/6-31+G(d,p)//B3LYP/6-31G(d,p) ^a	35.0
MP2/6-31+G(d,p)//MP2/6-31G(d,p) ^a	34.4

^a B3LYP/6-31G(d,p) thermodynamic corrections. $\Delta S = +43.6$ cal/mol*K.

A transition state search with the DFT method for the loss of N₂ by **1** located a transition structure **1-TS** in which the C(1)–N bond is elongated by about 0.8 Å ($d_{C-N} = 2.13$ Å). The DFT calculated activation parameters, $\Delta H^\ddagger = 25.4$ kcal/mol and $\Delta S^\ddagger = 12.5$ cal/mol K fall sort of the experimental data (*vide supra*). Single point calculations for **1-TS** at the MP2//DFT level of theory gave $\Delta H^\ddagger = 30.4$ kcal/mol in pyridine dielectric medium, which is lower by 6 kcal/mol than the enthalpy change for the complete reaction. In addition, the calculations demonstrated practically an energy plateau between $d_{C-N} =$

2.13 Å ($\Delta E_{\text{SCF}} = 33.95$ kcal/mol) and $d_{\text{C-N}} = 2.70$ Å ($\Delta E_{\text{SCF}} = 34.45$ kcal/mol), whereas ΔE_{SCF} for $d_{\text{C-N}} = 3.5$ Å is 36.6 kcal/mol and for the complete reaction is 37.8 kcal/mol.

Table 3. Calculated structural parameters for selected derivatives of {*closo*-1-CB₉}



	X = H 14	X = N ₂ ⁺ 1	X = • 25	X = + 19
<i>Geometry</i>				
C(1)–B(2) /Å	1.602	1.624	1.585	1.532
B(2)–B(3) /Å	1.836	1.885	1.849	1.928
B(2)–B(6) /Å	1.802	1.785	1.809	1.829
B(6)–B(10) /Å	1.700	1.711	1.698	1.678
B–C–B /°	108.3	110.2	111.2	125.8
<i>Natural Atomic Charge</i> ^c				
C(1)	-0.77	-0.52	-0.36	-0.34
B(2)	0.03	0.08	-0.01	0.07
B(6)	-0.19	-0.19	-0.18	0.11
B(10)	-0.17	-0.06	-0.20	-0.32
<i>Bonding</i> ^c				
C(1) exo	sp ^{2.03} (1.94)	sp ^{3.37} (1.96)	sp ^{3.97} (0.95)	sp ^{99.8} (0.67)

^a Optimized at the MP2/6-31G(d,p) level of theory at the C_{4v} point group symmetry. ^b C–N distance 1.337 Å, N–N distance, 1.149 Å. ^c NBO analysis.

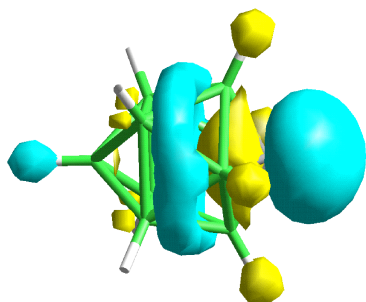


Figure 2. The MP2/6-31G(d,p) derived contour for the LUMO ($E = -1.57$ eV) of ylide **19**.

MP2-level calculations demonstrated that the carbenium ylide **19** is a zwitterionic species. The carbon exocyclic orbital is practically a pure p orbital and partially populated (-0.34 e) at the expense of the boron atoms in the lower belt (Table 3). The LUMO of **19** is primarily localized on the C(1) atom with a contribution from the lower belt of boron atoms (Figure 2).

The loss of electron density from the carbon exocyclic orbital markedly affects the geometry of the {*closo*-1-CB₉} cage (Table 3). Thus, the departure of N₂ by **1** results in a less pyramidalized apical carbon atom, contraction of the C–B interatomic distances, and significant expansion of the interbelt B–B bonds in the ylide **19** as compared to **1**.

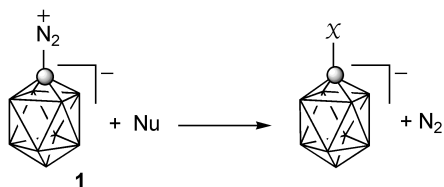
Reaction of the ylide with nucleophiles. The resulting electron deficient intermediate, carbenium ylide **19**, is a highly reactive electrophile. In the simplest case, it reacts with Lewis bases in a two-electron process giving C–substitution products such as **9**, **11a**, and **20**. The overall two-step nucleophilic substitution reactions (S_N1) of **1** are highly exothermic with the enthalpy change exceeding -30 kcal/mol and typically about -60

kcal/mol in vacuum (Table 4). Analysis of results for the four isomeric pyridine adducts **11a**[H]–**11d**[H] demonstrates that the most thermodynamically stable isomer is **11b**[H], while the least stable is the *N*-isomer **11a** (**11b**[H] > **11d**[H] > **11c**[H] > **11a**) in vacuum. The compounds have substantial dipole moments, up to 3 times of that for the starting dinitrogen derivative **1** (6.1 D), and significant solvent effect on the reaction's exotherm can be expected in polar media. Indeed, IPCM calculations in the dielectric medium increase the stability of all isomers, but the largest gain is observed for the C(3)-isomer **11c**[H]. Consequently, the ΔH for the formation of **11c**[H] in pyridine solutions is about 21 kcal/mol larger than in vacuum, which makes it the most exothermic and exoergic process among the formation of all regioisomers (Table 4). The exotherm for the formation of other regioisomers is smaller and the resulting order of thermodynamic stability follows: **11c**[H] > **11b**[H] > **11d**[H] > **11a**. Interestingly, in both sets of calculations the *N*-isomer **11a** is predicted to be the least thermodynamically stable.

MP2//DFT calculations demonstrated that the dipole moment of the zwitterionic compounds significantly depends on the solvent polarity (Table 4). For instance, with increasing polarity of the medium the dipole moment of **1** increases ($\mu = 6.1$ D, $\epsilon = 1$; $\mu = 8.1$ D, $\epsilon = 13.3$; $\mu = 8.4$ D, $\epsilon = 36.6$) due to increasing net negative charge at the 10 position from +0.062 for B(10) and +0.0013 for H(10) ($\epsilon = 13.3$) to +0.051 for B(10) and -0.0002 for H(10) ($\epsilon = 36.6$). This is consistent with the observed solvent effect on NMR spectra and higher nuclear shielding in CD₃CN as compared to benzene-*d*₆ solutions (*vide supra*).

Calculations in the dielectric medium also demonstrated that two of the protonated derivatives **11b[H]** and **11d[H]** are significantly stronger acids than pyridinium, and proton transfer to pyridine is moderately exothermic (Table 5). For the C(3) isomer **11c[H]** the process is practically thermoneutral. The resulting anions **11[-]** have very similar energies in pyridine dielectric medium with the C(4) isomer **11d[-]** slightly more stable than the C(2) isomer **11b[-]** and more stable by 1.7 kcal/mol than **11c[-]**.

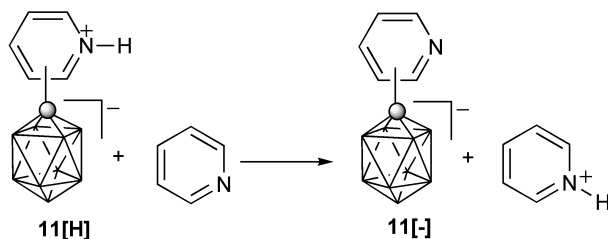
Table 4. Enthalpy change in substitution reactions of **1**.^a



Reagent	Product	χ	ΔH /kcal mol ⁻¹		Dipole /D	
			$\epsilon = 1$ ^b	$\epsilon = 13.3$ ^c	$\epsilon = 1$ ^b	$\epsilon = 13.3$ ^c
Me ₂ S	9a	Me ₂ S ⁺	-45.5	^d	12.8	^d
Pyridine	11a	1-C ₅ H ₅ N ⁺	-59.2	-67.2	15.1	18.6
	11b[H]	2-C ₅ H ₄ NH ⁺	-67.9	-76.4	15.7	19.1
	11c[H]	3-C ₅ H ₄ NH ⁺	-59.9	-81.4	19.2	24.2
	11d[H]	4-C ₅ H ₄ NH ⁺	-61.0	-75.4	19.2	24.2
MeCN	17	MeCN ⁺	-30.7	-34.7 ^e	14.0	17.4 ^e
NMe ₃	20	NMe ₃ ⁺	-60.0	^d	13.3	^d

^a MP2/6-31G(d,p)//B3LYP/6-31G(d,p) level with DFT thermodynamic corrections. ^b Vacuum calculations. ^c IPCM solvation model. ^d Not calculated. ^e Calculated for $\epsilon = 36.6$.

Table 5. Calculated free energy change in deprotonation reactions of **11**.^a



	b	c	d
ΔG_{298}	-5.9	+0.5	-7.3
kcal mol ⁻¹			

^a MP2/6-31G(d,p)//B3LYP/6-31G(d,p) calculations in with DFT thermodynamic corrections. IPCM solvation model $\epsilon = 13.3$.

Formation of pyridine derivatives **11**. The formation of four regioisomeric products **11a–11d** may involve either 2-electron or 1-electron process. Initially, we focused on the former and considered electrophilic reactions of the carbenium ylide **19** with pyridine.

The formation of the N(1) isomer (**11a**) can be envisioned as a simple one-step collapse of a Lewis acid (ylide **19**) and a Lewis base (pyridine) to form the C–N bond (Figure 3). Our attempts to locate the transition state for the reaction using the DFT method were unsuccessful, which indicates that the process may be practically barrierless. In contrast, the formation of the C-substituted isomers **11b–11d** involves a two-step process, with the initial formation of arenium zwitterions **21b–21d** followed by a proton transfer. The calculated energy for the arenium ions is much higher, by about 60 kcal/mol, than that for the direct adduct **11a**. Computational results indicate that the order of stability for zwitterions **21** follows: **21c** > **21b** > **21d** in both gas phase and the dielectric

medium; the latter stabilizes the highly polar intermediates by 10-13 kcal/mol relative to gas phase. Proton transfer from **21** to pyridine and the formation of anions **11[-]** is highly exothermic, which renders the process irreversible.

Even though transition state structures for the formation of **21** were not located and their energies were not calculated, it seems unlikely that they would be formed preferentially to the direct collapse of the reactants into the N(1) isomer **11a**. In addition, the formation of the C(2) regioisomer **11b**, experimentally observed as the major product, is not consistent with the relative stabilities of the arenium ions **21**. Instead, calculations strongly favor the C(3) isomer **21c**, which is consistent with the established regioselectivity of electrophilic substitution in pyridine.³⁰

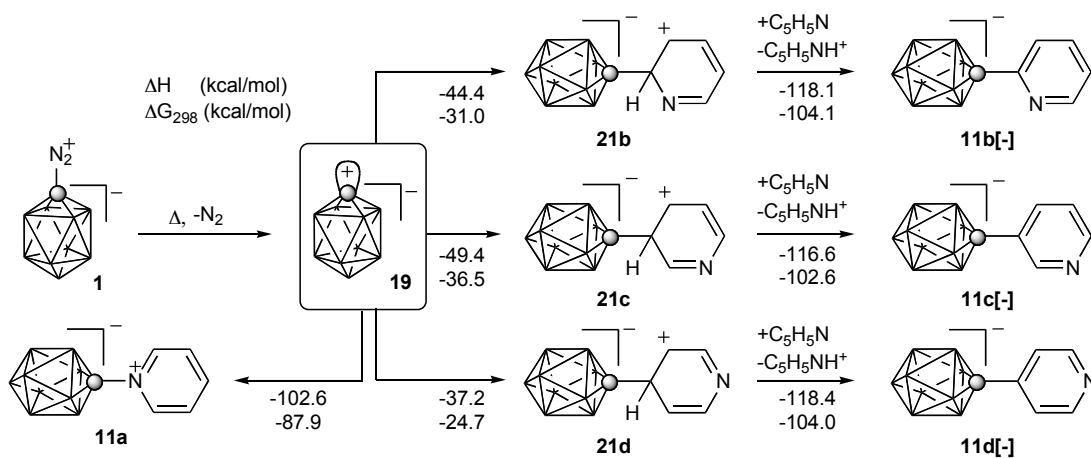


Figure 3. Electrophilic substitution of pyridine. Energy change relative to ylide **19** and pyridine (MP2/6-31G(d,p)//B3LYP/6-31G(d,p), $\epsilon = 13.3$). For the reaction with radical ion **25** the intermediates **27** are analogous to **21** with the delocalized unpaired spin instead of the positive charge.

An alternative mechanism for the formation of **11b–11d** may involve a radical

process initiated by the addition of pyridine to the electrophilic dinitrogen group of **1**. Indeed, both DFT- and MP2-level calculations located the pyridine adduct **22** on the potential energy surface. The formation of the highly polar azene **22** ($\mu = 23.2$ D) was found to be endothermic by 14.3 kcal/mol or endoergic by 24.8 kcal/mol at the MP2//DFT level of theory in pyridine dielectric medium ($\epsilon = 13.3$).

According to this mechanism azene **22** undergoes fragmentation with a homolytic cleavage of the N–pyridine bond leading to the radical ion pair **23** and **24** (Figure 4). The process is highly endothermic in gas phase ($\Delta H = 133.0$ kcal/mol), but it becomes more favorable in pyridine dielectric medium ($\Delta G_{298} = +44.5$ kcal/mol). The diazenyl radical **23** easily loses molecular nitrogen ($\Delta G_{298} = -24.8$ kcal/mol) and forms radical ion **25**. The dissociation of the C–N bond and the direct formation of radical anion **25** is also possible, although the second ion, pyridinediazenyl radical (**26**), was not located on the potential energy surface with the DFT method. The calculated overall enthalpy change for the formation of the ion pair and N_2 from **1** is +145.9 kcal/mol in gas phase, but in pyridine ($\epsilon = 13.3$) this energy is lowered to $\Delta H = 56.4$ kcal/mol or $\Delta G_{298} = 44.4$ kcal/mol (Figure 4).

NBO analysis indicates that the apical carbon atom in radical ion **25** has a significant negative charge density (-0.36) and the radical is expected to be moderately nucleophilic (Table 3). Therefore, it may react with a molecule of neutral pyridine (solvent), which leads to regioisomeric radical anion adducts **27** (analogous to zwitterions **21** in Figure 3). Results show that in gas phase the C(2) intermediate **27b**, which leads to the experimentally observed major product **11b**, is least favored and its regioisomers

are more stable by about 3-4 kcal/mol (stability order: **27c** > **27a**, **27d** > **27b**, Table 6). The IPCM calculations demonstrated diminished exotherms of the adduct formation in the dielectric medium, with the heat of formation for the C(2) adduct **27b** being least affected. Consequently, the order of stability of the intermediates is changed in pyridine; the N(1) adduct **27a**, leading to the unobserved **11a**, become the least favored, whereas **27b** is less stable than **27c** by only 1.4 kcal/mol (order of stability: **27c** > **27b** > **27d** > **27a**, Table 6). The resulting adducts **27b–27d** undergo a highly exothermic (about 115 kcal/mol) process leading to products **11b[–]–11d[–]** and involving either a hydrogen atom transfer or a sequence of electron followed by proton transfer with pyridinium radical **24**. A reaction of radical anion **25** with pyridine radical cation **24** is predicted to be highly exothermic and leading directly to **11a**.

Our initial attempts to locate transition state structures for either types of adducts, radicals **27** or zwitterions **21**, were unsuccessful and due to computational intensity were not pursued further.

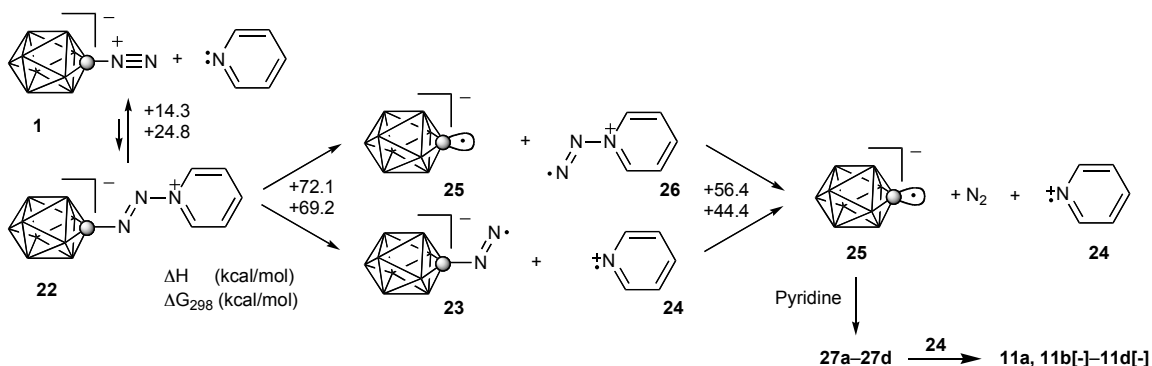
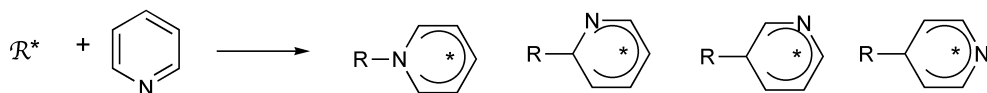


Figure 4. Formation of radical ion **25**. Enthalpy change relative to reactants calculated with MP2/6-31G(d,p)//B3LYP/6-31G(d,p) for the pyridine solution ($\epsilon = 13.3$).

Table 6. Calculated enthalpy change for reactions with pyridine.^a



React. interm.	*	Adduct	ϵ	N(1)	C(2)	C(3)	C(4)
R^*	*			a	b	c	d
19	+	21	1 ^b 13.3 ^c	-92.5 -102.6	-32.0 -44.4	-36.4 -49.4	-26.9 -37.2
25	•	27	1 ^b 13.3 ^c	-28.0 -22.9	-24.9 -23.4	-29.2 -24.8	-28.0 -23.1
$C_6H_5\cdot$ 31	•	32	1 ^b 13.3 ^c	-28.4 -26.0	-26.0 -25.3	-27.6 -28.4	-25.8 -28.0

^a MP2/6-31G(d,p)//B3LYP/6-31G(d,p) level with DFT thermodynamic corrections. ^b Vacuum calculations. ^c IPCM solvation model.

Phenylation of Pyridine. To provide a better support for the proposed radical process of formation of **11**, we also analyzed an analogous reaction between benzenediazonium ion and pyridine (Figure 5 and Table 6). According to the accepted mechanism, the formation of the *N*-phenylazopyridinium (**28**) is the first step in the free radical phenylation of pyridine, which leads to three regioisomeric *C*-phenylpyridines (**29**).³¹⁻³³ DFT calculations located the *N*-diazene **28** on the potential energy surface, and subsequent MP2//DFT calculations revealed that its formation is moderately endothermic ($\Delta H = +2.9$ kcal/mol, $\Delta G_{298} = +14.5$ kcal/mol) in pyridine dielectric medium (Figure 5). Homolytic cleavage of the N–N bond leading to the formation of phenyldiazenyl radical (**30**) and

radical cation **24** is significantly endoergic ($\Delta G_{298} = +51.7$ kcal/mol). This is partially compensated by the favorable decomposition of the diazenyl radical **30** and the formation of phenyl radical (**31**) and N_2 ($\Delta H = -11.6$ kcal/mol, $\Delta G_{298} = -21.5$ kcal/mol). Nevertheless, the overall process of formation of the phenyl radical is endothermic (Figure 5).

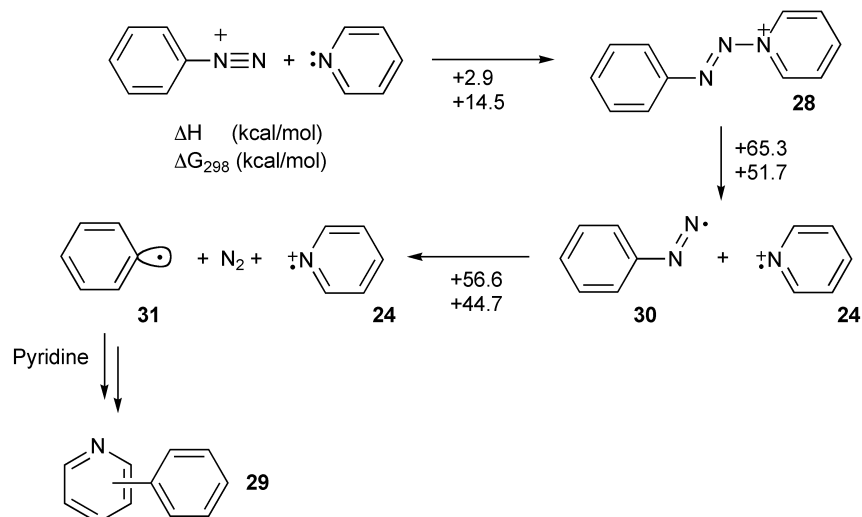


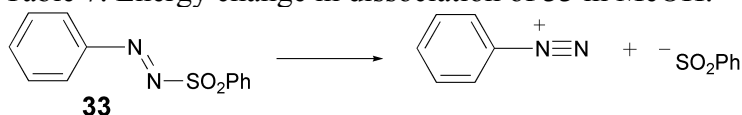
Figure 5. Formation of phenyl radical **31**. Energy change relative to reactants calculated with MP2/6-31G(d,p)//B3LYP/6-31G(d,p) for the pyridine solution ($\epsilon = 13.3$).

The addition of the resulting phenyl radical (**31**) to pyridine and the formation of the intermediates **32** is moderately exothermic with the highest exotherm calculated for the *N*-adduct **32a** (stability order: **32a** > **32c** > **32b** > **32d**) in gas phase (Table 6). The same calculations in dielectric medium decrease the reaction exotherm for **32a** and **32b** and increase the exotherm for **32c** and **32d**. Consequently, the order of the thermodynamic stability of the four intermediates is altered giving the preference for the C(3) isomer **32c** (stability order: **32c** > **32d** > **32a** > **32b**) in pyridine. Subsequent H^\bullet

transfer from **32** to **24** is highly exothermic ($\Delta H \approx -110$ kcal/mol) and gives the isomeric pyridines **29**. The calculated order of their thermodynamic stability (**29b** > **29d** ~ **29c**) is consistent with experimentally established trends in heats of formation.³⁴

Finally, we assessed the accuracy of the IPCM method in predicting the formation of ion pairs, such as **24** and **25**, by computing of the energy change for dissociation of azosulfone **33** and the formation of ion pair PhN_2^+ and PhSO_2^- in a dielectric medium. The experimentally³⁵ established association constant $K_{\text{assoc}} = 1.44 \times 10^5$ l/mol for the ion pair PhN_2^+ and PhSO_2^- in MeOH at 29 °C allows for the calculation of $\Delta G_{302} = +7.1$ kcal/mol for the dissociation of **33**. Our MP2//DFT calculations in gas phase demonstrated a high endotherm ($\Delta H = +67.9$ kcal/mol) for the dissociation process of **33** (Table 7). In the dielectric medium, however, the dissociation process of **33** becomes significantly more favorable reaching the value of $\Delta G_{302} = +12.6$ kcal/mol in MeOH. This represents a fairly good agreement between the theory and experiment, and indicates that MP2//DFT calculations underestimated the solvation of the ions by 5.5 kcal/mol. Consequently, stability of other ions in dielectric medium is most likely underestimated and their formation is more favorable than calculated.

Table 7. Energy change in dissociation of **33** in MeOH.^a



ϵ	ΔH / kcal mol ⁻¹	ΔG_{302} / kcal mol ⁻¹
1 ^b	67.9	56.1
30.9 ^{c,d}	24.5	12.6

^a MP2/6-31G(d,p)//B3LYP/6-31G(d,p) level with DFT thermodynamic corrections. ^b Vacuum calculations. ^c IPCM solvation model. ^d Value interpolated from data in ref³⁶.

Electronic Absorption Spectroscopy

Spectroscopic analysis of four derivatives **1**, **8**, **9a**, **11a**, and trimethylamine zwitterion **20**, provides convenient means to study electronic interactions between the {*closo*-1-CB₉} cage and the substituent at the C(1) position.

Among the five substituents, NMe₃ in **20** is the simplest and not possessing easily available electrons or accessible orbitals. Therefore, the electronic absorption spectrum of **20** closely resembles that of the parent [*closo*-1-CB₉H₁₀]⁻ anion (**14**) with the absorption tailing to about 250 nm and the maximum below 200 nm (Figure 6a). The presence of an electron pair in the SMe₂ substituent of **9a** resulted in the increased intensity of the band at about 200, appearance of a shoulder band at about 225 nm, and also a broad low intensity band at 272 nm. These spectral features are consistent with the transitions observed at about 230 nm and 200 nm for trialkylsulfonium salts.³⁷ It was also noted that the UV spectra of sulfonium salts are affected by the presence of molecular oxygen which gives rise to the appearance of CT bands.³⁷

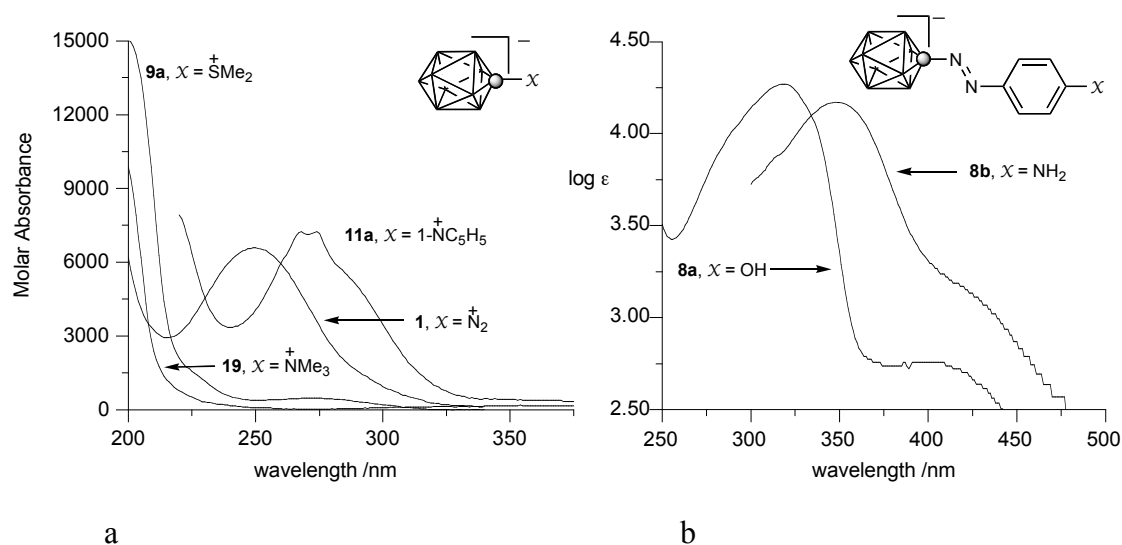


Figure 6. Electronic absorption spectra for selected compounds recorded in CH₃CN.

The dinitrogen, N₂, and pyridine groups are π substituents and their orbitals can interact with the electronic manifold of the {*closo*-1-CB₉} cage. Thus, the dinitrogen derivative **1** exhibits a single absorption band at 250 nm (Figure 6a). ZINDO//MP2 calculations revealed that **1** exhibits two $\pi \rightarrow \pi^*$ transitions, at 280 nm ($f = 0.49$) and a weaker at 242 nm ($f = 0.12$) in vacuum. The former involves the double degenerated HOMO, localized mostly on the cage, and the LUMO, localized primarily on the N₂ group (Figure 7). The higher energy transition is due to intra-cage excitations (HOMO \rightarrow LUMO+1). The same calculations conducted for **1** in the dielectric medium of the solvent ($\epsilon = 36.6$) revealed a substantial negative solvatochromic effect of the cage-to-substituent excitation and practically no solvent effect of the intra-cage excitation. Consequently, the two transitions merge into one, which is calculated at 247 nm ($f = 0.56$) and observed at 250 nm.

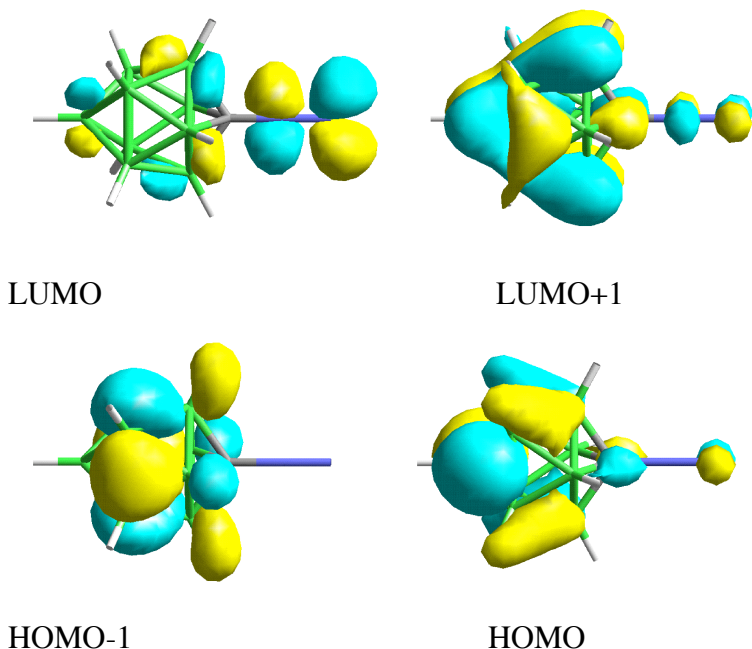


Figure 7. DFT – generated MO contours for **1**. For clarity only one part of each degenerated MO is shown.

Pyridine is the most complex substituent among the five groups; it has both the low-lying LUMO and also its own $\pi \rightarrow \pi^*$ transitions in the UV region. Consequently, the pyridine derivative **11a** is expected to exhibit three types electronic transitions: cage-ring, intra-ring, and intra-cage. The first two types apparently overlap and form a complex structure in the range of 240-300 nm (Figure 6a). The maximum of the broad, intense underlying band is estimated at 269 nm and attributed to the cage-to-ring CT transition. The upper fine structure has two maxima at 268 nm and 274 nm and represents pyridine B-band. Results of ZINDO//MP2 calculation for **11a** in dielectric medium ($\epsilon = 36.6$) support this assignment. The CT transition is calculated at 260 nm ($f = 0.32$) and involves the HOMO \rightarrow LUMO excitation (Figure 8) with a small contribution from the intra-cage

excitation (HOMO→LUMO+4). The pyridine B-band appears at 272 nm ($f = 0.08$) and involves HOMO-2→LUMO excitation. The same calculations for **11a** in vacuum give the CT transition at 361 nm ($f = 0.18$), which demonstrates a large negative solvatochromic effect (-1.34 eV) in this polar derivative (Table 4). The pyridine B-band experiences a smaller and positive solvatochromic shift (+0.37 eV).



Figure 8. DFT –generated HOMO and LUMO contours for **11a**.

Electronic spectra of the azo derivatives **8a** and **8b** exhibit absorption bands typical for azobenzenes.³⁸ The intense band of the $\pi \rightarrow \pi^*$ transition in azophenol **8a** appears at 318 nm ($\log \epsilon = 4.30$) and in azoaniline **8b** at 348 nm (Figure 6b), while the forbidden $n \rightarrow \pi^*$ transition is located at about 400 nm in both derivatives.

ZINDO//DFT calculations in MeCN dielectric medium ($\epsilon = 36.6$) demonstrated a low intensity transition at 445 nm ($f < 0.001$), which involves excitation from HOMO-2 and HOMO-4, localized on the nitrogen atom lone pairs and the cage, to the π symmetry orbitals LUMO+1 and LUMO+4, which are delocalized over the molecule with the main component from the {*closo*-1-CB₉} cage. The more intense transition is calculated at 329 nm ($f = 0.82$), which involves the excitation from HOMO, localized on the organic

fragment, mainly to the LUMO+1 and also to the LUMO+4 localized on the $\text{CB}_9\text{H}_9\text{-N=N}$ fragment (Figure 9).

In comparison to the azobenzene analogues, the electronic transitions of the $\{\textit{closo-1-CB}_9\}$ derivatives **8a** and **8b** are blue-shifted by 24-34 nm. For instance, absorption bands of 4-hydroxyazobenzene are recorded at 344 nm and 425 nm in CH_3CN .³⁹ In 4-aminoazobenzene both absorption bands overlap to form a broad band⁴⁰ with a maximum at 382 nm in CH_3CN .⁴¹

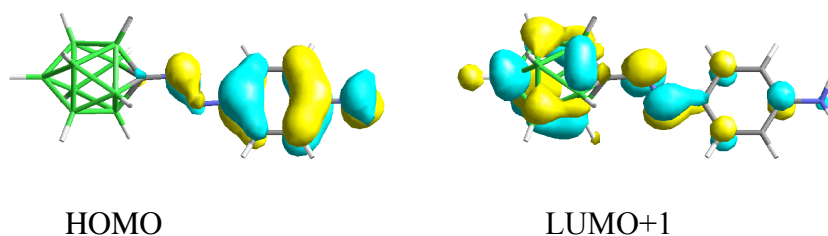


Figure 9. ZINDO –generated HOMO and LUMO contours for **8b**.

NMR Studies

The availability of several diverse derivatives of the $[\textit{closo-1-CB}_9\text{H}_{10}]^-$ cluster provided an opportunity to analyze the transmission of the substituent effect through the cage and compare the results to those for analogous benzene and $[\textit{closo-1-CB}_{11}\text{H}_{12}]^-$ derivatives. Thus, the relative NMR chemical shifts ($\Delta\delta$) for the antipodal B(10)-**H** were plotted versus the substituent σ_p values⁴² and the results are shown in Figure 10.

A Hammett plot of $\Delta\delta$ versus Hammett σ_p for ^1H NMR B(10)-**H** chemical shifts

showed good linear fit for several substituents (Figure 10a). The correlation factor r^2 is 0.94 for all substituents, and it increases to 0.99 if the two outlying data points ($X = \text{NH}_3$ and $X = \text{Cl}$) are removed. This change has little effect on the slope (ρ) of the linear fit, which slightly increases from 0.70 ± 0.05 to 0.73 ± 0.02 for the smaller data set. Interestingly, the slope for B(10)-**H** chemical shift is practically the same as that obtained for C(4)-**H** chemical shift in monosubstituted benzene derivatives ($\rho = 0.70 \pm 0.09$) after correction for anisotropic magnetic shielding⁴³ (see Supporting Information).

The Hammett plot of B(10) and B(12)⁴⁴ ¹¹B NMR chemical shifts for $\{\textit{closo-1-CB}_9\}$ and $\{\textit{closo-1-CB}_{11}\}$, respectively, showed that $\{\textit{closo-1-CB}_9\}$ ($\rho = 12.7 \pm 1.8$) appears to be significantly more sensitive than $\{\textit{closo-1-CB}_{11}\}$ ($\rho = 5.3 \pm 1.3$) to the nature of the C(1) substituent (Figure 10b).

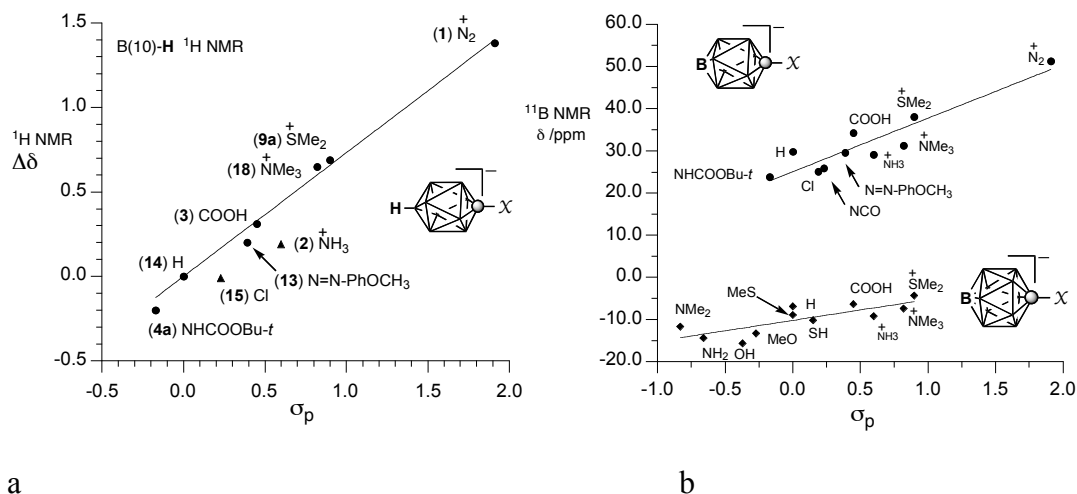


Figure 10. Relative ^1H (a) and absolute ^{11}B (b) NMR chemical shifts measured in CD_3CN for the antipodal position of $[\text{closo-1-CB}_9\text{H}_9\text{-1-X}]^-$ and $[\text{closo-1-CB}_{11}\text{H}_{11}\text{-1-X}]^-$ plotted against the substituent σ_p values. The σ_p parameters of the $-\text{N}=\text{N-Ph}$ and $-\text{NHCOOMe}$ groups were used for the substituents in **4a** and **13**, respectively. Best fit lines: (a) $y = 0.73x$, $r^2 = 0.990$; (b) $\{\text{closo-1-CB}_9\}$ $y = 12.7x + 25.1$, $r^2 = 0.86$; $\{\text{closo-1-CB}_{11}\}$ $y = 5.3x - 10.0$, $r^2 = 0.67$.

Discussion

Experiments demonstrated that the dinitrogen derivative **1** is stable in the solid state but decomposes in solutions. In MeCN the process is slow and the estimated half-life of **1** is $t_{1/2} = 91$ hrs at 25°C and $t_{1/2} = 2$ s at 90°C . The consistency of the measured high enthalpy of activation ΔH^\ddagger of 38.4 ± 0.8 kcal/mol with the calculated enthalpy change, ΔH , and the formation of a single product (**17**) support the heterolytic mechanism for the decomposition of **1** and the formation of the reactive intermediate **19** in MeCN . In addition, the unusually high experimental entropy of activation, ΔS^\ddagger (44.5 ± 2.5 cal/mol $\cdot\text{K}$) is similar to the calculated ΔS value of 43.6 cal/mol $\cdot\text{K}$. This suggests that the

dissociation process involves stretching the C–N bond to the edge of the Van der Waals contact between the atoms. Alternatively, solvent molecules are involved in the transition state, and the high value of ΔS^\ddagger reflects differential solvation of the ground and transition states. The proposed heterolytic unimolecular decomposition reaction of **1** is similar to that described for PhN_2^+ in polar aprotic solvents.⁴⁵ Interestingly, ΔG_{298}^\ddagger for **1** is higher by about 1.5 kcal/mol than that reported for PhN_2^+ .⁴⁵ Also **1** has a significantly higher ΔS^\ddagger than that measured for PhN_2^+ in MeCN (18.3 cal/mol*K) or in MeNO₂ (30.9 cal/mol*K).⁴⁵

A change of solvent or addition of a nucleophile dramatically accelerates the transformation of **1**, which is then usually fully consumed in less than 20 hrs at ambient temperature. This suggests that the simple mechanism of heterolytic dissociation of **1** and the formation of transient ylide **19** is inadequate.

A reaction of ylide **19** with pyridine is expected to give directly the N(1) adduct **11a** as the only or dominant product, since the process is favored kinetically (anticipated low activation barrier) and has a large exotherm ($\Delta H = -102.6$ kcal/mol). Support for this expectation is provided by the reported smooth transformations of similar dinitrogen derivatives of the [*closo*-B₁₀H₁₀]⁻² cluster with pyridine.^{2-4,6-8} Instead, the observed distribution of products in reaction of **1** with pyridine suggests a radical pathway, which is similar to the known Gomberg-Bachmann free radical arylation reaction.⁴⁶ In both reactions all C-substituted pyridine isomers are formed with the dominant proportions of the C(2) isomer.^{31,47} The radical mechanism for formation of **11** is supported also by

computational results, which demonstrate that the formation of radical ion **25** from **1** is equally feasible as the generation of Ph• (**31**) from PhN₂⁺.

From the mechanistic point of view, reaction of **1** in neat pyridine proceeds by either a heterolytic or homolytic pathway (Figure 11). The first and also the rate determining step in the former mechanism is a unimolecular first-order reaction, whereas the rate-limiting step in the radical pathway is pseudo-first order formation of diazenyl radical **23**, since [Pyridine] \approx const \gg [**1**]. At ambient temperature the radical process is significantly faster ($k_c \ll K_{eq}k_r$)⁴⁸ and the resulting radical anion **25** attacks the dominant neutral pyridine (solvent). The reaction between **25** and pyridine is also a pseudo-first order process. It is faster than the energetically more favorable (Table 4) ion recombination reaction of **25** and the pyridinium radical **24** (a second-order process), which, presumably, leads directly to the N(1) adduct **11a**. The attack of **25** on pyridine is calculated to be moderately exoergic (ΔG_{298} between -11.3 kcal/mol for **27a** and -13.7 kcal/mol for **27c**) and with sufficiently low activation barrier the process may be reversible leading to the thermodynamic intermediate **27**. The subsequent electron transfer (ET) from **27a** and hydrogen transfer (HT) from **27b–27d** to **24**⁴⁹ and the formation of **11a** and **11b[-]–11d[-]**, respectively, are highly exothermic ($\Delta H > 100$ kcal/mol in the dielectric medium) and considered irreversible. Therefore, the formation of **11b** as the major component of the mixture may arise either from the kinetic preference for the formation of intermediate **27b** (if the barrier is sufficiently high and the HT process is fast), or from the thermodynamic stability of **27b** (if the barrier is sufficiently low and the

HT process is slow). The latter implies that the calculations underestimated the stability of **27b** by about 2 kcal/mol relative to **27c**, which is not unreasonable. In fact, all C-substituted intermediates have comparable calculated energies within 2 kcal/mol in pyridine dielectric medium. It also needs to be remembered that the dielectric medium significantly destabilizes **27c** and has least effect on the energy of formation of **27b** (Table 6). Also, **27a** is thermodynamically least favorable intermediate, which is in agreement with its practical absence among the reaction products. A similar discrepancy between the calculated thermodynamic stability of the radical intermediates **32** and the distribution of the products **29** is found for the phenylation of pyridine (Table 6). Again, this may indicate that products formation is governed by kinetics (irreversible processes), or the relative energies are calculated with an error of ± 2 kcal/mol.

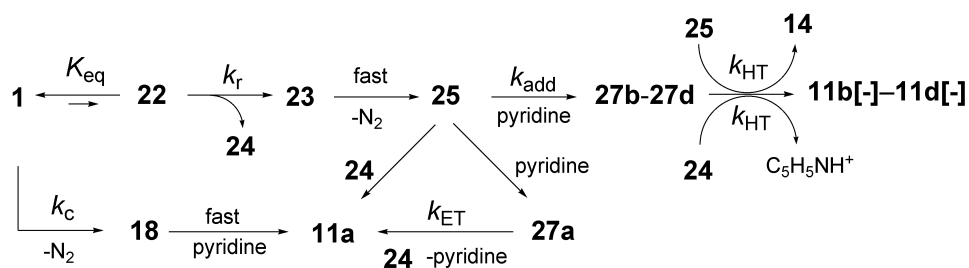


Figure 11. Proposed mechanism for the formation of pyridine derivatives **11**.

At higher temperatures the rate of formation of the ylide **19** becomes competitive with that of generation of the radical anion **25** ($k_c \sim K_{eq}k_r$) and consequently the N(1) isomer **11a** is formed in substantial amounts (Table 1).

In contrast to reactions of **1** in neat pyridine, in dilute solutions of pyridine in

benzene the ratio of **[24]**/**[Pyridine]** is greater and the more frequent encounters of radical anion **25** with **24** lead directly to the N(1) product **11a**, which is observed in 13% yield. Since the concentration of pyridine is low relative to that of benzene ($[\text{C}_6\text{H}_6]/[\text{Pyridine}] \approx 25$), addition of **25** to benzene effectively competes with the formation of adducts to pyridine, and $[\textit{closo-1-CB}_9\text{H}_9\text{-1-Ph}]^-$ (**16**) is formed as the major product. Calculations demonstrate that both addition reactions have comparable exotherms of $\Delta H = 23\text{-}25$ kcal/mol in pyridine dielectric medium. In methylene chloride solutions, the situation is similar and the radical anion **25** preferentially attacks the solvent giving the chloride $[\textit{closo-1-CB}_9\text{H}_9\text{-1-Cl}]^-$ (**15**) and the parent **14** in approximate ratio of 3:1 as the major products. Calculations indicate that abstraction of chlorine atom and hydrogen from CH_2Cl_2 are both exothermic processes ($\Delta G_{298} = -19.3$ and -18.6 kcal/mol, respectively) in dielectric medium $\epsilon = 13.3$. If the calculated free energy change for the process reflects the difference in energy of activation, the ratio 10:3 calculated from $\Delta\Delta G_{298}$ is in good agreement with the observed ratio of products. The $\bullet\text{CH}_2\text{Cl}$ radical reacts with pyridinium radical cation **24** leading to *N*-(chloromethyl)pyridinium, which was observed as the counterion in the crystal structure of the isolated chloride **15**.⁵⁰ An alternative mechanism, in which large amounts of **15** are formed by abstraction of Cl^- from CH_2Cl_2 by the ylide **19**, is less likely due to insufficient rate of the ylide formation.

The mechanism of pyridine-induced radical reactions of **1** is similar to the accepted mechanism of free radical arylation of pyridine with benzenediazonium salts.^{31-33,51} In both cases a stable adduct of pyridine to the N_2 group was located on PES

(compounds **22** and **28**). The relatively high energy of adducts **22** and **28** suggests that they are transient species formed at low concentration, and which give rise to the radical ion pairs. Further studies of reactions of arenediazonium salts indicated that the radical/cationic pathway correlates with the nucleophilicity of the solvent^{33,51} and does not necessarily involve a stable transient adduct but rather involves an intermolecular electron transfer (outer-sphere ET).³³ Thus, pyridine has one of the highest whereas acetonitrile has one of the lowest nucleophilicity parameter.^{51,52} Therefore, the former will induce radical generation, while the latter will favor cationic processes. This is indeed observed experimentally for decomposition of both **1** (present work) and benzenediazonium salts⁵³⁻⁵⁷ for which the corresponding acetamides are the main products in MeCN solutions (see Scheme 7).

The propensity of a nucleophile to induce radical reactions of **1** and PhN_2^+ can be assessed from the energetics of electron transfer (ET) between the diazonium and the donor calculated from ionization potential (I_p) and electron affinity (E_a) for a gas phase reaction, or from oxidation (E^{ox}) and reduction (E^{red}) potentials in solutions (Table 8). Calculations demonstrate that while the E_a for the two electrophiles, **1** and PhN_2^+ , are different in gas phase by over 3.5 eV, they are practically the same in MeCN solutions. The dielectric medium stabilizes charged molecules and consequently addition of an electron to **1** becomes more favorable, while reduction of PhN_2^+ is less exothermic in MeCN.

The calculated I_p values for the five reagents compare well to the experimental

data⁵⁸ with a systematic underestimation by about 0.3 eV. In MeCN dielectric medium the calculated I_p values are lower by 2-3 eV relative to gas phase. A comparison of the calculated ionization values to the experimental electrochemical data (Table 8) can be made only at a qualitative level, since all investigated processes are irreversible in solution and the observed current peak potentials do not represent thermodynamic processes. The calculated ionization potentials I_p generally follow the trend in experimental anodic peak potentials E_{pa}^{ox} for all reagents with the exception of Me₂S (Table 8). In agreement with calculations, the lowest oxidation potential is observed for the thioformamide and the highest for MeCN. The experimental E_{pa}^{ox} for Me₂S is higher by over 0.5 V than predicted, presumably due to complex chemical behavior of the radical cation.⁵⁹

A comparison of calculated electron affinities with the electrochemical data shows that reduction of **1** is more cathodic by 0.39 V than that of PhN₂⁺. The discrepancy between calculated solution E_a values and observed E_{pc} (Table 8) is presumably due to the difference in ion solvation (cation *vs.* anion) and solvent reorganization energy.

Table 8. Calculated adiabatic electron affinity (E_a) and ionization potential (I_p), and experimental electrochemical reduction/oxidation potentials for selected compounds.

Compound	Calculated ^a			Experimental ^b	
	$\epsilon = 1$ ^c	$\epsilon = 13.3$ ^d	$\epsilon = 36.6$ ^d	E_{pa}^{ox}/V	E_{pc}^{red}/V
	<i>Electron affinity /eV</i>				
1	2.11	3.69	3.76	-	-0.54
$C_6H_5N_2^+$	5.84	3.86	3.76	-	-0.16 ^e
	<i>Ionization potential /eV</i>				
Me ₂ S	8.29 (8.69) ^f	5.91	5.77	1.78 ^g	-
Me ₂ NCHS	7.94 (8.2) ^f	5.93	5.83	1.25	-
Pyridine	8.95 (9.26) ^f	6.82	6.72	Lit. ~1.5 ^h	-
CH ₂ Cl ₂	10.93 (11.33) ^f	8.40	8.27	~1.8 ⁱ	-
MeCN	12.10 (12.20) ^f	9.28	9.42	~2.4 ⁱ	-

^a MP2/6-31G(d,p)//B3LYP/6-31G(d,p) level with DFT enthalpic corrections. ^b Peak potential recorded in MeCN (0.05 M Bu₄NPF₆) versus SCE. ^c Vacuum calculations. ^d IPCM solvation model. ^e Lit. -0.17 (MeCN, SCE) ref⁶⁰. ^f Experimental data taken from ref⁵⁸. ^g Lit.⁵⁹ +1.71 V vs. SCE. ^h Recorded in neat pyridine.⁶¹ ⁱ Solvent electrochemical limit; ref⁶².

Calculated data in Table 9 demonstrates that ET between pyridine and PhN₂⁺ (outer-sphere process) and the formation of a radical ion pair is endothermic in pyridine

($\Delta G_{298} = 66.3$ kcal/mol) and practically the same in MeCN solution (Table 9), which corresponds to the difference in the measured current peak potentials of $\Delta E_p \approx 1.7$ V (Table 8). The same analysis for **1** and pyridine gives a similar value for the ET process in MeCN ($\Delta G_{298} = 65.3$ kcal/mol) but larger experimental electrochemical potential ($\Delta E_p \approx 2.0$ V).

Table 9. Calculated free energy change ΔG_{298} for the electron transfer process between **1** and compounds.^a



Nu \ \mathcal{R}	[<i>closo</i> -1-CB ₉ H ₉] ⁺ (1)			Ph-		
	$\epsilon = 1$ ^b	$\epsilon = 13.3$ ^c	$\epsilon = 36.6$ ^c	$\epsilon = 1$ ^b	$\epsilon = 13.3$ ^c	$\epsilon = 36.6$ ^c
Me ₂ S	138.8	47.4	43.0	53.7	44.4	43.9
Me ₂ NCHS	132.3	49.6	45.8	47.2	46.6	46.7
Pyridine	154.7	69.2	65.3	69.6	66.3	66.2
CH ₂ Cl ₂	200.9	106.0	101.4	115.8	103.0	102.3
MeCN	227.3	125.7	127.5	142.2	122.8	128.4

^a MP2/6-31G(d,p)//B3LYP/6-31G(d,p) level with DFT thermodynamic corrections. Energies in kcal/mol. ^b Vacuum calculations. ^c IPCM solvation model.

Calculations suggest that the ET process between **1** and Me₂S and also Me₂NCHS is more favorable and it should be faster than that with pyridine (Table 9). Both sulfur reagents have markedly lower I_p values relative to pyridine, and consequently ΔG_{298} values for electron transfer to **1** are lower by 20 kcal/mol or 1/3 than those for pyridine (Table 9). This is consistent with smaller ΔE_p of 1.79 V (Table 8) for the reaction of **1** and

Me₂NCHS and indicates that the formation of **10** and possibly also **9a** involves a radical process, which begins with outer-sphere ET (intermolecular) and formation of the radical ion pair.⁶³ In the case of Me₂S, the ion pair collapses to form the product **9a** (Scheme 12). Since the concentration of the ions is small and the rate of this bimolecular process is low, other processes take place, such as loss of proton and presumably abstraction of H. Consequently, the adduct **9a** is isolated only in 40% yield with the rest of the precursor forming a polymeric/decomposition products.

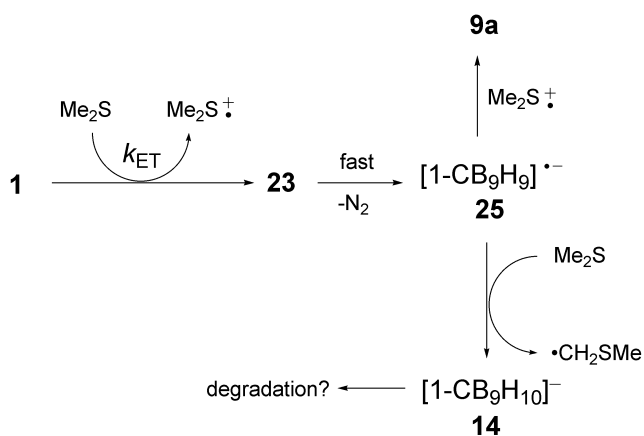


Figure 12. Proposed mechanism for the formation of **9a**.

The reaction with Me₂NCHS is much more efficient. Thionocarbonyls are known to react smoothly with C-centered radicals, often in a chain process, in which the weak S=C bond is eliminated.⁶⁴ Thus, it can be postulated that radical ion **25** preferentially attacks the sulfur atom giving rise to the C-centered transient radical **34** stabilized by both the N and S atoms (Figure 13). Subsequent ET to the Me₂NCHS radical cation gives product **10**. Overall, the preparation of dialkylsulfonium derivatives such as **9** is most

efficiently done in a two-step process using **10** as the intermediate.

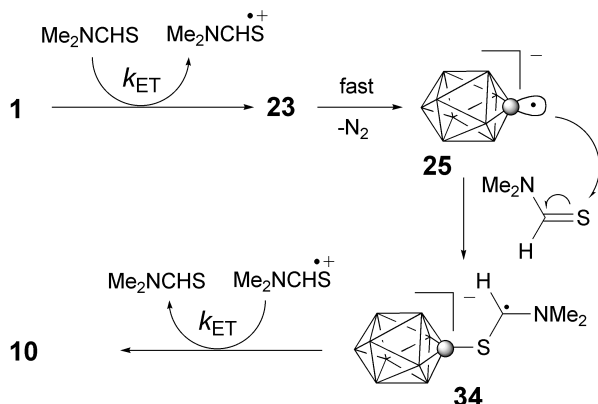


Figure 13. Proposed mechanism for the formation of **10**.

Solvents with high I_p (> 10 eV) and E_{pa} , such as MeCN and CH_2Cl_2 are not expected to transfer an electron to **1** and induce radical transformations of **1**. Therefore, the observed significantly accelerated decomposition of **1** in the weakly nucleophilic CH_2Cl_2 and benzene as compared to that in MeCN is surprising at first. The difference presumably lies in the stabilization of the counterion in the three solvents. In MeCN, the reaction of ylide **19** with the solvent leads to electrically neutral zwitterion **17**. Upon *in situ* hydrolysis of **17** with traces of water the resulting proton is reasonably well solvated by MeCN or can be associated with the acetamide carbonyl group. In contrast, proton resulting from the electrophilic attack of **19** on benzene and formation of [*closo*-1- CB_9H_9 -1-Ph] (**16**) is poorly solvated and stabilized. Therefore, H^+ may attack **1** and promote its decomposition, which leads to an autocatalytic process and possibly destruction of the boron cluster. Similarly, reaction of ylide **19** with CH_2Cl_2 leads to the strongly

electrophilic $+CH_2Cl$ ion, which presumably leads to accelerated decomposition of **1** and also cage destruction. Overall, slow decomposition of **1** through ylide **19** can be expected in solvents such as $MeNO_2$ with high I_p , for which adducts to **19** are relatively stable zwitterions (do not produce aggressive electrophiles), and have been demonstrated to promote heterolytic unimolecular decomposition of PhN_2^+ .⁴⁵ On the other hand, reagents with high nucleophilicity and low I_p , such as amines and sulfur compounds, are likely to induce radical transformations of **1**.

Analysis of electronic absorption spectra and chemical shifts revealed significant similarities between the $[closo-1-CB_9H_{10}]^-$ and benzene. Thus, electronic absorption spectra revealed substantial electronic communication between the $\{closo-1-CB_9\}$ cage and π substituents. This is consistent with our previous experimental and theoretical studies for the derivatives of $[B_{10}H_{10}]^{2-}$ and $C_2B_8H_{10}$.^{6-8,11,65-67} In the absence of π substituents the compounds are practically UV transparent. Since the cage is negatively charged, the electronic excitations of the zwitterionic derivatives such as **1** and **11a** involve the cage-to-substituent transitions, which exhibit strong solvatochromism^{6,8} and may find applications as NLO chromophores.

The Hammett analysis of NMR chemical shifts demonstrated similar ability to transmit electronic effects through the $[closo-1-CB_9H_{10}]^-$ cage and benzene ring, which is significantly higher than that found for the $[closo-1-CB_{11}H_{12}]^-$ derivatives. The stronger antipodal effect^{68,69} observed in the $\{closo-1-CB_9\}$ cluster relative to the $\{closo-1-CB_{11}\}$ may be related to the smaller size and higher electron density for the former as compared

to the latter. The only other Hammett correlation previously reported for boron clusters was for ^{13}C NMR chemical shifts of *C*-arylated *p*-carborane derivatives.⁷⁰ A comparison⁷¹ of the slope (ρ values) reported⁷⁰ for 1-aryl-*p*-carboranes with that for ^{13}C NMR chemical shifts of 4-substituted biphenyls demonstrates that transmission of substituent effect through the 12-vertex carborane cage is about 70% as effective as through the benzene ring (see Supporting Information). This finding is consistent with results presented in Figure10.

Summary and Conclusions

The present studies describe an alternative and reliable method for the preparation of amine **2** and dinitrogen derivative **1**, provide good understanding of the properties of the latter, and its usefulness as a synthetic intermediate in the preparation of more complex derivatives, including liquid crystals. The method for the formation of amino functionality through the COOH group permits the introduction of an antipodal substituent at the stage of [*closo*-2-CB₉H₉-2-COOH].¹⁶ Such compounds are being currently investigated in our laboratory.

In many respects dinitrogen derivative **1** displays behavior similar to that of benzenediazonium salt; it has similar stability, undergoes diazo coupling, reacts with pyridine and sulfur nucleophiles, and undergoes heterolysis in MeCN giving *N*-substituted acetamide. Detailed analysis of the experimental data and computational results revealed two mechanisms for the transformations of **1**; the closed-shell zwitterionic pathway

through ylide **19**, and an open-shell radical pathway involving radical anion **25**. The latter is analogous to the nucleophile-induced decomposition of PhN_2^+ and operates for reagents and solvents, which are good nucleophiles and/or electron donors (low I_p and low $E_{1/2}^{\text{ox}}$). In the absence of electron donors (reagents with high I_p and $E_{1/2}^{\text{ox}}$) dinitrogen **1** undergoes heterolytic cleavage of N_2 and gives products of electrophilic addition.

Experimental results demonstrated that **1** serves as a convenient precursor for the preparation dialkylsulfonium derivatives such as **9b**; the two-step process through **10**, a masked thiol generated *in situ*, is more efficient due to higher yield of the first step. Also diazocoupling of **1**, leading to azophenols such as **8**, is an efficient process, which has already been exploited for the preparation of ionic liquid crystals.¹⁵ In contrast, the preparation of *N*-substituted pyridine **11a**, which is of interest for investigation of molecular materials, is a low yield process of little synthetic value at present.

Spectroscopic investigation indicate significant electronic interactions between the {*closo*-1- CB_9 } cage and π substituents, which indicates a possibility of control of photophysical properties in specifically designed molecular materials.

Overall, results demonstrate that the dinitrogen **1** is an attractive compound for further mechanistic investigation and synthetic applications.

Computational Details

Quantum-mechanical calculations were carried out with the B3LYP^{72,73} and MP2(fc)⁷⁴ methods with the 6-31G(d,p) basis set using the Gaussian 98 computational package.⁷⁵ Geometry optimizations were undertaken using appropriate symmetry constraints and tight convergence limits. Vibrational frequencies were obtained with the B3LYP/6-31G(d,p) method and were used to characterize the nature of the stationary points and to obtain thermodynamic parameters. Zero-point energy (ZPE) corrections were scaled by 0.9806.⁷⁶ Population analysis for single point calculations (MP2//DFT) was performed using the Density keyword. For MP2-level calculations of open-shell species the spin projected energies were used for comparative studies. The IPCM solvation model⁷⁷ was used with default parameters.

Experimental Section

Reagents and solvents were obtained commercially. Solvents were dried and deoxygenated before use, and reagents were used as supplied. ZnCl₂ was dried by heating at ~100 °C under vacuum. Reactions were carried out under dry Ar, subsequent manipulations conducted in air. NMR spectra were obtained at 128.4 MHz (¹¹B), 100.6 MHz (¹³C), and 400.1 MHz (¹H) in CD₃CN unless otherwise specified. ¹H NMR and ¹³C NMR spectra were referenced to the solvent. ¹¹B NMR chemical shifts are relative to the resonance of an external boric acid sample in CH₃OH that was set to 18.1 ppm. IR

spectra were recorded in the solid state using an AT-IR accessory.

UV spectra were recorded in UV-grade CH₃CN. All compounds were in concentration of 0.7–5 x 10⁻⁵ M. Extinction coefficients were obtained by fitting the maximum absorbance against concentration in agreement with Beer's law.

Electrochemical analysis was conducted in dry MeCN with Bu₄NPF₆ (0.05 M) as the supporting electrolyte and using freshly polished glassy carbon working electrode with the Ag/AgCl reference electrode. The scanning rate was 1V/s. Following literature recommendations,⁶⁰ the concentration of compounds **1** and PhN₂⁺ was set at 0.6 mM and the reported data was taken from the first scan. Continuous scanning of the electrochemical window (+0.7 to -1.0 V) resulted in shifting of the observed cathodic peak to more negative potentials due to electrode passivation by electrografting of Ph• or [*closo*-1-CB₉H₉] radicals. Peak potentials were referenced by adding small amounts of ferrocene to the solution and E-chem scan for each compound was referenced to the ferrocene couple which was assumed to be 0.31 V versus SCE (MeCN, 0.2 M LiClO₄).⁷⁸

Preparation of [*closo*-1-CB₉H₉-1-N₂] (1**).**

A suspension of [*closo*-1-CB₉H₉-1-NHBoc]⁻ NEt₄⁺ (**4a**[NEt₄], 0.21 g, 0.57 mmol) in a 1:3 mixture of conc. HCl in CH₃OH (10 mL) was gently heated until all solid dissolved and stirring was continued at rt for 18 hrs. Water (15 mL) was added and CH₃OH was removed *in vacuo*. Conc. HCl (3 mL) was added, and [*closo*-1-CB₉H₉-1-NH₃] (**2**) was extracted into Et₂O (3 x 15 mL). The organic layers were combined, dried

(Na₂SO₄), and evaporated *in vacuo* to give 0.120 g (166% yield) of crude amine **2** as a transparent glassy solid: ¹H NMR δ 0.61 (q, *J* = 145 Hz, 4H), 1.74 (q, *J* = 156 Hz, 4H), 5.46 (q, *J* = 156 Hz, 1H), 8.55 (s); [lit.¹² ¹H NMR δ 0.81 (4H), 2.34 (4H), 5.53 (1H), 10.15 (3H)]; ¹³C NMR δ 66.6; ¹¹B NMR δ, -25.5 (d, *J* = 141 Hz, 4B), -16.8 (d, *J* = 152 Hz, 4B), 29.1 (d, *J* = 159 Hz, 1B); [lit.¹² ¹¹B NMR δ -25.8 (4B), -16.8 (4B), 29.2 (1B)]; IR 3182 and 3162 (N-H) cm⁻¹.

Crude amine **2** was dissolved in a 1:1 mixture of AcOH/H₂O (1 mL), and an aqueous solution of NaNO₂ (0.043 g, 0.63 mmol) in H₂O (2 mL) was added dropwise (~1 drop/sec) at 0 °C. Reaction temperature was maintained for 30 min, H₂O (2 mL) was added, and a precipitate was filtered and dried giving 0.066 g (80% yield) of [*closo*-1-CB₉H₉-1-N₂] (**1**) as a white crystalline solid: dec ~87 °C (Δ*H* = 148 kJ/mol, DSC); ¹H NMR (CD₃CN) δ 0.96 (q, *J* = 150 Hz, 4H), 2.51 (q, *J* = 167 Hz, 4H), 6.65 (q, *J* = 164 Hz, 1H); ¹H NMR (benzene-*d*₆) δ 1.10-3.20 (m, 8H), 7.87 (q, *J* = 170 Hz, 1H); ¹¹B NMR (CD₃CN) δ -22.1 (d, *J* = 149 Hz, 4B), -8.6 (d, *J* = 167 Hz, 4B), 51.3 (d, *J* = 167 Hz, 1B); ¹¹B NMR (benzene-*d*₆) δ -20.6 (d, *J* = 147 Hz, 4B); -6.8 (d, *J* = 163 Hz, 4B), 57.0 (d, *J* = 179 Hz, 1B) IR 2250 (N₂) cm⁻¹; UV (CH₃CN), λ_{max} 250 nm, (log ε = 3.82).

Preparation of [*closo*-1-CB₉H₉-1-NHBoc]⁻ NEt₄⁺ (4a**).**

A suspension of [*closo*-1-CB₉H₉-1-COOH]⁻ NEt₄⁺ (**3**[NEt₄], 1.14 g, 3.88 mmol) [¹¹B{¹H} NMR δ -23.6 (4B), -15.4 (4B), 34.2 (1B); IR 1678 (C=O) cm⁻¹] in anhydrous CH₂Cl₂ (10 mL) was treated with 2 M (COCl)₂ in CH₂Cl₂ (2.2 mL, 4.3 mmol). Vigorous

bubbling of CO and CO₂ gases was observed followed by the dissolution of the substrate and the formation of a slight yellow solution. The solution was stirred for 75 min at rt, filtered to remove insoluble particulates, and the solvent removed *in vacuo* to give 1.20 g of crude [*closo*-1-CB₉H₉-1-COCl]⁻ NEt₄⁺ (**5[NEt₄]**) as a white solid: [¹¹B {¹H} NMR δ -23.1 (4B), -13.5 (4B), 38.5 (1B); IR 1776 (C=O) cm⁻¹].

Crude [*closo*-1-CB₉H₉-1-COCl]⁻ NEt₄⁺ (**5[NEt₄]**, 1.20 g, 3.85 mmol) was dissolved in anhydrous CH₂Cl₂ (10 mL) and added via syringe to solid anhydrous ZnCl₂ (0.052 g, 0.38 mmol) under N₂ atmosphere. The reaction mixture was cooled to 0 °C and Me₃SiN₃ (0.55 mL, 4.2 mmol) was added. The reaction mixture was stirred at 0 °C for an additional 30 min after which it was warmed to rt and stirred for 4 hrs. The reaction mixture was poured into ice-cold H₂O (50 mL) and extracted with CH₂Cl₂ (3 x 30 mL). The organic layers were combined, dried (MgSO₄), filtered, and the solvent was removed *in vacuo* giving 1.11 g [*closo*-1-CB₉H₉-1-CON₃]⁻ NEt₄⁺ (**6[NEt₄]**) as a white crystalline solid: [¹¹B {¹H} NMR δ -23.3 (4B), -14.8 (4B), 36.4 (1B); IR 2360, 2339, and 2142 (N₃), 1691 (C=O) cm⁻¹]. Crude product was contaminated with about 15% of carboxylic acid **3[NEt₄]**.

Crude [*closo*-1-CB₉H₉-1-CON₃]⁻ NEt₄⁺ (**6[NEt₄]**, 1.11 g, 3.49 mmol) was dissolved in anhydrous CH₃CN (15 mL) and refluxed for 1 hr. The reaction was cooled to rt, solvent removed, and the residue dried *in vacuo* giving 1.11 g of crude [*closo*-1-CB₉H₉-1-NCO]⁻ NEt₄⁺ (**7[NEt₄]**) as a slight yellow solid: [¹¹B {¹H} NMR δ -26.1 (4B), -

16.0 (4B), 25.1 (1B); IR 2262 (N=C=O)].

A solution of anhydrous *tert*-butanol (15 mL), anhydrous CH₃CN (5 mL), and crude [*closo*-1-CB₉H₉-1-NCO]⁻ NEt₄⁺ (**7**[NEt₄], 1.04 g, 3.58 mmol) was stirred at 90 °C for 2 hr after which solvents were removed leaving 1.20 g of crude [*closo*-1-CB₉H₉-1-NHBoc]⁻ NEt₄⁺ (**4a**[NEt₄]) as a yellow solid. The crude solid was dissolved in CH₂Cl₂ and passed through a silica gel plug buffered with 1% NEt₃ in CH₂Cl₂. Elution with a buffered CH₃CN/CH₂Cl₂ solution (1% NEt₃, 20% CH₃CN, 79% CH₂Cl₂) afforded 0.68 g (48% yield based on starting acid **3**[NEt₄]) of pure [*closo*-1-CB₉H₉-1-NHBoc]⁻ NEt₄⁺ (**4a**[NEt₄]) as a slight yellow solid: mp 140 °C; ¹H NMR δ 0.45 (q, *J* = 143 Hz, 4H), 1.19 (t, *J* = 7.3 Hz, 12H), 1.49 (s, 9H), 1.67 (q, *J* = 156 Hz, 4H), 3.14 (q, *J* = 7.3 Hz, 8H), 5.07 (q, *J* = 151 Hz, 1H), 7.12 (s, 1H); ¹³C NMR δ 7.7 (N⁺CH₂CH₃), 28.6 (C(CH₃)₃), 47.3 (C(CH₃)₃), 53.0 (N⁺CH₂CH₃), 156.0 (C=O), carbon associated with {*closo*-1-CB₉} cluster was not observed, minor signals at 9.0 and 53.5 ppm were attributed to excess NEt₄⁺Br⁻; ¹¹B NMR δ -26.2 (d, *J* = 135 Hz, 4B), -17.2 (d, *J* = 152 Hz, 4B), 23.8 (d, *J* = 158 Hz, 1B); IR 3505 (N-H), 1737 (C=O) cm⁻¹. Anal. Calcd. for C₁₄H₃₉B₉N₂O₂: C, 46.10; H, 10.78; N, 7.38. Found: C, 46.26; H, 10.76; N, 7.53.

Subsequent fractions produced 0.56 g of a 30:70 mixture of and [*closo*-1-CB₉H₉-1-COOH]⁻ NEt₄⁺ (**3**[NEt₄]) and [*closo*-1-CB₉H₉-1-NH₂]⁻ NEt₄⁺ (**2**[NEt₄]): ¹H NMR δ 1.23 (t, *J* = 7.2 Hz, 12H), 3.19 (q, *J* = 8.0 Hz, 8H), 7.31 (s, 2H); ¹¹B {¹H} NMR δ -26.1 (4B), -17.1 (4B), 24.1 (1B), [lit.¹² data for (**2**[NHEt₃]): ¹H NMR δ 0.91 (4H), 1.69 (4H),

5.40 (1H), 8.52 (2H); ^{11}B NMR δ -25.8 (4B), -17.2 (4B), 26.0 (1B)].

Reaction of Isocyanate **7** with 1:1 Mixture of 18% HCl and CH₃OH

A suspension of crude [*closo*-1-CB₉H₉-1-NCO]⁻ NEt₄⁺ (**7**[NEt₄], 0.55 g, 1.89 mmol) in a 1:1 mixture of 18% HCl in CH₃OH (25 mL) was stirred at 80 °C for 2 hrs. Methanol was removed *in vacuo* and a white precipitate formed. The precipitate was filtered, washed with H₂O, and dried (0.420 g). The mother liquor was neutralized with NaOH (checked by pH paper), and the solution was allowed to sit overnight upon which additional precipitation was filtered, washed with H₂O, and dried (0.240 g). Analysis of the first precipitate (0.420 g) by ^{11}B { ^1H } NMR showed approximately a 1:1 ratio of carboxylic acid **3**[NEt₄] amine **2**[NEt₄]: ^1H NMR δ 1.23 (t, J = 7.2 Hz, 12H), 3.19 (q, J = 8.0 Hz, 8H), 7.31 (s, 2H); ^{11}B { ^1H } NMR δ -26.1 (4B), -17.1 (4B), 24.1 (1B).

After extracting the first precipitate (0.420 g) into Et₂O from aqueous HCl, [*closo*-1-CB₉H₉-1-NHCOOMe]⁻ NEt₄⁺ (**4b**[NEt₄]) [δ B(10) -26.2 (4B), -17.1 (4B), 24.1 (1B)] was also observed since ^{11}B NMR still showed a doublet at 24.1 ppm with a new doublet at 29.1 ppm for expected **2**. The second precipitate (0.240 g) was demonstrated to be approximately 90% pure carbamate **4b**[NEt₄] on the basis of the analysis of the acid extract: (**4b**[H₃O]): ^1H NMR δ 3.85 (s, 3H), 5.19 (q, J = 156 Hz, 1H) 8.56 (s, 1H); ^{11}B { ^1H } NMR δ -26.1 (4B), -17.1 (4B), 24.4 (1B); IR 3378 (N-H), 1741 (C=O) cm⁻¹.

Attempts to further purify [*closo*-1-CB₉H₉-1-NHCOOMe]⁻ H₃O⁺ (**4b**[H₃O]) were unsuccessful due to poor separation from **2** and **3**[H₃O] on SiO₂. Amine **2** was liberated

from the methyl carbamate under basic conditions (10% aqueous NaOH, ambient temperature, overnight).

Reactions of **1** with Activated Aromatics

A. Diazocoupling of **1** with Stoichiometric Amounts of Phenolate

An orange solution of [*closo*-1-CB₉H₉-1-N₂] (**1**, 0.040 g, 0.27 mmol) and a 1:1 solution of phenol (0.025 g, 0.27 mmol) and 20% NEt₄⁺ OH⁻ in H₂O (0.2 mL) in CH₃CN (2 mL) was stirred for 24 hrs. Solvent was removed *in vacuo* leaving crude product as a solid residue. The residue was passed through a short silica gel plug (1:4 CH₃CN/CH₂Cl₂) giving 0.057 g of a 5:1 mixture of single **8a**[NEt₄] and double **12**[2NEt₄] diazocoupling products. Analysis of the mixture gave the following data for **12**[2NEt₄]: ¹H NMR (characteristic signals) δ 7.24 (d, *J* = 8.9 Hz, 1H), 8.01 (dd, *J*₁ = 8.8 Hz *J*₂ = 2.4 Hz, 1H), 8.50 (s, 1H); MS (FAB): *m/z* (381-390) max at 386 (100%); FAB-HRMS(-): calcd. for C₈H₂₂B₁₈N₄O *m/z*: 388.3469; found: 388.3486. ¹¹B NMR signals for double and mono diazocouplings products were indistinguishable and are labeled as: ¹¹B NMR δ -24.5 (4B), -16.4 (4B), 29.3 (1B).

B. Diazocoupling with Excess Phenolate

A red solution of phenol (0.52 g, 5.53 mmol), NMe₄⁺ OH⁻ · 5 H₂O (1.00 g, 5.53 mmol), and [*closo*-1-CB₉H₉-1-N₂] (**1**, 0.160 g, 1.1 mmol) in CH₃CN (8 mL) was stirred for 18 hr at rt. The solvent was evaporated giving a deep red viscous oil (1.23 g). The oil was acidified with 10 % HCl (20 mL) and extracted into Et₂O (3 x 10 mL). The organic

layers were combined and evaporated to give crude acid extract, which was purified by column chromatography (1:4 CH₃CN/CH₂Cl₂) giving 0.224 g (81% yield) of [*closo*-1-CB₉H₉-1-(N₂-C₆H₄-4-OH)]⁻ H₃O⁺ (**8a**[H₃O]) as a yellow-orange oil after carefully drying over P₂O₅: ¹H NMR δ 5.46 (q, *J* = 158 Hz, 1H), 6.97 (d, *J* = 8.8 Hz, 2H); 7.50 (s, 1H), 7.79 (d, *J* = 8.8 Hz, 2H); ¹¹B{¹H} NMR δ -24.5 (4B), -16.5 (4B), 29.4 (1B).

Water (3 mL) and NMe₄⁺ OH⁻ · 5 H₂O (0.16 g, 0.90 mmol) were added followed by 10 % HCl added dropwise until an orange solid precipitated which was washed with H₂O, filtered, and dried giving 0.170 g (50% yield) of [*closo*-1-CB₉H₉-1-(N₂-C₆H₄-4-OH)]⁻ NMe₄⁺ (**8a**[NMe₄]): mp 115 °C; ¹H NMR δ 3.08 (s, 12H), 5.45 (q, *J* = 152 Hz, 1H), 7.04 (d, *J* = 8.7 Hz, 2H), 7.77 (d, *J* = 8.8 Hz, 2H), proton associated with OH was not observed; ¹¹B NMR δ -24.5 (d, *J* = 137 Hz, 4B), -16.5 (d, *J* = 151 Hz, 4B), 29.3 (d, *J* = 160 Hz, 1B); IR: 3365 (O-H), 1505 and 1482 (N=N) cm⁻¹; UV (CH₃CN), λ_{max} (log ε) 319 nm (4.27), 400 (2.76); MS (FAB): *m/z* (237-242) max at 239 (100%); FAB-HRMS(-): Calcd. for C₁₁H₂₆B₉N₃O *m/z*: 241.1944; found: 241.1931. Anal. Calcd. for C₁₁H₂₆B₉N₃O: C, 42.12; H, 8.36; N, 13.40. Found: C, 43.03; H, 8.57; N, 13.28.

C. Diazocoupling with Excess Aniline

An orange solution of aniline (0.23 mL, 2.58 mmol) and [*closo*-1-CB₉H₉-1-N₂] (**1**, 0.075 g, 0.51 mmol) dissolved in CH₃CN (2 mL) was stirred for 18 hr at rt. The solvent was removed, 10 % HCl (25 mL) was added, and the solution was extracted with Et₂O (3 x 10 mL). The organic layers were combined and evaporated to give 0.170 g of

crude acid extract, which was purified by column chromatography (1:4 CH₃CN/CH₂Cl₂). The resulting material was dried over P₂O₅ giving 0.130 g (106% yield) of [*closo*-1-CB₉H₉-1-(N₂-C₆H₄-4-NH₂)]⁻ H₃O⁺ (**8b**[H₃O]) as a deep red viscous oil: ¹H NMR δ 6.88 (d, *J* = 8.8 Hz, 2H), 7.77 (d, *J* = 8.8 Hz, 2H); ¹¹B{¹H} NMR δ -24.6 (d, *J* = 175 Hz, 4B), -16.3 (d, *J* = 153 Hz, 4B), 29.6 (d, *J* = 139 Hz, 1B).

Water (3 mL) and NMe₄⁺ OH⁻ · 5H₂O (0.11 g, 0.60 mmol) was added followed by 10% HCl added dropwise until an orange solid precipitated which was washed with H₂O, filtered, and dried giving 0.130 mg (80% yield) of [*closo*-1-CB₉H₉-1-(N₂-C₆H₄-4-NH₂)]⁻ NMe₄⁺ (**8b**[NMe₄]): mp 115 °C; ¹H NMR δ 3.06 (s, 12H), 5.41 (q, *J* = 149 Hz, 1H), 6.76 (d, *J* = 8.7 Hz, 2H), 7.69 (d, *J* = 8.7 Hz, 2H), protons associated with NH₂ were not observed; ¹¹B NMR δ -24.6 (d, *J* = 137 Hz, 4B), -16.6 (d, *J* = 146 Hz, 4B), 28.8 (d, *J* = 152 Hz, 1B); IR: 3469 and 3368 (N-H), 2551 and 2526 (B-H), 1481 and 1432 (N=N) cm⁻¹; UV (CH₃CN), λ_{max} (log ε) 348 nm (4.17), 410 sh. Anal. Calcd. for C₁₁H₂₇B₉N₄: C, 42.26; H, 8.70; N, 17.92. Found: C, 42.37; H, 8.95, N, 17.63.

Reaction of 1 with Sulfur Compounds.

A. Reaction with Dimethyl Sulfide

A yellow solution of [*closo*-1-CB₉H₉-1-N₂] (**1**, 0.062 g, 0.43 mmol) in Me₂S (3 mL) was stirred for 18 hr at rt, and the solvent was removed leaving a yellow solid. The crude product was passed through a silica gel plug (CH₂Cl₂) giving 0.030 g (40% yield) of [*closo*-1-CB₉H₉-1-S(CH₃)₂] (**9a**) as an off-white solid. Product was further purified

via recrystallization (cold 1,2-dichloroethane) for analyses (^1H and ^{11}B NMR), which were identical with literature result.¹²

B. Reaction with N,N-Dimethylthioformamide

A yellow solution of [*closo*-1- CB_9H_9 -1- N_2] (**1**, 0.050 g, 0.34 mmol) and freshly distilled N,N-dimethylthioformamide (2.0 mL, 23.1 mmol) was stirred overnight at rt. Excess Me_2NCHS was removed by vacuum distillation (80 °C, 0.25 mm Hg) leaving crude product as a slight yellow solid. The crude product was washed with toluene until the decant was no longer yellow giving 0.069 g of crude [*closo*-1- CB_9H_9 -1- $\text{SCHN}(\text{CH}_3)_2$] (**10**) containing ~20% Me_2NCHS by ^1H NMR: mp 230 °C dec; ^1H NMR major signals δ 3.45 (s, 3H), 3.64 (s, 3H), 5.70 (q, $J = 160$ Hz, 1H), 9.79 (s, 1H); minor signals for Me_2NCHS δ 3.19 (s, 3H), 3.25 (s, 3H), 9.13 (s, 1H); $^{11}\text{B}\{^1\text{H}\}$ NMR major signals δ -23.6 (4B), -14.2 (4B), 34.2 (1B); MS (FAB): m/z (204-210) max at 207 (100%); FAB-HRMS(+): Calcd. for $\text{C}_4\text{H}_{16}\text{B}_9\text{NS}$ m/z : 209.1841; found; 209.1856.

Reactions of 1 with Pyridine.

A. Neat Pyridine at Room Temperature

An orange solution of [*closo*-1- CB_9H_9 -1- N_2] (**1**, 0.056 g, 0.38 mmol) and pyridine (2 mL) was stirred for 18 hrs at rt. Excess pyridine was removed *in vacuo* leaving 0.120 g of a red oil that slowly crystallized. The crude reaction mixture was purified using a Chromatotron (1:10 $\text{CH}_3\text{CN}/\text{CH}_2\text{Cl}_2$) giving 0.030 g (40% yield) of [*closo*-1- CB_9H_9 -1-(2-

C₅H₅N)] (**11b**[H]) as a yellowish solid.

The more polar components were eluted with MeCN and evaporated to dryness giving 0.055 g of a semi-solid material. This material was dissolved in 10 % HCl (10 mL) and extracted with Et₂O (3 x 5 mL). The organic layers were combined, dried (Na₂SO₄), and evaporated giving 0.025 g of orange semi-solid product. The crude material was washed with CH₂Cl₂ leaving 0.010 g of a yellowish solid, which was identified as a mixture of **11d**[H] (4-isomer) and **11c**[H] (3-isomer) by 1D ¹H and 2D ¹H-¹H COSY NMR (Figure S1). The CH₂Cl₂ wash contained 0.015 g of about 80% pure mixture of the two isomers.

Using spectroscopic information obtained for purified products the ratio of products **11c**, **11d** and **14** in the crude polar fraction was calculated as 17:10:6.

B. Neat Pyridine Hot

Hot pyridine (~90 °C, 2 mL) was added to [*closo*-1-CB₉H₉-1-N₂] (**1**, 0.10 g, 0.68 mmol). The reaction mixture immediately turned dark red, and a precipitate formed. The temperature was maintained for 20 min, and after cooling, solvent was removed *in vacuo* leaving 0.160 g of a red oil. The oil was passed through a short silica gel plug, which was eluted first with a 1:4 CH₂Cl₂/hexane mixture giving 0.023 g (17% yield) of [*closo*-1-CB₉H₉-1-(1-C₅H₅N)] (**11a**) as a white crystalline solid. Using MeCN as the eluent, 0.11 g of the more polar fraction was collected, which was acidified with 10% HCl (10 mL) and extracted with Et₂O (3x5 mL). The organic layers were combined, dried (Na₂SO₄),

and evaporated giving 0.081 g of orange semi-solid product. ^{11}B NMR analysis revealed the presence of four doublets in the low field region identified as **11b[H]**, **11c[H]**, **11d[H]** and **14** in a ratio of approximately 10:9:4:2.

C. Dilute solution of Pyridine in CH_2Cl_2

An orange mixture of [*closo*-1- CB_9H_9 -1- N_2] (**1**, 0.042 g, 0.29 mmol), anhydrous pyridine (0.10 mL, 1.2 mmol), and anhydrous CH_2Cl_2 (2.5 mL) was stirred for 18 hrs at rt. Inorganic salts were filtered and washed with CH_3CN . Solvent was evaporated leaving 100 mg of an orange film that contained **11a**, **11b**, **14**, and **15[PyrH]** in a ratio of 17:7:20:56 ratio, respectively, by $^{11}\text{B}\{^1\text{H}\}$ NMR analysis. The film was passed through a silica gel plug (CH_2Cl_2) giving 6 mg of **11a** as the first fraction. Elution with 1:10 $\text{CH}_3\text{CN}/\text{CH}_2\text{Cl}_2$ gave 0.026 g of crude (~55% purity by $^{11}\text{B}\{^1\text{H}\}$ NMR) [*closo*-1- CB_9H_9 -1- Cl] $^-$ (**15[PyrH]**). The 0.026 g was further purified on another silica gel plug (1:10 $\text{CH}_3\text{CN}/\text{CH}_2\text{Cl}_2$) giving 2.6 mg of ~90% pure **15[PyrH]** for which analysis was performed.

XRD analysis of a single crystal grown from the reaction mixture demonstrated the *N*-chloromethylpyridinium cation associated with the [*closo*-1- CB_9H_9 -1- Cl] $^-$ (**15[PyrCH₂Cl]**).⁵⁰ A singlet possibly related to the *N*-chloromethylpyridinium cation was observed in crude reaction mixture [^1H NMR (CD_3CN) δ 7.13 (s, 2H); lit.⁷⁹ (DMSO) δ 6.74 (s, 2H)], but unambiguous identification of other signals associated with the pyridine moiety in both the crude reaction mixture (overlap from other signals) and after

chromatography (disappearance of singlet at 7.13 ppm) was not possible.

D. Dilute solution of Pyridine in Benzene

A colorless solution of [*closo*-1-CB₉H₉-1-N₂] (**1**, 0.042 g, 0.29 mmol), anhydrous pyridine (0.10 mL, 1.2 mmol), and anhydrous C₆H₆ (2.5 mL) was stirred for 18 hrs at rt. The solvent was removed leaving 0.039 g of a semi-solid material that contained **11a**, **11b**[**H**], and **16** presumably with pyridinium as the counterion, **16**[**PyrH**], in an approximate ratio of 2:3:11 ratio by ¹¹B {¹H} NMR analysis.

11a (1-isomer): mp 220 °C dec; ¹H NMR δ 5.80 (q, *J* = 158 Hz, 1H), 8.10 (t, *J* = 5.9 Hz, 2H), 8.60 (t, *J* = 7.8 Hz, 1H), 9.48 (d, *J* = 5.7 Hz, 2H); ¹¹B NMR δ -24.2 (d, *J* = 141 Hz, 4B), -14.1 (d, *J* = 153 Hz, 4B), 33.1 (d, *J* = 157 Hz, 1B); UV (CH₃CN), λ_{max} (log ε) 271 nm (3.8); MS (FAB): *m/z* (193-199) max at 197 (100%); FAB-HRMS(+): calcd. for C₆H₁₄NB₉ *m/z*: 199.1964; found; 199.1947. Anal. Calcd. for C₆H₁₄B₉N: C, 36.49; H, 7.15; N, 7.09. Found: C, 37.74; H, 7.41; N, 7.04.

11b[**H**] (2-isomer): mp 240 °C dec; ¹H NMR δ 5.86 (q, *J* = 156 Hz, 1H), 7.92 (t, *J* = 6.6 Hz, 1H), 8.47 (d, *J* = 8.0 Hz, 1H), 8.55 (m, 2H); ¹¹B NMR δ -22.8 (d, *J* = 140 Hz, 4B), -13.9 (d, *J* = 150 Hz, 4B), 37.2 (d, *J* = 160 Hz, 1B); MS (FAB): *m/z* (194-200) max at 197 (100%); FAB-HRMS(+): calcd. for C₆H₁₄B₉N *m/z*: 199.1964; found; 199.1966.

11c[**H**] and **11d**[**H**] Mixture: ¹H NMR (major signals attributed to **11c**[**H**]) δ 8.05 (t, *J* = 6.3 Hz, 1H), 8.60 (d, *J* = 6.0 Hz, 1H), 9.03 (d, *J* = 8.2 Hz, 1H), 9.09 (d, *J* = 6.3 Hz, 1H);

^{11}B NMR δ -22.9 (4B), -14.5 (4B), 33.9 (1B); ^1H NMR (minor signals attributed to **11d[H]**) δ 8.42 (d, $J = 5.9$ Hz, 2H), 8.61 (d, $J = 6.0$, 2H); ^{11}B NMR δ -22.9 (4B), -13.8 (4B), 35.9 (1B); MS (FAB): m/z (193-199) max at 196 (100%); FAB-HRMS(-): Calcd. for $\text{C}_6\text{H}_{13}\text{NB}_9$ m/z : 198.1885; found; 198.1883.

14[PyrH]: ^1H NMR δ 8.03 (t, $J = 7.2$ Hz, 2H), 8.58 (t, $J = 8.0$ Hz, 1H), 8.69 (d, $J = 5.6$ Hz, 2H); ^{11}B $\{^1\text{H}\}$ NMR δ -24.7 (4B), -19.3 (4B), 29.8 (1B).

15[PyrH]: ^1H NMR δ 5.26 (q, $J = 154$ Hz, 1H), 7.96 (t, $J = 7.1$ Hz, 2H), 8.50 (t, $J = 7.9$ Hz, 1H), 8.67 (d, $J = 5.3$ Hz, 2H); ^{11}B $\{^1\text{H}\}$ NMR δ -25.4 (4B), -14.9 (4B), 26.0 (1B); MS (FAB): m/z (151-156) max at 154 (100%); FAB-HRMS(-): calcd. for $\text{CB}_9\text{H}_9\text{Cl}$ m/z : 155.1230; found: 155.1214.

16[NEt₄]: An authentic sample was used for identification of **16[PyrH]** in crude reaction mixture. ^1H NMR δ 1.18 (t, $J = 7.3$ Hz, 12H), 3.13 (q, $J = 7.3$ Hz, 8H), 5.33 (q, $J = 153$ Hz, 1H), 7.29 (t, $J = 7.3$ Hz, 1H), 7.37 (t, $J = 7.4$ Hz, 2H), 7.89 (t, $J = 7.0$ Hz, 2H); ^{11}B $\{^1\text{H}\}$ NMR δ -23.6 (4B), -15.5 (4B), 29.6 (1B). [lit.⁸⁰ ^{11}B $\{^1\text{H}\}$ NMR (acetone- d_6) δ -24.4 (4B), -16.1 (4B), 27.1 (1B)].

Preparation of [*closo*-1-CB₉H₉-1-SC₅H₁₀] (**9b**).

A yellow solution of crude **10** (0.069 g, 0.334 mmol), $\text{NMe}_4^+ \text{OH}^- \cdot 5 \text{H}_2\text{O}$ (0.150 g, 0.83 mmol), and 1,5-dibromopentane (0.046 mL, 0.34 mmol) in anhydrous CH_3CN (10 mL) was stirred for 24 hrs at rt. Insoluble salts were filtered and rinsed with CH_2Cl_2 .

Solvent was evaporated, and the solid residue was passed through a short silica gel plug (CH_2Cl_2) giving 0.067 g of crude **9b**. Further purification via recrystallization (toluene/iso-octane mixture) gave 0.038 g (50% yield) of [*closo*-1- CB_9H_9 -1-(1- SC_5H_{10})] (**9b**) as a white crystalline solid: mp 230 °C dec; ^1H NMR δ 1.66 (qt, $J_1 = 13.4$ Hz, $J_2 = 3.2$ Hz, 2H), 2.04 (m, 2H), 2.40 (m, 2H), 3.64 (td, $J_1 = 12.6$ Hz, $J_2 = 2.3$ Hz, 2H), 4.10 (br d, $J = 11.8$ Hz, 2H), 5.96 (q, $J = 159$ Hz, 1H); ^{11}B NMR δ -23.8 (d, $J = 142$ Hz, 4B), -15.3 (d, $J = 154$ Hz, 4B), 38.2 (d, $J = 146$ Hz, 1B). Anal. Calcd. for $\text{C}_6\text{H}_{19}\text{B}_9\text{S}$: C, 32.67; H, 8.68. Found: C, 33.19; H, 8.62.

Preparation [*closo*-1- CB_9H_9 -1-(N_2 - C_6H_4 -4- OCH_3)] $^-$ NMe_4^+ (13**[NMe_4]).**

A yellow solution of [*closo*-1- CB_9H_9 -1-(N_2 - C_6H_4 -4- OH)] $^-$ NMe_4^+ (**8a**[NMe_4], 0.055 g, 0.18 mmol) and $\text{NMe}_4^+ \text{OH}^- \cdot 5\text{H}_2\text{O}$ (0.032 g, 0.18 mmol) in anhydrous CH_3CN (8 mL) was slightly heated until the color darkened signifying deprotonation. After cooling, CH_3I (0.013 mL, 0.21 mmol) was added, and the solution was stirred for 24 hrs at rt. Precipitation was filtered and solvent removed giving 0.075 g of crude product as a yellow crystalline material. The crude material was passed through a short silica gel plug (1:4 $\text{CH}_3\text{CN}/\text{CH}_2\text{Cl}_2$) giving 0.054 g (95% yield) of [*closo*-1- CB_9H_9 -1-(N_2 - C_6H_4 -4- OCH_3)] $^-$ NMe_4^+ (**13**[NMe_4]) as a light yellow solid: mp 210 °C dec; ^1H NMR δ 3.06 (s, 12H), 3.89 (s, 3H), 5.47 (q, $J = 153$ Hz, 1H), 7.09 (d, $J = 9.2$ Hz, 2H), 7.87 (d, $J = 9.2$ Hz, 2H); ^{11}B NMR δ -24.5 (d, $J = 141$ Hz, 4B), -16.4 (d, $J = 155$ Hz, 4B), 29.6 (d, $J = 149$ Hz, 1B); IR: 1503 and 1482 (N=N), 1249 (C-O) cm^{-1} ; UV (CH_3CN), λ_{max} (log ϵ) 319 nm (4.23), 409 (2.8). Anal. Calcd. for $\text{C}_{12}\text{H}_{28}\text{B}_9\text{N}_3\text{O}$: C, 43.99; H, 8.61; N, 12.82. Found: C,

43.75; H, 8.49; N, 12.57.

Preparation of [*closo*-1-CB₉H₁₀]⁻C₅H₆N⁺ (14[PyrH]).

Equimolar amounts of pyridine and trifluoroacetic acid were mixed and allowed to cool to form a hygroscopic solid. ¹H NMR analysis in CD₃CN showed three broad aromatic signals [¹H NMR δ 7.90 (m, 2H), 8.38 (m, 1H), 8.80 (m, 2H)]. A small portion of [*closo*-1-CB₉H₁₀]⁻NEt₄⁺ was dissolved in 10% HCl and extracted with Et₂O (3x). The organic layers were combined and H₂O was added. The Et₂O was removed *in vacuo*, and the aqueous layer was filtered. A slight molar excess of pyridinium trifluoroacetate was added to form a precipitate, which was filtered, washed with H₂O, and dried. ¹H NMR δ 8.03 (t, *J* = 7.2 Hz, 2H), 8.58 (t, *J* = 8.0 Hz, 1H), 8.69 (d, *J* = 5.6 Hz, 2H); ¹¹B {¹H} NMR δ -24.7 (4B), -19.28 (4B), 29.8 (1B).

Preparation of [*closo*-1-CB₉H₉-1-NHCOCH₃] (18[H₃O]).

In a NMR tube, [*closo*-1-CB₉H₉-1-N₂] (**1**, 5 mg, 0.034 mmol) was heated (70 °C) in anhydrous CD₃CN (dried over 4 Å MS) for 1 hr. ¹¹B NMR showed the presence of two species [B(10) δ 37.4 and 30.5] in approximately a 1:1 ratio. Solvent was removed *in vacuo*, and the crude product (5 mg) was dissolved in moist CD₃CN. The sample was stored openly in the freezer for 10 min to ensure that moisture was introduced. ¹¹B NMR showed the presence of only one species [B(10) δ 30.5]. A similar experiment was performed in CH₃CN for which the final product was analyzed to verify the identify of acetamide **18**[H₃O]: ¹H NMR δ 0.56 (q, *J* = 107 Hz, 1H), 1.76 (q, *J* = 115 Hz, 1H), 2.55

(s, 3H), 5.66 (q, $J = 116$ Hz, 1H) 10.6 (s, 1H); ^{11}B NMR δ -25.7 (d, $J = 142$ Hz, 4B), -16.6 (d, $J = 155$ Hz, 4B), 29.0 (d, $J = 141$ Hz, 4B); MS (FAB): m/z (174-178) max at 176 (100%); FAB-HRMS(-): calcd. for $\text{C}_3\text{H}_{13}\text{B}_9\text{NO}$ m/z : 178.1835; found: 178.1838.

Analysis of the original reaction mixture permitted assignment of the ^{11}B NMR chemical shifts of nitrilium adduct **17**: ^{11}B NMR δ -24.6 (4B), -13.5 (4B), 37.4 (4B). The ratio of these two species in the initial decomposition of **1** varied between experiments due to different residual H_2O content.

Preparation of [*closo*-1- CB_9H_9 -1- $\text{N}(\text{CH}_3)_3$] (**20**)

Compound **20** was prepared following literature procedure¹² using amine **2** and Me_2SO_4 .

Acknowledgment

Financial support for this work was received from the National Science Foundation (DMR-0111657 and DMR-0606317). We thank Mr. Andrzej Balinski for his technical assistance with isolation of **11b[H]**.

References

- (1) Hertler, W. R.; Knoth, W. H.; Muetterties, E. L. *J. Am. Chem. Soc.* **1964**, *86*, 5434-5439.
- (2) Hertler, W. R.; Knoth, W. H.; Muetterties, E. L. *Inorg. Chem.* **1965**, *4*, 288-293.

- (3) Knoth, W. H.; Hertler, W. R.; Muetterties, E. L. *Inorg. Chem.* **1965**, *4*, 280-287.
- (4) Knoth, W. H. *J. Am. Chem. Soc.* **1966**, *88*, 935-939.
- (5) Leyden, R. N.; Hawthorne, M. F. *Inorg. Chem.* **1975**, *14*, 2444-2446.
- (6) Balinski, A.; Januszko, A.; Harvey, J. E.; Brady, E.; Kaszynski, P.; Young, V. G., Jr. unpublished results.
- (7) Kaszynski, P.; Huang, J.; Jenkins, G. S.; Bairamov, K. A.; Lipiak, D. *Mol. Cryst. Liq. Cryst.* **1995**, *260*, 315-331.
- (8) Kaszynski, P.; Douglass, A. G. *J. Organomet. Chem.* **1999**, *581*, 28-38.
- (9) Komura, M.; Nakai, H.; Shiro, M. *J. Chem. Soc., Dalton Trans.* **1987**, 1953-1956.
- (10) Bragin, V. I.; Sivaev, I. B.; Bregadze, V. I.; Votnova, N. A. *J. Organomet. Chem.* **2005**, *690*, 2847-2849.
- (11) Kaszynski, P.; Pakhomov, S.; Young, V. G., Jr. *Collect. Czech. Chem. Commun.* **2002**, *67*, 1061-1083.
- (12) Jelinek, T.; Stibr, B.; Plesek, J.; Thornton-Pett, M.; Kennedy, J. D. *J. Chem. Soc., Dalton Trans.* **1997**, 4231-4236.
- (13) Kaszynski, P.; Lipiak, D. In *Materials for Optical Limiting*; Crane, R., Lewis, K., Stryland, E. V., Khoshnevisan, M., Eds.; MRS: Boston, 1995; Vol. 374, p 341-347.

- (14) Fendrich, W.; Harvey, J. E.; Kaszynski, P. *Inorg. Chem.* **1999**, *38*, 408-410.
- (15) Ringstrand, B.; Kaszynski, P. Monobe, H. *J. Mater. Chem.* **2009**, *19*, 4805-4812;
Ringstrand, B. Kaszynski, P.; Januszko, A.; Young, V. G. Jr. *J. Mater. Chem.* **2009**, *19*,
9204-9212.
- (16) Ringstrand, B.; Balinski, A.; Franken, A.; Kaszynski, P. *Inorg. Chem.* **2005**, *44*,
9561-9566.
- (17) Banthorpe, D. V. In *The Chemistry of the Azido Group*; Patai, Ed.; Wiley: NY,
1971, p 405.
- (18) Banthorpe, D. V. In *The Chemistry of the Azido Group*; Patai, Ed.; Wiley: NY,
1971, p 397.
- (19) Krow, G.; Damodaran, K. M.; Michener, E.; Miller, S. I.; Dalton, D. R. *Synth.*
Commun. **1976**, *6*, 261-267.
- (20) Warren, J. D.; Press, J. B. *Synth. Commun.* **1980**, *10*, 107-110.
- (21) Shioiri, T.; Ninomiya, K.; Yamada, S. *J. Am. Chem. Soc.* **1972**, *94*, 6203-6205.
- (22) Wallace, R. G.; Barker, J. M.; Wood, M. L. *Synthesis* **1990**, *12*, 1143-1144.
- (23) Prakash, G. K. S.; Iyer, P. S.; Arvanaghi, M.; Olah, G. A. *J. Org. Chem.* **1983**, *48*,
3358-3359.
- (24) Rawal, V. H.; Zhong, H. M. *Tetrahedron Lett.* **1994**, *35*, 4947-4950.

- (25) Laszlo, P.; Polla, E. *Tetrahedron Lett.* **1984**, 25, 3701-3704.
- (26) Paraskewas, S. M.; Danopoulos, A. A. *Synthesis* **1983**, 638-340.
- (27) Franken, A.; Kilner, C. A.; Thornton-Pett, M.; Kennedy, J. D. *Inorg. Chem. Comm.* **2002**, 5, 581-584.
- (28) Ringstrand, B.; Bateman, D.; Shoemaker, R. K.; Janousek, Z. *Collect. Czech. Chem. Comm.* **2009**, 74, 419-431.
- (29) Jelinek, T.; Kilner, C. A.; Thornton-Pett, M.; Kennedy, J. D. *Chem. Commun.* **2001**, 1790-1791.
- (30) Eicher, T.; Hauptmann, S. in *The Chemistry of Heterocycles*, Georg Thieme Verlag, New York 1995, pp 273-276, and references therein.
- (31) Abramovitch, R. A.; Saha, J. G. *Tetrahedron* **1965**, 21, 3297-3303.
- (32) Zollinger, H. *Acc. Chem. Res.* **1973**, 6, 335-341.
- (33) Galli, C. *Chem. Rev.* **1988**, 88, 765-792.
- (34) Ribeiro da Silva, M. A. V.; Matos, M. A. R.; Rio, C. A.; Morais, V. M. F.; Wang, J.; Nichols, G.; Chickos, J. S. *J. Phys. Chem. A* **2000**, 104, 1774-1778.
- (35) Ritchie, C. D.; Saltiel, J. D.; Lewis, E. S. *J. Am. Chem. Soc.* **1961**, 83, 4601-4605.

- (36) Le Fèvre, R. J. W. *Trans. Faraday Soc.* **1938**, *34*, 1127-1132.
- (37) Ohkubo, K.; Yamabe, T. *J. Org. Chem.* **1971**, *36*, 3149–3155.
- (38) Jaffé, H. H. *Theory and applications of ultraviolet spectroscopy*, Wiley, New York, 1962, pp 276-286.
- (39) Kojima, M.; Nebashi, S.; Ogawa, K.; Kurita, N. *J. Phys. Org. Chem.* **2005**, *18*, 994-1000.
- (40) Korolev, B. A.; Titova, S. P.; Ufimtsev, V. N. *J. Org. Chem. USSR* **1971**, *7*, 1228-1231.
- (41) Uno, B.; Matsuhisa, Y.; Kano, K.; Kubota, T. *Chem. Pharm. Bull.* **1984**, *32*, 1691-1698.
- (42) Hansch, C.; Leo, A.; Taft, R. W. *Chem. Rev.* **1991**, *91*, 165-195.
- (43) Figeys, H. P.; Flammang, R. *Mol. Phys.* **1967**, *12*, 581-587.
- (44) Jelinek, T.; Plesek, J.; Hermanek, S.; Stibr, B. *Collect. Czech. Chem. Commun.* **1986**, *51*, 819-829.
- (45) Ishida, K.; Kobori, N.; Kobayashi, M.; Minato, H. *Bull. Chem. Soc. Japan* **1970**, *43*, 285-286.
- (46) Dermer, O. C.; Edmison, M. T. *Chem. Rev.* **1957**, *57*, 77-122. Bachmann, W. E., Hoffman, R. A. *Org. React.* **1944**, *2*, 224-261.

- (47) Beadle, J. R.; Korzeniowski, S. H.; Rosenberg, D. E.; Garcia-Slanga, B. J.; Gokel, G. W. *J. Org. Chem.* **1984**, *49*, 1594-1603.
- (48) From the steady-state approximation considering that the rate of decomposition of adduct **23** is much slower than the reverse reaction.
- (49) Since $[26] \approx [25]$, radical anion **26** competes with **25** for the hydrogen from **28** leading to the observed low yield (~5%) of **14**.
- (50) Carr, M. J.; Kaszynski, P.; Franken, A.; Kennedy, J. D., unpublished results.
- (51) Szele, I.; Zollinger, H. *Helv. Chim. Acta* **1978**, *61*, 1721-1729.
- (52) Maria, P.-C.; Gal, J.-F. *J. Phys. Chem.* **1985**, *89*, 1296-1304.
- (53) Kice, J. L.; Gabrielsen, R. S. *J. Org. Chem.* **1970**, *35*, 1004-1015.
- (54) Makarova, L. G.; Nesmeyanov, A. N. *Bull Akad. Sci. USSR, Div. Chem. Sci.* **1954**, 887-891.
- (55) Kobayashi, M.; Minato, H.; Yamada, E.; Kobori, N. *Bull. Chem. Soc. Japan* **1970**, *43*, 215-219.
- (56) Kobayashi, M.; Minato, H.; Kobori, N. *Bull. Chem. Soc. Japan* **1970**, *43*, 219-223.
- (57) Kobori, N.; Kobayashi, M.; Minato, H. *Bull. Chem. Soc. Japan* **1970**, *43*, 223-225.

- (58) NIST Standard Reference Database Number 69 (<http://webbook.nist.gov/chemistry/>) and references therein.
- (59) Cottrell, P. T.; Mann, C. K. *J. Electrochem. Soc.* **1969**, *116*, 1499-1503.
- (60) Andrieux, C. P.; Pinson, J. *J. Am. Chem. Soc.* **2003**, *125*, 14801-14806.
- (61) Turner, W. R.; Elving, P. J. *Anal. Chem.* **1965**, *37*, 467-469.
- (62) Baizer, M. M. and Lund, H. *Organic Electrochemistry*, Marcel Dekker, New York, 2nd Ed, 1983, and references therein.
- (63) No stable adduct of Me₂S to **1** nor to PhN₂⁺ was located on the PES with the DFT method.
- (64) Barton, D. H. R.; Crich, D.; Motherwell, W. B. *Tetrahedron* **1985**, *41*, 3901-3924.
- (65) Kaszynski, P. In *Anisotropic Organic Materials-Approaches to Polar Order*; Glaser, R., Kaszynski, P., Eds.; ACS Symposium Series: Washington, D.C., 2001; Vol. 798, p 68-82.
- (66) Pakhomov, S.; Kaszynski, P.; Young, V. G., Jr. *Inorg. Chem.* **2000**, *39*, 2243-2245.
- (67) Kaszynski, P.; Kulikiewicz, K. K.; Januszko, A.; Douglass, A. G.; Tilford, R. W.; Pakhomov, S.; Patel, M. K.; Radziszewski, G. J.; Young, V. G., Jr. unpublished results.
- (68) Hermanek, S.; Plesek, J.; Gregor, V.; Stirb, B. *Chem. Commun.* **1977**, 561-563.

Hermanek, S. *Chem. Rev.* **1992**, *92*, 325-362.

(69) Bühl, M.; Schleyer, P. v. R.; Havlas, Z.; Hnyk, D.; Hermanek, S. *Inorg. Chem.* **1991**, *30*, 3107-3111.

(70) Fox, M. A.; MacBride, H. J. A.; Peace, R. J.; Wade, K. *J. Chem. Soc., Dalton Trans.* **1998**, 401-411.

(71) For details see Supporting Information.

(72) Becke, A. D. *J. Chem. Phys.* **1993**, *98*, 5648-5652.

(73) Lee, C.; Yang, W.; Parr, R. G. *Phys. Rev. B*, **1988**, *37*, 785-789.

(74) Møller, C.; Plesset, M. S. *Phys. Rev.* **1934**, *46*, 618-622; Head-Gordon, M.; Pople, J. A.; Frisch, M. J. *Chem. Phys. Lett.* **1988**, *153*, 503-506.

(75) Gaussian 98, Revision A.9, M. J. Frisch, G. W. Trucks, H. B. Schlegel, G. E. Scuseria, M. A. Robb, J. R. Cheeseman, V. G. Zakrzewski, J. A. Montgomery, Jr., R. E. Stratmann, J. C. Burant, S. Dapprich, J. M. Millam, A. D. Daniels, K. N. Kudin, M. C. Strain, O. Farkas, J. Tomasi, V. Barone, M. Cossi, R. Cammi, B. Mennucci, C. Pomelli, C. Adamo, S. Clifford, J. Ochterski, G. A. Petersson, P. Y. Ayala, Q. Cui, K. Morokuma, D. K. Malick, A. D. Rabuck, K. Raghavachari, J. B. Foresman, J. Cioslowski, J. V. Ortiz, A. G. Baboul, B. B. Stefanov, G. Liu, A. Liashenko, P. Piskorz, I. Komaromi, R. Gomperts, R. L. Martin, D. J. Fox, T. Keith, M. A. Al-Laham, C. Y. Peng, A. Nanayakkara, M. Challacombe, P. M. W. Gill, B. Johnson, W. Chen, M. W. Wong, J. L. Andres, C. Gonzalez, M. Head-Gordon, E. S. Replogle, and J. A. Pople, Gaussian, Inc., Pittsburgh PA, 1998.

(76) Scott, A. P.; Radom, L. *J. Phys. Chem.* **1996**, *100*, 16502-16513.

(77) Foresman, J. B.; Keith, T. A.; Wiberg, K. B.; Snoonian, J.; Frisch, M. J. *J. Phys. Chem.* **1996**, *100*, 16098–16104.

(78) A. J. Bard and L. R. Faulkner *Electrochemical Methods: Fundamentals and Applications*, 2nd Ed, Wiley, Hoboken, 2001.

(79) Anders, E.; Opitz, A.; Wermann, K.; Wiedel, B.; Walther, M.; Imhof, W.; Gorls, H. *J. Org. Chem.* **1997**, *64*, 3113-3121.

(80) Franken, A.; Jelinek, T.; Taylor, R. G.; Ormsby, D. L.; Kilner, C. A.; Clegg, W.; Kennedy, J. D. *J. Chem. Soc. Dalton Trans.* **2006**, *48*, 5753-5769.

The Anionic Amino Acid [*closo*-1-CB₉H₈-1-COO-10-NH₃]⁻ and Dinitrogen Acid [*closo*-1-CB₉H₈-1-COOH-10-N₂] as Key Precursors to Advanced Materials: Synthesis and Reactivity.

Reproduced with permission from Ringstrand, B.; Kaszynski, P.; Young, V. G. Jr.; Janousek, Z. *Inorg. Chem.* **2010**, *49*, 1166-1179. Copyright 2011 American Chemical Society. Available online: <http://pubs.acs.org/doi/abs/10.1021/ic9021323>

The goal of this work was to investigate functional group transformations at the B(10) position of the [*closo*-1-CB₉H₁₀]⁻ anion with emphasis on the N₂⁺ group. The Pd-catalyzed amination of the B-I bond in iodo acid **1** with an ammonia equivalent provided access to the 10-amino acid **4**, and its diazotization gave 10-N₂ acid **5**. The importance of this work was in opening up the B(10) vertex of the [*closo*-1-CB₉H₁₀]⁻ anion for substitution with onium fragments, which provides access to polar materials of type **II** (see Dissertation Synopsis and Guide).

My role in this work was performing synthesis and characterization of all compounds and conducting all physical-organic studies, which included UV-vis spectroscopy, NMR temperature-dependent studies to determine the activation parameters of thermal decomposition of [*closo*-1-CB₉H₈-1-COOMe-10-N₂] (**11**) in benzonitrile, and electrochemical measurements on **11** and [*closo*-1-CB₉H₈-1-COO-10-

N₂]⁻ (**5**⁻) to determine their redox properties.

This work was initially conceived at Vanderbilt University under my own direction but was partly continued at the Czech Academy of Sciences, Institute of Inorganic Chemistry located in Rez, Czech Republic in the summer of 2008. It was later completed at Vanderbilt University in the fall of 2008. Dr. Zbynek Janousek hosted me during my stay in the Czech Republic. Dr. Victor G. Young, Jr. from the University of Minnesota at the Twin Cities performed single crystal X-ray measurements on compounds **5**, **6**, and **8**. Dr. Piotr Kaszynski performed quantum mechanical calculations to support experimental data collected during the project.

Abstract

Amino acid [*closo*-1-CB₉H₈-1-COO-10-NH₃]⁻ (**4**) was prepared by amination of iodo acid [*closo*-1-CB₉H₈-1-COOH-10-I]⁻ (**1**) with LiHMDS in a practical and reproducible manner. The apparent dissociation constants, pK₂ = 5.6 and pK₁ >11, were measured for [*closo*-1-CB₉H₈-1-COO-10-NH₃]⁻ (**4**[NMe₄]) in 50% aq. EtOH. Diazotization of **4** with NO⁺PF₆⁻ under mildly basic conditions afforded stable dinitrogen acid [*closo*-1-CB₉H₈-1-COOH-10-N₂]⁻ (**5**). Activation parameters ($\Delta H^\ddagger = 33.9 \pm 1.4$ kcal mol⁻¹ and $\Delta S^\ddagger = 10 \pm 3.5$ cal mol⁻¹ K⁻¹) for thermolysis of its methyl ester [*closo*-1-CB₉H₈-1-COOMe-10-N₂]⁻ (**11**) in PhCN were established, and the heterolysis of the B–N bond is believed to be the rate-determining step. Electrochemical analysis showed a partially reversible reduction process for **11** ($E_{1/2}^{\text{red}} = -1.03$ V) and **5**⁻ ($E_{1/2}^{\text{red}} = -1.21$ V), which are

more cathodic than reduction of [*closo*-1-CB₉H₉-1-N₂] (**17**).

The dinitrogen acid **5** was reacted with pyridine and *N,N*-dimethylthioformamide, to form pyridine acid **6** and protected mercapto acid **7**, respectively, through a boronium ylide intermediate **18**. Compound **7** was converted to sulfonium acid **8**. The molecular and crystal structures for **5** [C₂H₉B₉N₂O₂ monoclinic, *P*2₁/*n*, *a* = 7.022(2) Å, *b* = 11.389(4) Å, *c* = 12.815(4) Å, β = 96.212(5)°; *V* = 1018.8(6) Å³, *Z* = 4,], **6** [C₇H₁₄B₉NO₂, monoclinic, *P*2₁/*n*, *a* = 14.275(4) Å, *b* = 12.184(3) Å, *c* = 30.538(8) Å, β = 95.377(4)°; *V* = 5288(3) Å³, *Z* = 16], and **8** [C₇H₁₉B₉O₂S, monoclinic, *P*₂1/*c*, *a* = 15.988(5) Å, *b* = 19.377(6) Å, *c* = 9.655(3) Å, β = 98.348(5)°; *V* = 2959.4(16) Å³, *Z* = 8] were determined by X-ray crystallography and compared with results of DFT and MP2 calculations.

Electronic structures of **5**, **6**, and related species were elucidated with electronic spectroscopy and assessed computationally at the B3LYP/6-31G(d,p), MP2/6-31G(d,p), and ZINDO//MP2 levels of theory.

Introduction

closo-Carbaborates^{1,2} [*closo*-1-CB₉H₁₀]⁻ (**A**)³ and [*closo*-1-CB₁₁H₁₂]⁻ (**B**)^{4,5} (Figure 1) are becoming increasingly important building blocks for advanced materials such as ionic liquids,⁶ lithium ion battery electrolytes,⁷ ionic liquid crystals,⁸ polar liquid crystals,⁹ NLO materials,¹⁰ and also agents for Boron Neutron Capture Therapy¹¹⁻¹³ (BNCT) and Photodynamic Therapy^{11,14,15} (PDT). The attractiveness of these clusters

stems largely from their electronic features which are manifested in complete charge delocalization, low nucleophilicity,¹⁶ and chemical stability under ambient conditions due to sigma-aromaticity of the skeleton.^{1,4,17,18} In BNCT and PDT applications, the lipophilic nature of these anions assists otherwise hydrophobic molecules to cross cellular membranes in biological systems. On the other hand, the geometry of the clusters is suitable for the construction of anisometric molecules¹⁹ as has been demonstrated for their electrically neutral carborane analogs.²⁰⁻²⁷

The 12-vertex carbaborate, [*closo*-1-CB₁₁H₁₂]⁻, has been relatively more accessible and many functionalization methods have been devised.²⁸⁻³¹ In contrast, the chemistry of the 10-vertex analog is less developed in part due to its lesser availability, and in part to differences in reactivity. For instance, while the electrophilic substitution of the {*closo*-1-CB₁₁} cage occurs preferentially at the B(12) position,^{10,28,29} the electrophilic attack on the {*closo*-1-CB₉} takes place almost exclusively at the B(6) position (Figure 1).^{8,32} The inability to form derivatives with substituents in the antipodal positions (the 1,10-disubstitution pattern) was the major obstacle in applications of the [*closo*-1-CB₉H₁₀]⁻ cluster as a structural element for anisometric molecules and materials such as liquid crystals.

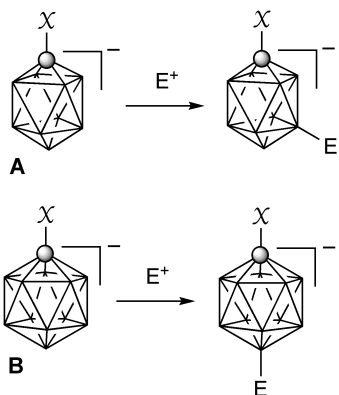
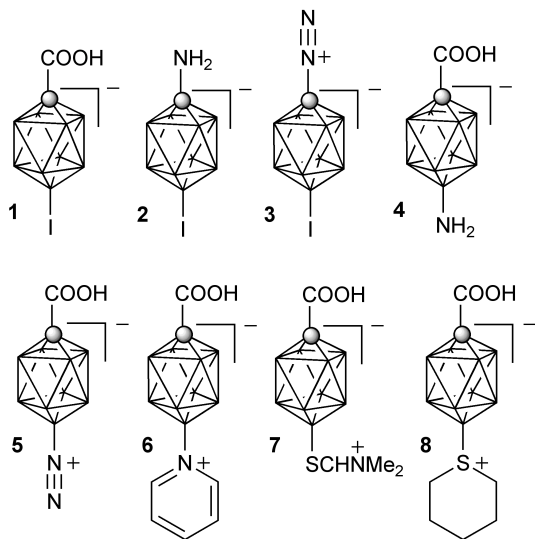


Figure 1. Substitution pattern in carbaborates **A** and **B**. Each vertex represents a BH fragment, and the sphere is a carbon atom.

This situation changed when Brelochs discovered³³ a new method for preparing the parent [*closo*-1-CB₉H₁₀]⁻ and *C*-substituted derivatives.³⁴⁻³⁶ The method not only simplified access to the {1-CB₉} cluster, but also permitted the introduction of a substituent at the B(10) position.³⁷ The next milestone in the chemistry of the [*closo*-1-CB₉H₁₀]⁻ cluster was the preparation of an isomerically pure 1,10-heterobifunctionalized derivative, the iodo acid **1**.³⁸ We have demonstrated that the iodine in **1** can be used to introduce alkyl groups in Pd-catalyzed coupling reactions with alkylzinc reagents.^{8,9} The COOH group in the iodo acid was transformed to the NH₂ group in amine **2** and subsequently to the stable dinitrogen group, N₂, in **3**.⁸ The relatively high stability of the N₂ group at the apical position appears to be general for 10-vertex *closo*-boranes,³⁹ and several such derivatives of [*closo*-B₁₀H₁₀]²⁻ have been prepared and used as intermediates to obtain nitrogen,⁴⁰⁻⁴⁵ sulfur,^{45,46} phosphorus,⁴⁷ oxygen,^{43,48} and even carbon^{43,49} substituted {*closo*-B₁₀} clusters. Similar stability and synthetic value of the dinitrogen

group was recently found for [*closo*-1-CB₉H₉-1-N₂]; its reactivity is similar to that of benzenediazonium and permits the introduction of heteroatoms at the C(1) position of the cluster.⁵⁰ These new findings were exploited in the preparation of the first anion-driven ionic liquid crystals⁸ and positive Δε additives to nematic materials.⁹ In contrast, the analogous dinitrogen derivatives of the 12-vertex *closo*-boranes are highly unstable,³⁹ and their usefulness as synthetic intermediates is limited.

Now, we report another important step in the chemistry of the {*closo*-1-CB₉} cluster, the preparation of amino acid **4** and its dinitrogen derivative **5**, which completes the development of key 1,10-heterobifunctional derivatives of the [*closo*-1-CB₉H₁₀]⁻ cluster and opens new horizons for applications of this cluster in advanced materials and biological investigations.



Here we describe the preparation of amino acid **4** from readily available [*closo*-1-CB₉H₈-1-COOH-10-I]NMe₄⁺ (**1**[NMe₄]),³⁸ its diazotization, and formation of the

nitrogen derivative [*closo*-1-CB₉H₈-1-COOH-10-N₂] (**5**). The latter is extensively characterized by structural, spectroscopic, thermochemical, and electrochemical methods aided by quantum-mechanical calculations. Several transformations of the dinitrogen acid **5** are demonstrated including conversion to pyridinium **6** and acid **7** containing a protected mercapto functionality. The latter was converted further to sulfonium acid **8**. Both, pyridinium acid **6** and sulfonium acid **8** were structurally characterized, and simple transformations (esterification) of the carboxyl group were demonstrated.

Results

*Synthesis of [*closo*-1-CB₉H₈-1-COOH-10-NH₂] (4)*

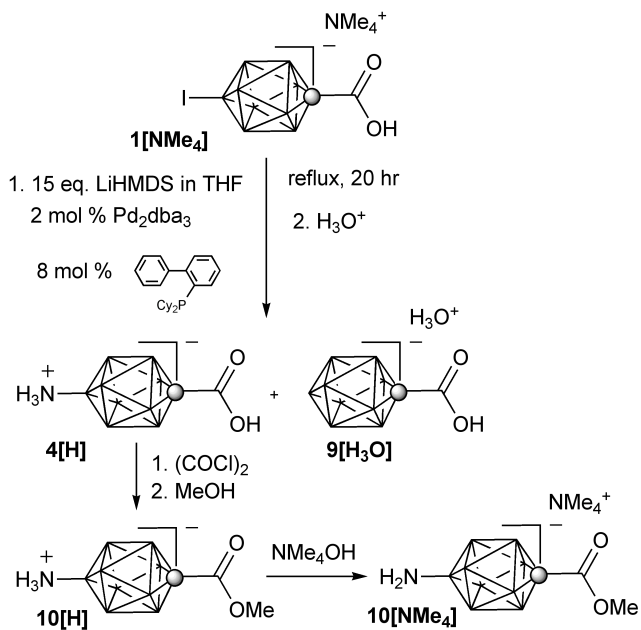
Amination of iodo acid **1** with ammonia equivalents was envisioned using the Buchwald-Hartwig conditions.⁵¹ However, the reactions could not be run in toluene, a common solvent used for typical amination reactions, because of the low solubility of the **1**[NMe₄] salt. Also, harsh bases such as alkali *tert*-butoxides could not be used in this process due to possible attack on the {*closo*-1-CB₉} cage. For these reasons THF was the solvent of choice, and Cs₂CO₃ was the preferred base.

Our initial attempts at aminating **1** were unsuccessful. Reactions of the iodo acid **1**[NMe₄] with aqueous NH₃, according to the literature procedure,⁵² or 2 equivalents of diallylamine⁵³ with Cs₂CO₃ and 2 mol% Pd₂dba₃/8 mol% S-Phos⁵⁴ in refluxing THF showed no product formation after 24 hr. Similar reactions using the latter conditions

with 5 equivalents of benzophenone imine,⁵⁵ or *tert*-butylcarbamate⁵⁶ were slow, taking at least 5 days to complete. Attempts to perform the amination of ethyl ester of iodo acid **1**[NMe₄] using these conditions failed, and no reaction was observed after several days.

Metal salts of hexamethyldisilazane (HMDS) as the ammonia equivalent were more promising. A reaction of **1**[NMe₄] with 5 equivalents of Zn(HMDS)₂⁵⁷ and [HPCy₃]⁺BF₄⁻, as the phosphine ligand precursor, in THF was approximately 10% complete after 24 hrs at reflux. However, deiodinated product, acid [*closo*-1-CB₉H₉-1-COOH] (**9**), was the major product observed by ¹¹B NMR. Reactions with LiHMDS^{58,59} as the ammonia equivalent were more successful although deiodination of **1** was still observed. Brief optimization of the reaction conditions revealed that by increasing the amounts of LiHMDS to 15 equivalents and using 2-(dicyclohexylphosphine)biphenyl as the phosphine ligand, the ratio of amino acid **4**[H] to parent acid **9**[H₃O] improved to 5:1 (Scheme 1).⁶⁰ Excess of LiHMDS beyond 15 equivalents did not improve the ratio. When [HP(*t*-Bu)₃]BF₄ was used as the phosphine ligand source, the parent [*closo*-1-CB₉H₁₀]⁻ anion was obtained as the major product apparently by deiodination at the B(10) vertex and decarboxylation at the C(1) vertex of iodo acid **1**. A summary for the results for optimization of the LiHMDS reaction is presented in the SI.

Scheme 1



Separation of the amino acid $4[\text{H}]$ from acid $9[\text{H}_3\text{O}]$ was accomplished by preferential extraction of the $9[\text{NEt}_4]$ ion pair with CH₂Cl₂ from an aqueous solution of the two products containing Et₄N⁺Br⁻. After acidification, the protonated amino acid $4[\text{H}]$ was extracted to ether and isolated in purity greater than 90% (by ¹¹B NMR) and in yields ranging from 40% to 50%. The protonated form of the amino acid [*closo*-1-CB₉H₈-1-COOH-10-NH₃] ($4[\text{H}]$) was treated with 0.9 equivalent of Me₄N⁺OH•5H₂O to obtain pure salt $4[\text{NMe}_4]$ after washing with ether followed by boiling MeCN. Acidification of $4[\text{NMe}_4]$ and extraction to ether provided a convenient method for the preparation of pure $4[\text{H}]$. The two products, $4[\text{H}]$ and $9[\text{H}_3\text{O}]$, can also be separated by chromatography, but with lower overall yield.

[*closo-1-CB₉H₈-1-COOH-10-N₂*] (**5**)

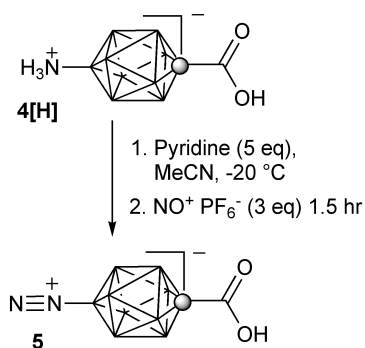
Diazotization of amino acid **4** was surprisingly difficult. Attempts to diazotize **4**[**H**] in aqueous AcOH, conditions used for the parent amine [*closo-1-CB₉H₉-1-NH₃*],⁵⁰ were unsuccessful and only the starting amino acid was recovered. A similar result was obtained with NO⁺PF₆⁻ as the diazotizing reagent under conditions used for weakly nucleophilic anilines.⁶¹ When amino acid **4**[**H**] was allowed to react with 2.5 equivalents of NO⁺PF₆⁻ overnight at room temperature instead at -20 °C, a new species with lower boron cage symmetry (according to ¹¹B NMR) and *m/z* of 271 (FAB-MS) was formed as the sole product. This result suggests that amino acid **4** was substituted, presumably at the B(6) vertex, which is preferred in electrophilic attack on the [*closo-1-CB₉H₁₀*]⁻ cluster.^{8,32} Attempts to further elucidate the structure were not made.

The negative results for the diazotization of **4** under typical conditions prompted us to conduct more detailed investigations. Diazotization of methyl ester of acid **4**, [*closo-1-CB₉H₈-1-COOMe-10-NH₂*]⁻ (**10**[**NMe₄**], Scheme 1) with NO⁺PF₆⁻ resulted in complete conversion of **10**[**NMe₄**], and the formation of two products in 85:15 ratio with a significantly shielded B(10) nucleus. Analysis revealed that the major product was the protonated amino ester **10**[**H**], while the minor product with a more shielded B(10) nucleus ($\Delta\delta = -26.7$ ppm) was the expected dinitrogen ester **11**. The complete and clean transformation of ester **10**[**NMe₄**] to **11** was accomplished by addition of pyridine to the reaction mixture. A similar approach was taken for diazotization of acid **4**[**H**]. Initially,

the reaction was conducted in neat pyridine, but brief optimization⁶² led to MeCN containing 5.0 equivalents of pyridine as the appropriate medium for the reaction. The yield of isolated dinitrogen acid [*closo*-1-CB₉H₈-1-COOH-10-N₂] (**5**) was about 80% after chromatographic separation (Scheme 2). Diazotization of crude **4**[H] give a lower yield of about 60%. In none of the diazotization reactions in the presence of pyridine, was the formation of **6** observed (*vide infra*).

Other bases such as NaH or solid K₂CO₃ were less effective and incomplete conversion was observed even with large excess of NO⁺PF₆⁻.

Scheme 2



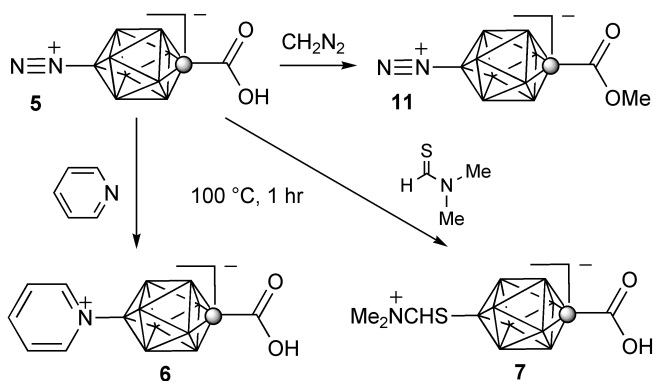
Reactivity of [*closo*-1-CB₉H₈-1-COOH-10-N₂] (**5**)

Reactions of dinitrogen acid **5** in neat pyridine and *N,N*-dimethylthioformamide gave pyridinium acid **6** and masked mercaptan **7**, respectively, as the sole products (Scheme 3). Masked mercaptan **7** was isolated as a crude product and used without further purification, whereas pyridinium **6** was isolated in 90% yield after

chromatographic separation. In contrast to [*closo*-1-CB₉H₉-1-N₂],⁵⁰ reaction of dinitrogen **5** required heating to about 100 °C, which is typical for reactions of *B*-dinitrogen derivatives of [*closo*-B₁₀H₁₀]²⁻.⁴⁰⁻⁴⁹

The acid **5** also reacted smoothly with diazomethane to give methyl ester **11** in 78% yield (Scheme 3). This provides an alternative to the formation of **11** by diazotization of amino ester **10**.

Scheme 3

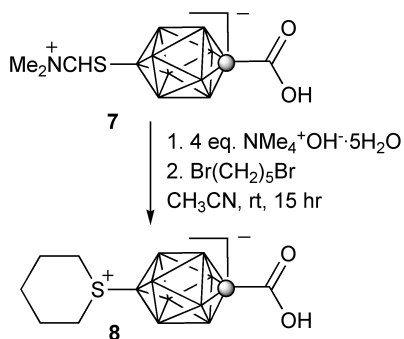


The synthetic utility of the protected mercaptan **7** was demonstrated by formation of sulfonium derivative **8** under hydrolytic conditions in the presence of a base and 1,5-dibromopentane. The optimized reaction required 4 equivalents of base ($\text{Me}_4\text{N}^+\text{OH}^-$), and the product **8** was isolated by chromatographic methods in 60% yield (Scheme 4). With fewer equivalents of base, the *S*-alkylation competed with alkylation of the carboxyl group.

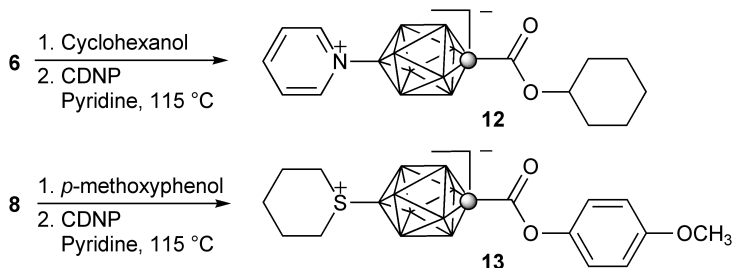
Finally, chemical transformations of the carboxyl group in the presence of the onium fragments in acids **6** and **8** were demonstrated. Thus, using 2-chloro-3,5-

dinitropyridine (CDNP) as a condensation agent,⁶³ zwitterion **6** was converted to an ester of a secondary alcohol (**12**), and acid **8** gave an ester of a phenol (**13**) in 75% and 54% yields, respectively (Scheme 5). Identical reactions with DCC were less clean and efficient.

Scheme 4



Scheme 5

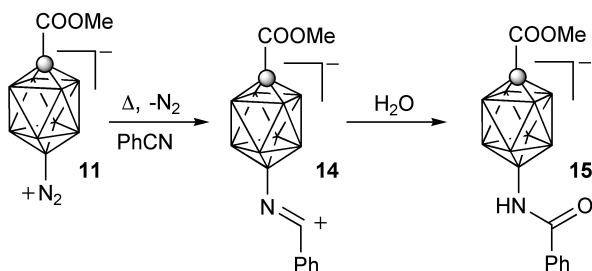


Reaction with PhCN and kinetic data for [closo-1- CB_9H_8 -1-COOMe-10- N_2] (**11**)

Decomposition of dinitrogen ester **11** in dry PhCN at elevated temperatures (> 100 °C) gave a single product identified as zwitterion **14**. Upon addition of moist PhCN to the reaction mixture, the zwitterion **14** was converted quantitatively to benzamide **15** (Scheme 6), which was isolated and partially characterized. An attempt to thermolyze **11**

in MeCN was unsuccessful and no trace of product was observed after 1 hrs at 80 °C. The clean transformation of **11** in PhCN to a single product permitted kinetics analysis of this reaction, which is believed to involve the heterolytic cleavage of the B–N bond as the rate-determining step.

Scheme 6



Thus, kinetics of decomposition of **11** in dry PhCN was followed by ¹¹B NMR spectroscopy in a temperature range of 125 °C – 140 °C.⁶² Intensities of the disappearing B(10) signal at 19.8 ppm and the growing peak at 29.1 ppm were used to calculate the ratio of **11** to **14**. Standard kinetic analysis using the Eyring equation found $\Delta H^\ddagger = 33.9 \pm 1.4 \text{ kcal mol}^{-1}$, $\Delta S^\ddagger = 10.0 \pm 3.5 \text{ cal mol}^{-1} \text{ K}^{-1}$, and $\Delta G^\ddagger_{298} = 30.9 \pm 1.4 \text{ kcal mol}^{-1}$.

Similar studies with the carboxylate anion of **5** could not be performed due to the insolubility of salt **5**[NMe₄] in PhCN, even at 140 °C.

Molecular and Crystal Structures

Colorless crystals of **5**, **6**, and **8** were grown by slow evaporation of a CH₂Cl₂ solution containing a few drops of MeOH. Solid-state structures for all three compounds were determined by X-ray diffraction⁶⁴ and selected bond lengths and angles are shown

in Table 1.

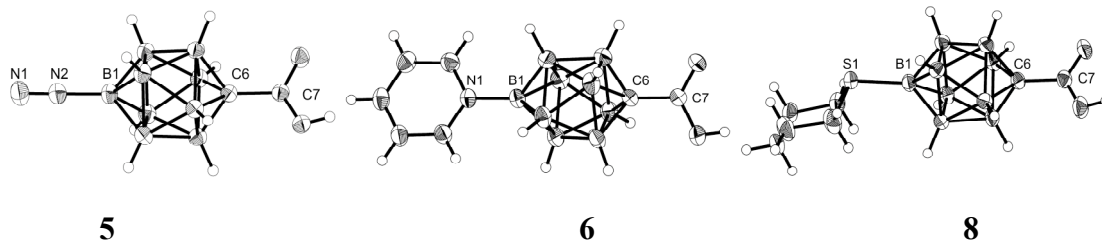


Figure 2. Thermal ellipsoid diagram representations of selected molecules of [*closo*-1-CB₉H₈-1-COOH-10-N₂] (**5**), [*closo*-1-CB₉H₈-1-COOH-10-C₅H₅N] (**6**), and [*closo*-1-CB₉H₈-1-COOH-10-C₅H₁₀S] (**8**), and drawn at 50 % probability. Selected interatomic distances and angles for **5**, **6**, and **8** are listed in Table 1.

Table 1. Selected Experimental and Calculated Bond Lengths and Angles for [*closo*-1-CB₉H₈-1-COOH-10-N₂] (**5**), [*closo*-1-CB₉H₈-1-COOH-10-C₅H₅N] (**6**), and [*closo*-1-CB₉H₈-1-COOH-10-C₅H₁₀S] (**8**).

Distances / Å	5		6		8	
	Exp. ^a	Calcd. ^b	Exp. ^a	Calcd. ^b	Exp. ^a	Calcd. ^b
B(10)-X ^c	1.4981(17) ^{d,e}	1.461 ^d	1.525 ^d	1.520 ^d	1.858 ^f	1.854 ^f
B(10)-B ^c	1.6702	1.674	1.676	1.676	1.680	1.676
C _{cage} -B ^c	1.6053	1.602	1.601	1.603	1.607	1.604
C _{cage} -C _{COOH} ^c	1.4859(16)	1.489	1.482	1.484	1.485	1.485
C(1)⋯B(10) ^c	3.429	3.436	3.471	3.465	3.478	3.463
Angles / °						
X-B-B ^c	127.3 ^d	127.6 ^d	128.7 ^d	128.5 ^d	128.6 ^f	128.4 ^f
C _{COOH} -C _{cage} -B ^c	125.0	125.1	125.4	125.3	125.4	125.3

^a See footnote ⁶⁴. ^b MP2/6-31G(d,p) level geometry optimization at C_s (**5** and **8**) or C₁ (**6**) point group symmetry for monomeric acids. ^c Average value for all equivalent bonds or angles in all unique molecules. Numbering system according to the chemical structure. ^d X = N. ^e The N-N distance: experimental 1.0905(15) Å and calculated 1.138 Å. ^f X = S.

All three acids form dimeric structures in the solid state. In the crystal of dinitrogen acid **5**, the two monomers are related by an inversion center. In contrast, the dimeric pair in the solid structure of **8** is unsymmetrical and both monomeric acids are unique molecules, while in the crystal of pyridinium acid **6**, there are four unique molecules (two unsymmetrical unique dimers).

The carboxyl group in each acid adopts a pseudo-staggered conformation relative to the {*closo*-1-CB₉} cage. The deviation of the COOH group from the ideal staggered orientation varies from as little as 5°, observed in the solid-state structure of **5** and one of the molecules of **6**, to 18° in acid **8** and 20° in two molecules of pyridinium acid **6**. The pair of carboxyl groups is ideally co-planar in **5**, nearly co-planar in pyridinium acid **6** (the interplanar angle of about 8°), and significantly off co-planarity in sulfonium acid **8** (the interplanar angle of 20°).

The B-N bond length of 1.4981(17) Å observed in **5** is similar to 1.489(6) Å and 1.499(2) Å reported for [*closo*-B₁₀H₉-1-N₂]⁻ ⁶⁵ and [*closo*-B₁₀H₈-1,10-(N₂)₂],⁶⁶ respectively. Also the observed N-N distance in **5** (1.0905(15) Å) is close to those reported for the {*closo*-B₁₀} analogs (1.097(6) Å and 1.091(2) Å).

The pyridine ring in **6** adopts a nearly ideal staggered orientation relative to the {*closo*-1-CB₉} cage in one dimer (2° and 4° off the ideal conformation), while in the other pair the deviation is larger (18° and 20°). As a result, the interplanar angle between the COOH and C₅H₅N groups, measured using the first three atoms from the cage, deviates

about 15° from the ideal 45° (see Figure 3) in each molecule. The overall interplanar angle between the pyridinium rings in the two unique dimers is 1.5° and 6.4°.

The orientation of the thiacyclohexane ring in acid **8** is 15° in one monomer and 30° in another monomer away from the ideal staggered conformation in which the sulfur lone pair eclipses the B–B bond (Figure 3). The staggered conformation has been found to be the conformation minimum in theoretical models (*vide infra*) and observed in solid-state structures of closely related sulfonium derivatives of [*closo*-B₁₀H₁₀]²⁻.^{67,68} For instance, in the structure of [*closo*-B₁₀H₈-1,10-(SMe₂)₂] the two SMe₂ groups are about 2° and 16° away from the ideal staggered conformation, and the B–S bond length (1.866(3) Å) is similar to that observed in **8**.⁶⁷

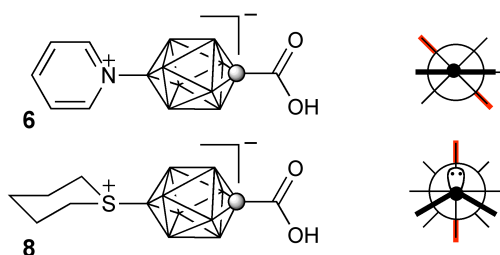


Figure 3. Extended Newman projection along the long molecular axes of **6** and **8** showing the staggered (minimum) conformations. The bars represent the substituents, and the filled circle is the nitrogen or sulfur atom.

Analysis of the {*closo*-1-CB₉} cage geometry indicates that the pyramidalization of the B(10) apex is greater for more electronegative onium substituents. The X–B(10) distance is smaller and consequently the B(10)⋯C(1) separation is markedly shorter in **5** with the most electronegative substituent N₂⁺ (σ_p = 1.91)⁶⁹ than in the sulfonium **8** (SMe₂⁺

$\sigma_p = 0.90$)⁶⁹ and pyridinium analogs (Table 1). Similar observations were found for derivatives of $C_2B_{10}H_{12}$.^{39,70}

Computational Analysis.

To shed more light on properties of **5** and its reactions with nucleophiles, we conducted quantum-mechanical calculations initially at the B3LYP/6-31G(d,p) level of theory to establish conformational minima and to obtain thermodynamic corrections. The resulting structures were used as starting points to optimize geometry and calculate the SCF energies at the MP2/6-31G(d,p) level of theory. For comparison purpose, properties of the anion **5**⁻, the parent [*closo*-1-CB₉H₉-10-N₂] (**16**), and its isomer [*closo*-1-CB₉H₉-1-N₂] (**17**)⁵⁰ were also considered at the same level of theory. Computational results are shown in Figure 4, Tables 2 and 3, and equilibrium geometries are provided in the Supporting Information.

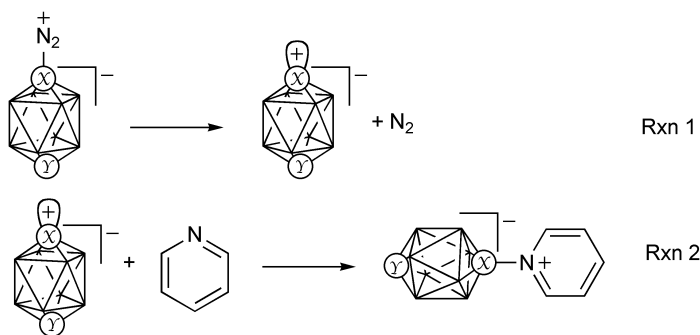
Initially, the performance of the adopted computational protocol was tested on acids **5**, **6**, and **8**, whose solid-state structures were established experimentally. Both DFT and MP2 methods well reproduced the experimentally observed conformational minima of the substituents in the three compounds (Figure 3). Detailed comparison of the theoretical and experimental bond lengths demonstrated that the MP2-level geometry optimizations performed better with the mean difference of 0.0001 ± 0.006 Å (absolute mean 0.005 ± 0.004 Å) than the DFT method (mean error = -0.006 ± 0.008 Å, absolute

mean error 0.007 ± 0.007 Å).⁷¹ Selected results for the MP2/6-31G(d,p) calculations are shown in Table 1.

Formation, structure and reactivity of the boronium ylides.

Experimental results indicate that reactions of **5** involve boronium ylide **18**. Calculations demonstrated that its formation by heterolytic cleavage of the B–N bond in **5** is endothermic by 41.8 kcal/mol (Table 2) and practically identical to that calculated for ester [*closo*-1-CB₉H₈-1-COOMe-10-N₂] (**11**). This enthalpy change is nearly the same as the formation of the parent B(10) boronium ylide **19** from [*closo*-1-CB₉H₉-10-N₂] (**16**), and significantly larger, by about 8 kcal/mol, than the formation of the carbonium ylide **20** from [*closo*-1-CB₉H₉-1-N₂] (**17**).⁵⁰ Interestingly, the heterolysis of the carboxylate anion **5**⁻ is easier by nearly 5 kcal/mol than that of the protonated form, acid **5**. The computational results are consistent with experimental data for dinitrogen derivatives **11** (*vide supra*) and **17**.⁵⁰ The calculated larger change of free energy, $\Delta\Delta G_{298} = 10.8$ kcal/mol, in the formation of ylide **18** as compared to **20** in gas phase corresponds to the observed higher activation energy $\Delta\Delta G_{298}^{\ddagger} = 5.8$ kcal/mol for the thermolysis of **11** relative to **17** in a dielectric medium.

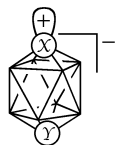
Table 2. Calculated reaction energies for selected dinitrogen derivatives of the {*closo*-1-CB₉} in gas phase.^a



Compound		Rxn 1		Rxn 2		Rxn 1+2	
	X	Y	ΔH /kcal mol ⁻¹	ΔH /kcal mol ⁻¹	ΔH /kcal mol ⁻¹	ΔH /kcal mol ⁻¹	ΔH /kcal mol ⁻¹
			$\Delta G_{298} /kcal mol^{-1}$	$\Delta G_{298} /kcal mol^{-1}$	$\Delta G_{298} /kcal mol^{-1}$	$\Delta G_{298} /kcal mol^{-1}$	$\Delta G_{298} /kcal mol^{-1}$
5	B	CCOOH	18	41.8	6	-88.6	-46.8
				31.1		-76.2	-45.1
5⁻	B	CCOO ⁻	18⁻	37.0	6⁻	-70.5	-33.5
				26.2		-57.9	-31.7
16	B	CH	19	41.1	21	-86.8	-45.7
				30.3		-74.6	-44.3
17	C	BH	20	33.3	22	-92.5	-59.2
				20.3		-77.7	-57.4

^a MP2/6-31G(d,p) level with DFT thermodynamic corrections.

Table 3. Calculated structural parameters for selected ylides. ^a



	X = B Y = CCOOH 18	X = B Y = CCOO ⁻ 18⁻	X = B Y = CH 19	X = C Y = BH 20
<i>Geometry</i>				
C(1)-B / Å	1.598 ^b	1.591	1.594	1.532
B(2)-B(3) / Å	1.872 1.855	1.848 1.840	1.861	1.928
B(2)-B(6) / Å	1.810 ^b	1.820 ^b	1.812	1.829
B(6)-B(7) / Å	1.931 ^b	1.916	1.928	1.894
B(10)-B _{avrg} / Å	1.628 ^b	1.624 1.630	1.628	1.678
B-C-B _{avrg} / °	111.0	110.0	111.3	125.8
B-B(10)-B _{avrg} / °	114.0 113.7	113.0 112.4	113.8	105.9
<i>Natural Atomic Charge^c</i>				
C(1)	-0.74	-0.72	-0.79	-0.34
B(2)	0.08	0.07	0.05	0.07
B(6)	-0.20	-0.21	-0.21	-0.11
B(10)	0.45	0.34	0.44	-0.32
<i>Bonding^c</i>				

χ exo	sp ^{18.4} (0.18)	sp ^{29.7} (0.25)	sp ^{18.8} (0.18)	sp ¹⁰⁰ (0.64)
LUMO /eV	-0.03	3.21	0.21	-1.57

^a Optimized at the MP2/6-31G(d,p) level of theory at the C_s (**18**), C_{2v} (**18**⁻) or C_{4v} (**19** and **20**) point group symmetry. ^b Average value. ^c NBO analysis.

The reactivity of the ylides was assessed from their reactions with pyridine. The results show that trapping of ylides **18**, **19**, and **20**, by pyridine and the formation of the corresponding adducts **6**, **21**, and **22**⁵⁰ is highly exothermic (about 90 kcal/mol) and the order of the thermal effect follows **20** > **18** > **19** (Table 2). The exotherm for the reaction of the carbonium ylide **20** with pyridine is greater than that for its isomeric boronium ylide **19** by 5.7 kcal/mol. Deprotonation of ylide **18** has a significant effect on its reactivity, and trapping of carboxylate boronium ylide **18**⁻ with pyridine has a nearly 18 kcal/mol lower exotherm relative to that of **18**.

The large exotherm for the second reaction (Table 2) overcompensates the endotherm for the ylide generation, and the overall process of transforming dinitrogen derivatives to their pyridine products is exothermic (Table 2). The relatively low energy of formation of carbonium ylide **20** and its high reactivity results in a larger overall enthalpy change for the transformation of [*closo*-1-CB₉H₉-1-N₂] (**17**) than for the B(10) analogs **5** and **16** by about 13 kcal/mol. Transformation of the deprotonated acid **5**, the anion **5**⁻, has the lowest overall exotherm, which is lower by 13.5 kcal/mol than that for the acid **5**.

The observed reactivity of the ylides is related to their electronic structures. Both types of ylides, the boronium and carbonium, have LUMO localized mainly on the exocyclic orbital of the electron deficient atom with some density on the non-adjacent boron atom belt. This contribution of the boron belt is more pronounced for the carbonium ylide **20** than for the boronium analog (Figure 4). NBO analysis of the MP2 wave function demonstrates that the B(10) atom in the boronium ylides is electropositive, while the C(1) atom in carbonium ylide **20** is electronegative. The two types of ylides also display a difference in hybridization of the exo-cage orbital: the carbonium ylide has a practically pure *p* character, while a small fraction of an *s* orbital is mixed into the *p* orbital in the boronium ylides.

Deprotonation of the COOH group in **18** and the formation of the carboxylate ylide **18⁻** has a large effect on the boronium center: it increases the electron density on the exo-cage hybrid by nearly 40%, which consequently increases the *p* content of the hybrid and the energy of the LUMO by nearly 3.5 eV. These results, the charge density and the LUMO energy, are consistent with the reactivity of the ylides towards pyridine: the lower the energy of the LUMO the higher exotherm of the reaction (Table 2).

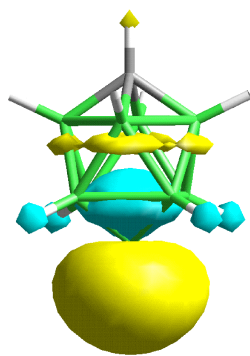
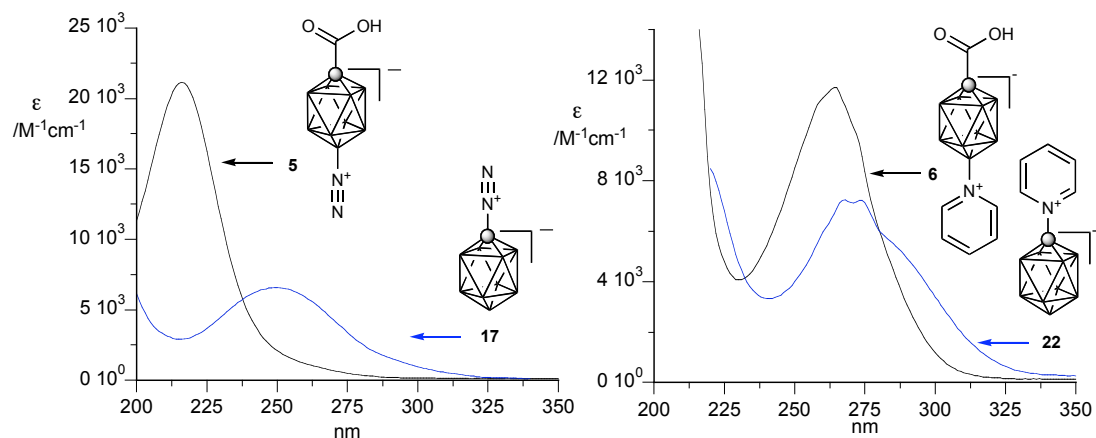


Figure 4. The MP2/6-31G(d,p) derived contour for the LUMO ($E = 0.21$ eV) of ylide **19**. Nearly identical contours are found for **18** and **18**⁻.

Electronic Absorption Spectroscopy

Electronic interactions between onium substituents and the {*closo*-1-CB₉} cluster were probed using electronic absorption spectroscopy. The UV spectra of dinitrogen acid **5** and pyridinium acid **6** show strong absorption bands at 216 nm and 263 nm, respectively (Figure 5). The observed absorption bands are blue-shifted and have higher intensity relative to similar derivatives with the onium substituent at the C(1) vertex: [*closo*-1-CB₉H₉-1-N₂] (**17**)⁵⁰ and [*closo*-1-CB₉H₉-1-NC₅H₅] (**22**).⁵⁰ A particularly strong shift of 34 nm is observed for the pair **5** and **17**.



a

b

Figure 5. Electronic absorption spectra for a) dinitrogen acid **5** and [*closo*-1-CB₉H₉-1-N₂] (**17**), and b) pyridinium acid **6** and [*closo*-1-CB₉H₉-1-NC₅H₅] (**22**) recorded in CH₃CN.

ZINDO//MP2/6-31G(d,p) level calculations revealed that both isomeric dinitrogen derivatives **16** and **17** exhibit similar two main $\pi \rightarrow \pi^*$ transitions. For [*closo*-1-CB₉H₉-10-N₂] (**16**), both transitions involve a combination of two excitations: from the double degenerate HOMO, with the density localized mostly on the {1-*closo*-CB₉} cage, to the double degenerate LUMO, which is localized on the N₂ fragment, and the intracage HOMO→LUMO+2 excitation. In MeCN dielectric medium, energy for both transitions shifts and for the C(1) isomer **17** merge into one absorption band at 249 nm (exp.⁵⁰ 250 nm). In contrast, the two transitions for the B(10) isomer **16** constitute separate absorption bands at 223 ($f = 0.56$) and 232 nm ($f = 0.67$). Similar calculations for the dinitrogen acid **5** showed a significantly larger number of transitions in the 220-250 nm region mainly due to the lower molecular symmetry (C_s vrs C_{4v}) and the involvement of the COOH group. Nevertheless, the main transitions in **5** are essentially the same,

$\pi_{\text{cage}} \rightarrow \pi_{\text{cage}}^*$ and $\pi_{\text{cage}} \rightarrow \pi_{\text{N}_2}^*$, as those observed for **16** and involve orbitals shown in Figure 6. In MeCN dielectric medium, the two main transitions for **5** are calculated at 226 ($f = 0.50$) and 236 nm ($f = 0.54$), which may appear as one broad absorption band in the UV spectrum. The experimental absorption band in **5** (Figure 5) is 15 nm blue-shifted relative the average position of the calculated bands.

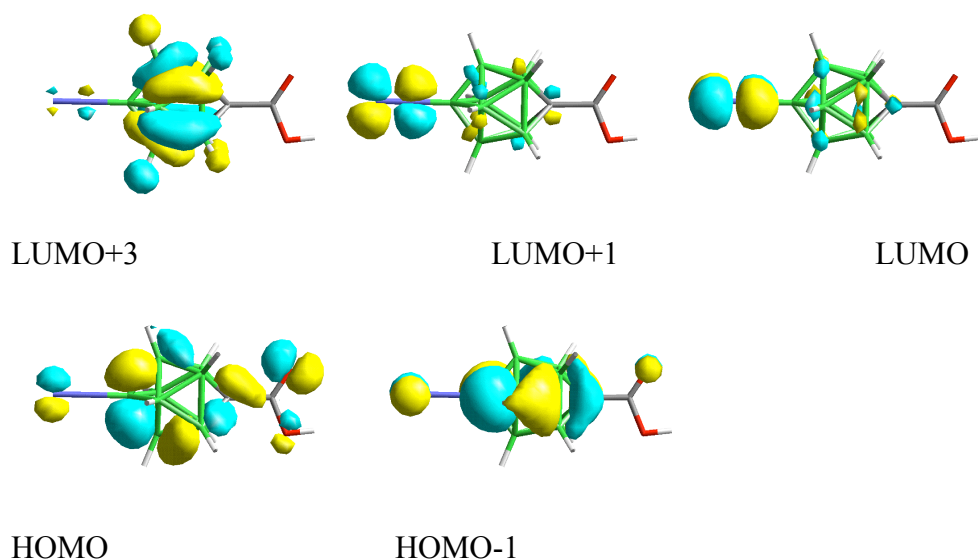


Figure 6. ZINDO – generated MO contours for **5**.

The calculated blue shift of about 20 nm for the absorption band in **16** relative to **17** is consistent with a 34 nm shift observed for the pair of **5** and **17** (Figure 5a). Analysis of the MP2 wave functions for **16** and **17** demonstrated a wider HOMO-LUMO gap (~ 1.1 eV) in the B(10) (former) than in the C(1) (latter) isomer, due mainly to an increase of the energy of the LUMO (+0.68 eV). This can be rationalized by lower electronegativity of the B(10) than the C(1) atom and consequently higher electron density on the N_2

fragment.

Dissociation Constants Measurements

The apparent dissociation constant pK for the amino acid **4[NMe₄]** was measured by potentiometric titration in 50% aq. EtOH (v/v). For comparison purposes, the apparent pK values for the parent acid [*closo*-1-CB₉H₉-1-COOH]⁻ (**9**) and benzoic acid were also measured in the same solvent.

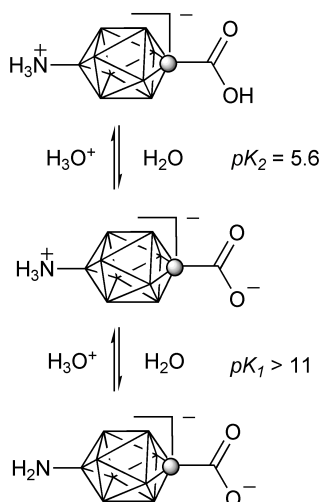


Figure 7. Apparent ionization constants pK for **4** in 50% EtOH (v/v) at 24 °C.

The results in Figure 7 for titrations of **4[NMe₄]** with acid show that the apparent pK_2 value for dissociation of the COOH in [*closo*-1-CB₉H₈-1-COOH-10-NH₃]⁺NMe₄⁻ (**4[H]**) is 5.61±0.08, which is similar to that measured for benzoic acid in the same solvent ($pK = 5.51$, lit.⁷² $pK = 5.67$, lit.⁷³ $pK = 5.80$). Titration of **4[NMe₄]** with a base

gave only the lower limit ($pK_1 > 11$) for the apparent dissociation constant of the NH_3^+ group. A comparison of the pK_2 value for **4** with that for the parent acid [*closo*-1- CB_9H_9 -1-COOH]⁻ (**9**[NEt_4], $pK = 6.36$) shows that the presence of the NH_3^+ group in the antipodal B(10) position of **4**[**H**] shifts the pK value by about -0.8. The solution of the amino acid salt **4**[NMe_4] is slightly basic in 50% EtOH with a pH of about 8.6

Discussion

The reactions reported here demonstrate the strong effect of the antipodal substituent and the impact of the negatively charged cage upon reactivity. For instance, the amination reaction of iodo acid **1** and the formation of amino acid **4** represents a rare example of *B*-amination⁷⁴ and the first example of Pd-catalyzed amination of a boron cluster with an ammonia equivalent. The reactivity of the iodine at the B(10) position appears to be highly sensitive to the substituent at the C(1) vertex; it is inactive in the presence of an alkoxy carbonyl substituent, but undergoes substitution when the carboxylate group is present in the antipodal position. This result is consistent with our previous observations of Pd-catalyzed Negishi-type alkylation of the iodo acid **1** and its ester.⁸ Both results suggest that the moderately electron withdrawing alkoxy carbonyl substituent ($\sigma_p = 0.45$)⁶⁹ at C(1) completely deactivates the B(10)-I bond towards oxidative addition of Pd(0) or shuts down the transmetalation step in the catalytic cycle. On the other hand, the carboxylate group ($\sigma_p = 0.00$)⁶⁹ at the C(1) position allows for the

reaction to proceed to completion.

The two substituents, COOR and COO⁻, have similar effect on reactivity of dinitrogen derivatives **5** and **5⁻**. However, analysis of computational results indicates that deprotonation of the COOH group in **5** and the formation of the carboxylate anion COO⁻ in **5⁻** has a more pronounced effect on the reactivity than can be expected on the basis of Hammett σ parameters.⁶⁹ It appears that the ionization of the COOH group injects significant electron density into the {*closo*-1-CB₉} cage and to the B(10) position in particular. This is evident from the calculated higher reactivity of the anion **5⁻**, and also higher charge density at the B(10) position and lower electrophilicity of the boronium ylide **18⁻**, as compared to the analogous carboxylic acid derivatives (**5** and **18**) and the parent boronium ylide **19** (Tables 2 and 3). These results indicate that the relative impact of the antipodal substituents on reactivity of the {*closo*-1-CB₉} derivatives follows: COOH ~ COOR ~ H > COO⁻, which is different than the order of the Hammett parameter values σ_p (COOH ~ COOR > COO⁻ ~ H).⁶⁹

The amino group in **4** is unusually basic. The measured *pK* for the conjugate acid appears to be higher than that reported for quinuclidinium in the same solvent (*pK* = 10.2)⁷⁵. A consequence of this basicity is the facile protonation of the NH₂ group and the formation of the zwitterion [*closo*-1-CB₉H₈-10-NH₃-1-COOH] (**4[H]**). The zwitterionic structure is consistent with ¹¹B NMR spectra for **4[H]** and its derivatives. The B(10) nucleus has nearly the same chemical shift in **4[H]** and its methyl ester **10[H]** (37.0 and 37.1 ppm, respectively). Treatment of the ester with 1 equivalent of NMe₄OH leads to

deshielding of the B(10) nucleus by nearly 10 ppm, which is consistent with the presence of the NH₂ group in **10**[NMe₄]. On the other hand, neutralization of **4**[H] with 1 equivalent of NMe₄OH results in 3.4 ppm shielding of the B(10) nucleus in CD₃OD solvent. Since the B(10) nucleus is shielded by 5.9 ppm after deprotonation of dinitrogen acid **5** and formation of **5**⁻[NMe₄] in CD₃CN, the structure of **4**[NMe₄] is consistent with the zwitterion [*closo*-1-CB₉H₈-1-COO-10-NH₃]. Interestingly, addition of another equivalent of NMe₄OH to the solution of **4**[NMe₄] does not affect the chemical shift of the B(10) nucleus, which may suggest that the pK for the NH₃⁺ group is > 15 in CD₃OD.⁷⁶

The high basicity of the amino group in **4**, is also evident from its chemical reactivity: upon protonation in **4**[H] it becomes completely inert towards electrophiles such as acid chlorides and NO⁺. Thus, the zwitterion **4**[H] can be converted to methyl ester **10** in high yield apparently through the acid chloride [*closo*-1-CB₉H₈-1-COCl-10-NH₃] (Scheme 1). Also, the total resistance of **4**[H] to diazotization in aqueous medium is in sharp contrast to the same reaction of *p*-aminobenzoic acid.⁷⁷ The high basicity of the amino group and consequently tight N–H bond in the ammonio group is also evident from the observed ¹J_{N-H} = 34 and 42 Hz found for **4**[H] and **10**[H] in CD₃CN solutions, respectively.⁷⁸

The high basicity observed for the amino group in **4** is consistent with reports for other amino-*closo*-borates and our calculations. For instance, the amines [*closo*-B₁₀H₉-1-NH₂]²⁻ and [*closo*-B₁₂H₁₁NH₂]²⁻ are highly basic and “the *N*-protonated forms of these amino compounds could be isolated directly from alkaline solutions.”⁷⁹ A similar

observation was made for [*closo*-B₁₂H₁₁NHMe₂]⁻ which “is such a weak acid that OH⁻ does not remove the proton from the quaternary nitrogen”.⁸⁰ It was also reported that [*closo*-B₁₀H₈-1,10-(NH₂)₂]²⁻ could not be diazotized in aqueous medium “possibly because the concentration of these anions in aqueous acid solution is negligible”.^{43,81} A comparison of experimental data for [*closo*-1-CB₁₁H₁₁-1-NH₃] (*pK_a* = 6.0 in 50% EtOH²⁸ or H₂O³¹) and [*closo*-1-CB₁₁H₁₁-2-NH₃] indicates that the *B*-ammonio derivative is significantly less acidic than the former isomer by more than 5.5 units.³¹ These experimental results are supported by computational data which show a difference in *pK_a* for the two amines of about 7 units, and estimate the *pK_a* value for [*closo*-B₁₂H₁₁NH₃]⁻ at about 20!³¹ Our calculations shown in Figure 8 also demonstrate that the *B*-amino *closo*-borates are significantly more basic than the *C*-amino isomers, and that the amine basicity follows the order {*closo*-B₁₂} > {*closo*-1-CB₉} > {*closo*-CB₁₁}. These findings are consistent with the observed difference in reactivity of [*closo*-1-CB₉H₉-1-NH₃], which can be diazotized under aqueous acidic conditions,⁵⁰ and the [*closo*-1-CB₉H₈-1-COOH-10-NH₃] (**4**[**H**]), which requires a stronger base for a successful diazotization. To our knowledge, the preparation of **5** is the first example of diazotization under homogenous basic conditions.⁸²

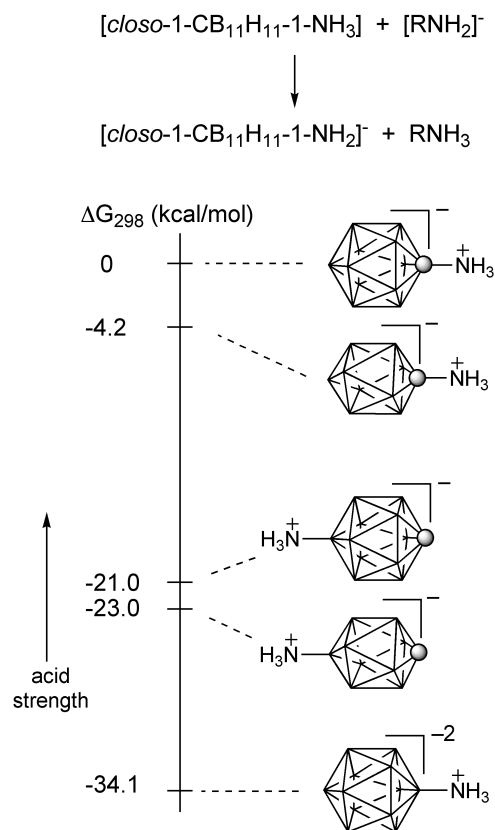
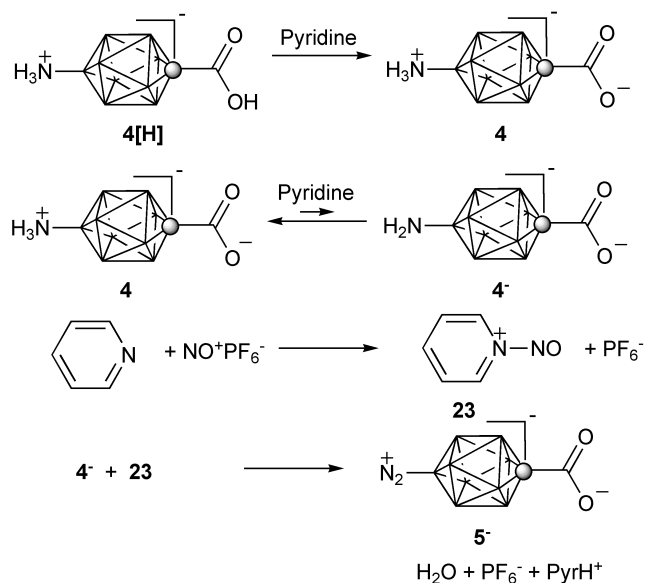


Figure 8. Free energy change for the acid-base reaction shown on the top obtained at the MP2/6-31+G(d,p)/MP2/6-31G(d,p) level of theory with DFT thermodynamic corrections in 50% EtOH dielectric medium ($\epsilon = 52.5$).

The reaction of $NO^+PF_6^-$ with **4**[**H**] in the presence of pyridine is a complex process in which the base serves a dual role: it deprotonates the NH_3 group and presumably reacts with $NO^+PF_6^-$ to form an alternative diazotizing reagent, the *N*-nitrosopyridinium ion^{83,84} (**23**). It can be postulated that the formation of **5** involves initial deprotonation of the COOH group in **4**[**H**] and subsequent proton-transfer equilibrium between the NH_3^+ group and pyridine (Scheme 7). On the basis of the measured pK values, the equilibrium is significantly shifted to the left and the required ambident anion

4⁻ is present in low concentrations. The subsequent addition of NO⁺PF₆⁻ leads to the formation of cation **23**. Although, the ambident ion **4** may compete with pyridine for NO⁺, the green color⁸⁵ developing immediately upon addition of a portion of NO⁺PF₆⁻ to the solution and fading to clear/yellowish suggests that cation **23** is formed preferentially and serves as the main diazotizing reagent for **4**⁻. The reaction requires excess NO⁺PF₆⁻, since at least one equivalent is presumably consumed by water formed during diazotization.

Scheme 7



The reactivity of the B(10) dinitrogen acid **5** is distinctly different from that of C(1) dinitrogen derivative **17**.⁵⁰ Unlike dinitrogen species **17**, where identical reactions with nucleophiles occur at ambient temperature,⁵⁰ reactions of dinitrogen acid **5** require heating to about 100 °C. The observed relatively high thermal stability of **5** is consistent

with behavior of apical dinitrogen derivatives of the [*closo*-B₁₀H₁₀]²⁻ cluster.⁴⁰⁻⁴⁹

The most striking difference in reactivity of the C(1) and B(10) dinitrogen derivatives is, however, the regioselectivity of their reactions with pyridine. While the former (**17**) gives a mixture of C-substituted pyridines as the sole products,⁵⁰ reactions of **5** with hot pyridine leads to the exclusive formation of the *N*-isomer, pyridine acid **6**. The formation of **6** is consistent with reactions of other *B*-dinitrogen derivatives of [*closo*-B₁₀H₁₀]²⁻ with pyridine^{42,43,45,86} (Figure 9).

The observed diametrically different regioselectivities for the reactions of **5** and **17** are consistent with different mechanistic pathways and reactive intermediates involved in transformation of each dinitrogen derivative. Thus, for reactions of **17** we postulated⁵⁰ the nucleophile-induced formation of radical anion [*closo*-1-CB₉H₉]^{·-} (**24**, Figure 9) and its reaction with pyridine in accordance with the Gomberg-Bachmann mechanism for arylation with arenediazonium salts. The formation of the radical intermediates in this process requires dinitrogen precursors with high electron affinity (low reduction potential). Our previous experiments demonstrated that reduction of **17** is more cathodic than that of PhN₂⁺ by about 0.4 V (Table 5), which apparently is still low enough for a nucleophile to trigger the radical ion mechanism for **17**.⁵⁰ In contrast, reduction of dinitrogen ester **11** is more difficult by 0.56 V than **17** or by nearly 1 V relative to PhN₂⁺. This apparently renders the nucleophile-induced formation of radical too slow for effective competition with the alternative process involving boronium ylide. Deprotonation of the dinitrogen acid **5** in pyridine solutions increases further the

reduction potential to $E_{1/2} = -1.25$ V, which makes the electron transfer from the nucleophile even more unfavorable, and at the same time the heterolytic cleavage of the B–N bond and the formation of the ylide **18**[•] is predicted to be easier (Table 2).

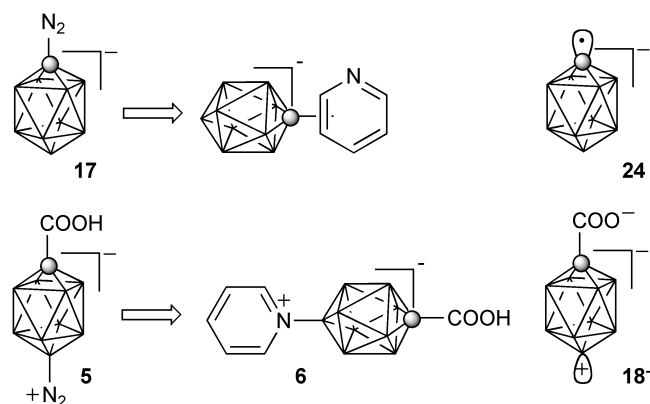


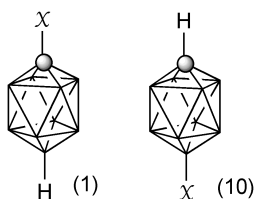
Figure 9. Regioselectivity of reaction of **5** and **17** with pyridine.

Table 5. Calculated gas phase adiabatic electron affinity (E_a) and experimental electrochemical reduction potentials for selected compounds.

Compound	Calculated ^a	Experimental ^b	
	E_a /eV	$E_{1/2}^{\text{red}}$ /V	$E_{\text{pc}}^{\text{red}}$ /V
$\text{C}_6\text{H}_5\text{N}_2^+$	5.45	^d	-0.16 ^{e,f}
[<i>closo</i> -1-CB ₉ H ₉ -1-N ₂] (17)	2.06	^d	-0.54 ^e
[<i>closo</i> -1-CB ₉ H ₈ -10-N ₂ -1-COOMe] (11)	1.00	-1.03 ^g	-1.10
[<i>closo</i> -1-CB ₉ H ₉ -10-N ₂] (16)	0.60	-	-
[<i>closo</i> -1-CB ₉ H ₈ -10-N ₂ -1-COO] ⁻ (5)	-1.97	-1.21 ^g	-1.34

^a MP2/6-31G(d,p) level with DFT enthalpic corrections. ^b Recorded in MeCN (0.05 M Bu₄NPF₆) versus SCE. ^c Peak potential. ^d Irreversible process. ^e Ref.⁵⁰ ^f Lit. -0.17 (MeCN, SCE) ref ⁸⁷. ^g Process partially reversible.

Table 6. Relative thermodynamic stability for selected pairs of isomers. ^a



X	$\Delta H = H_{(1)} - H_{(10)}$ ^b /kcal mol ⁻¹
N ₂ (17 and 16)	52.4
+ ^c (20 and 19)	44.6
Pyridinium (22 and 21)	38.9

^a MP2/6-31G(d,p) level with DFT enthalpic corrections. ^b Difference in enthalpy of formation between the (1) and (10) isomers shown above. ^c Vacant orbital in ylides.

Finally, a comment on the relative stability of the 1- and 10- isomers. Calculations indicate that the B(10) isomers are significantly more thermodynamically stable than the C(1) analogs (Table 6). For the pairs of compounds in Table 6 the calculated difference in the enthalpy of formation is about 39 kcal/mol for the pyridinium derivatives **21** and **22**, and as high as 52.4 kcal/mol for the isomers **16** and **17** containing the strongly electron withdrawing dinitrogen substituent. The calculated high stability of the B(10)-N₂ isomer is consistent with the experimental results and appears to be general for apical derivatives of the [closo-B₁₀H₁₀]²⁻ cluster; similarly to **5** and **11** they are isolable stable compounds^{40,42,43,68,86,88} and serve as important intermediates in the preparation of a variety of derivatives of the {closo-B₁₀} cluster. The higher stability of the B-N₂ vs C-N₂ isomer is consistent with the UV spectra indicating a higher HOMO-LUMO gap due to

lower charge separation of the B–N bond as compared to the C–N analog.

Summary and Conclusions

A practical and reproducible method for converting iodo acid **1**[NMe₄] to amino acid **4**[NMe₄] and subsequently to stable dinitrogen acid **5** has been developed. The latter undergoes thermolysis at about 100 °C and forms boronium ylide **18**, which is efficiently trapped by a nucleophilic solvent. The synthetic utility of this reaction was demonstrated with high yield preparation of pyridine acid **6** and protected mercapto acid **7**. Experimental results and theoretical analysis showed that the B(10) dinitrogen derivatives, such as **5**, are less electrophilic and more thermodynamically stable than the isomeric C(1) dinitrogen derivatives, such as **17**. Therefore, the former derivatives react solely through the heterolytic cleavage of the B(10)–N bond and boronium ylide intermediates. In contrast, the C(1)-N₂ derivatives undergo nucleophile-induced homolytic cleavage of the C–N bond, which leads to radical anion formation. The two distinct mechanistic pathways result in different regiochemical outcome of reaction of **5** and **17** with pyridine.

Computational results indicate that the reactivity of the dinitrogen derivatives and the stability of the resulting boronium ylides can be controlled to some extent by antipodal substituents at the C(1) vertex.

Overall, the demonstrated Pd-catalyzed transformations of iodo acid **1** (alkylation

and amination) and access to amino acid **4[NMe₄]** open new opportunities for the incorporation of the [*closo*-1-CB₉H₁₀]⁻ cluster into more complex molecular architectures, such as anisometric molecules. Our current work concentrates on applying this methodology in the development of polar liquid crystalline materials for electro-optical applications.

Computational Details

Quantum-mechanical calculations were carried out with the B3LYP^{89,90} and MP2(fc)⁹¹ methods with 6-31G(d,p) basis set using the Gaussian 03 package.⁹² Geometry optimizations were undertaken using appropriate symmetry constraints and tight convergence limits. Vibrational frequencies were used to characterize the nature of the stationary points and to obtain thermodynamic parameters. Zero-point energy (ZPE) corrections were scaled by 0.9806.⁹³ Hybridization parameters and natural charges were obtained using the NBO algorithm supplied in the Gaussian 03 package.⁹² Population analysis of the MP2 wavefunction (MP2//MP2) was performed using the DENSITY(MP2) keyword. The IPCM solvation model⁹⁴ was used with default parameters and $\epsilon = 52.5$ for EtOH/H₂O (1:1, v/v) at 25 °C, which was interpolated from the reported values for EtOH/H₂O mixtures.⁹⁵

Excitation energies for derivatives of the {*closo*-1-CB₉} cluster were obtained at their MP2 determined geometries using the INDO/2 algorithm (ZINDO)⁹⁶ as supplied in

Cerius2 suite of programs and including all electrons and orbitals in the CI. ZINDO calculations with the solvation model (Self Consistent Reaction Field) used cavity radii derived from the MP2 calculations with the VOLUME and DENSITY(MP2) keyword. The list of used cavity radii is provided in the SI.

Experimental Section

Reagents and solvents were obtained commercially. Pyridine was distilled from KOH and stored over 4 Å molecular sieves. *N,N*-dimethylthioformamide was distilled (80 °C, 0.25 mm Hg) prior to use. CH₃OH and CH₂Cl₂ were freshly distilled from CaH₂. Both DMF and cyclohexanol were dried over 4 Å molecular sieves. All other reagents were used as supplied. Reactions were carried out under Ar, and subsequent manipulations were conducted in air. NMR spectra were obtained at 128.4 MHz (¹¹B) and 400.1 MHz (¹H) in CD₃CN or CD₃OD as specified. ¹H NMR spectra were referenced to the solvent, and ¹¹B NMR chemical shifts were referenced to an external boric acid sample in CH₃OH that was set to 18.1 ppm. IR spectra were recorded in the solid state using an AT-IR accessory. Ultraviolet absorption spectra were recorded in CH₃CN and molar absorptivity was established by fitting 4 data points in accordance to Beer's law.

Temperature-Dependent NMR Study of the Decomposition of **11** in Benzonitrile.

The temperature-dependent NMR kinetic study of [*closo*-1-CB₉H₈-1-COOMe-10-N₂] (**11**) was performed on a 400 MHz NMR at 140 °C, 135 °C, 130 °C, and 125 °C in

non-deuterated PhCN, which was dried over 4Å molecular sieves for 24 hrs before use. Each experiment was performed with 5 mg of **11** dissolved in 0.6 mL of PhCN. A NMR tube filled with an equivalent volume of PhCN was used for tuning and shimming (1D) at the desired temperature. $^{11}\text{B}\{-^1\text{H}\}$ NMR experiments were executed using a time-delay controlled by the NMR console of 113.26 seconds. Each experiment consisted of 128 scans to improve resolution and reduce baseline noise. For experiments at 140 °C and 135 °C, each data point reflects one experiment whereas two experiments were recorded for each data point at 130 °C and 125 °C.

Dissociation Constant pK Measurements

Apparent dissociation constants were determined for **4**[NMe₄], **9**[NEt₄], and benzoic acid by potentiometric titration at 24 °C. The pH of the half-equivalent point at which $[\text{HA}] = [\text{A}^-]$ was taken as the apparent pK of the acid HA as described in the Henderson-Hasselbach equation.^{62,97} No corrections for solvent effect (e.g. for 50% aqueous ethanol a correction of $\Delta pK_a = +0.23$ is recommended)⁹⁸ or ion activity were made. Selected compound was dissolved in EtOH/H₂O (1:1 vol/vol, ~0.01 M) and covered with parafilm to minimize evaporation of solvent. Neutralization was achieved under stirring with 0.05 M NaOH or 0.05M HCl in EtOH/H₂O (1:1, vol/vol), which was added in 50 µL increments using a digital pipette. The pH electrode was calibrated in aqueous buffer (pH = 4.0, 7.0, and 10.0) followed by soaking in EtOH/H₂O (1:1 vol/vol) for 4 hrs or until the pH reading stabilized. After addition of titrant, the pH was recorded upon stabilization (~30 seconds). For **9**[NEt₄] and benzoic acid two titrations gave pK

values within 0.01. The pK_2 for **4[NMe₄]** was obtained as an average of 4 titrations (5.61 \pm 0.08).

Electrochemical Measurements

Electrochemical analysis was conducted in dry, degassed (with Ar) MeCN with Bu₄NPF₆ (0.05 M) as the supporting electrolyte using a freshly polished glassy carbon working electrode with the Ag/AgCl reference electrode. The scanning rate was 1 V/s. Following literature recommendations,⁸⁷ the concentration of compounds **11** and **5** [NMe₄] was set at 0.6 mM and the reported data was taken from the first scan. Continuous scanning of the electrochemical window (+0.8 to -2.0 V) resulted in little shifting of the observed cathodic and anodic peak potentials, which suggests no surface modification of the electrode surface by products of the initial reduction process. Peak potentials were referenced by adding small amounts of ferrocene to the solution and E-chem scans for each compound were referenced to the ferrocene couple which was assumed to be 0.31 V versus SCE (MeCN, 0.2 M LiClO₄)⁹⁹ or 0.35 V vs Ag/AgCl electrode.

Preparation of [*closo*-1-CB₉H₈-1-COO-10-NH₃]⁻NMe₄⁺ (**4[NMe₄]**)

[*closo*-1-CB₉H₈-1-COOH-10-I]⁻NMe₄⁺ (**1[NMe₄]**, 1.00 g, 2.75 mmol) was added to a solution of lithium hexamethyldisilazane (LiHMDS, 41.2 mL, 41.3 mmol, 1.0 M in THF) at rt under Ar. The light orange suspension was stirred vigorously for 15 mins or until the suspension became more fine and disperse. Pd₂dba₃ (0.050 g, 0.055 mmol) and

2-(dicyclohexylphosphino)biphenyl (0.077 g, 0.22 mmol) were added, and the reaction was stirred at reflux for 20 hr. After several minutes at reflux, the reaction mixture turned dark brown. The reaction was cooled to 0 °C, and 10% HCl (100 mL) was added slowly. The THF was removed *in vacuo* giving a dark orange solution. The orange solution was extracted with Et₂O (3x30 mL), the Et₂O layers were combined, dried (Na₂SO₄), and evaporated at slightly elevated temperature (~40 °C) to ensure complete removal of trimethylsilanol. ¹¹B NMR of the crude material revealed a 70:30 ratio of amino acid **4[H]** to parent acid **9[H₃O]**.

The crude brown/orange material was redissolved in Et₂O, and H₂O (10 mL) was added. The Et₂O was removed *in vacuo* or until bubbling became less vigorous. The aqueous layer was filtered, and the process was repeated two more times (the insoluble material presumably contains a B(10)-phosphonium derivative). The aqueous layers were combined, and NEt₄⁺Br⁻ (0.578 g, 2.75 mmol) was added resulting in precipitation of a white solid. CH₂Cl₂ (20 mL) was added, and the biphasic system was stirred vigorously until the H₂O layer became clear (~30 mins). The CH₂Cl₂ was separated, and the process was repeated once more. The H₂O layer was filtered, reacidified with conc. HCl (5 mL), and extracted with Et₂O (3 x 10 mL). The Et₂O layers were combined, washed with H₂O, dried (Na₂SO₄), and evaporated giving 0.260 g amino acid [*closo*-1-CB₉H₈-1-COOH-10-NH₃] (**4[H]**) with purity > 90% by ¹¹B NMR.

Crude amino acid [*closo*-1-CB₉H₈-1-COOH-10-NH₃] (**4[H]**, 0.194 g, 1.08 mmol) was dissolved in CH₃OH (5 mL) and NMe₄⁺OH⁻•5H₂O (0.180 g, 0.993 mmol,) was

added. The mixture was stirred for 1 hr, CH₃OH was removed *in vacuo*, and the residue was washed with Et₂O and then with boiling MeCN (2x) to give 0.221 g (88% recovery, 44% overall yield) of pure amino acid [*closo*-1-CB₉H₈-1-COO-10-NH₃]⁻NMe₄⁺ (**4**[NMe₄]) as a fluffy off-white solid: mp > 260 °C; ¹H NMR (CD₃OD) δ 0.5-2.4 (br m, 8H), 3.19 (s, 12H), resonance for NH₃ was not observed; ¹¹B NMR (CD₃OD) δ -22.8 (d, *J* = 155 Hz, 4B), -17.4 (d, *J* = 149 Hz, 4B), 34.7 (s, 1B); IR 3400-2800 br (N-H), 2539 (B-H), 1555 and 1383 cm⁻¹. Anal. Calcd for C₆H₂₃B₉N₂O₂: C, 28.53; H, 9.18; N, 11.09. Calcd for C₆H₂₃B₉N₂O₂•H₂O: C, 26.63; H, 9.31; N, 10.35. Found: C, 26.88; H, 9.43; N, 10.10.

Preparation of [*closo*-1-CB₉H₈-1-COOH-10-NH₃] (**4**[H]).

Amino acid [*closo*-1-CB₉H₈-1-COO-10-NH₃]⁻NMe₄⁺ (**4**[NMe₄], 0.055 g, 0.22 mmol) was dissolved in 10% HCl (2 mL) and the solution was extracted with ether (3x2 mL). The organic layers were combined, washed with H₂O (2 mL), dried (Na₂SO₄), and the solvent evaporated. The white solid residue was dried in vacuum to give 0.039 g (~100% yield) of pure acid [*closo*-1-CB₉H₈-1-COOH-10-NH₃] (**4**[H]) as a white solid: mp > 260 °C; ¹H NMR (CD₃CN) δ 0.5-2.4 (m, 8H), 6.6 (br t, *J* = 37 Hz, 3H), 9.6 (brs); (CD₃OD) δ 0.5-2.4 (m, 8H), 7.8 (br s, 1.2H); ¹¹B NMR (CD₃CN) δ -22.6 (d, *J* = 141 Hz, 4B), -16.8 (d, *J* = 158 Hz, 4B), 37.0 (s, 1B); (CD₃OD) δ -22.6 (d, *J* = 152 Hz, 4B), -16.8 (d, *J* = 145 Hz, 4B), 38.1 (s, 1B); IR 3300 – 2800 br (N-H and O-H), 2571 (B-H), 1671 (C=O) cm⁻¹; FAB-HRMS(-), calcd. for C₂H₁₀B₉NO₂ *m/z*: 179.1549; found: 179.1534.

Preparation of [*closo*-1-CB₉H₈-1-COOH-10-N₂] (**5**)

Amino acid [*closo*-1-CB₉H₈-1-COOH-10-NH₃] (**4**[H]), 0.105 g, 0.59 mmol) was suspended in anhydrous CH₃CN (2 mL) under Ar. Anhydrous pyridine (0.240 mL, 2.93 mmol) was added, and the mixture was sonicated for 5 mins. The reaction mixture was cooled to -15 °C, and nitrosonium hexafluorophosphate (NO⁺PF₆⁻, 0.310 g, 1.77 mmol) was added in five portions at 5 minute intervals. Addition of NO⁺PF₆⁻ resulted in a green/blue homogeneous solution that slowly faded to colorless, and the solution became more yellow as more NO⁺PF₆⁻ was introduced. Once all NO⁺PF₆⁻ was added, the reaction was stirred for 1.5 hr at -15 °C.

The reaction mixture was evaporated to dryness (the flask was kept at cold water bath), 10% HCl (10 mL) was added, and the mixture was stirred vigorously until all solids had dissolved (~20 mins). The aqueous solution was extracted with Et₂O (3 x 5 mL), the Et₂O layers were combined, washed with H₂O, dried (Na₂SO₄), and evaporated to dryness giving 0.107 g of crude dinitrogen acid **5**. The crude product was passed through a short silica gel plug (CH₃OH/CH₂Cl₂, 1:19, R_f = 0.2) giving 0.087 g (78% yield) of dinitrogen acid [*closo*-1-CB₉H₈-1-COOH-10-N₂] (**5**) as a white solid, which was recrystallized from aqueous MeOH containing a few drops of acetone: mp 174-177 °C dec; ¹H NMR (CD₃CN) δ 1.0-2.7 (br m, 8H), 10.0 (br s, 1H); ¹¹B NMR (CD₃CN) δ -15.5 (d, *J* = 158 Hz, 4B), -13.6 (d, *J* = 169 Hz, 4B), 20.3 (s, 1B); IR 2291 (N₂) cm⁻¹; UV (CH₃CN), λ_{max} 216 nm (log ε = 4.33); FAB-HRMS(-), calcd. for C₂H₉B₉N₂O₂ *m/z*: 192.1502; found: 192.1501. Anal. Calcd for C₂H₉B₉N₂O₂: C, 12.62; H, 4.76; N, 14.71;

Found: C, 13.06; H, 4.87; N, 14.58.

Preparation of [*closo*-1-CB₉H₈-1-COOH-10-(1-NC₅H₅)] (6)

A slight yellow solution of [*closo*-1-CB₉H₈-1-COOH-10-N₂] (5, 0.048 g, 0.25 mmol) and anhydrous pyridine (3.0 mL, 37.1 mmol) was stirred at 100 °C for 1 hr. As the reaction progressed, bubbling of N₂ became evident. Excess pyridine was removed *in vacuo*, 10% HCl (10 mL) was added to the residue, and the solution was extracted with Et₂O (3 x 5 mL). The Et₂O layers were combined, washed with H₂O, dried (Na₂SO₄), and evaporated giving 0.060 g of crude pyridinium acid 6 as a slight yellow solid. The crude product was passed through a short silica gel plug (CH₃OH/CH₂Cl₂, 1:19, R_f = 0.4) giving 0.054 g (90% yield) of acid [*closo*-1-CB₉H₈-1-COOH-10-(1-NC₅H₅)] (6) as an off-white solid, which was further purified by recrystallization from EtOH/H₂O (3x): mp 258-260 °C; ¹H NMR (CD₃CN) δ 1.0-2.5 (br m, 8H), 8.03 (t, *J* = 7.2 Hz, 2H), 8.50 (t, *J* = 7.8 Hz, 1H), 9.31 (d, *J* = 5.2 Hz, 2H); ¹¹B NMR (CD₃CN) δ -20.9 (d, *J* = 131 Hz, 4B), -16.2 (d, *J* = 160 Hz, 4B), 42.2 (s, 1B); UV (CH₃CN), λ_{max} 264 nm, (log ε = 4.07); FAB-HRMS(+), calcd. for C₇H₁₄B₉NO₂ *m/z*: 243.1862; found: 243.1853. Anal. Calcd for C₇H₁₄B₉NO₂: C, 34.81; H, 5.84; N, 5.80. Found: C, 35.46; H, 5.86; N, 5.89.

Preparation of [*closo*-1-CB₉H₈-1-COOH-10-SCHN(CH₃)₂] (7)

A solution of [*closo*-1-CB₉H₈-1-COOH-10-N₂] (5, 0.061 g, 0.32 mmol) and freshly distilled Me₂NCHS (3.0 mL, 35.2 mmol) was stirred at 100 °C for 1 hr. As the reaction progressed, bubbling of N₂ became evident. Excess Me₂NCHS was removed by

vacuum distillation (95 °C, 1.5 mm Hg) leaving crude product as an off-white crystalline solid. The crude product was washed with toluene giving 0.076 g (95% yield) of crude protected mercaptan [*closo*-1-CB₉H₈-1-COOH-10-SCHN(CH₃)₂] (**7**) containing ~5% of Me₂NCHS by ¹H NMR: mp 250-253 °C dec; ¹H NMR major signals (CD₃CN) δ 0.6-2.5 (br m, 8H), 3.50 (s, 3H), 3.57 (s, 3H), 9.49 (s, 1H); minor signals for Me₂NCHS: δ 3.19 (s, 3H), 3.25 (s, 3H), 9.12 (s, 1H); ¹¹B NMR (CD₃CN) major signals δ -20.4 (d, *J* = 144 Hz, 4B), -15.3 (d, *J* = 155 Hz, 4B), 35.2 (s, 1B); FAB-HRMS(+), calcd. for C₅H₁₆B₉NO₂S *m/z*: 253.1739; found: 253.1734.

Preparation of [*closo*-1-CB₉H₈-1-COOH-10-(1-SC₅H₁₀)] (8**)**

A solution of crude protected mercaptan [*closo*-1-CB₉H₈-1-COOH-10-SCHN(CH₃)₂] (**7**, 0.065 g, 0.26 mmol) in anhydrous CH₃CN (4 mL) was treated with a solution of NMe₄⁺OH⁻·5H₂O (0.236 g, 1.3 mmol) in anhydrous CH₃CN (6 mL) resulting in the formation of a white precipitate. 1,5-Dibromopentane (36 μL, 0.26 mmol) was added and the reaction mixture was stirred for 24 hrs at rt. The reaction mixture was evaporated to dryness and stirred in a methanol solution (4 mL) of NaOH (0.01 g, 0.250 mmol) at 50 °C for 4 hrs, to hydrolyze small amounts of ester. Solvent was removed to dryness and 10% HCl (10 mL) was added. The suspension was stirred vigorously with Et₂O (5 mL) until the aqueous layer became homogeneous. The Et₂O layer was separated, and the aqueous layer was further extracted with Et₂O (2 x 5 mL). The Et₂O layers were combined, washed with H₂O, dried (Na₂SO₄), and evaporated leaving 0.064 g of crude sulfonium acid **8** as an orange crystalline film. The crude material was passed

through a short silica gel plug (CH₃OH/CH₂Cl₂, 1:19, R_f = 0.4) and washed with hot hexane giving 0.037 g 54% yield) of [*closo*-1-CB₉H₈-1-COOH-10-(1-SC₅H₁₀)] (**8**) as an off-white solid. The product was recrystallized from aq EtOH and then from toluene to give colorless blades of acid **8** as a solvate with toluene (1:1). The solvent was removed by heating at 100 °C in vacuum for 2 hr: mp 232-233 °C; ¹H NMR (CD₃CN) δ 0.6-2.5 (br m, 8H), 1.60-1.75 (m, 2H), 1.93-2.05 (m, 2H), 2.29-2.33 (m, 2H), 3.36 (td, *J*₁ = 12.2 Hz, *J*₂ = 2.4 Hz, 2H), 3.66 (dm, *J* = 12.4 Hz, 2H), 9.71 (brs, 1H); ¹¹B NMR (CD₃CN) δ -20.2 (d, *J* = 149 Hz, 4B), -14.8 (d, *J* = 160 Hz, 4B), 32.1 (s, 1B); FAB-HRMS(+), calcd. for C₇H₁₉B₉O₂S *m/z*: 266.1943; found: 266.1933. Anal. Calcd for C₇H₁₉B₉O₂S: C, 31.78; H, 7.24. Found: C, 32.00; H, 7.27.

Preparation of [*closo*-1-CB₉H₈-1-COOMe-10-NH₃] (**10**[H])

A suspension of [*closo*-1-CB₉H₈-1-COOH-10-NH₃] (**4**[H], 0.025 g, 0.14 mmol) in anhydrous CH₂Cl₂ (2 mL) containing (COCl)₂ (0.15 mL, 0.29 mmol, 2.0 M in CH₂Cl₂) was treated with anhydrous DMF (0.1 mL, 1.4 mmol). Intense bubbling ensued followed by dissolution of the substrate, and the reaction was stirred at rt for an additional 30 mins. Solvents were removed to complete dryness leaving a light yellow residue of acid chloride [*closo*-1-CB₉H₈-1-COCl-10-NH₃]: ¹H NMR (CD₃CN) δ 8.38 (br t, *J* = 34 Hz); ¹¹B NMR (CD₃CN) δ -22.6 (d, *J* = 140 Hz, 4B), -15.3 (d, *J* = 158 Hz, 4B), 41.4 (s, 1B).

The crude chloride was dissolved in anhydrous CH₃OH (5 mL) and refluxed for 1 hr. The reaction was evaporated to dryness, suspended in Et₂O (5 mL), and treated with

5% HCl (10 mL). The Et₂O layer was separated, and the aqueous layer was further extracted with Et₂O (2x5 mL). The Et₂O layers were combined, washed with H₂O, dried (Na₂SO₄), and evaporated to dryness giving 0.026 g (96% yield) of **10[H]** as slight yellow microcrystals: mp > 260 °C; ¹H NMR (CD₃CN) δ 0.5-2.50 (br m, 8H), 3.92 (s, 3H), 6.58 (br t, *J* = 42 Hz, 3H) [¹H-¹⁴N} 6.57 (s, 3H)]; ¹¹B NMR (CD₃CN) δ -22.6 (d, *J* = 142 Hz, 4B), -16.8 (d, *J* = 156 Hz, 4B), 37.1 (s, 1B); IR 3277 and 3126 (N-H), 2569 (B-H), 1724 (C=O); ESI-HRMS (+) calcd. for C₃H₁₄B₉NNaO₂ *m/z*: 217.1798; found: 217.1778.

Preparation of [*closo*-1-CB₉H₈-1-COOMe-10-N₂] (**11**)

A cooled solution (~ 0 °C) of [*closo*-1-CB₉H₈-1-COOH-10-N₂] (**5**, 0.028 g, 0.15 mmol) in anhydrous Et₂O (2.0 mL) and diazomethane (generated from 0.076 g, 0.74 mmol of *N*-methyl-*N*-nitrosoourea) were stirred for 1 hr. The reaction mixture was evaporated to dryness giving 42 mg of crude product as a white solid. The crude material was passed through a short silica gel plug (CH₂Cl₂, R_f = 0.5) giving 24 mg (78% yield) of [*closo*-1-CB₉H₈-1-COOMe-10-N₂] (**10**) as a white crystalline solid. An analytical sample was prepared by recrystallization from EtOH/H₂O (slow evaporation of EtOH): mp 132-134 °C dec; ¹H NMR (CD₃CN) δ 1.2-2.7 (br m, 8H), 3.97 (s, 3H); ¹¹B NMR (CD₃CN) δ -15.5 (d, *J* = 163 Hz, 4B), -13.6 (d, *J* = 169 Hz, 4B), 20.4 (s, 1B); IR 2611, 2588, and 2558 (B-H), 2296 (N₂), 1735 (C=O), 1321 (C-O) cm⁻¹; ESI-HRMS(+); calcd. for C₃H₁₁B₉N₂NaO₂ *m/z*: 229.1556; found: 229.1551. Anal. Calcd for C₃H₁₁B₉N₂O₂: C,

17.63; H, 5.42; N, 13.70; Found: C, 18.08; H, 5.60; N, 13.39.

Ester [*closo*-1-CB₉H₈-1-(COOC₆H₁₁)-10-(1-NC₅H₅)] (12)

A red/orange solution of pyridinium acid [*closo*-1-CB₉H₈-1-COOH-10-(1-NC₅H₅)] (**6**, 30 mg, 0.124 mmol), dry cyclohexanol (15 mg, 0.150 mmol), and 2-chloro-3,5-dinitropyridine (25 mg, 0.124 mmol) in anhydrous pyridine (2 mL) was stirred at reflux under Ar. The ratio of peaks at 5.07 ppm and 9.31 ppm in ¹H NMR (CD₃CN) was monitored until the desired 1:2. ratio was achieved. If the reaction was not complete, additional equivalents of alcohol and 2-chloro-3,5-dinitropyridine were added and heating was continued. Excess pyridine was removed to dryness giving a red/orange crystalline film. The film was treated with 10% HCl and extracted into Et₂O (3x). The Et₂O layers were combined, washed with H₂O, dried (Na₂SO₄), and evaporated to dryness. The crude product was further purified by passing through a short silica gel plug (hexane/CH₂Cl₂; 3:7). The eluent was filtered through a cotton plug, and the product was recrystallized (5x) from iso-octane/toluene mixtures in the freezer. Ester **12** was obtained in 75% yield as colorless blades (R_f = 0.5 in CH₂Cl₂): mp 175-177 °C; ¹H NMR (CD₃CN) δ 0.8-2.5 (br m, 8H), 1.30-1.69 (m, 6H), 1.73-1.83 (m, 2H), 1.90-2.03 (m, 2H), 5.07 (tt, *J*₁ = 8.6 Hz, *J*₂ = 3.8 Hz, 1H), 8.02 (t, *J* = 7.2 Hz, 2H), 8.50 (t, *J* = 7.8 Hz, 1H), 9.31 (d, *J* = 5.3 Hz, 2H) and peaks of toluene at 2.32 (s, 1.5H), 7.12-7.26 (m, 2.5H); ¹¹B NMR (CD₃CN) δ -21.0 (d, *J* = 145 Hz, 4B), -16.3 (d, *J* = 158 Hz, 4B), 42.0 (s, 1B). Anal. Calcd. for C₁₃H₂₄B₉NO₂: C, 48.25; H, 7.47; N, 4.33. Calcd for C₁₃H₂₄B₉NO₂•1/2C₇H₈: C,

53.60; H, 7.63; N, 3.79. Found: C, 53.21; H, 7.64; N, 3.85.

Ester [*closo*-1-CB₉H₈-1-(COOC₆H₄OMe)-10-(1-SC₅H₁₀)] (13)

The ester was prepared from sulfonium acid [*closo*-1-CB₉H₈-1-COOH-10-(1-SC₅H₁₀)] (**8**) and *p*-methoxyphenol as described for **12**. The ratio of peaks at 3.82 ppm and 7.01 ppm in ¹H NMR (CD₃CN) was monitored until the desired 3:2 ratio was achieved. Ester **13** was isolated in 54% yield as colorless needles (R_f = 0.6 in CH₂Cl₂): mp 158-160 °C; ¹H NMR (CD₃CN) δ 0.7-2.7 (br m, 8H), 1.61-1.73 (m, 2H), 1.90-2.05 (m, 2H), 2.30-2.34 (m, 2H), 3.38 (td, *J*₁ = 12.2 Hz, *J*₂ = 2.2 Hz, 2H), 3.69 (br d, *J* = 12.6 Hz, 2H), 3.82 (s, 3H), 7.01 (d, *J* = 9.0 Hz, 2H), 7.22 (d, *J* = 9.0 Hz, 2H); ¹¹B NMR (CD₃CN) δ -20.1 (d, *J* = 140 Hz, 4B), -14.4 (d, *J* = 159 Hz, 4B), 33.0 (s, 1B). Anal. Calcd. for C₁₄H₂₅B₉O₃S: C, 45.36; H, 6.80; Found: C, 45.63; H, 6.79.

Preparation of [*closo*-1-CB₉H₈-1-COO-10-N₂]⁻NMe₄⁺ (5⁻[NMe₄])

A solution of dinitrogen acid [*closo*-1-CB₉H₈-1-COOH-10-N₂] (**5**, 0.035 g, 0.182 mmol) in CH₃OH (0.5 mL) was treated with NMe₄⁺OH⁻•5H₂O (3.1 mL, 0.182 mmol, 0.0588 M in CH₃OH). The homogeneous mixture was evaporated and the residue was dried in vacuum to give 0.048 g (quantitative yield) of 5⁻[NMe₄] as a slight yellow solid: mp >260 °C; ¹H NMR (CD₃CN) δ 1.0-2.5 (br m, 8H), 3.14 (s, 12H); ¹¹B NMR (CD₃CN) δ -15.4 (d, *J* = 141 Hz, 4B), -14.4 (d, *J* = 141 Hz, 4B), 14.4 (s, 1B); IR 2569 (B-H), 2290 (N₂), 1602 (C=O) cm⁻¹.

Reaction of Amino Acid 4[H] with Nitrosonium Hexafluorophosphate at Room Temperature

In a NMR tube, amino acid [*closo*-1-CB₉H₈-1-COOH-10-NH₃] (**4[H]**, 0.010 g, 0.056 mmol) was dissolved in CD₃CN. Without pyridine, NO⁺PF₆⁻ (0.016 g, 0.092 mmol; 1.6 eq) was added, and the reaction was allowed to stand at rt overnight. ¹¹B NMR analysis showed the formation of a new species with apparent substitution on the boron cage: ¹¹B NMR (CD₃CN) δ -25.1 (d, *J* = 143 Hz, 1B), -19.5 (d, *J* = 140 Hz, 2B), -15.8 (d, *J* = 230 Hz, 2B), -14.0 (d, *J* = 235 Hz, 2B), -13.2 (s, 1B), 32.5 (s, 1B); FAB-MS(-): *m/z* 268-274 (max at 271, 100%).

Preparation of [*closo*-1-CB₉H₈-1-COOMe-10-NH₂]⁻NMe₄⁺ (**10[NMe₄]**)

The salt was prepared by treating [*closo*-1-CB₉H₈-1-COOMe-10-NH₃] (**10[H]**, 10 mg, 0.052 mmol) with NMe₄⁺OH⁻•5H₂O (9 mg, 0.050 mmol) dissolved in CH₃OH (3 mL). The solution was evaporated to dryness giving 12 mg (87% yield) of **10[NMe₄]** as a slight yellow film: ¹H NMR (CD₃CN) δ 0.5-2.50 (br m, 8H), 3.06 (s, 12H), 3.87 (s, 3H); ¹¹B NMR (CD₃CN) δ -25.8 (d, *J* = 139 Hz, 4B), -19.0 (d, *J* = 158 Hz, 4B), 47.0 (s, 1B).

Generation of [*closo*-1-CB₉H₈-1-COOMe-10-NHCOPh]⁻H₃O⁺ (**15[H₃O]**)

A solution of [*closo*-1-CB₉H₈-1-COOMe-10-N₂] (**11**, 0.005 g,) in dry PhCN (0.6 mL) was heated at 125-140 °C for 1-2 hr in a NMR tube. Progress of the reaction was monitored by ¹¹B NMR spectroscopy (see kinetic experiment above). After no more starting **11** was present, the excess PhCN was distilled off from the solution containing mostly the ylide [*closo*-1-CB₉H₈-1-COOMe-10-NCPh] (**14**) [¹¹B NMR major

signals (PhCN) δ -18.8 (d, $J = 150$ Hz, 4B), -15.1 (d, $J = 154$ Hz, 4B), 29.0 (s, 1B)]. The residue was treated with moist CD₃CN to form *in situ* [*closo*-1-CB₉H₈-1-COOMe-10-NHCOPh]⁻H₃O⁺ (**15**[H₃O]): ¹H NMR major signals (95%) (CD₃CN) δ 1.0-2.5 (br m, 8H), 3.90 (s, 3H), 7.48-7.55 (m, 2H), 7.58 (t, $J = 6.2$ Hz, 1H), 7.93 (d, $J = 7.4$ Hz, 2H); ¹¹B NMR (CD₃CN) major signals (95%) δ -24.0 (d, $J = 138$ Hz, 4B), -17.6 (d, $J = 152$ Hz, 4B), 40.1 (s, 1B); ESI-HRMS(-), calcd. for C₁₀H₁₇B₉NO₃ m/z : 298.2046; found: 298.2054.

Reaction of Nitrosonium Hexafluorophosphate and Pyridine. Formation of 23.

Nitrosonium hexafluorophosphate (0.110 g, 0.63 mmol) was added to anhydrous pyridine (0.05 mL, 0.63 mmol) in anhydrous CH₃CN (1.5 mL) at -15 °C. The solution turned green immediately and stirring was continued for 20 min. Solvents were removed to dryness giving an off-white solid: ¹H NMR (CD₃CN) δ 7.91 (t, $J = 5.1$ Hz, 2H), 8.41 (t, $J = 5.9$ Hz, 1H), 8.83 (d, $J = 4.2$ Hz, 2H). Lit.⁸⁴ for the SbCl₆⁻ salt: ¹H NMR (CD₃CN) δ 8.09 (t, 2H), 8.62 (t, 1H), 9.00 (d, 2H).

Pyridine: ¹H NMR (CD₃CN) δ 7.29-7.33 (m, 2H), 7.72 (tt, $J_1 = 7.7$ Hz, $J_2 = 1.8$ Hz, 1H), 8.56 (d, $J = 4.1$ Hz, 2H).

Acknowledgments

We thank two undergraduate students Sarah Muller and Breanna Stein, and also to Mr. Matthew Casella for technical assistance with the preparation of **1**[NMe₄]. This project was supported by the NSF grant (DMR-0606317 and DMR-0907542). BR thanks for support while visiting Academy of Sciences of the Czech Republic (NSF CHE-0446688 and OISE-0532040). ZJ was supported by Grant Contact (project ME857) and the Ministry of Education, Youth, and Sports of the Czech Republic (project LC523).

References

- (1) Stibr, B. *Chem. Rev.* **1992**, *92*, 225-250.
- (2) Sivaev, I. B.; Kayumov, A.; Yakushev, A. B.; Solntsev, K. A.; Kuznetsov, N. T. *Koord. Khim.* **1989**, *15*, 1466-1477.
- (3) Nestor, K.; Stibr, B.; Kennedy, J. D.; Thornton-Pett, M.; Jelinek, T. *Collect. Czech. Chem. Commun.* **1992**, *57*, 1262-1268.
- (4) Körbe, S.; Schreiber, P. J.; Michl, J. *Chem. Rev.* **2006**, *106*, 5208-5249.
- (5) Michl, J. *Pure Appl. Chem.* **2008**, *80*, 429-446.
- (6) Larsen, A. S.; Holbrey, J. D.; Tham, F. S.; Reed, C. A. *J. Am. Chem. Soc.* **2000**, *122*, 7264-7272. Nieuwenhuyzen, M.; Seddon, K. R.; Teixidor, F.; Puga, A. V.; Viñas, C. *Inorg. Chem.* **2009**, *48*, 889-901.
- (7) Ivanov, S. V.; Casteel, W. J.; Bailey, W. H. *US Pat. Appl.* 2007, US 2007189946. Pez, G. P.; Ivanov, S. V.; Dantsin, G.; Casteel, W. J.; Lehmann, J. F. *Eur. Pat. Appl.*

2007, EP 1763099.

(8) Ringstrand, B.; Kaszynski, P.; Monobe, H. *J. Mater. Chem.* **2009**, *19*, 4805-4812.

(9) Ringstrand, B.; Kaszynski, P.; Young, V. G., Jr.; Januszko, A. *J. Mater. Chem.* **2009**, *19*, 9204-9212.

(10) Grüner, B.; Janousek, Z.; King, B. T.; Woodford, J. N.; Wang, C. H.; Vsetecka, V.; Michl, J. *J. Am. Chem. Soc.* **1999**, *121*, 3122-3126.

(11) Sivaev, I. B.; Bregadze, V. V. *Eur. J. Inorg. Chem.* **2009**, 1433-1450.

(12) Wilbur, D. S.; Hamlin, D. K.; Srivastava, R. R.; Chyan, M.-K. *Nucl. Med. Biol.* **2004**, *31*, 523-530.

(13) Sivaev, I. B.; Bregadze, V. I.; Kuznetsov, N. T. *Russ. Chem. Bull., Int. Ed.* **2002**, *51*, 1362-1374.

(14) Ol'shevskaya, V. A.; Zaitsev, A. V.; Luzgina, V. N.; Kondratieva, T. T.; Ivanov, O. G.; Kononova, E. G.; Petrovskii, P. V.; Mironov, A. F.; Kalinin, V. N.; Hofmann, J.; Shtil, A. A. *Bioorg. Med. Chem.* **2006**, *14*, 109-120.

(15) Ol'shevskaya, V. A.; Nikitina, R. G.; Zaitsev, A. V.; Luzgina, V. N.; Kononova, E. G.; Morozova, T. G.; Drozhzhina, V. V.; Ivanov, O. G.; Kaplan, M. A.; Kalinin, V. N.; Shtil, A. A. *Org. Biomol. Chem.* **2006**, *4*, 3815-3821.

(16) Reed, C. A. *Acc. Chem. Res.* **1998**, *31*, 133-139. Strauss, S. H. *Chem. Rev.* **1993**, *93*, 927-942. Krossing, I.; Raabe, I. *Angew. Chem. Int. Ed.* **2004**, *43*, 2066-2090.

- (17) King, R. B. *Russ. Chem. Bull.* **1993**, *42*, 1283-1291.
- (18) Schleyer, P. v. R.; Najafian, K. *Inorg. Chem.* **1998**, *37*, 3454-3470.
- (19) Bullen, N. J.; Franken, A.; Kilner, C. A.; Kennedy, J. D. *Chem. Commun.* **2003**, 1684-1685.
- (20) Muller, J.; Base, K.; Magnera, T.; Michl, J. *J. Am. Chem. Soc.* **1992**, *114*, 9721-9722.
- (21) Schöberl, U.; Magnera, T. F.; Harrison, R. M.; Fleischer, F.; Pflug, J. L.; Schwab, P. F. H.; Meng, X.; Lipiak, D.; Noll, B. C.; Allured, V. S.; Rudalevige, T.; Lee, S.; Michl, J. *J. Am. Chem. Soc.* **1997**, *119*, 3907-3917.
- (22) Yang, X.; Jiang, W.; Knobler, C. B.; Hawthorne, M. F. *J. Am. Chem. Soc.* **1992**, *114*, 9719-9721.
- (23) Schwab, P. F. H.; Levin, M. D.; Michl, J. *Chem. Rev.* **1999**, *99*, 1863-1933.
- (24) Kaszynski, P.; Douglass, A. G. *J. Organomet. Chem.* **1999**, *581*, 28-38.
- (25) Kaszynski, P.; Pakhomov, S.; Tesh, K. F.; Young, V. G., Jr. *Inorg. Chem.* **2001**, *40*, 6622-6631.
- (26) Pakhomov, S.; Kaszynski, P.; Young, V. G., Jr. *Inorg. Chem.* **2000**, *39*, 2243-2245.
- (27) For other recent publications see: Januszko, A.; Glab, K. L.; Kaszynski, P. *Liq. Cryst.* **2008**, *35*, 549-553. Nagamine, T.; Januszko, A.; Ohta, K.; Kaszynski, P.; Endo, Y.

Liq. Cryst. **2008**, *35*, 865-884. Januszko, A.; More, K. M.; Pakhomov, S.; Kaszynski, P.; O'Neill, M.; Wand, M. D. *J. Mater. Chem.* **2004**, *14*, 1544-1553. Januszko, A.; Glab, K. L.; Kaszynski, P.; Patel, K.; Lewis, R. A.; Mehl, G. H.; Wand, M. D. *J. Mater. Chem.* **2006**, *16*, 3183-3192. Jasinski, M.; Jankowiak, A.; Januszko, A.; Bremer, M.; Pauluth, D.; Kaszynski, P. *Liq. Cryst.* **2008**, *35*, 343-350.

(28) Jelinek, T.; Plesek, J.; Hermanek, S.; Stibr, B. *Collect. Czech. Chem. Commun.* **1986**, *51*, 819-829.

(29) Jelinek, T.; Baldwin, P.; Scheidt, W. R.; Reed, C. A. *Inorg. Chem.* **1993**, *32*, 1982.

(30) Jelinek, T.; Plesek, J.; Mares, F.; Hermanek, S.; Stibr, B. *Polyhedron* **1987**, *6*, 1981-1986.

(31) Finze, M. *Chem. Eur. J.* **2009**, *15*, 947-962.

(32) Ivanov, S. V.; Rockwell, J. J.; Miller, S. M.; Anderson, O. P.; Solntsev, K. A.; Strauss, S. H. *Inorg. Chem.* **1996**, *35*, 7882-7891.

(33) Brellochs, D. In *Contemporary Boron Chemistry*; Davidson, M. G., Hughes, A. K., Marder, T. B., Wade, K., Eds.; Royal Society of Chemistry: Cambridge, England, 2000, p 212-214.

(34) Jelinek, T.; Kilner, C. A.; Thornton-Pett, M.; Kennedy, J. D. *Chem. Commun.* **2001**, 1790-1791.

(35) Franken, A.; Carr, M. J.; Clegg, W.; Kilner, C. A.; Kennedy, J. D. *Dalton Trans.* **2004**, 3552-3561.

- (36) Sivaev, I. B.; Starikova, Z. A.; Petrovskii, P. V.; Bregadze, V. I.; Sjöberg, S. J. *Organomet. Chem.* **2005**, *690*, 2790-2795.
- (37) Franken, A.; Kilner, C. A.; Thornton-Pett, M.; Kennedy, J. D. *Collect. Czech. Chem. Comm.* **2002**, *67*, 869-912.
- (38) Ringstrand, B.; Balinski, A.; Franken, A.; Kaszynski, P. *Inorg. Chem.* **2005**, *44*, 9561-9566.
- (39) Kaszynski, P.; Pakhomov, S.; Young, V. G., Jr. *Collect. Czech. Chem. Commun.* **2002**, *67*, 1061-1083.
- (40) Hertler, W. R.; Knoth, W. H.; Muetterties, E. L. *J. Am. Chem. Soc.* **1964**, *86*, 5434-5439.
- (41) Knoth, W. H.; Hertler, W. R.; Muetterties, E. L. *Inorg. Chem.* **1965**, *4*, 280-287.
- (42) Hertler, W. R.; Knoth, W. H.; Muetterties, E. L. *Inorg. Chem.* **1965**, *4*, 288-293.
- (43) Knoth, W. H. *J. Am. Chem. Soc.* **1966**, *88*, 935-939.
- (44) Naoufal, D.; Grüner, B.; Bonnetot, B.; Mongeot, H. *Polyhedron* **1999**, *18*, 931-939.
- (45) Kaszynski, P.; Huang, J.; Jenkins, G. S.; Bairamov, K. A.; Lipiak, D. *Mol. Cryst. Liq. Cryst.* **1995**, *260*, 315-331.
- (46) Komura, M.; Nakai, H.; Shiro, M. *J. Chem. Soc., Dalton Trans.* **1987**, 1953-1956.

- (47) Naoufal, D.; Bonnetot, B.; Mongeot, H.; Grüner, B. *Collect. Czech. Chem. Comm.* **1999**, *64*, 856-864.
- (48) Bragin, V. I.; Sivaev, I. B.; Bregadze, V. I.; Votnova, N. A. *J. Organomet. Chem.* **2005**, *690*, 2847-2849.
- (49) Knoth, W. H. *Organometallics* **1985**, *4*, 207-208.
- (50) Ringstrand, B.; Kaszynski, P.; Franken, A. *Inorg. Chem.* **2009**, *48*, 7313-7329.
- (51) Abaev, V. T.; Serdyuk, O. V. *Russ. Chem. Rev.* **2008**, *77*, 177-192.
- (52) Xia, N.; Taillefer, M. *Angew. Chem. Int. Ed.* **2009**, *48*, 337-339.
- (53) Jaime-Figueroa, S.; Liu, Y.; Muchowski, J. M.; Putman, D. G. *Tetrahedron Lett.* **1998**, *39*, 1313-1316.
- (54) Charles, M. D.; Schultz, P.; Buchwald, S. L. *Org. Lett.* **2005**, *7*, 3965-3968.
- (55) Wolfe, J. P.; Ahman, J.; Sadighi, J. P.; Singer, R. A.; Buchwald, S. L. *Tetrahedron Lett.* **1997**, *38*, 6367-6370.
- (56) Hartwig, J. F.; Kawatsura, M.; Hauck, S. I.; Shaughnessy, K. H.; Alcazar-Roman, L. M. *J. Org. Chem.* **1999**, *64*, 5575-5580.
- (57) Lee, D.-Y.; Hartwig, J. F. *Org. Lett.* **2005**, *7*, 1169-1172.

- (58) Lee, S.; Jørgensen, M.; Hartwig, J. F. *Org. Lett.* **2001**, *3*, 2729-2732.
- (59) Huang, X.; Buchwald, S. L. *Org. Lett.* **2001**, *3*, 3417-3419.
- (60) Amination reactions of a mixture of 6- and 10-iodo isomers [*closo*-1-CB₉H₈-1-COOH-6-I]⁻ and [*closo*-1-CB₉H₈-1-COOH-10-I]⁻ (**1**) under the same conditions demonstrated similar reactivity of both isomers.
- (61) Lipilin, D. L.; Belyakov, P. A.; Strelenko, Y. A.; Churakov, A. M.; Smirnov, O. Y.; Ioffe, S. L.; Tartakovskiy, V. A. *Eur. J. Org. Chem.* **2002**, 3821-3826.
- (62) For details see Supporting Information.
- (63) Takimoto, S.; Abe, N.; Kodera, Y.; Ohta, H. *Bull. Chem. Soc. Jpn.* **1983**, *56*, 639-640.
- (64) Crystal data for **5** (CCDC no. 744000): C₂H₉B₉N₂O₂ monoclinic, *P*2₁/*n*, *a* = 7.022(2) Å, *b* = 11.389(4) Å, *c* = 12.815(4) Å, β = 96.212(5)°; *V* = 1018.8(6) Å³, *Z* = 4, *T* = 173(2) K, *l* = 0.71073 Å, *R*(F²) = 0.0384 or *R*_w(F²) = 0.1006 (for 1945 reflections with *I* > 2*s*(*I*)). Crystal data for **6** (CCDC no. 743999): C₇H₁₄B₉NO₂, monoclinic, *P*2₁/*n*, *a* = 14.275(4) Å, *b* = 12.184(3) Å, *c* = 30.538(8) Å, β = 95.377(4)°; *V* = 5288(3) Å³, *Z* = 16, *T* = 173(2) K, *l* = 0.71073 Å, *R*(F²) = 0.0541 or *R*_w(F²) = 0.1358 (for 7029 reflections with *I* > 2*s*(*I*)). Crystal data for **8** (CCDC no. 744001): C₇H₁₉B₉O₂S, monoclinic, *P*2₁/*c*, *a* = 15.988(5) Å, *b* = 19.377(6) Å, *c* = 9.655(3) Å, β = 98.348(5)°; *V* = 2959.4(16) Å³, *Z* = 8, *T* = 173(2) K, *l* = 0.71073 Å, *R*(F²) = 0.0428 or *R*_w(F²) = 0.0979 (for 4900 reflections with *I* > 2*s*(*I*)). For details see Supporting Information.
- (65) Ng, L.-L.; Ng, B. K.; Shelly, K.; Knobler, C. B.; Hawthorne, M. F. *Inorg. Chem.* **1991**, *30*, 4278-4280.
- (66) Whelan, T.; Brint, P.; Spalding, T. R.; McDonald, W. S.; Lloyd, D. R. *J. Chem.*

Soc. Dalton Trans. **1982**, 2469-2473.

(67) Hall, H. D.; Ulrich, B. D.; Kultyshev, R. G.; Liu, J.; Liu, S.; Meyers, E. A.; Gréau, S.; Shore, S. G. *Collect. Czech. Chem. Comm.* **2002**, *67*, 1007-1024.

(68) Schramm, K. D.; Ibers, J. A. *Inorg. Chem.* **1977**, *16*, 3287-3293.

(69) Hansch, C.; Leo, A.; Taft, R. W. *Chem. Rev.* **1991**, *91*, 165-195.

(70) Hnyk, D.; Holub, J.; Hofmann, M.; Schleyer, P. v. R.; Robertson, H. E.; Rankin, D. W. H. *J. Chem. Soc., Dalton Trans.* **2000**, 4617 - 4622.

(71) Statistical analysis for a total of 90 bond lengths in acids **5**, **6**, and **8** excluding the C–O and N–N distances.

(72) Niazi, M. S. K.; Mollin, J. *Bull. Chem. Soc. Jpn.* **1987**, *60*, 2605-2610.

(73) Wilcox, C. F., Jr.; McIntyre, J. S. *J. Org. Chem.* **1965**, *30*, 777-780.

(74) Mukhin, S. N.; Kabytaev, K. Z.; Zhigareva, G. G.; Glukhov, I. V.; Starikova, Z. A.; Bregadze, V. I.; Beletskaya, I. P. *Organometallics* **2008**, *27*, 5937-5942.

(75) Hoefnagel, A. J.; Hoefnagel, M. A.; Wepster, B. M. *J. Org. Chem.* **1981**, *46*, 4209–4211.

(76) *pK* values measured in MeOH are higher than those in 50% EtOH. For PhCOOH the difference is 0.86; Bright, W. L.; Briscoe, H. T. *J. Phys. Chem.* **1933**, *37*, 787-796.

(77) For example: Morita Y.; Agawa, T. *J. Org. Chem.* **1992**, *57*, 3658-3662; McNab, H.; Monahan, L. C. *J. Chem. Soc. Perkin Trans. 1* **1989**, 419-424.

(78) A $^1J_{\text{N-H}} = 46$ Hz for a partially collapsed triplet was reported for anhydrous NH_3 ; Ogg, R. A. Jr.; Ray, J. D. *J. Chem. Phys.* **1957**, *26*, 1515-1516.

(79) Hertler, W. R.; Raasch, M. S. *J. Am. Chem. Soc.* **1964**, *86*, 3661-3668.

(80) Knoth, W. H.; Miller, H. C.; England, D. C.; Parshall, G. W.; Muettertiese, E. L. *J. Am. Chem. Soc.* **1962**, *84*, 1056-1057.

(81) The author in ref 43 quotes a preliminary $[\text{pK}_a]_{(\text{MeCN})}$ value of 12.2 for $[\text{closo-B}_{10}\text{H}_8-1,10-(\text{NH}_2)_2]^{2-}$. Experimental details have not been published.

(82) A reaction of $[\text{closo-B}_{10}\text{H}_8-1,10-(\text{NH}_2)_2]^{2-} 2\text{Na}^+$ prepared *in situ* in diglyme with NOCl was reported in ref 43 to give $[\text{closo-B}_{10}\text{H}_8-1,10-(\text{N}_2)_2]$ in a low yield.

(83) Olah, G. A.; Olah, J. A.; Overchuk, N. A. *J. Org. Chem.* **1965**, *30*, 3373-3376.

(84) Lee, K. Y.; Kochi, J. K. *J. Chem. Soc. Perkin. Trans. 2* **1994**, 237-245.

(85) A similar green color was formed in a reaction between pyridine and NO^+PF_6^- in the absence of **4**, and also reported in literature (see reference 83).

(86) Leyden, R. N.; Hawthorne, M. F. *Inorg. Chem.* **1975**, *14*, 2444-2446.

- (87) Andrieux, C. P.; Pinson, J. *J. Am. Chem. Soc.* **2003**, *125*, 14801-14806.
- (88) Knoth, W. H. *J. Am. Chem. Soc.* **1972**, *94*, 104-109.
- (89) Becke, A. D. *J. Chem. Phys.* **1993**, *98*, 5648-5652.
- (90) Lee, C.; Yang, W.; Parr, R. G. *Phys. Rev. B*, **1988**, *37*, 785-789.
- (91) Møller, C.; Plesset, M. S. *Phys. Rev.* **1934**, *46*, 618-622; Head-Gordon, M.; Pople, J. A.; Frisch, M. J. *Chem. Phys. Lett.* **1988**, *153*, 503-506.
- (92) Gaussian 03, Revision D.01, M. J. Frisch, G. W. Trucks, H. B. Schlegel, G. E. Scuseria, M. A. Robb, J. R. Cheeseman, J. A. Montgomery, Jr., T. Vreven, K. N. Kudin, J. C. Burant, J. M. Millam, S. S. Iyengar, J. Tomasi, V. Barone, B. Mennucci, M. Cossi, G. Scalmani, N. Rega, G. A. Petersson, H. Nakatsuji, M. Hada, M. Ehara, K. Toyota, R. Fukuda, J. Hasegawa, M. Ishida, T. Nakajima, Y. Honda, O. Kitao, H. Nakai, M. Klene, X. Li, J. E. Knox, H. P. Hratchian, J. B. Cross, V. Bakken, C. Adamo, J. Jaramillo, R. Gomperts, R. E. Stratmann, O. Yazyev, A. J. Austin, R. Cammi, C. Pomelli, J. W. Ochterski, P. Y. Ayala, K. Morokuma, G. A. Voth, P. Salvador, J. J. Dannenberg, V. G. Zakrzewski, S. Dapprich, A. D. Daniels, M. C. Strain, O. Farkas, D. K. Malick, A. D. Rabuck, K. Raghavachari, J. B. Foresman, J. V. Ortiz, Q. Cui, A. G. Baboul, S. Clifford, J. Cioslowski, B. B. Stefanov, G. Liu, A. Liashenko, P. Piskorz, I. Komaromi, R. L. Martin, D. J. Fox, T. Keith, M. A. Al-Laham, C. Y. Peng, A. Nanayakkara, M. Challacombe, P. M. W. Gill, B. Johnson, W. Chen, M. W. Wong, C. Gonzalez, and J. A. Pople, Gaussian, Inc., Wallingford CT, 2004.
- (93) Scott, A. P.; Radom, L. *J. Phys. Chem.* **1996**, *100*, 16502-16513.
- (94) Foresman, J. B.; Keith, T. A.; Wiberg, K. B.; Snoonian, J.; Frisch, M. J. *J. Phys. Chem.* **1996**, *100*, 16098-16104.
- (95) Hasted, J. B. in *Water a Comprehensive Treatise*, F. Franks, Ed.; Plenum Press,

New York 1973, Vol 2, pp 421.

(96) Zerner, M. C. in *Reviews of Computational Chemistry*, K. B. Lipkowitz and D. B. Boyd, Eds.; VCH Publishing, New York, 1991, Vol. 2, pp 313-366, and references therein.

(97) Albert, A.; Serjeant, E. P. *The Determination of Ionization Constants: A Laboratory Manual*, 2nd ed.; Chapman and Hall Ltd: London, 1971.

(98) Rubino, J. T.; Berryhill, W. S. *J. Pharmac. Sci.* **1986**, 75, 182-186.

(99) A. J. Bard and L. R. Faulkner *Electrochemical Methods: Fundamentals and Applications*, 2nd Ed, Wiley, Hoboken, 2001.

Polar Derivatives of the [*closo*-1-CB₉H₁₀]⁻ Cluster as Positive $\Delta\epsilon$ Additives to Nematic Hosts.

Reproduced by permission of Ringstrand, B.; Kaszynski, P.; Januszko, A.; Young, V. G. Jr. *J. Mater. Chem.* **2009**, *19*, 9204-9212. Copyright 2009 The Royal Society of Chemistry. Available online: <http://pubs.rsc.org/en/content/articlelanding/2009/jm/b913701g>

This work describes the synthesis and characterization of quinuclidinium (**1**) and sulfonium (**2**) zwitterionic derivatives of the [*closo*-1-CB₉H₁₀]⁻ anion (calculated $\mu \approx 16$ D) as the first examples of polar materials type **I**, where the onium fragment is substituted at the C(1) vertex. The goal was to determine the solubility of the additives in nematic hosts and their effect on the dielectric anisotropy ($\Delta\epsilon$) of the bulk material. Results demonstrated that **1** and **2** were soluble in **CI Ester** and significantly increased $\Delta\epsilon$ of the bulk material. However, the additives were prone to aggregation, which limits their practical use.

My role in this work was to synthesize and characterize all compounds using the methodology developed earlier in my dissertation studies (see Part II, Chapters 1 and 2). I was also responsible for preparing the solutions of zwitterionic derivative **2** in nematic hosts and performing the dielectric measurements using the Liquid Crystal Analysis System (LCAS).

Dr. Victor G. Young, Jr. of University of Minnesota at the Twin Cities performed single crystal X-ray analysis on compound **1**. Dr. Adam Januszko prepared and measured solutions of derivative **1**. In addition, Dr. Januszko trained me how to operate the Liquid Crystal Analysis System (LCAS) in order to measure the dielectric properties of solutions of **2** in nematic hosts. Dr. Piotr Kaszynski performed quantum mechanical calculations that permitted the dielectric results for **1** and **2** to be analyzed using the Maier-Meier relationship.

Abstract

Polar ($\mu \approx 16$ D) and UV transparent > 250 nm quinuclidinium (**1**) and sulfonium (**2**) zwitterionic derivatives of the [*closo*-1-CB₉H₁₀]⁻ anion were synthesized and studied as additives to nematic hosts. The molecular and crystal structures for **1** [C₁₉H₄₄B₉N triclinic, P-1, $a = 9.766(2)$ Å, $b = 10.481(3)$ Å, $c = 12.098(3)$ Å, $\alpha = 93.804(9)^\circ$, $\beta = 90.249(10)^\circ$, $\gamma = 102.587(10)^\circ$, $Z = 2$] were determined by X-ray crystallography and compared with the results of HF/6-31G(d) calculations. Low concentration solutions (< 10 mol%) of **1** and **2** in **ClEster** host ($\Delta\epsilon = -0.59$) were investigated using thermal and dielectric methods. The results for **1** and **2** showed the virtual [T_{NI}] of 139 °C and 92 °C, and a $\Delta\epsilon$ extrapolated to infinite dilution of 70 ± 1 and 61 ± 2 , respectively. Dielectric results were analyzed using the Maier-Meier relationship and calculated molecular parameters. The apparent order parameter S_{app} was found to be 0.63 and 0.50 for **1** and **2**,

respectively, which is smaller than that for the pure host ($S = 0.66$). Analysis of the Kirkwood factors g obtained for each concentration gave an association constant K of 63 ± 2 and 37 ± 1 (model 1) for the assumed dimerization of molecules ($2M \rightleftharpoons M_2$) of **1** and **2**, respectively, in solutions of **CI Ester**.

Introduction

Nearly all liquid crystal (LC) electrooptical devices, such as flat panel displays,^{1,2} rely on the so-called Fréedericksz transition,³ where polar oriented molecules re-orientate in an external electric field resulting in a change of the optical properties of the bulk material.^{4,5} The threshold voltage (V_{th}) for the reorientation of the LC molecules is inversely proportional to the square root of dielectric anisotropy, $\Delta\epsilon$, which in turn is proportional to the molecular dipole moment and its orientation relative to the main molecular axis, $\sim \mu^2(1-3\cos^2\beta)$. Therefore, the larger the dipole moment, the lower the threshold voltage ($V_{th} \sim 1/\mu$).

Liquid crystals with positive dielectric anisotropy ($\Delta\epsilon > 0$) are typically designed by using polar terminal substituents, such as $-\text{CN}$,⁶ $-\text{NCS}$,⁷ and F ,² or heterocycles, such as pyrimidine⁸ or dioxane⁹ as part of the rigid core, with the net dipole moment oriented along the long molecular axis.^{2,10,11} Dipole moments associated with these molecular fragments are moderate and generally do not exceed 5 D (e.g., for benzonitrile¹² $\mu = 4.52$ D). Much larger molecular dipole moments are observed for zwitterions,¹³ and for some

compounds values near 16 D have been measured.^{14,15} Anisometric compounds (elongated molecular shapes) possessing such large dipole moments could serve as effective low-concentration polar additives that significantly increase $\Delta\epsilon$ of the liquid crystalline material. However, most zwitterions have geometries incompatible with a typical nematic LC material, which limits their usefulness in electrooptical applications. To date only three classes of zwitterionic mesogens, pyrazo[1,2-*a*]pyrazoliumolates,¹⁶ syndones,¹⁷ and *N*-pyridinio-4-alkoxybenzamides,¹⁸ have been reported but their compatibility with nematic materials has not been investigated. A class of zwitterions that are particularly attractive for the design of polar mesogens or additives to nematic materials is based on monocarbaborates **A** and **B** (Figure 1).¹⁹⁻²¹

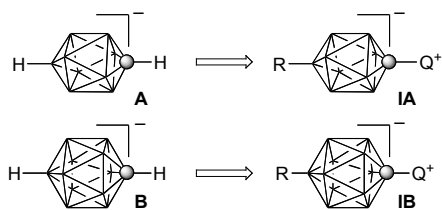
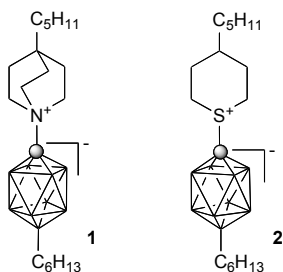


Figure 1. The structures of the ionic $[\textit{closo}\text{-}1\text{-CB}_9\text{H}_{10}]^-$ and $[\textit{closo}\text{-}1\text{-CB}_{11}\text{H}_{12}]^-$ clusters (**A** and **B**), and their polar derivatives (**IA** and **IB**). Each vertex represents a BH fragment, the sphere is a carbon atom, and Q^+ stands for an onium group such as an ammonium, sulfonium, or pyridinium.

closo-Monocarbaborates $[\textit{closo}\text{-}1\text{-CB}_9\text{H}_{10}]^-$ and $[\textit{closo}\text{-}1\text{-CB}_{11}\text{H}_{12}]^-$ (**A** and **B**, Fig. 1) belong to an extensive family of *closo*-boranes, which are characterized by sigma-aromaticity and complete negative charge delocalization.²¹ The geometry of the two clusters, **A** and **B**, appears to be appropriate for the formation of calamitic liquid crystals, as is indicated by results for their electrically neutral isostructural *p*-

carborane analogues.²²⁻²⁶ Extensive experimental data demonstrate that both *p*-carboranes support liquid crystalline phase formation, and their derivatives strongly prefer nematic over smectic phases. Therefore, clusters **A** and **B** substituted in the antipodal positions with appropriate groups are expected to exhibit LC state or at least be compatible with the nematic phase. The use of an onium fragment, Q⁺, as one of the substituents introduces a substantial dipole moment oriented along the long molecular axis (Figure 1). Our previous calculations²¹ demonstrated that the dipole moment expected from such derivatives of clusters **A** and **B** can exceed 15 D, which is difficult to obtain in organic non-zwitterionic species.

The unique properties of *closo*-boranes and opportunities to engineer highly polar and oriented materials for electrooptical applications prompted us to investigate the two monocarbaborates **A** and **B** as the centerpiece of rod-like compounds **IA** and **IB** (Figure 1). In this paper, we focus on the 10-vertex system, the [*closo*-1-CB₉H₁₀]⁻ anion **A**. We establish the method for the introduction of alkyl and appropriate onium fragments into the {*closo*-1-CB₉} cage and prepare first two such derivatives, **1** and **2**, from the isomerically pure iodo acid²⁷ [*closo*-1-CB₉H₈-1-COOH-10-I]⁻. We investigate both derivatives as additives to nematic hosts, and study such binary mixtures by thermal and dielectric methods. The dielectric data is analyzed with the aid of the Maier-Meier relationship, which uses molecular parameters derived from quantum-mechanical calculations. Finally, we quantify behavior **1** and **2** in the nematic solution by deriving the association constant *K* from the dielectric data.



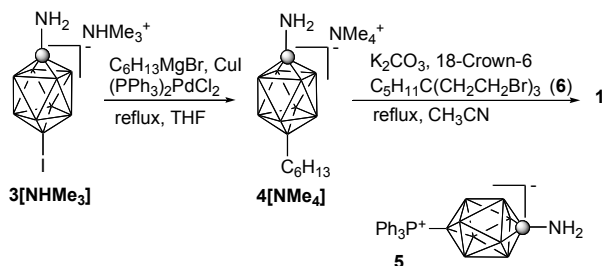
Results

Synthesis

Derivatives **1** and **2** were prepared starting from iodo amine²⁸ **3** by a combination of alkylative cyclization at the C(1) vertex and Pd(0) catalyzed coupling at the B(10) vertex.

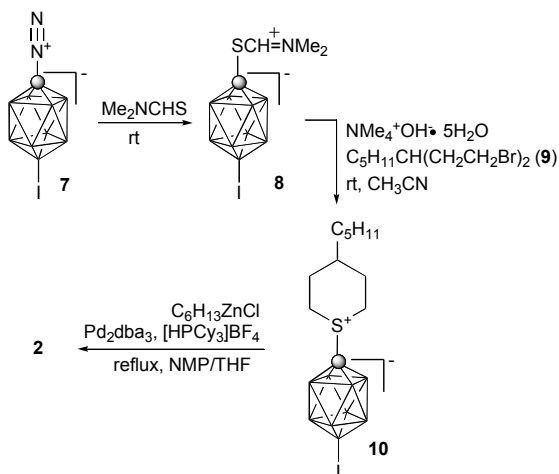
For quinuclidinium derivative **1**, iodo amine **3**[NMe₃] was reacted with excess hexylmagnesium bromide in the presence of CuI and Pd(0) giving hexyl amine **4**[NMe₄] in 33% yield. Phosphonium adduct **5** was isolated as a by-product in 20% yield and partially characterized. The formation of an adduct similar to **5** was also observed in the Pd-catalyzed hexylation of iodo acid [*closo*-1-CB₉H₈-1-COOH-10-I]⁻ NMe₄⁺ using tricyclohexylphosphine as a ligand.²⁸ Alkylation of amine **4**[NMe₄] with tribromide²⁹ **6** in the presence of a base under phase-transfer catalysis conditions gave quinuclidinium derivative **1** in 33% yield (Scheme 1).

Scheme 1



The introduction of the sulfonium fragment at the C(1) vertex and formation of **2** was envisioned by using a dinitrogen functionality in analogy to the preparation of [*closo*-1-CB₉H₉-1-SC₅H₁₀] from [*closo*-1-CB₉H₉-1-N₂].³⁰ Our initial experiments with diazotization of hexyl amine **4**[NMe₄] demonstrated that the corresponding dinitrogen derivative [*closo*-1-CB₉H₈-1-N₂-10-C₆H₁₃] was an unstable oil that was difficult to purify and handle. Therefore, we focused on iodo dinitrogen derivative **7**, which we previously prepared in high yield from amine **3** and isolated as a stable, crystalline solid, suitable for further synthetic transformations.²⁸ Thus, the dinitrogen derivative **7** was reacted at ambient temperature with Me₂NCHS to form protected mercaptan **8**, which upon reactions with dibromide³¹ **9** under hydrolytic conditions gave sulfonium derivative **10** in 39% overall isolated yield. The hexyl group was introduced at the B(10) position by reacting **10** with hexylzinc chloride under Negishi conditions, previously used for the hexylation of iodo acid²⁸ [*closo*-1-CB₉H₈-1-COOH-10-I]NMe₄⁺, giving sulfonium derivative **2** in 58% yield (Scheme 2).

Scheme 2



Thermal Properties

Calorimetric (DSC) and optical (POM) analyses revealed that both polar derivatives **1** and **2** are high melting solids ($> 200\text{ }^\circ\text{C}$) and neither forms liquid crystalline phases. DSC demonstrated two transitions for each compound corresponding to a Cr-Cr transition and melting (Table 1). The solid-solid transition in quinuclidinium **1** is a high energy, broad peak spread over 40 K with a maximum at $126\text{ }^\circ\text{C}$. The melting at $363\text{ }^\circ\text{C}$ has a similar high endotherm and is accompanied by rapid decomposition. The analogous transitions for the sulfonium **2** occur at lower temperatures at which the compound is thermally stable. An additional transition at $86\text{ }^\circ\text{C}$ (2.3 kJ/mol) was detected in a one-year-old sample of **2**. After heating this sample to $150\text{ }^\circ\text{C}$ followed by conditioning at ambient temperature for 5 hrs the transitions at $66\text{ }^\circ\text{C}$ and $86\text{ }^\circ\text{C}$ were replaced with new transitions at $55\text{ }^\circ\text{C}$ and $77\text{ }^\circ\text{C}$, respectively. After 20 hrs at ambient temperature the original transition at $66\text{ }^\circ\text{C}$ partially reappeared in addition to the other two transitions.

The isotropic phase of **2** supercools by 12 K before crystallization.

POM observations of samples of **1** and **2** revealed practically no change in the appearance of the crystals at the solid-solid transitions.

Table 1. Transition temperatures ($^{\circ}\text{C}$) and enthalpies (kJ/mol in parentheses) for **1** and **2**.^a

1 $\mathcal{A} =$	2 $\mathcal{A} =$
Cr_1 109 Cr_2 363 I (dec) (21.6) (19.0)	Cr_1 66 Cr_2 209 I ^b (21.1) (10.9)

^a Cr-crystal, I-isotropic. ^b A second Cr-Cr transition at 86 $^{\circ}\text{C}$ (2.3 kJ/mol) was observed in aged sample.

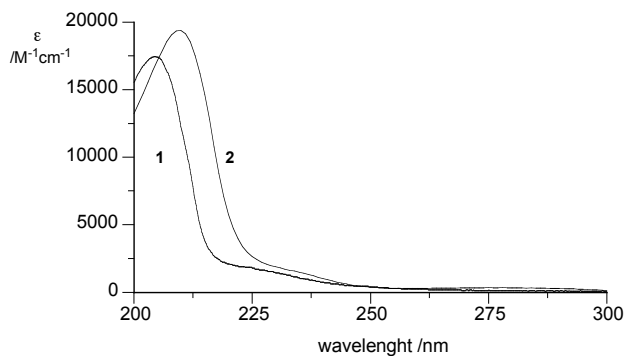


Figure 2. Electronic absorption spectra of **1** and **2** recorded in MeCN.

Electronic Absorption

Spectroscopic analysis demonstrated that both compounds are practically transparent above 250 nm (Figure 2). The quinuclidinium derivative **1** and the sulfonium **2** have high-energy absorption bands with the maximum at 204.5 nm and 210 nm, respectively, and with a shoulder feature at about 230 nm. The spectra recorded for **1** and **2** are similar to those obtained for [1-*closo*-CB₉H₉-1-NMe₃]³⁰ and [1-*closo*-CB₉H₉-1-SMe₂]³⁰ with the absorption bands shifted to lower energies (10 nm for **2**) presumably due to the presence of the alkyl group at the B(10) position.

Molecular and Crystal Structures

Colorless, triclinic crystals of **1** were grown from a toluene/*iso*-octane mixture by slow evaporation. The solid-state structure for **1** was determined by X-ray diffraction³² and pertinent interatomic dimensions are shown in Figure 3.

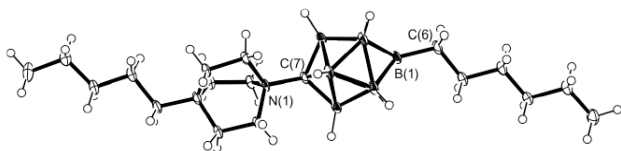


Figure 3. Thermal ellipsoid diagram representation of quinuclidinium **1** drawn at 50 % probability. Pertinent interatomic dimensions: C(7)–N(1) 1.505(2) Å, C(6)–B(1) 1.593(3) Å, avrg B–C(7) 1.619 Å, avrg B–B(1) 1.715 Å, C–N(1) avrg 1.525 Å. Quinuclidine cage twist avrg 18.8°.

Crystallographic analysis revealed that the unit cell is occupied by two identical molecules of **1** that are related through an inversion center. The separation between the long axes of the molecules in the unit cell is about 5.8 Å. In the crystal structure,

molecules of **1** form infinite sheets perpendicular to the *ab* plane with alternating antiparallel arrangement.

In a molecule of **1**, the C(7)–N(1) distance between the quinuclidine ring and {*closo*-1-CB₉} cage is 1.505(3) Å and the average B–C(7) distance is 1.619 Å. These distances are slightly longer by 0.007 Å and 0.011 Å, respectively, than those reported for the analogous trimethylamino derivative [1-*closo*-CB₉H₉-1-NMe₃].³³ Similar differences are observed in the pair of 1-quinuclidine and 1-NMe₃ derivatives of the {*closo*-1-CB₁₁} cluster.³⁴ The quinuclidine ring in **1** is twisted by an average value of 18.8°, which is larger than the average value of 8.3° found in a similar derivative of {*closo*-1-CB₁₁}.³⁴ This is presumably due to the shorter C_{cage}–N distance in the former than in the latter compound. The pyramidalization angle³⁵ α of the nitrogen atom in the quinuclidine ring is 21.2°, which is practically the same as in the quinuclidinium derivative of the {*closo*-1-CB₁₁}³⁴ and also in the quinuclidine–1-boraadamantane complex.³⁶

The dimensions of the {*closo*-1-CB₉} cage are similar to those reported for [1-*closo*-CB₉H₉-1-NMe₃].³³ Both alkyl groups are generally in all-*trans* conformations with dihedral angles little deviating from the ideal 180°. The largest deviation from planarity is observed for the pentyl group in which the angle defined by C _{α} –C _{β} –C _{γ} –C _{δ} is 166°. The two alkyl groups, the hexyl and the pentyl, deviate from the ideal staggered conformations with the {*closo*-1-CB₉} cage and quinuclidine ring by about 10° and 8°, respectively. Also, the orientation of the quinuclidine ring relative to the {*closo*-1-CB₉}

cage is about 6° off the ideal staggered conformation.

The angle between the two alkyl chain planes in **1**, as defined by $C_\alpha-C_\beta-C_\gamma$ in each chain, is 11° .

Computation of Molecular Properties

The experimental structure of **1** is well reproduced by the HF/6-31G(d) level calculations.³⁷ The quinuclidine and the {1-*closo*-CB₉} cage adopt a staggered conformation in the ground state (Figure 4), which is consistent with the solid state structure of [1-*closo*-CB₉H₉-1-Me₃N].³³ In contrast, in **1** the two rings are 8.6° away from the staggered conformation, presumably to minimize the inert-planar angle between the two alkyl chains.

The alkyl chains prefer pseudo-staggered conformations relative to the cage and the ring, which results in 22° angle between the alkyl group planes, each defined by the $C_\alpha-C_\beta-C_\gamma$ atoms, in the global conformational minimum of **1**. Similar conformational preferences are found in sulfonium **2**. The orientation of the pentyl chain is staggered with respect to the thiacyclohexane ring, which results in a wider interplanar angle between the alkyl chains (41°), and consequently less linear molecular shape than that of **1** in the global conformational minimum.

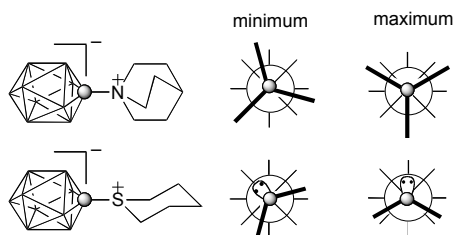


Figure 4. Extended Newman projection along the long molecular axes of **1** and **2** showing main conformations. The bars represent the substituent and the circle is the nitrogen or sulfur atom.

The HF level calculations demonstrated a substantial longitudinal dipole moment, $\mu_{||}$, exceeding 15 D for both molecules (Table 2). The transverse component of the dipole, μ_{\perp} , is small, which results in a nearly parallel orientation of the net molecular dipole along the long molecular axes ($\beta = 9^\circ$). The magnitude and, to some degree, orientation of the dipole moment in **1** and **2** depends on the strength of the dielectric medium. IPCM calculations revealed an approximately linear dependence of the dipole moment in **1** and **2** on ϵ of the medium in the range of $\epsilon = 1$ (vacuum) to $\epsilon = 4.6$.³⁷

Polarizability tensors α for **1** and **2** were obtained using the B3LYP method. Results shown in Table 2 demonstrate that polarizability α and its anisotropy, $\Delta\alpha$, calculated for both compounds are consistent with those for typical two-ring liquid crystalline compounds.³⁸

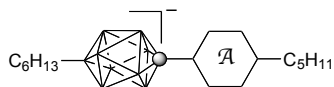
Binary Mixtures

Both zwitterions exhibited low solubility in nematic hosts containing a significant

fraction of aliphatic groups. Thus, mixtures with concentration of **1** >2.5 mol% in **5CB**, 1.8 mol% in **6-CHBT**, and 2.7 mol% in ZLI-1132 were not homogenous either in the isotropic phase or upon cooling to ambient temperature. Much greater solubility of **1** was observed in ester **CI Ester**,³⁹ and solutions up to 6 mol% were obtained. The solutions were apparently supersaturated, and after several weeks at ambient temperature some microcrystals of **1** were formed in solutions with concentration >2 mol%. The sulfonium derivative **2** exhibits greater solubility in organic solvents, and solutions up to nearly 10 mol% in **CI Ester** were obtained. This is consistent with the lower melting point of **2** as compared to **1**.

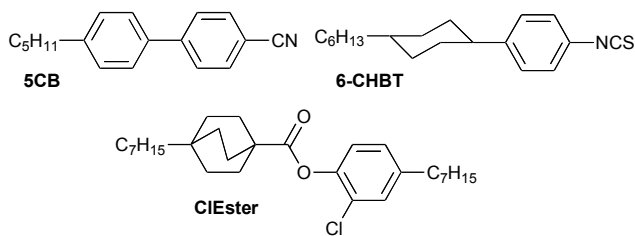
DSC analysis of the solutions in **CI Ester** demonstrated a linear increase of the clearing temperature T_{NI} with increasing concentration of **1** (Figure 5). Extrapolation of data in Figure 5 gave the virtual $[T_{NI}]$ for quinuclidinium **1** of 139 ± 1.3 °C. In contrast, solutions of sulfonium **2** in **CI Ester** exhibit a non-linear dependence of T_{NI} on concentration. The virtual temperature $[T_{NI}]$ calculated for **2** using the 9.5 mol% data point is 92 °C, which is nearly 50 K lower than $[T_{NI}]$ for **1**.

Table 2. Calculated molecular parameters for **1** and **2**.^a



A	1	2
$\mu_{ } / \text{D}$	15.9	15.3
μ_{\perp} / D	2.9	2.6
μ / D	16.1	15.5
$\beta / ^{\circ}{}^b$	9	9
$\Delta\alpha / \text{\AA}^3$	25.1	25.8
$\alpha_{\text{avrg}} / \text{\AA}^3$	44.3	44.8

^a Vacuum dipole moments obtained with the HF/6-31G(d) method and electronic polarizabilities at the B3LYP/3-21G level of theory. ^b Angle between the net dipole vector μ and $\mu_{||}$. For details see the electronic supporting information.



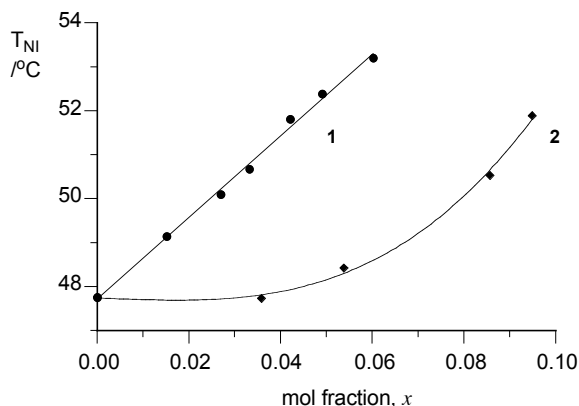


Figure 5. A plot of peak temperature of the N-I transition for binary mixtures of quinuclidinium **1** (circles) and sulfonium **2** (diamonds) in **ClEster**. Best fit line for **1**: $T_{NI} = 90.8(\pm 1.3)x + 47.8$

Dielectric Measurements

The addition of small amounts of the zwitterion **1** or **2** to the **ClEster** host possessing small negative dielectric anisotropy ($\Delta\epsilon = -0.59$) dramatically changed its dielectric properties (Figure 6). The parallel component of dielectric permittivity, $\epsilon_{||}$, of the material significantly increased, while the perpendicular component, ϵ_{\perp} , was little affected by the additive (Figure 6). In consequence, $\Delta\epsilon$ increased and the negative $\Delta\epsilon$ host was transformed to a positive $\Delta\epsilon$ material. The observed effect on material's dielectric properties is consistent with the magnitude and orientation of the molecular dipole moment in the additive, and indicated good alignment in the nematic host. In addition, temperature dependence studies of dielectric parameters of one of the solutions demonstrated no anomalous behavior in the temperature range of the nematic phase (Figure 6). Thus, the results indicate that both zwitterions **1** and **2** are compatible with the

nematic host.

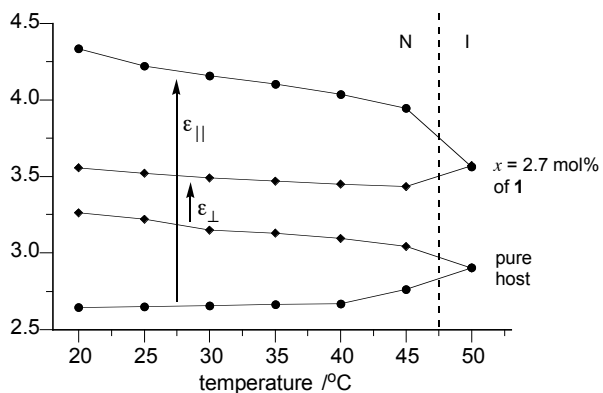


Figure 6. Dielectric permittivity tensors ($\epsilon_{||}$ circles and ϵ_{\perp} diamonds) for the host, **CI Ester**, and 2.7 mol% solution of **1** as a function of temperature. Estimated standard deviation for $\epsilon_{||}$ and ϵ_{\perp} is 0.1.

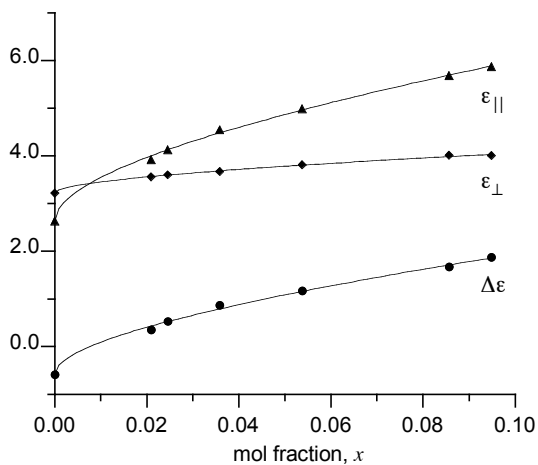


Figure 7. Plot of $\epsilon_{||}$ (triangles), ϵ_{\perp} (diamonds), and $\Delta\epsilon$ (circles) vs. concentration of **2** in **CI Ester** at 25 °C.

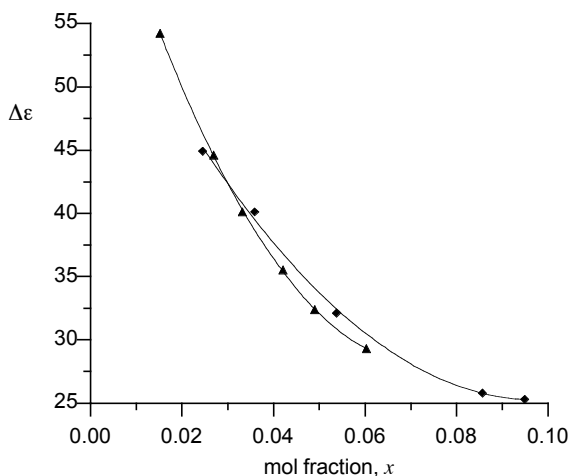


Figure 8. Plot of extrapolated $\Delta\epsilon$ vs. concentration of **1** (triangles) and **2** (diamonds) in **ClEster** fitted to a second order polynomial.

A plot of dielectric permittivity parameters measured for each solution at ambient temperature showed a non-linear dependence on concentration of the zwitterion (Figure 7). This suggests a change of nature of the additive caused e.g. by aggregation.

Using equation 1, which reflects additive properties of dielectric permittivity, dielectric anisotropy $\Delta\epsilon$ of the pure zwitterion can be calculated for each individual concentration of **1** and **2** in **ClEster**. The resulting extrapolated $\Delta\epsilon$ values were fitted to a second-order polynomial⁴⁰ and the curves for quinuclidinium **1** and sulfonium **2** are shown in Figure 8. Extrapolation to infinite dilution ($x \rightarrow 0$) yielded $\Delta\epsilon$ value of 70 ± 1 for **1** and 61 ± 2 for **2**. Similar analysis for the ϵ_{\parallel} component gave 88 ± 1 and 84 ± 1 for **1** and **2**, respectively.³⁷

Dielectric Data Analysis

Extrapolated dielectric data for **1** and **2** were analyzed quantitatively using the Maier-Meier equation,⁴¹ which relates bulk parameters of the nematic phase, dielectric anisotropy $\Delta\varepsilon$ and order parameter S , with molecular parameters, dipole moment μ and polarizability α (equation 2).⁴²

Considering the Maier-Meier relationship (equation 2) and results of dielectric measurements (*vide supra*), extrapolated dielectric parameters for the zwitterions depend on the Kirkwood factor⁴³ g (equation 3), apparent order parameter⁴⁴ S_{app} , temperature T , and concentration c . For $T = constant$ and at a given concentration c of the additive, dielectric parameters $\varepsilon_{||}$, ε_{\perp} , and $\Delta\varepsilon$ depend on g and S_{app} . The two unknowns, S_{app} and g , were found for **1** and **2** by solving simultaneously the Maier-Meier expressions for $\varepsilon_{||}$ and ε_{\perp} .³⁷

$$\Delta\varepsilon = \sum_i x_i \Delta\varepsilon_i \quad \text{Eq 1}$$

$$\Delta\varepsilon = \frac{NFh}{\varepsilon_0} \left\{ \Delta\alpha - \frac{F\mu_{eff}^2}{2k_B T} (1 - 3 \cos^2 \beta) \right\} S \quad \text{Eq 2}$$

$$\mu_{eff}^2 = g\mu^2 = \left(\frac{c-a}{c} \right) \mu^2 \quad \text{Eq 3}$$

$$K = \frac{[M_2]}{[M]} = \frac{a}{2(c-a)^2} \quad \text{Eq 4}$$

$$a = \frac{4Kc + 1 - \sqrt{8Kc + 1}}{4K} \quad \text{Eq 5}$$

$$g = \frac{\sqrt{8Kc + 1} - 1}{4Kc} \quad \text{Eq 6}$$

Initially, the medium was assumed to be the pure host, and the effect of the additive on dielectric properties of the solution was ignored. Analysis using dipole moments obtained in vacuum ($\epsilon = 1$) gave practically constant order parameter $S_{app} = 0.63 \pm 0.01$ for **1** and $S_{app} = 0.50 \pm 0.01$ for **2** in the entire range of concentrations. The Kirkwood factor g was diminishing in a nonlinear mode from 0.38 to 0.21 for **1** and from 0.42 to 0.24 for **2** with increasing concentration of the additive. When larger dipole moments calculated for the dielectric medium of the host ($\epsilon = 3.03$) were used for the analysis, the order parameters remained the same, while the g factors were smaller by about 20% for both additives. A plot of resulting g values is shown in Figure 9.³⁷

For comparison purposes dielectric parameters of the additives were calculated for ideal compatibility with ($S_{app} = S_{host} = 0.66$) and solubility ($g = 1$) in the host. The resulting dielectric values $\epsilon_{||}$ and $\Delta\epsilon$ for the pure zwitterions in **ClEster** are 178 and 147, respectively, for quinuclidinium **1**, and 170 and 140 for sulfonium **2**. Calculations of S_{app} and g using dielectric parameters extrapolated to infinite dilution ($x = 0$, Figure 8) gave 0.62 and 0.50, respectively for **1** and 0.52 and 0.55 for **2**. The results indicate that the calculated dipole moments μ are overestimated by the HF computational method by about 30%.⁴⁵

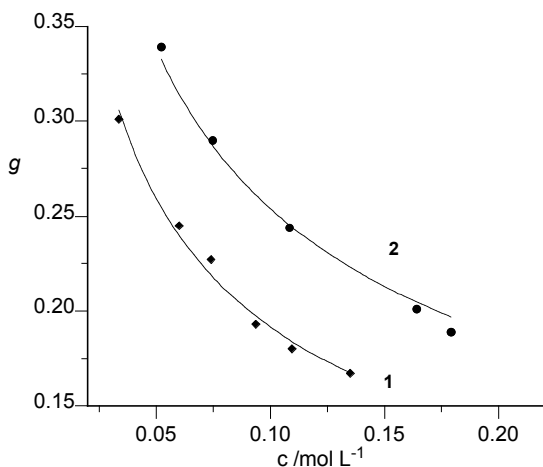


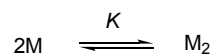
Figure 9. A plot of calculated Kirkwood parameter g for **1** (diamonds) and **2** (circles) vs concentration c . Dipole calculated at $\epsilon = 3.03$ (model 2). Fitting function shown as equation 6.

Since the zwitterions significantly increase dielectric permittivity of the solutions, their dipole moments may vary with concentration. Also the reaction field parameters h and F (equation 2; see the electronic supporting information) change appropriately with the increasing dielectric strength of the solution. Calculations using adjusted dipole moment of the additive and constant reaction field parameters demonstrated a drop in the value of the Kirkwood factor by about 10%. When all three parameters, μ , h , and F , were treated as a function of ϵ , the Kirkwood factor was smaller by an additional 5%. While the adjustments of these parameters affected the g factor, the apparent order parameter S_{app} for each zwitterion was practically unchanged.

The calculated small value of the Kirkwood factor demonstrates that a significant fraction of the zwitterions exists as aggregates, and the changing values of g indicate that

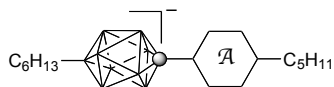
the degree of aggregation increases with the increasing concentration of the additive. The observed aggregation of the zwitterion molecules M in dilute solutions can be approximated with a simple model of dimerization shown in Scheme 3.

Scheme 3



Assuming that the dimer M_2 has no dipole moment, $\mu = 0$, the dielectric data can be used to calculate the constant K for the monomer-dimer equilibrium process shown in Scheme 3. At equilibrium, the concentration of the dimer M_2 is $0.5a$ and the monomer is $c-a$, where c is the concentration of the zwitterion in **CI Ester** solution expressed in mol/L. This leads to equation 4 for K , which is transformed to the expression for a (equation 5). The effective dipole moment μ_{eff}^2 is related to the dipole moment μ^2 by the Kirkwood factor g , which can be expressed as a fraction of monomeric molecules (equation 3). Substitution of equation 5 into equation 3 and solving for g leads to equation 6, in which g is a function of concentration c and K is the association constant.

Table 3. Association constant K for **1** and **2**.^a



model	Parameters	$K / L mol^{-1}$	
		1	2
1	μ for $\epsilon = 1$	63 ± 2	37 ± 1
2	μ for $\epsilon = 3.03$	110 ± 2.5	58 ± 1
3	μ for variable ϵ	122 ± 3	68 ± 3
4	μ , h , and F for variable ϵ	145 ± 5	89 ± 6

^a See text for details

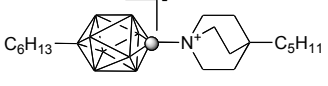
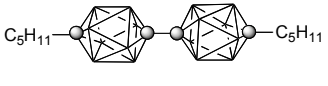
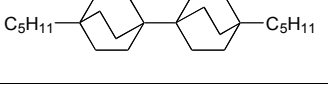
Fitting the Kirkwood factors g obtained for values of μ calculated in vacuum (model 1 in Table 3) to the single parameter function (equation 6) gives the association constant K of 63 L/mol for quinuclidinium **1** and about a 40% smaller value, 37 L/mol, for the sulfonium **2**. For the g values calculated for the dielectric strength of the host (model 2, Table 3), the association constant K values are 75% and 57% bigger, respectively, due to larger calculated dipole moments for **1** and **2**. The constant K increased further when g was derived from adjustable dipole moments (model 3), and the largest, 145 L/mol and 89 L/mol for **1** and **2**, respectively, for g calculated with adjustable dipoles and reaction field parameters (model 4). Incidentally, the correlation factors for fitting data derived from adjustable parameters (models 3 and 4) to equation 6 are

progressively worse than those for the fixed value of dipole moment values (models 1 and 2). This is reflected in higher uncertainty of the K values obtained in the former models as compared to those in models 1 and 2.

Discussion

The structure of the $\{closo-1-CB_9\}$ cluster permits the design of anisometric molecules characterized by high compatibility with the nematic phase. This is evident from the high virtual clearing points, $[T_{NI}] > 90$ °C, and high apparent order parameters, $S_{app} > 0.5$, for both additives in **CI Ester** host. The $[T_{NI}]$ for quinuclidinium **1** (139 °C) is higher by nearly 50 K than the $[T_{NI}]$ of sulfonium **2**, and favorably compares to $[T_{NI}]$ values for similar, non-polar two-ring compounds **11** and **12** measured in a different host (Table 4).⁴⁶ Interestingly, the $[T_{NI}]$ for **1** is close to an average of the $[T_{NI}]$ values for the two analogues **11** and **12**. Considering the difference in the alkyl chain length and that the measurements were performed in different hosts, the result indicates a rather modest effect of high dipole moment on phase stability.

Table 4. N-I transition temperatures for selected compounds.

Compound		$[T_{NI}]_a$ /°C	T_{NI} /°C
1		138 ^b	^c
11		75 ^d	98 ^d
12		171 ^d	^e

^a Virtual N-I transition temperature. ^b Determined in **CI Ester** host. This work. ^c Not observed. ^d Ref⁴⁶. ^e Sm-I transition at 244 °C; ref⁴⁶.

The observed difference of 47 K in $[T_{NI}]$ values for the two zwitterions **1** and **2** is consistent with poorer alignment of molecules of the latter with the nematic director of the host than those of quinuclidinium **1**. Experimental results demonstrate that **1** aligns well with the host since the apparent order parameter, $S_{app} = 0.63$, is similar to that of the pure host ($S = 0.66$).³⁸ In contrast, the S_{app} value for sulfonium **2** is markedly lower (0.50).

The difference in behavior of the two zwitterions in a nematic phase is related, in part, to their conformational properties and the ability to adopt a co-planar orientation of the terminal alkyl chains. For the quinuclidinium **1** the two alkyl chains are 23° off co-planarity, while for the sulfonium **2** the inter-planar angle is nearly twice larger, according to *ab initio* modeling. The quinuclidinium **1** can, however, adopt even more

favorable configuration (11° inter-planar angle in the solid state) apparently without much thermodynamic penalty, as evident from the XRD analysis. Presumably, this greater conformational flexibility contributed to the higher $[T_{NI}]$ value of **1**. The high inter-planar angle calculated for **2** (43°) is similar to that calculated and observed experimentally⁴⁷ for alkyl derivatives of 10-vertex carborane derivative, such as **11** in Table 4, which is a consequence of the cage symmetry.^{21,47} It is presumably for this reason that binary mixtures involving many 10-vertex *closo*-borane derivatives, including **2** (Figure 5), exhibit a non-linear concentration dependence of T_{NI} for low mole fractions.^{46,48,49}

Besides the unfavorable orientation of the terminal alkyl groups in the conformational ground state of **2**, epimerization at the sulfur center in **2** and the formation of the *cis* isomer (**2-cis**, Figure 10) may also contribute to the low dynamic anisometry of the molecule, and, consequently, lower $[T_{NI}]$ value as compared to **1**. Such epimerization and *cis/trans* equilibrium shown for **2** in Figure 10 is anticipated on the basis of our findings for another 10-vertex cluster derivative.⁵⁰

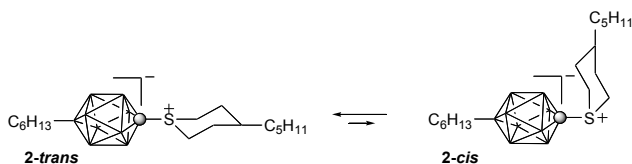


Figure 10. The *trans* and *cis* isomers of **2**.

Both compounds **1** and **2** have significant dipole moments oriented along the long molecular axis. This, considering their good alignment with the nematic director, renders both compounds as highly effective positive $\Delta\epsilon$ additives. For instant, 1 mol% concentration of the zwitterion increases $\Delta\epsilon$ of the **CI Ester** host by about +0.60 for **1** and +0.54 for **2**. Unfortunately, both compounds have rather low solubility in typical nematic hosts, and their possible applications in electrooptical devices will require structural modifications. Analysis of the two zwitterions demonstrates that lowering symmetry of **1** to that of **2** decreases the melting point by about 150 K, increases solubility by nearly 2 fold, and also lowers tendency to association (lower K value). Thus, further dissymmetrization of **2**, by e.g. modifying the alkyl chains, is expected to improve the solubility without significant compromising its effectiveness as a high $\Delta\epsilon$ additive.

The Maier-Meier analysis provides a convenient method for quantitative understanding of the behavior of the additives in solutions. As we already demonstrated for other binary mixtures,^{26,51} the calculated apparent order parameter S_{app} indicates the degree of alignment of the additive with the nematic director, and hence its steric compatibility with the host. In previous analyses,^{26,51} the dielectric parameters were changing linearly with the concentration of the additive giving a constant value of the Kirkwood factor g . The non-linear behavior of the dielectric data for solutions of **1** and **2**, and consequently variable Kirkwood factor g , indicate aggregation of the solute, which is expected for highly polar compounds in weakly polar media. Unlike in previous studies, the effect of **1** and **2** on dielectric properties of the solution is substantial and proper

analysis of the data may require inclusion of the dielectric effect of the additive on μ and reaction field parameters h and F . As the calculated dipole increases in the higher dielectric strength medium, the additives are more associated and smaller Kirkwood factors g are obtained.

Further analysis demonstrated that for hypothetical ideal solutions of **1** and **2** in **CI Ester** (high order parameter, $S_{app} = S_{host}$, and no aggregation, $g = 1$) the dielectric parameters of the pure additives are about twice of those extrapolated to infinite dilution ($x \rightarrow 0$) from the real solutions. This is in part due to the lower S_{app} of the additives and in part to apparent overestimation of the dipole moment at the HF level of theory.⁴⁵ Assuming that the extrapolated dielectric values are reliable, the actual dipole moment of **1** and **2** is about 11 D.

Since the Kirkwood factor g derived from the Maier-Meier equation is related to the fraction of non-associated molecules, it can be used to calculate association constant K for a simple dimerization process. The actual molecular process leading to lowering the effective dipole moment is presumably more complex; it may involve larger number of molecules in the aggregates and incomplete compensation of the dipole moment especially at higher concentrations.⁵² Nevertheless, such a simplistic treatment of the molecular association provides a convenient and quantitative description of non-linear dielectric systems such as solutions of **1** and **2** in **CI Ester**. Moreover, the calculated association constant K offers a means for quantitative comparison of different highly polar additives. Out of the four models of treatment of the molecular dipole moment of

the additive (Table 3), the most complete, but also most expensive computationally, appears to be model 4 in which all three parameters, μ , h and F , are function of the additive's concentration. However, for practical purpose of comparing behavior of various polar additives, the simplest model involving molecular dipole moment calculated in vacuum is appropriate.

Summary and Conclusions

Synthetic access to a new class of highly effective, low concentration, positive dielectric anisotropy additives to nematic materials has been developed. The first two examples, zwitterions **1** and **2**, have been prepared and characterized in a nematic host. Solution dielectric data was analyzed with the aid of the Maier-Meier relationship and quantum-mechanical calculations, which provided a convenient protocol for the quantitative understanding of the behavior of polar additives in solutions and for the comparison of their properties. Data indicates that quinuclidinium **1** exhibits higher compatibility with the nematic phase (higher apparent order parameter S_{app} and higher $[T_{NI}]$) than the sulfonium **2**. However, the sulfonium **2** is more soluble and has a markedly lower association constant K .

Further tailoring of the properties of this class of zwitterions for practical applications will involve structural modification of **1** and **2** to increase their solubility.

Computational Details

Quantum-mechanical calculations were carried out using Gaussian 98⁵³ suite of programs. Geometry optimizations for unconstrained conformers of **1** and **2** with the most extended molecular shapes were undertaken at the HF/6-31G(d) and B3LYP/3-21G levels of theory using default convergence limits. Dipole moments of **1** and **2** for analysis with the Maier-Meier theory were obtained using the HF/6-31G(d) method, and exact electronic polarizabilities were calculated at the B3LYP/3-21G level of theory. The latter are considered to be underestimated by about 10%. Dipole moment components μ and polarizability tensors α were calculated in Gaussian standard orientation of each molecule (charge based), which is close to the principal moment of inertia coordinates (mass based). The IPCM solvation model⁵⁴ was used with default parameters to obtain molecular dipole moment components for dielectric strength ϵ of the medium: 2.84, 3.03, 4.00, and 4.62. The resulting linear dependence $\mu(\epsilon)$ was used to calculate molecular dipole moments of the additive for each solution.

Experimental Section

Binary Mixtures Preparation. Solutions of **1** or **2** in host **ClEster** (~10 mg) were prepared in an open vial with agitation using a closed-end capillary tube with moderate heating supplied by a heat gun. The binary mixtures were analyzed by polarized optical microscopy (POM) to ensure that the mixtures were homogeneous. The mixtures were

then allowed to condition for 3 hr at room temperature. The clearing temperature of each homogeneous mixture was determined by DSC at the peak of the transition.

Electrooptical Measurements. Dielectric properties of solutions of zwitterions **1** and **2** in **CI Ester** were measured by a Liquid Crystal Analytical System (LCAS - Series II, LC Analytical Inc.) using GLCAS software version 0.951, which implements literature procedures for dielectric constants.⁵⁵ The homogeneous binary mixtures were loaded into ITO electrooptical cells by capillary forces with moderate heating supplied by a heat gun. The cells (about 4 μm thick, electrode area of 0.581 cm^2 and anti-parallel rubbed polyimide layer 2°–3° pretilt) were obtained from LCA Inc., and their precise thickness (± 0.05 μm) was measured by LCAS using the capacitance method before the cells were filled. The filled cells were heated to an isotropic phase and were cooled to room temperature before measuring the dielectric properties. Default parameters were used for measurements: triangular shaped voltage bias ranging from 0.1–20 V at 1 kHz frequency. The threshold voltage V_{th} was measured at a 10% change. For each mixture, the measurement was repeated seven times for two cells. The first two measurements for each cell were discarded as conditioning measurements, and the remaining total ten results were averaged to calculate the mixture's parameters. Dielectric parameters of the pure host **CI Ester** were measured in similar cells in which the electrode area (0.28 cm^2) was covered with a surfactant to impose a homeotropic alignment.

Synthetic and Characterization Details

Reagents and solvents were obtained commercially. Solvents were dried and deoxygenated before use, and reagents were used as supplied. ZnCl_2 was dried by heating at ~ 100 °C under vacuum. The concentration of Grignard or organozinc reagents were determined by I_2 titration.⁵⁶ Reactions were carried out under dry Ar, subsequent manipulations conducted in air.

NMR spectra were obtained at 128.4 MHz (^{11}B) and 400.1 MHz (^1H) in CD_3CN or CDCl_3 unless otherwise specified. ^1H NMR spectra were referenced to CD_3CN (1.93 ppm) or CDCl_3 (7.24 ppm). ^{11}B NMR chemical shifts are relative to the resonance of an external boric acid sample in CH_3OH that was set to 18.1 ppm. IR spectra were recorded in the solid state using an AT-IR accessory. Elemental analysis was provided by Atlantic Microlab, GA.

Thermal analysis was obtained using a TA Instruments 2920 differential scanning calorimeter (DSC). Transition temperatures (onset) and enthalpies were obtained using small samples (0.3-0.6 mg) and a heating rate of 5 K min^{-1} under a flow of nitrogen gas.

UV spectra were recorded in UV-grade CH_3CN . All compounds were in concentration of $0.4\text{--}4 \times 10^{-5}$ M. Extinction coefficients were obtained by fitting the maximum absorbance against concentration in agreement with Beer's law.

Preparation of [*closo*-1-CB₉H₈-1-NC₁₂H₂₃-10-C₆H₁₃] (1)

A mixture of [*closo*-1-CB₉H₈-1-NH₂-10-C₆H₁₃]⁻ NMe₄⁺ (**4**[NMe₄], 0.190 g, 0.65 mmol), 3,3-bis(2-bromoethyl)-1-bromooctane²⁹ (**9**, 0.26 g, 0.65 mmol), 18-crown-6 (0.011 g, 0.042 mmol), and anhydrous K₂CO₃ (0.248 g, 1.79 mmol) were refluxed in anhydrous CH₃CN (20 mL) under inert atmosphere for 9 days. The reaction mixture was filtered, washed with CH₂Cl₂, and solvents removed giving a semi-crystalline yellow-brown solid. The solid was passed through a short silica-gel plug (CH₂Cl₂) giving 0.270 g of crude product, which was washed with iso-octane and cold CH₃OH giving 0.130 g of a white residue. The white residue was further purified via column chromatography (hexanes/CH₂Cl₂, 1:2) giving 0.080 g (33% yield) of [*closo*-1-CB₉H₈-1-NC₁₂H₂₃-10-C₆H₁₃] (**1**) as a white crystalline solid. The final product was further purified by recrystallization (iso-octane/toluene mixture): mp 363 °C dec (DSC); ¹H NMR (CDCl₃) δ 0.40-2.80 (br m, 8H), 0.80-1.00 (m, 6H), 1.12-1.50 (m, 10H), 1.52-1.70 (m, 4H), 1.81-1.95 (m, 2H) 2.01-2.15 (m, 8H), 4.10-4.30 (m, 6H); ¹¹B NMR (CDCl₃) δ -26.4 (d, *J* = 141 Hz, 4B), -18.5 (d, *J* = 110 Hz, 4B), 46.4 (s, 1B). Anal. Calcd. for C₁₉H₄₄B₉N: C, 59.45; H, 11.55; N, 3.65. Found: C, 59.57; H, 11.65; N, 3.78.

Preparation of [*closo*-1-CB₉H₈-1-SC₁₀H₂₀-10-C₆H₁₃] (2)

To a three-necked flask under inert atmosphere attached with reflux condenser, a glass stopcock, and septum containing Pd₂dba₃ (5 mg, 0.005 mmol) and [HPCy₃]₃BF₄ (8 mg, 0.022 mmol) was added an anhydrous NMP/THF mixture (6 mL, 1:2). A solution

$C_6H_{13}ZnCl$ (3 mL, 2.14 mmol, 0.712 M) [prepared from $C_6H_{13}MgBr$ (3 mL, 2.14 mmol, 0.712 M) and anhydrous $ZnCl_2$ (0.300 g, 2.20 mmol)] was added resulting in the formation of a yellow/orange suspension that slowly turned green. [*closo*-1- CB_9H_8 -1- $SC_{10}H_{20}$ -10-I] (**10**, 0.114 g, 0.274 mmol) dissolved in anhydrous THF (2 mL) was added via syringe, the septum replaced with a glass stopcock, and the reaction was stirred at 85 °C. Reaction progress was monitored at 24 hr intervals by ^{11}B NMR analysis. If the reaction was incomplete, additional equivalents of Pd_2dba_3 , $[HPCy_3]BF_4$, and $C_6H_{13}ZnCl$ were added and stirring continued at 85 °C. After 72 hr, the reaction was quenched with a saturated solution of NH_4Cl (10 mL), extracted into Et_2O (3 x 5 mL), dried (Na_2SO_4) and evaporated. NMP was removed via vacuum distillation (0.5 mm Hg, 50 °C) giving 0.212 g of crude product. The crude product was purified via column chromatography (CH_2Cl_2 /hexane, 1:1) giving 0.060 g (58% yield) of [*closo*-1- CB_9H_8 -1- $SC_{10}H_{20}$ -10- C_6H_{13}] (**2**) as a yellowish solid. The final product was further purified by washing with hot hexane and recrystallization (toluene/iso-octane mixture): mp 209 °C (DSC); 1H NMR ($CDCl_3$) δ 0.40-2.80 (br m, 8H), 0.92 (t, $J = 6.5$ Hz, 6H), 1.33-1.40 (m, 13H), 1.51-1.63 (m, 2H), 1.62-1.80 (m, 2H), 1.85-1.95 (m, 2H), 2.05-2.14 (m, 2H), 2.50 (br d, $J = 11.6$ Hz, 2H), 3.60-3.72 (m, 2H), 4.07 (br d, $J = 11.7$ Hz, 2H); ^{11}B NMR ($CDCl_3$) δ -24.5 (d, $J = 146$ Hz, 4B), -16.2 (d, $J = 149$ Hz, 4B), 54.1 (s, 1B). Anal. Calcd. for $C_{17}H_{41}B_9S$: C, 54.47; H, 11.02. Found: C, 54.69; H, 11.17.

Preparation of [*closo*-1- CB_9H_8 -1- NH_2 -10- C_6H_{13}] $^-$ NMe_4^+ (**4**[NMe_4])

To a three-necked flask under inert atmosphere attached with reflux condenser, a

glass stopcock, and septum containing iodo amine [*closo*-1-CB₉H₈-1-NH₂-10-I]⁻ NMe₃⁺ (**3**[NMe₃], 0.635 g, 1.98 mmol) [¹¹B NMR (CD₃CN) δ -22.0 (d, *J* = 144 Hz, 4B), -16.3 (d, *J* = 157 Hz, 4B), 10.8 (1B)] dissolved in anhydrous THF (20 mL) was added C₆H₁₃MgBr (9.9 mL, 19.8 mmol, 2.0 M). A bubbler was attached, and the reaction mixture was heated at reflux for 30 min. (PPh₃)₂PdCl₂ (0.186 g, 0.26 mmol) and CuI (0.075 g, 0.393 mmol) were added, and the reaction was stirred at reflux, and reaction progress was monitored by ¹¹B NMR at 24 hr intervals. If the reaction was incomplete, additional equivalents of C₆H₁₃MgBr, (PPh₃)₂PdCl₂, and CuI were added and heating continued. A 5% HCl solution (200 mL) was added, and the reaction mixture was extracted with Et₂O (3 x 50 mL). The organic layers were combined, dried (Na₂SO₄), filtered, and evaporated giving 1.60 g of an oily brown residue. The residue was purified by column chromatography (CH₃CN/CH₂Cl₂, 1:4) giving 0.140 g of crude acid extract [*closo*-1-CB₉H₈-1-NH₂-10-C₆H₁₃]⁻ H₃O⁺ [¹¹B {¹H} NMR (CD₃CN) δ -26.5 (4B), -18.1 (4B), 39.4 (1B)]. Water (5 mL) and NMe₄⁺ OH⁻ · 5H₂O (0.109 g, 0.60 mmol) were added producing a milky suspension. Solvents were removed to dryness *in vacuo* giving 0.190 g (33% yield) of [*closo*-1-CB₉H₈-1-NH₂-10-C₆H₁₃]⁻ NMe₄⁺ (**4**[NMe₄]) as a colorless film that slowly crystallized: ¹H NMR (CD₃CN) δ 0.40-2.80 (br m, 8H), 0.91 (t, *J* = 7.0 Hz, 3H), 1.30-1.40 (m, 4H), 1.45-1.59 (m, 2H), 1.73-1.83 (m, 4H), 3.08 (s, 12H); ¹¹B {¹H} NMR δ -26.5 (4B), -18.2 (4B), 36.2 (1B); MS (FAB): *m/z* (216-220) max at 219 (100 %); FAB-HRMS(-): Calcd. for C₈H₂₂B₉O₂ *m/z*: 220.2668; found; 220.2670.

Identification of [*closo*-1-CB₉H₈-1-NH₂-10-PPh₃] (**5**).

Crude phosphonium adduct **5** (158 mg, 20% yield) of was isolated by column chromatography (CH₃CN/CH₂Cl₂, 1:9) during the purification of amine **4** as a slight yellow residue. An analytical sample was prepared by washing crude **5** with hot hexane, hot ethanol, and then recrystallized (cold toluene/CH₃CN mixture): mp 300 °C (DSC); ¹H NMR (CD₃CN) δ 7.57-7.65 (m, 6H), 7.69-7.76 (m, 3H), 7.78-7.88 (m, 6H); ¹¹B NMR (CD₃CN) δ -20.6 (d, *J* = 144 Hz, 4B), -14.5 (d, *J* = 154 Hz, 4B), 15.6 (d, *J* = 196 Hz, 1B); ³¹P NMR (CD₃CN) δ 9.7 (q, *J* = 196 Hz); MS (FAB): *m/z* 393-398 (max at 396, 100%); FAB-HRMS(+): Calcd. for C₁₉H₂₅B₉NP *m/z*: 397.2562; found; 397.2542. Anal. Calcd. for C₁₉H₂₅B₉NP: C, 57.67; H, 6.37; N, 3.54. Found: C, 56.87; H, 6.19; N, 3.33.

Preparation of [*closo*-1-CB₉H₈-1-SCHN(Me)₂-10-I] (**8**)

A yellow solution of [*closo*-1-CB₉H₈-1-N₂-10-I]²⁸ (**7**, 0.200 g, 0.74 mmol) and freshly distilled Me₂NCHS (3.0 mL) was stirred at rt for 6 hr. Excess Me₂NCHS was removed by vacuum distillation (80 °C, 0.25 mm Hg) leaving 0.296 g of crude product as a slight yellow oil that slowly crystallized. The crude product was washed with toluene until the decant was no longer yellow giving 0.245 g (100% yield) of crude [*closo*-1-CB₉H₉-1-SCHN(Me)₂-10-I] (**8**) as yellowish solid: ¹H NMR (CD₃CN) (major signals) δ 3.46 (s, 3H), 3.65 (s, 3H), 9.74 (s, 1H), (minor signals attributed to Me₂NCHS) δ 3.19 (s, 3H), 3.25 (s, 3H), 9.14 (s, 1H); ¹¹B NMR (CD₃CN) δ -19.6 (d, *J* = 146 Hz, 4B), -13.9 (d, *J* = 156 Hz, 4B), 20.0 (s, 1B); MS (FAB): *m/z* (331-335) max at 333 (100 %); FAB-

HRMS(+): Calcd. for C₄H₁₄B₉INS *m/z*: 334.0729; found; 334.0731.

Preparation of [*closo*-1-CB₉H₈-1-SC₁₀H₂₀-10-I] (10)

A yellow solution of crude [*closo*-1-CB₉H₈-1-SCHN(Me)₂-10-I] (**8**, 0.245 g, 0.74 mmol), NMe₄⁺ OH⁻ · 5H₂O (0.145 g, 0.80 mmol), and 1-bromo-3-(2-bromoethyl)octane (0.220 g, 0.74 mmol) in anhydrous CH₃CN (5 mL) was stirred at rt for 12 hr. The reaction mixture was filtered and evaporated to dryness. The resulting residue was washed with hexane giving 0.43 g of crude product. The crude product was passed through a short silica gel plug (CH₂Cl₂/hexane, 1:1) giving 0.120 g (39% yield based on **7**) of [*closo*-1-CB₉H₈-1-SC₁₀H₂₀-10-I] (**10**) as the fast-moving component, which was further purified by recrystallization (toluene/iso-octane mixture): mp 230 °C; ¹H NMR (CD₃CN) δ 0.40-2.80 (br m, 8H), 0.90 (t, *J* = 6.9 Hz, 3H), 1.31-1.35 (m, 8H), 1.71-1.76 (m, 3H), 2.41 (m, 2H), 3.66 (t, *J* = 11.8 Hz, 2H), 4.13 (d, *J* = 11.1 Hz, 2H); ¹¹B NMR (CD₃CN) δ -19.8 (d, *J* = 152 Hz, 4B), -15.0 (d, *J* = 164 Hz, 4B), 23.2 (s, 1B). Anal. Calcd. for C₁₁H₂₈B₉IS: C, 31.71; H, 6.77. Found: C, 31.69; H, 6.86.

Acknowledgments

Financial support for this work was received from the National Science Foundation (DMR-0606317). XRD results were obtained using ChemMatCARS Sector 15, which is principally supported by the NSF/DoE under grant number CHE-0535644, the Advanced Photon Source, which is supported by the U. S. Department of Energy,

Office of Science, Office of Basic Energy Sciences, under Contract No. DE-AC02-06CH11357. We thank Prof. R. Dabrowski for his generous gift of **CI Ester**.

References

- (1) Sage, I. C. In *Handbook of Liquid Crystals*; Demus, D., Goodby, J. W., Gray, G. W., Spiess, H.-W., Vill, V., Eds.; Wiley-VCH: New York, 1998; Vol. 1, p 731-762.
- (2) Kirsch, P.; Bremer, M. *Angew. Chem., Int. Ed.* **2000**, *39*, 4216-4235.
- (3) Fréedericksz, V.; Zolina, V. *Trans. Faraday. Soc.* **1933**, *29*, 919-930.
- (4) Blinov, L. M.; Chigrinov, V. G. *Electrooptic Effects in Liquid Crystal Materials*; Springer-Verlag: New York, 1994.
- (5) Blinov, L. M. In *Handbook of Liquid Crystals*; Demus, D., Goodby, J. W., Gray, G. W., Spiess, H.-W., Vill, V., Eds.; Wiley-VCH: New York, 1998; Vol. 1, p 477-534.
- (6) For example: Gray, G. W.; Harrison, K. J.; Nash, J. A. *Electron. Lett.* **1973**, *9*, 130-131; Eidenschink, R.; Erdmann, D.; Krause, J.; Pohl, L. *Angew. Chem., Int. Ed. Engl.* **1977**, *16*, 100.
- (7) Dabrowski, R.; Dziaduszek, J.; Szczucinski, T. *Mol. Cryst. Liq. Cryst.* **1984**, *102*, 155-160; Dabrowski, R.; Dziaduszek, J.; Szczucinski, T. *Mol. Cryst. Liq. Cryst.* **1985**, *124*, 241-257; Dabrowski, R.; Dziaduszek, J.; Drzewinski, W.; Czuprynski, K.; Stolarz, Z. *Mol. Cryst. Liq. Cryst.* **1990**, *191*, 171-176.
- (8) For example: Zaszke, H. *J. Prakt. Chem.* **1975**, *317*, 617-630; Kraus, G.;

Zaschke, H. J. *Prakt. Chem.* **1981**, 323, 199-206.

(9) Vorbrodt, H.-M.; Deresch, S.; Kresse, H.; Wiegeleben, A.; Demus, D.; Zaschke, H. J. *Prakt. Chem.* **1981**, 323, 902-913.

(10) Demus, D. In *Handbook of Liquid Crystals*; Demus, D., Goodby, J. W., Gray, G. W., Spiess, H.-W., Vill, V., Eds.; Wiley-VCH: New York, 1998; Vol. 1, p 133-187.

(11) Toyne, K. J. In *Thermotropic Liquid Crystals*; Gray, G. W., Ed.; Wiley: New York, 1987; pp 28-63, and references therein.

(12) Wohlfart, K.; Schnell, M.; Grabow, J.-U.; Küpper, J. *J. Mol. Spectr.* **2008**, 247, 119-121.

(13) McKillip, W. J.; Sedor, E. A.; Culbertson, B. M.; Wawzonek, S. *Chem. Rev.* **1973**, 73, 255-281.

(14) Serbutoviez, C.; Nicoud, J.-F.; Fischer, J.; Ledoux, I.; Zyss, J. *Chem. Mater.* **1994**, 6, 1358-1368.

(15) Alcalde, E.; Pérez, L.; Fayet, J. P.; Vertut, M. C. *Chem. Lett.* **1991**, 845-848; and references therein.

(16) Künkemeier-Schröder, B.; Koch, A.-C.; Pelzl, G.; Friedrichsen, W. *Liq. Cryst.* **1993**, 15, 559-561.

(17) Yelamaggad, C. V.; Mathews, M.; Hiremath, U. S.; Rao, D. S. S.; Prasad, S. K. *Tetrahedron Lett.* **2005**, 46, 2623-2626; Yelamaggad, C. V.; Mathews, M.; Hiremath, U. S.; Rao, D. S. S.; Prasad, S. K. *Chem. Commun.* **2005**, 1552-1554.

- (18) Kise, H.; Nishisaka, Y.; Asahara, T.; Seno, M. *Chem. Lett.* **1978**, 1235-1238.
- (19) Kaszynski, P.; Huang, J.; Jenkins, G. S.; Bairamov, K. A.; Lipiak, D. *Mol. Cryst. Liq. Cryst.* **1995**, *260*, 315-332.
- (20) Kaszynski, P.; Lipiak, D. In *Materials for Optical Limiting*; Crane, R., Lewis, K., Stryland, E. V., Khoshnevisan, M., Eds.; MRS: Boston, 1995; Vol. 374, p 341-347.
- (21) Kaszynski, P.; Douglass, A. G. *J. Organomet. Chem.* **1999**, *581*, 28-38, and references therein.
- (22) Kaszynski, P.; Pakhomov, S.; Young, V. G. Jr. *Collect. Czech. Chem. Commun.* **2002**, *67*, 1061-1083; Pakhomov, S.; Kaszynski, P.; Young, V. G. Jr. *Inorg. Chem.* **2000**, *39*, 2243-2245; Balinski, A.; Januszko, A.; Harvey, E. J.; Brady, E.; Kaszynski, P.; Young, V. G. Jr. unpublished results; Kaszynski, P. In *Anisotropic Organic Materials*; Glaser, R. and Kaszynski, P. Eds.; ACS Symposia: Washington D.C., **2001**; Vol. 798, p 68-82.
- (23) Januszko, A.; Kaszynski, P.; Wand, M. D.; More, K. M.; Pakhomov, S.; O'Neill, M. *J. Mater. Chem.* **2004**, *14*, 1544-1553; Jasinski, M.; Jankowiak, A.; Januszko, A.; Bremer, M.; Pauluth, D.; Kaszynski, P. *Liq. Cryst.* **2008**, *35*, 343-350.
- (24) Ohta, K.; Januszko, A.; Kaszynski, P.; Nagamine, T.; Sasnouski, G.; Endo, Y. *Liq. Cryst.* **2004**, *31*, 671-682; Januszko, A.; Kaszynski, P. *Liq. Cryst.* **2008**, *35*, 705-710.
- (25) For other recent publications see: Ringstrand, B.; Vroman, J.; Jensen, D.; Januszko, A.; Kaszynski, P.; Dziaduszek, J.; Drzewinski, W. *Liq. Cryst.* **2005**, *32*, 1061-1070; Januszko, A.; Glab, K. L.; Kaszynski, P. *Liq. Cryst.* **2008**, *35*, 549-553; Nagamine, T.; Januszko, A.; Ohta, K.; Kaszynski, P.; Endo, Y. *Liq. Cryst.* **2008**, *35*, 865-884.
- (26) Januszko, A.; Glab, K. L.; Kaszynski, P.; Patel, K.; Lewis, R. A.; Mehl, G. H.;

Wand, M. D. *J. Mater. Chem.* **2006**, *16*, 3183-3192.

(27) Ringstrand, B.; Balinski, A.; Franken, A.; Kaszynski, P. *Inorg. Chem.* **2005**, *44*, 9561-9566.

(28) Ringstrand, B.; Kaszynski, P.; Monobe, H. *J. Mater. Chem.* **2009**, *19*, 4805-4812.

(29) Bairamov, K. A.; Douglass, A. G.; Kaszynski, P. *Synth. Commun.* **1998**, *28*, 527-540.

(30) Ringstrand, B.; Kaszynski, P.; Franken, A. *Inorg. Chem.* **2009**, *48*, 7313-7329.

(31) Thomas, J.; Clough, D. *J. Pharm. Pharmacol.* **1963**, *15*, 167-177; Volynskii, N. P.; Shcherbakova, L. P. *Bull. Acad. Sci. USSR, Div. Chem. Sci.* **1979**, *28*, 1006-1009.

(32) Crystal data for **1** (CCDC # 731853): C₁₉H₄₄B₉N triclinic, P-1, $a = 9.766(2) \text{ \AA}$, $b = 10.481(3) \text{ \AA}$, $c = 12.098(3) \text{ \AA}$, $\alpha = 93.804(9)^\circ$, $\beta = 90.249(10)^\circ$, $\gamma = 102.587(10)^\circ$; $V = 1205.7(5) \text{ \AA}^3$, $Z = 2$, $T = 95(2) \text{ K}$, $\mu = 0.49595 \text{ \AA}$, $R(F2) = 0.0641$ or $R_w(F2) = 0.1789$ (for 3664 reflections with $I > 2\sigma(I)$).

(33) Jelinek, T.; Stibr, B.; Plesek, J.; Thornton-Pett, M.; Kennedy, J. D. *J. Chem. Soc., Dalton Trans.* **1997**, 4231-4236.

(34) Douglass, A. G.; Janousek, Z.; Kaszynski, P.; Young, V. G., Jr. *Inorg. Chem.* **1998**, *37*, 6361-6365.

(35) The pyramidalization angle α is defined as the N-C-* angle, where * represents the mid-point between the carbon atoms adjacent to N.

- (36) Kaszynski, P.; Pakhomov, S.; Gurskii, M. E.; Erdyakov, S. Y.; Starikova, Z. A.; Lyssenko, K. A.; Antipin, M. Y.; Young, V. G., Jr.; Bubnov, Y. N. *J. Org. Chem.* **2009**, *74*, 1709-1720.
- (37) For details see the Electronic Supplementary Information.
- (38) Urban, S.; Kedzierski, J.; Dabrowski, R. *Z. Naturforsch.* **2000**, *55A*, 449-456.
- (39) Dabrowski, R.; Jadzyn, J.; Czerkas, S.; Dziaduszek, J.; Walczak, A. *Mol. Cryst. Liq. Cryst.* **1999**, *332*, 61-68.
- (40) The data can more properly be fitted to a hyperbolic function such as $y = a/(x+b)$ giving slightly bigger extrapolated dielectric values with significantly higher uncertainty. The Maier-Meier calculations using these extrapolated dielectric parameters give g values that are very similar to those obtained from the quadratic function extrapolation. The polynomial appears to describe well the dielectric data for $x < 0.1$. More in the ESI.
- (41) Maier, W.; Meier, G. *Z. Naturforsch.* **1961**, *16A*, 262-267 and 470-477.
- (42) Urban, S. in *Physical Properties of Liquid Crystals: Nematics*, D. Dunmur, A. Fukuda, and G. Luckhurst, Eds; IEE, London, 2001, pp 267-276.
- (43) Bordewijk, P. *Physica*, **1974**, *75*, 146-156.
- (44) Local orientational parameter of the additive in the host.
- (45) The dipole moment for the [*closo*-1-CB₁₁H₁₁-12-C₇H₆] zwitterion is calculated as 14.3 D in benzene dielectric medium (HF/6-31G(d) method), while the measured value is 11.25 D (B. Grüner, Z. Janousek, B. T. King, J. N. Woodford, C. H. Wang, V. Vsetecka, J. Michl *J. Am. Chem. Soc.* **1999**, *121*, 3122-3126).

- (46) Piecek, W.; Kaufman, J. M.; Kaszynski, P. *Liq. Cryst.* **2003**, *30*, 39-48.
- (47) Kaszynski, P.; Pakhomov, S.; Tesh, K. F.; Young, V. G., Jr. *Inorg. Chem.* **2001**, *40*, 6622-6631.
- (48) Douglass, A. G.; Both, B.; Kaszynski, P. *J. Mater. Chem.* **1999**, *9*, 683-686.
- (49) Czuprynski, K.; Kaszynski, P. *Liq. Cryst.* **1999**, *26*, 775-778.
- (50) Miniewicz, A.; Samoc, A.; Samoc, M.; Kaszynski, P. *J. Appl. Phys.* **2007**, *102*, 033108.
- (51) Nagamine, T.; Januszko, A.; Kaszynski, P.; Ohta, K.; Endo, Y. *J. Mater. Chem.* **2006**, *16*, 3836-3843.
- (52) For instant: Kedziora, P.; Jadzyn, J. *Acta Phys. Polon. A.* **1990**, *A77*, 605-610; Kedziora, P.; Jadzyn, J. *Mol. Cryst. Liq. Cryst.* **1990**, *192*, 31-37.
- (53) Gaussian 98, Revision A.7, M. J. Frisch, G. W. Trucks, H. B. Schlegel, G. E. Scuseria, M. A. Robb, J. R. Cheeseman, V. G. Zakrzewski, J. A. Montgomery, Jr., R. E. Stratmann, J. C. Burant, S. Dapprich, J. M. Millam, A. D. Daniels, K. N. Kudin, M. C. Strain, O. Farkas, J. Tomasi, V. Barone, M. Cossi, R. Cammi, B. Mennucci, C. Pomelli, C. Adamo, S. Clifford, J. Ochterski, G. A. Petersson, P. Y. Ayala, Q. Cui, K. Morokuma, D. K. Malick, A. D. Rabuck, K. Raghavachari, J. B. Foresman, J. Cioslowski, J. V. Ortiz, A. G. Baboul, B. B. Stefanov, G. Liu, A. Liashenko, P. Piskorz, I. Komaromi, R. Gomperts, R. L. Martin, D. J. Fox, T. Keith, M. A. Al-Laham, C. Y. Peng, A. Nanayakkara, C. Gonzalez, M. Challacombe, P. M. W. Gill, B. Johnson, W. Chen, M. W. Wong, J. L. Andres, C. Gonzalez, M. Head-Gordon, E. S. Replogle, and J. A. Pople, Gaussian, Inc., Pittsburgh PA, 1998.
- (54) Foresman, J. B.; Keith, T. A.; Wiberg, K. B.; Snoonian, J.; Frisch, M. J. *J. Phys.*

Chem. **1996**, *100*, 16098–16104.

(55) Wu, S. T.; Coates, D.; Bartmann, E. *Liq. Cryst.* **1991**, *10*, 635-646.

(56) Krasovskiy, A.; Knochel, P. *Synthesis* **2006**, *5*, 890-891.

How Much Can an Electric Dipole Stabilize a Nematic Phase? Polar and Non-Polar Isosteric Derivatives of [closo-1-CB₉H₁₀]⁻ and [closo-1,10-C₂B₈H₁₀].

Reproduced by permission of Ringstrand, B.; Kaszynski, P. *J. Mater. Chem.* **2010**, *20*, 9613-9615.
Copyright 2010 The Royal Society of Chemistry. Available online:
<http://pubs.rsc.org/en/content/articlelanding/2010/jm/c0jm02876b>

This paper addresses one of the most fundamental questions in the field of liquid crystals, which is how much does an electric dipole affect mesophase stability. During the 120 years of research and studying of liquid crystals, this question had only been addressed computationally since appropriate models (i.e. liquid crystalline molecules) did not exist to permit experimental studies. Until now, changing the molecular dipole of a molecule typically resulted in changes to either the molecule's geometry and/or conformational properties. Here, we used an isosteric replacement of a non-polar C–C fragment with a polar B–N fragment in pairs of molecules that increases the molecular dipole by 12 D with little change to the molecule's geometry and/or conformational properties.

My role in this work was the synthesis and characterization of both pairs of isosteric polar/non-polar molecules. The polar nematics **1b-5b** were prepared following

methodology established earlier in my dissertation studies (Part II, Chapters 1 and 3). For the non-polar nematics **1a-5a**, the parent [*closo*-1,10-C₂B₈H₁₀] cluster was arylated with 4-iodoanisole, demethylated, alkylated with 1-heptyltosylate, lithiated and carboxylated with CO₂, and lastly esterified.

Dr. Piotr Kaszynski performed theoretical analysis to calculate the dipole moments of the polar **1b-5b** and non-polar **1a-5a** nematics.

Abstract

Replacement of a C–C fragment with a N⁺–B[–] fragment leads to pairs of isosteric non-polar/polar nematics with a difference in the calculated molecular dipole moment of about 12 D. Contrary to the expectations, the uniform increase of the dipole moment does not affect phase stability equally, and a strong dependence on the substituent structure is observed. For one of the polar derivatives (**5b**, $\mu = 20$ D) a record high dielectric anisotropy ($\Delta\epsilon = 113$) was measured in dilute nematic solutions.

Introduction

Dynamic shape anisotropy of molecules is considered to be the main factor responsible for the formation of the liquid crystalline state.¹ Earlier molecular theories of the nematic state included shape and electronic polarizability of the mesogens.² However,

most liquid crystals of technological importance possess a dipole moment, which permits electro-optical switching³ and applications in the display industry.⁴ Therefore, the impact of the dipole moment on phase properties has been of intense interest, and numerous simulations⁵ of the nematic phase have appeared over the past two decades.^{6,7} These results suggest that for a given increase of the dipole moment there is certain degree of phase stabilization. Experimental verifications of these predictions are hampered by the lack of appropriate molecular models in which *only* polarity can be modified.


Typically, change of the molecular dipole moment is associated with alteration of the molecular geometry and conformational dynamics, which themselves affect phase behavior. Recently, we suggested that the N^+-B^- fragment can serve as an isosteric polar replacement for the C-C fragment in liquid crystalline molecules.⁸ Such a replacement would have negligible impact on molecular geometry and dynamics, and the change in phase properties would be due solely to the molecular dipole. Therefore, we have focused on zwitterionic derivatives of [*closo*-1-CB₉H₁₀]⁻ and their 10-vertex *p*-carborane, [*closo*-1,10-C₂B₈H₁₀], analogues. Here we report the first experimental assessment of the dipole moment effect on phase stability in 5 pairs of *isosteric* and *isoelectronic* molecules using non-polar/polar mesogens **1–5** shown in Table 1.

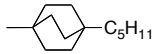
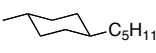
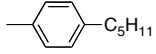
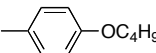
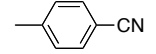
Results and Discussion

Analysis of molecular models for mesogens **1–5** at the B3LYP/6-31G(d,p) level

of theory in gas phase demonstrated that replacement of C–C with N⁺–B[–] results in significant change of the molecular dipole moment and negligible change in electronic polarizability and geometry. Thus, the replacement increases the longitudinal component of the dipole $\mu_{||}$ by about 12 D and the transverse component μ_{\perp} by an average of 1.7 D (Table 1).⁹ At the same time electronic polarizability $\alpha_{||}$ and $\Delta\alpha$ increase by about 1.8 Å³ and 1.5 Å³, respectively, or about 3%. The polar molecules are longer by 8.4 ± 2 pm or ~0.3% as a result of minor expansion of the aryl–cage bond and the {*closo*-1-CB₉} cage by 3.8 ± 0.06 pm and 9.4 ± 0.08 pm, respectively, and contraction of the aryl ring and cage–COO bond by -2.7 ± 0.3 pm and -0.8 ± 0.04 pm, respectively.¹⁰ Since the only significant change upon polar substitution is the increase of the dipole moment by about the same value, phase stability should be affected in a similar way in all five pairs of compounds.

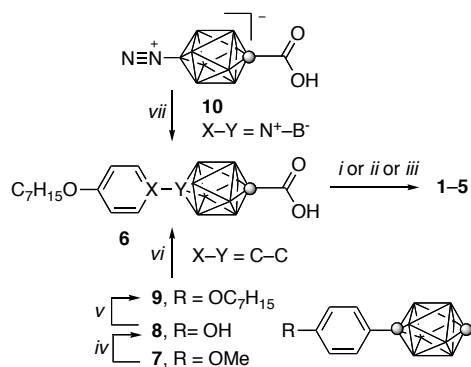
Table 1. Calculated molecular dipole moment components for **1–5**.^a



	R	X-Y	$\mu_{ }$ /D	μ_{\perp} /D
1		a: C–C b: N ⁺ –B ⁻	1.3 13.2	1.7 3.2
2		a: C–C b: N ⁺ –B ⁻	1.5 13.3	1.5 3.3
3		a: C–C b: N ⁺ –B ⁻	2.0 14.0	1.4 3.3
4		a: C–C b: N ⁺ –B ⁻	1.3 13.3	1.9 3.7
5		a: C–C b: N ⁺ –B ⁻	8.1 20.2	0.5 1.8

^a Obtained at the B3LYP/6-31G(d,p) level of theory in Gaussian standard orientation. In the cluster each vertex represents a BH fragment and the sphere is a carbon atom. For details see electronic supporting information.

Scheme 1



i: 2-Chloro-3,5-dinitropyridine (CDNP) and ROH, heat; *ii*: 1. $(\text{COCl})_2$, 2. ROH and Et_3N ;
iii: 1. $(\text{COCl})_2$, 2. ROH, heat; *iv*: BBr_3 ; *v*: $\text{C}_7\text{H}_{15}\text{OTs}$, K_2CO_3 ; *vi*: 1. BuLi, 2. CO_2 , 3. H_3O^+ ; *vii*: 4- $\text{C}_7\text{H}_{15}\text{OC}_5\text{H}_4\text{N}$, heat.

Colorless esters **1–5** were prepared from acid **6** and appropriate phenol or alcohol either directly or through acid chloride (Scheme 1). Acid **6a** ($\text{X}-\text{Y} = \text{C}-\text{C}$) was prepared in three steps from 1-(4-methoxyphenyl)-*p*-carborane **7**, which was obtained by arylation of *p*-carborane according to a similar literature procedure¹¹ (Scheme 1). Acid **6b** ($\text{X}-\text{Y} = \text{N}^+-\text{B}^-$) was obtained in 88% yield by thermolysis of dinitrogen acid¹² **10** in excess 4-heptyloxy pyridine.

Optical and thermal analyses demonstrated that all derivatives **1–5** exhibit exclusively the nematic phase (Table 2). The observed nematic behavior for the non-polar compounds **1a–5a** is consistent with results for other mesogens containing *p*-carborane.¹³ The absence of smectic phases in **1b–5b**, typically observed in polar three-ring liquid crystals, is surprising and highly unusual. This can be attributed to the presence of the carborane unit near the molecule's center, which destabilizes layered

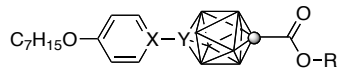
molecular organization.¹³

A comparison of transition temperatures for the two series of compounds demonstrates that the polar derivatives **1b–5b** have higher melting points than the non-polar analogues **1a–5a**, and the increase ranges from 50 K for **5** to 87 K for **1**. The most interesting aspect of the two series is, however, the comparison of the N-I transition temperatures (Fig. 1). For the polar alicyclic derivatives **1b** and **2b**, the nematic phase is stabilized by about 55 K relative to the non-polar analogues **1a** and **2a**. This effect is much smaller for the benzene derivatives **3–5**; the nematic phase is most stabilized in **4b** although by only $\Delta T_{\text{NI}} = 18$ K and *destabilized* by $\Delta T_{\text{NI}} = -4$ K in the nitrile **5b** relative to the *p*-carborane analogues. The trend in ΔT_{NI} for **3–5** follows the Hammett σ_p values and correlates well with the field parameters of the substituents.¹⁴ Thus, results in Figure 1 indicate that the effect of the dipole moment on phase stability is not only a function of its magnitude and orientation, but most importantly, the molecular structure.

The observed variation of the electric dipole effect on phase relative stability (ΔT_{NI}) in the isosteric pairs can be due to the difference in the mean distance r between the molecules or to the magnitude of the effective dipole moment μ_{eff} in the nematic phase, since both quantities define the dipole-dipole interaction energy E_{dip} .^{15,16} If considering intermolecular separation only, the largest mean distance r and consequently lowest E_{dip} in the series is expected for **1** and **2** with the most voluminous groups; conversely smallest r and largest E_{dip} is expected for the nitrile **5**. The trend in E_{dip} is

opposite to that observed for ΔT_{NI} in the pairs of mesogens.

Table 2. Transition temperatures for **1–5**.^a



	X-Y	Cr		N		I
1	a: C-C	•	74	•	174 ^b	•
	b: N ⁺ -B ⁻	•	161	•	231	•
2	a: C-C	•	64	•	107	•
	b: N ⁺ -B ⁻	•	148	•	161	•
3	a: C-C	•	45	•	105	•
	b: N ⁺ -B ⁻	•	120	(•)	114)	•
4	a: C-C	•	64	•	138	•
	b: N ⁺ -B ⁻	•	122	•	156	•
5	a: C-C	•	79	•	133	•
	b: N ⁺ -B ⁻	•	128	(•)	129)	•

^a Cr-crystal, N-nematic, I-isotropic. Temperatures obtained on heating at 5 K min⁻¹. Enthalpies are listed in the ESI. ^b Recorded at 10 K min⁻¹.

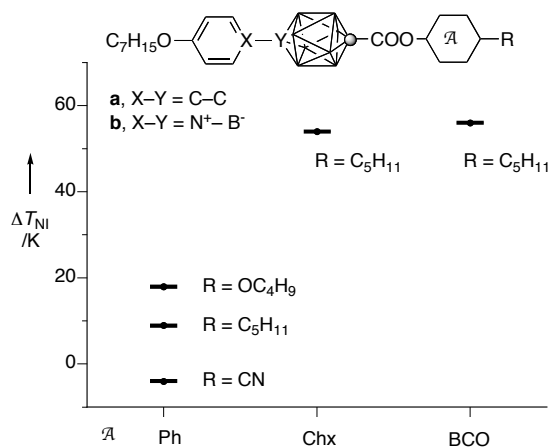
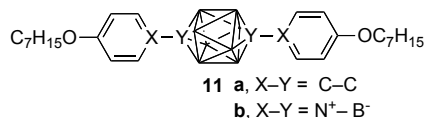


Figure 1. A plot of the ΔT_{NI} between polar (**1b – 5b**) mesogens and their non-polar analogues (**1a – 5a**).

In general, the magnitude of the dipole moment depends on the dielectric strength

of the medium; it is largest in gas phase ($\epsilon = 1$) and diminishes with increasing ϵ .¹⁷ For instance, the dipole moment for MeCN is smaller in CS₂ solutions ($\epsilon = 2.63$) than in gas phase by 22% and for nitrobenzene the difference is 13%.¹⁷ This suggests that alicyclic substituents, bicyclo[2.2.2]octane in **1** and cyclohexane in **2**, have a lower screening effect on the molecular dipole than the benzene ring in **3–5** in the condensed phase. Consequently, E_{dip} is larger for **1** and **2**, which, in turn, leads to greater stabilization of the parallel alignment of the molecules (the Keesom orientation¹⁵) and higher relative stability of the nematic phase in these pairs of molecules. In the isostructural derivative **3**, the dielectric screening of the benzene ring reduces the strength of the dipole moment, which results in lower phase stabilization. It appears, that the substituent on the benzene ring further modulates the strength of this dielectric screening, and its field impacts stabilization of the nematic phase.¹⁶

While this report concentrates on polar nematic, it should also be mentioned that the isosteric replacement of C–C with N⁺–B⁻ can lead to liquid crystals with large linear quadrupole. An example is the pair **11a**¹⁸ and **11b**.¹⁹ Analysis revealed that the most significant difference between these two C₂-symmetric molecules is in their longitudinal component of the primitive quadrupole moment: $Q_{xx} = -172 \text{ D}\text{\AA}$ for the non-polar **11a** and $Q_{xx} = -61 \text{ D}\text{\AA}$ for the polar **11b**.²⁰ The calculated nearly 3-fold change in Q_{xx} corresponds to the observed 120 K higher T_{NI} for the polar **11b** than for the non-polar analogue **11a**. This surprisingly strong nematic phase stabilization is consistent with results of Gay-Berne modeling²¹ and presumably occurs by interaction of local dipole moments.



Polar nematics, such as **1b–5b**, are of interest as high $\Delta\epsilon$ additives in formulation of mixtures for LCD applications.⁴ Low concentration solution studies of **3b** in a weakly polar nematic host²² at 24 °C gave an extrapolated $\Delta\epsilon$ of 42. The same measurements for the pair **5a** and **5b**, show that the replacement of C–C in the former with N⁺–B⁻ in **5b** results in an increase of dielectric anisotropy $\Delta\epsilon$ by 98 to a record value of 113! There are very few materials with $\Delta\epsilon > 40$,²³ and to our knowledge, the extrapolated value of $\Delta\epsilon$ for **5b** is the highest ever recorded for a nematic material.²⁴

Summary and Conclusions

We have demonstrated that the isosteric polar replacement of the C–C fragment with the N⁺–B⁻ fragment in pairs of mesogenic compounds is a new and powerful tool in addressing fundamental and applied aspects of liquid crystal research. The substitution in compounds **1–5** introduces a substantial longitudinal dipole moment, whose effect on phase properties depends on the nature of the substituent distant from the zwitterion. This suggests that simulation of a realistic nematic phase requires atomistic models.²⁵ The present findings constitute an important contribution to the understanding of the role of an electric dipole on phase stability, offer experimental verification of current theoretical models, and guide development of new high $\Delta\epsilon$ materials for electro-optical applications.

Experimental Section

Reagents and solvents were obtained commercially. DME was distilled over potassium in the presence of benzophenone. Pyridine, dichloromethane, and NEt_3 were distilled over CaH_2 . DMF was dried over 4 Å molecular sieves. *n*-Heptyl tosylate was prepared according to literature.¹ CuCl was freshly purified by suspending it in 5% H_2SO_4 followed by filtration of CuCl as a white precipitate. The collected CuCl was washed with cold EtOH , Et_2O , and then dried *in vacuo* at 100 °C for 1 hr. All other reagents were used as supplied. Reactions were carried out under Ar, and subsequent manipulations were conducted in air. NMR spectra were obtained at 128.4 MHz (^{11}B) and 400.1 MHz (^1H) in CD_3CN or CDCl_3 . ^1H NMR spectra were referenced to the solvent, and ^{11}B NMR chemical shifts were referenced to an external boric acid sample in CH_3OH that was set to 18.1 ppm.

General Procedure for Preparation of Esters 1–5

Method A A red/orange solution of acid **6b** (0.25 mmol), alcohol or phenol (0.28 mmol), DMAP (0.25 mmol), and 2-chloro-3,5-dinitropyridine (CDNP, 0.25 mmol) in anhydrous pyridine (1 mL) was stirred at reflux under Ar. Reaction progress was monitored by ^1H NMR of a small aliquot in CD_3CN . If the reaction was incomplete, additional equivalents of CDNP were added and heating continued (6-48 hrs). Excess pyridine was removed to dryness giving a red/orange crystalline film. The film was

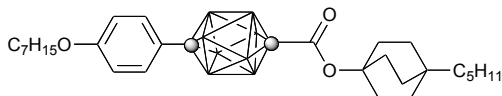
treated with 10% HCl and extracted into Et₂O (3x). The Et₂O layers were combined, washed with a sat. solution of NaHCO₃, dried (Na₂SO₄), and evaporated. The crude product was further purified by passage through a short silica gel plug (CH₂Cl₂/hexane mixture), filtered through a cotton plug, and recrystallized.

Method B A mixture of acid **6** (0.25 mmol) and anhydrous CH₂Cl₂ (1 mL) was treated with a 0.5 M solution of (COCl)₂ in CH₂Cl₂ (0.75 mL, 0.375 mmol) and 0.1 M solution of anhydrous DMF in CH₂Cl₂ (0.25 mL, 0.025 mmol) at rt. The mixture began to bubble, and the reaction became homogeneous (for **6b** the reaction mixture starts as a suspension). After 30 mins, the light yellow solution was evaporated to dryness, redissolved in anhydrous CH₂Cl₂ (1 mL), and phenol (1.5 equivalents) and a 0.5 M solution of freshly distilled NEt₃ in CH₂Cl₂ (0.25 mL, 0.75 mmol) were added. The reaction was stirred overnight at rt, evaporated to dryness, passed through a short silica gel plug (CH₂Cl₂/hexane mixture), filtered through a cotton plug, and recrystallized. Calculated yields for esters **1a-5a** are for the purest fractions only. The mass of the impure fractions amounted to approximately 15-20% of the total yield on average.

Method C. The acid chloride derived from acid **6** (0.25 mmol) was generated as in Method B. Without purification, the chloride, excess alcohol (~1 mmol), and freshly distilled pyridine (0.1 mL) were added. The mixture was heated for 3 days at 90 °C protected from moisture. At times, the reaction was cooled to rt, and minimal anhydrous CH₂Cl₂ was added to wash the sides of the flask. The product was purified as in Method B. Calculated yields for esters **1a-5a** are for the purest fractions only. The mass of the

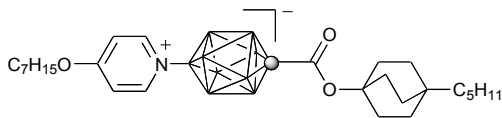
impure fractions amounted to approximately 15-20% of the total yield on average.

Ester of 10-(4-heptyloxyphenyl)-*p*-carborane-1-carboxylic acid and 4-pentylbicyclo[2.2.2]octan-1-ol (1a).



It was obtained using Method C in 56% yield after chromatography (CH₂Cl₂/hexane, 1:19). Ester **1a** was purified by recrystallization from CH₃CN/toluene (2x) at -20 °C, pentane (4x) at -40 °C, and *iso*-octane at -20 °C giving colorless crystals: mp 74 °C (DSC); ¹H NMR (400 MHz, CDCl₃, 25 °C, CHCl₃): δ = 1.50-3.40 (br m, 8H), 0.85-0.94 (m, 6H), 1.07-1.43 (m, 14H), 1.48 (quint, *J* = 5.7 Hz, 2H), 1.59 (br t, *J* = 7.9 Hz, 6H), 1.82 (quint, *J* = 6.9 Hz, 2H), 2.16 (br t, *J* = 7.8 Hz, 6H), 4.01 (t, *J* = 6.5 Hz, 2H), 6.95 (d, *J* = 8.7 Hz, 2H), 7.32 (d, *J* = 8.7 Hz, 2H); ¹¹B NMR (128.4 MHz, CDCl₃, 25 °C, B(OH)₃/MeOH): δ = -10.2 (d, *J* = 154 Hz). Anal. Calcd. For C₂₉H₅₀B₈O₃: C, 65.33; H, 9.45. Found: C, 65.43; H, 9.54.

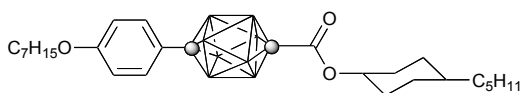
Ester of [*clos*-1-C B₉H₈-1-COOH-10-(1-(4-C₇H₁₅O)-C₅H₄N)] and 4-pentylbicyclo[2.2.2]octan-1-ol (1b).



It was obtained using Method A. After heating for 3 days and additional amounts of both CDNP and alcohol, most starting acid remained unreacted. Ester **1b** was isolated in 9% yield after chromatography (CH₂Cl₂/hexane, 3:7) and was recrystallized from *iso*-octane/toluene (4x) giving colorless leaflets: mp 161 °C (DSC); ¹H NMR (400 MHz,

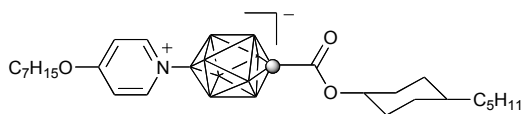
CDCl₃, 25 °C, CHCl₃): δ = 0.75-2.60 (br m, 8H), 0.86 (t, J = 7.1 Hz, 3H), 0.90 (t, J = 6.7 Hz, 3H) 1.04-1.12 (m, 2H), 1.14-1.24 (m, 4H), 1.25-1.44 (m, 8H), 1.46-1.55 (m, 2H), 1.56 (br t, J = 8.0 Hz, 6H), 1.92 (quint, J = 7.1 Hz, 2H), 2.18 (br t, J = 8.0 Hz, 6H), 4.27 (t, J = 6.5 Hz, 2H), 7.23 (overlapping with CHCl₃, 2H), 9.06 (d, J = 7.3 Hz, 2H); ¹¹B {¹H} NMR (128.4 MHz, CDCl₃, 25 °C, B(OH)₃/MeOH): δ = -20.9 (4B), -16.1 (4B), 41.2 (s, 1B). MS (ESI): m/z (554-559) max at 557 (100 %); ESI-HRMS(+): Calcd. for C₂₇H₅₀B₉NNaO₃ m/z : 558.4526; found; 558.4542.

Ester of 10-(4-heptyloxyphenyl)-*p*-carborane-1-carboxylic acid and 4-*trans*-pentylcyclohexanol (2a).



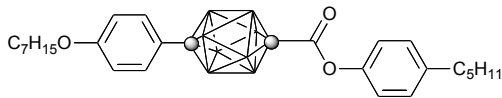
It was obtained using Method C in 50% yield after chromatography (CH₂Cl₂/hexane, 1:19). Ester **2b** was purified by recrystallization from CH₃CN (3x) at -20 °C and pentane (3x) at -20 °C giving colorless crystals: mp 64 °C (DSC); ¹H NMR (500 MHz, CDCl₃, 25 °C, CHCl₃): δ = 1.50-3.40 (br m, 8H), 0.90 (t, J = 5.6 Hz, 3H), 0.91 (t, J = 5.6 Hz, 3H), 1.04-1.15 (m, 2H), 1.18-1.42 (m, 15H), 1.44-1.57 (m, 4H), 1.82 (quint, J = 7.2 Hz, 2H), 1.87 (br d, J = 12.4 Hz, 2H), 2.17 (br d, J = 12.2 Hz, 2H), 4.02 (t, J = 6.6 Hz, 2H), 5.00 (tt, J_1 = 11.1 Hz, J_2 = 4.5 Hz, 1H), 6.96 (d, J = 8.8 Hz, 2H), 7.68 (d, J = 8.8 Hz, 2H); ¹¹B NMR (128.4 MHz, CDCl₃, 25 °C, B(OH)₃/MeOH): δ = -10.1 (d, J = 152 Hz). Anal. Calcd. For C₂₇H₄₈B₈O₃: C, 63.94; H, 9.54. Found: C, 63.96; H, 9.51.

Ester of [*closo*-1-CB₉H₈-1-COOH-10-(1-(4-C₇H₁₅O-C₅H₄N))] and 4-*trans*-pentylcyclohexanol (2b**).**



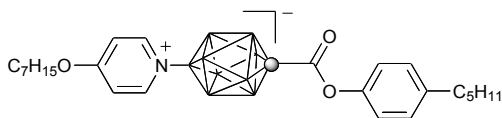
It was obtained using Method A. The peaks at 4.33 ppm and 4.94 ppm in ¹H NMR (CD₃CN) were monitored until the desired 2:1 ratio was achieved. Ester **2b** was isolated in 40% yield after chromatography (CH₂Cl₂/hexane, 3:7) and was recrystallized from *iso*-octane/toluene (5x) at -20 °C giving colorless leaflets: mp 148 °C (DSC); ¹H NMR (400 MHz, CDCl₃, 25 °C, CHCl₃): δ = 0.75-2.60 (br m, 8H), 0.85-0.97 (m, 6H), 1.03-1.16 (m, 2H), 1.18-1.45 (m, 17H), 1.47-1.60 (m, 2H), 1.85 (br d, *J* = 12.8 Hz, 2H), 1.94 (quint, *J* = 7.0 Hz, 2H), 2.20 (br d, *J* = 12.7 Hz, 2H), 4.29 (t, *J* = 6.5 Hz, 2H), 5.04 (tt, *J*₁ = 11.0 Hz, *J*₂ = 4.2 Hz, 1H), 7.26 (overlap with CHCl₃, 2H), 9.08 (d, *J* = 7.0 Hz, 2H); ¹¹B NMR (128.4 MHz, CDCl₃, 25 °C, B(OH)₃/MeOH): δ = -20.9 (d, *J* = 126 Hz, 4B), -16.1 (d, *J* = 124 Hz, 4B), 41.2 (s, 1B). Anal. Calcd. for C₂₅H₄₈B₉NO₃: C, 59.11; H, 9.52; N, 2.76. Found: C, 59.39; H, 9.58; N, 2.77.

Ester of 10-(4-heptyloxyphenyl)-*p*-carborane-1-carboxylic acid and 4-pentylphenol (3a).



It was obtained using Method B in 79% yield after chromatography (CH₂Cl₂/hexane, 1:19). Ester **3a** was purified by recrystallization from CH₃CN (3x) at -20 °C and pentane (3x) at -20 °C giving colorless leaflets: mp 45.0 °C (DSC); ¹H NMR (400 MHz, CDCl₃, 25 °C, CHCl₃): δ = 1.50-3.40 (br m, 8H), 0.91 (t, *J* = 6.9 Hz, 6H), 1.27-1.43 (m, 10H), 1.49 (quint, *J* = 7.3 Hz, 2H), 1.65 (quint, *J* = 7.5 Hz, 2H), 1.83 (quint, *J* = 7.0 Hz, 2H), 2.64 (t, *J* = 7.7 Hz, 2H), 4.03 (t, *J* = 6.5 Hz, 2H), 6.98 (d, *J* = 8.7 Hz, 2H), 7.22 (d, *J* = 8.5 Hz, 2H), 7.27 (d, *J* = 8.6 Hz, 2H), 7.71 (d, *J* = 8.7 Hz, 2H); ¹¹B NMR (128.4 MHz, CDCl₃, 25 °C, B(OH)₃/MeOH): δ = -9.9 (d, *J* = 163 Hz). Anal. Calcd. For C₂₇H₄₂B₈O₃: C, 64.71; H, 8.45. Found: C, 64.98; H, 8.47.

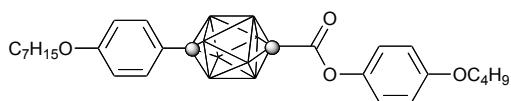
Ester of [closo-1-CB₉H₈-1-COOH-10-(1-(4-C₇H₁₅O-C₅H₄N))] with *p*-pentylphenol (3b).



It was obtained using Method A. The peaks at 2.66 ppm and 4.34 ppm in ¹H NMR (CD₃CN) were monitored until the desired 1:1 ratio was achieved. Ester **3b** was isolated in 64% yield after chromatography (CH₂Cl₂/hexane, 3:7) and purified by recrystallization from *iso*-octane/toluene (5x) at -20 °C giving colorless leaflets: mp 120 °C (DSC); ¹H NMR (400 MHz, CD₃CN, 25 °C, CHD₂CN): δ = 0.80-2.60 (br m, 8H), 0.91 (t, *J* = 6.7 Hz, 6H), 1.29-1.44 (m, 10H), 1.45-1.54 (m, 2H), 1.65 (quint, *J* =

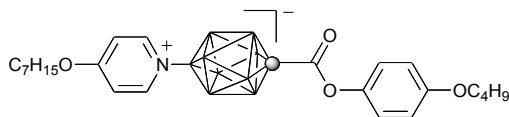
7.4 Hz, 2H), 1.88 (quint, $J = 7.2$ Hz, 2H), 2.66 (t, $J = 7.7$ Hz, 2H), 4.34 (t, $J = 6.6$ Hz, 2H), 7.20 (d, $J = 8.4$ Hz, 2H), 7.31 (d, $J = 8.4$ Hz, 2H), 7.41 (d, $J = 7.3$ Hz, 2H), 9.06 (d, $J = 7.1$ Hz, 2H); ^{11}B NMR (128.4 MHz, CD_3CN , 25 °C, $\text{B}(\text{OH})_3/\text{MeOH}$): $\delta = -21.3$ (d, $J = 156$ Hz, 4B), -16.1 (d, $J = 172$ Hz, 4B), 42.2 (s, 1B). Anal. Calcd. for $\text{C}_{25}\text{H}_{42}\text{B}_9\text{NO}_3$: C, 59.83; H, 8.43; N, 2.79. Found: C, 59.92; H, 8.44; N, 2.78.

Ester of 10-(4-heptyloxyphenyl)-*p*-carborane-1-carboxylic acid and 4-butoxyphenol (4a).



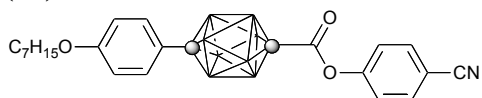
It was obtained using Method B in 79% yield after chromatography ($\text{CH}_2\text{Cl}_2/\text{hexane}$, 1:19). Ester **4a** was purified by recrystallization from CH_3CN (3x) at -20 °C, pentane (3x) at -20 °C, hexane (1x) at -20 °C, and *iso*-octane (1x) at 0 °C giving colorless needles: mp 64 °C (DSC); ^1H NMR (400 MHz, CDCl_3 , 25 °C, CHCl_3): $\delta = 1.50\text{-}3.40$ (br m, 8H), 0.91 (t, $J = 6.8$ Hz, 3H), 0.99 (t, $J = 7.4$ Hz, 3H), 1.29-1.43 (m, 6H), 1.46-1.57 (m, 4H), 1.79 (quint, $J = 7.1$ Hz, 2H), 1.82 (quint, $J = 7.1$ Hz, 2H), 3.99 (t, $J = 6.5$ Hz, 2H), 4.03 (t, $J = 6.6$ Hz, 2H), 6.96 (d, $J = 9.0$ Hz, 2H), 6.98 (d, $J = 8.7$ Hz, 2H), 7.22 (d, $J = 9.0$ Hz, 2H), 7.71 (d, $J = 8.7$ Hz, 2H); ^{11}B NMR (128.4 MHz, CDCl_3 , 25 °C, $\text{B}(\text{OH})_3/\text{MeOH}$): $\delta = -9.9$ (d, $J = 179$ Hz, 8B). Anal. Calcd. For $\text{C}_{26}\text{H}_{40}\text{B}_8\text{O}_4$: C, 62.07; H, 8.01. Found: C, 61.89; H, 7.98.

Ester of [*closo*-1-CB₉H₈-1-COOH-10-(1-(4-C₇H₁₅O-C₅H₄N))] and 4-butoxyphenol (4b).



It was obtained using Method B in 79% yield after chromatography (CH₂Cl₂/hexane, 3:7). Ester **4b** was purified by recrystallization from aq. EtOH (3x) at rt giving colorless leaflets: mp 122 °C (DSC); ¹H NMR (400 MHz, CDCl₃, 25 °C, CHCl₃): δ = 0.75-2.60 (br m, 8H), 0.92 (t, *J* = 6.8 Hz, 3H), 0.99 (t, *J* = 7.4 Hz, 3H), 1.30-1.45 (m, 6H), 1.49-1.58 (m, 4H), 1.80 (quint, *J* = 7.0 Hz, 2H), 1.95 (quint, *J* = 7.0 Hz, 2H), 3.98 (t, *J* = 6.5 Hz, 2H), 4.31 (t, *J* = 6.5 Hz, 2H), 6.95 (d, *J* = 9.0 Hz, 2H), 7.26 (d, *J* = 9.0 Hz, 2H), 7.28 (d, *J* = 7.4 Hz, 2H), 9.10 (d, *J* = 7.3 Hz, 2H); ¹¹B NMR (128.4 MHz, CDCl₃, 25 °C, B(OH)₃/MeOH): δ = -20.7 (d, *J* = 128 Hz, 4B), -15.7 (d, *J* = 177 Hz, 4B), 42.1 (s, 1B). Anal. Calcd. For C₂₄H₄₀B₉NO₄: C, 57.21; H, 8.00; N, 2.78. Found: C, 57.17; H, 7.95; N, 2.82.

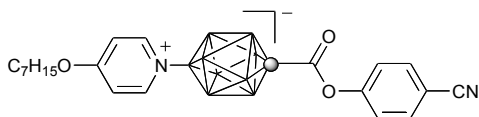
Ester of 10-(4-heptyloxyphenyl)-*p*-carborane-1-carboxylic acid and 4-cyanophenol (5a).



It was obtained using Method B in 39% yield after chromatography (CH₂Cl₂/hexane, 1:19). Ester **5a** was purified by recrystallization from CH₃OH (3x) at -20 °C, hexane (2x) at -20 °C, *iso*-octane (1x) at -20 °C, and pentane (2x) at -20 °C giving colorless needles: mp 79 °C (DSC); ¹H NMR (400 MHz, CDCl₃, 25 °C, CHCl₃): δ = 1.50-3.40 (br m, 8H), 0.91 (t, *J* = 6.9 Hz, 3H), 1.28-1.43 (m, 6H), 1.45-1.52 (m, 2H), 1.83

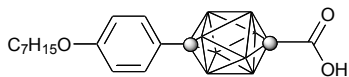
(quint, $J = 7.0$ Hz, 2H), 4.03 (t, $J = 6.6$ Hz, 2H), 6.98 (d, $J = 8.7$ Hz, 2H), 7.49 (d, $J = 8.6$ Hz, 2H), 7.70 (d, $J = 8.7$ Hz, 2H), 7.80 (d, $J = 8.7$ Hz, 2H); ^{11}B NMR (128.4 MHz, CDCl_3 , 25 °C, $\text{B}(\text{OH})_3/\text{MeOH}$): $\delta = -9.8$ (d, $J = 173$ Hz). Anal. Calcd. For $\text{C}_{23}\text{H}_{31}\text{B}_8\text{NO}_3$: C, 60.58; H, 6.85; N, 3.07. Found: C, 60.54; H, 6.89; N, 3.01.

Ester of [*closo*-1- CB_9H_8 -1-COOH-10-(1-(4- $\text{C}_7\text{H}_{15}\text{O}$ - $\text{C}_5\text{H}_4\text{N}$))] and 4-cyanophenol (5b**).**



It was obtained using Method B in 91% yield after chromatography ($\text{CH}_2\text{Cl}_2/\text{hexane}$, 1:1). Ester **5b** was purified by washing with boiling pentane (2x) and recrystallization from aq. EtOH (1x) at -20 °C, CH_3OH (1x) at -20 °C, and CH_3OH (1x) at -40 °C giving colorless blades: mp 128 °C (DSC); ^1H NMR (400 MHz, CDCl_3 , 25 °C, CHCl_3): $\delta = 1.50$ -3.40 (br m, 8H), 0.92 (t, $J = 6.8$ Hz, 3H), 1.30-1.38 (m, 4H), 1.39-1.46 (m, 2H), 1.48-1.56 (m, 2H), 1.95 (quint, $J = 7.0$ Hz, 2H), 4.31 (t, $J = 6.5$ Hz, 2H), 7.30 (d, $J = 7.3$ Hz, 2H), 7.51 (d, $J = 8.7$ Hz, 2H), 7.77 (d, $J = 8.7$ Hz, 2H), 9.09 (d, $J = 7.2$ Hz, 2H); ^{11}B NMR (128.4 MHz, CDCl_3 , 25 °C, $\text{B}(\text{OH})_3/\text{MeOH}$): $\delta = -20.7$ (d, $J = 142$ Hz, 4B), -15.6 (d, $J = 151$ Hz, 4B), 42.8 (s, 1B). Anal. Calcd. For $\text{C}_{21}\text{H}_{31}\text{B}_9\text{N}_2\text{O}_3$: C, 55.22; H, 6.84; N, 6.13. Found: C, 55.45; H, 6.83; N, 6.09.

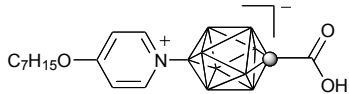
Preparation of 10-(4-heptyloxyphenyl)-*p*-carborane-1-carboxylic acid (6a**).**



A solution of 1-(4-heptyloxyphenyl)-*p*-carborane (**9**) (1.00 g, 3.22 mmol) in

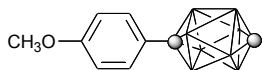
anhydrous THF (20 mL) at 0 °C was treated with *n*-BuLi (1.61 mL, 3.86 mmol, 2.4 M in hexanes). The reaction mixture was warmed to rt, and the solution developed a slight yellow tint. The solution was cooled back to 0 °C, and dry CO₂ was bubbled through the solution for 15 min upon which the solution became colorless. The reaction mixture was evaporated to dryness and washed with pentane. Et₂O (10 mL) and 10% HCl (30 mL) were added, and the Et₂O was separated. The aqueous layer was further extracted with Et₂O (3 x 10 mL). The organic layers were combined, washed with H₂O, dried (Na₂SO₄), and evaporated to dryness. The tacky white solid was washed with hot H₂O (2x) to remove residual valeric acid and dried *in vacuo* providing 1.06 g of crude acid **6a** (93% yield). The acid was further purified via recrystallization from aq. MeOH (3x), CH₃CN (2x), and *iso*-octane (2x). Despite repeated recrystallizations an unknown impurity (~10%) was still present as evident by ¹H NMR (doublet at 7.74 (*J* = 8.8 Hz) ppm): mp 156-157 °C; ¹H NMR (400 MHz, CDCl₃, 25 °C, CHCl₃): δ = 1.50-3.50 (br m, 8H), 0.91 (t, *J* = 6.9 Hz, 3H), 1.28-1.43 (m, 6H), 1.44-1.53 (m, 2H), 1.83 (quint, *J* = 7.0 Hz, 2H), 4.03 (t, *J* = 6.6 Hz, 2H), 6.97 (d, *J* = 8.8 Hz, 2H), 7.69 (d, *J* = 8.8 Hz, 2H); ¹¹B NMR (128.4 MHz, CDCl₃, 25 °C, B(OH)₃/MeOH): δ = -9.9 (d, *J* = 144 Hz, 8B); IR (solid): 2607 (B-H) and 1710 (C=O) cm⁻¹. Anal. Calcd. for C₁₆H₂₈B₈O₃: C, 54.15; H, 7.95. Found: C, 53.92; H, 8.11.

Preparation of [*closo*-1-CB₉H₈-1-COOH-10-(1-(4-C₇H₁₅O)-C₅H₄N)] (6b).



A slight yellow solution of [*closo*-1-CB₉H₈-1-COOH-10-N₂] (**10**, 0.095 g, 0.50 mmol) and 4-heptyloxy-pyridine (3.0 mL) was stirred at 100 °C for 1 hr. As the reaction progressed, bubbling of N₂ became evident. Excess 4-heptyloxy-pyridine was removed via Kugel-Rohr distillation (140 °C, 0.5 mmHg). 10 % HCl (10 mL) was added to the crude product, and the solution was extracted with Et₂O (3 x 5 mL). The Et₂O layers were combined, washed with H₂O, dried (Na₂SO₄), and evaporated giving 0.175 g of crude acid **6b**. The crude product was passed through a short silica gel plug (CH₃OH/CH₂Cl₂, 1:19, R_f = 0.4) giving 0.156 g (88% yield) of pure acid **6b** as a white crystalline solid. A small portion of the product was passed through a cotton plug and recrystallized from aq. EtOH (4x) giving an analytical sample: mp 208-210 °C; ¹H NMR (400 MHz, CD₃CN, 25 °C, CHD₂CN): δ = 0.60-2.50 (br m, 8H), 0.90 (t, *J* = 6.8 Hz, 3H), 1.28-1.43 (m, 6H), 1.44-1.53 (m, 2H), 1.87 (quint, *J* = 7.0 Hz, 2H), 4.33 (t, *J* = 6.6 Hz, 2H), 7.39 (d, *J* = 7.2 Hz, 2H), 9.04 (d, *J* = 6.9 Hz, 2H), 9.64 (br s, 1H); ¹¹B NMR (128.4 MHz, CD₃CN, 25 °C, B(OH)₃/MeOH): δ = -21.4 (d, *J* = 137 Hz, 4B), -16.5 (d, *J* = 158 Hz, 4B), 42.5 (s, 1B). Anal. Calcd. for C₁₄H₂₈B₉NO₃: C, 47.28; H, 7.93; N, 3.94. Found: C, 47.54; H, 8.06; N, 3.93.

Preparation of 1-(4-methoxyphenyl)-*p*-carborane (7)



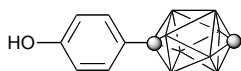
A solution of 10-vertex *p*-carborane (1.00 g, 8.31 mmol) dissolved in anhydrous DME (35 mL) at 0 °C under an inert atmosphere was treated with *n*-BuLi (4.2 mL, 9.97 mmol, 2.4 M in hexanes). After warming to rt, dry pyridine (5.0 mL, 61.6 mmol) and freshly prepared CuCl (1.23 g, 12.47 mmol) were added. The mixture was refluxed for 30 min upon which a dark red/purple solution formed. The reaction was cooled down to rt, and 4-iodoanisole (0.971 g, 4.15 mmol) was added in one portion and refluxing was then continued for 24 hrs. The light red/purple mixture was allowed to cool, treated with Et₂O (100 mL) and H₂O (5 mL). After 2 hrs, the blue/green copper salts were filtered off, the filtrate acidified with 10 % HCl (100 mL), and extracted with Et₂O (3 x 20 mL). The Et₂O layers were combined, dried (Na₂SO₄), and evaporated to dryness. The crude material was purified by column chromatography (CH₂Cl₂:hexane, 1:9) providing 1.10 g (59% yield) of mono-substituted product **7** ($R_f = 0.3$ in CH₂Cl₂/hexane, 1:9) as a colorless liquid that slowly crystallized. Further elution provided 0.722 g (26% yield) of 1,10-bis(4-methoxyphenyl)-*p*-carborane ($R_f = 0.05$ in CH₂Cl₂/Hexane, 1:9) as a white crystalline solid. The mono-substituted product **7** was used without further purification. The di-substituted product was washed with boiling CH₃OH (2x) and boiling EtOH (1x) and then recrystallized from *iso*-octane/toluene mixtures (5x).

An analytical sample of 1-(4-methoxyphenyl)-*p*-carborane (**7**) was obtained in 90% yield by methylation of phenol **8** with MeOTs as described for **9**. The product was

recrystallized from *iso*-octane (1x) at -40 °C, hexane (1x) at -40 °C, and *iso*-octane (1x) at -78 °C followed by sublimation (60-70 °C, 2 mm Hg). Colorless needles: mp 55-57 °C; ¹H NMR (400 MHz, CDCl₃, 25 °C, CHCl₃): δ = 2.11 (q, *J* = 162 Hz, 4H), 2.28 (q, *J* = 150 Hz, 4H), 3.86 (s, 3H), 6.82 (br s, 1H), 6.98 (d, *J* = 8.8 Hz, 2H), 7.74 (d, *J* = 8.8 Hz, 2H); ¹¹B {¹H} NMR (128.4 MHz, CDCl₃, 25 °C, B(OH)₃/MeOH): δ = -12.8 (4B), -10.2 (4B). Anal. Calcd. for C₉H₁₆B₈O: C, 47.68; H, 7.11. Found: C, 47.67; H, 7.24.

1,10-Bis(4-methoxyphenyl)-*p*-carborane: mp 193-194 °C; ¹H NMR (400 MHz, CDCl₃, 25 °C, CHCl₃): δ = 2.42 (q, *J* = 157 Hz, 8H), 3.88 (s, 6H), 6.98 (d, *J* = 8.8 Hz, 4H), 7.74 (d, *J* = 8.8 Hz, 4H); ¹¹B NMR (128.4 MHz, CDCl₃, 25 °C, B(OH)₃/MeOH): δ = -10.4 (d, *J* = 155 Hz). Anal. Calcd for C₂₈H₄₆B₈O₂: C, 67.11; H, 9.25. Found: C, 67.28; H, 9.29.

Preparation of 1-(4-hydroxyphenyl)-*p*-carborane (8).

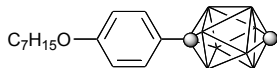


Method A. A solution of 1-(4-methoxyphenyl)-*p*-carborane (**7**, 1.10 g, 4.86 mmol) in anhydrous CH₂Cl₂ (5 mL) was treated with BBr₃ (4.86 mL, 4.86 mmol, 1.0 M in CH₂Cl₂) at 0 °C. The light red solution was warmed to rt and stirred overnight upon which it became dark red. Reaction progress and product formation were monitored by TLC (CH₂Cl₂, R_f = 0.35). Water (50 mL) was added, the CH₂Cl₂ layer was separated, and the H₂O was further extracted with CH₂Cl₂ (3 x 15 mL). The organic layers were combined, dried (MgSO₄), and evaporated to dryness. The crude product was isolated via column

chromatography (CH₂Cl₂/Hexane, 1:1) giving 0.926 g (90% yield) of phenol **8** as a white fluffy solid. An analytical sample of **8** was obtained by recrystallization from *iso*-octane (3x) followed by aq. CH₃OH (3x): mp 142-143 °C; ¹H NMR (400 MHz, CDCl₃, 25 °C, CHCl₃): δ = 2.10 (q, *J* = 162 Hz, 4H), 2.30 (q, *J* = 162 Hz, 4H), 4.82 (s, 1H), 6.84 (br s, 1H), 6.90 (d, *J* = 8.6 Hz, 2H), 7.68 (d, *J* = 8.6 Hz, 2H); ¹¹B NMR (128.4 MHz, CDCl₃, 25 °C, B(OH)₃/MeOH): δ = -12.8 (d, *J* = 161 Hz, 4B), -10.2 (d, *J* = 162 Hz, 4B). Anal. Calcd. for C₈H₁₄B₈O: C, 45.18; H, 6.63. Found: C, 45.18; H, 6.84.

Method B A light orange solution of 4-ethynylanisole (3.04 g, 23.0 mmol) and nonaborane B₉H₁₃•SMe₂ (1.98 g, 11.5 mmol) in dry toluene (30 mL) was refluxed for 30 min upon which the solution became dark red with vigorous bubbling. The solvent was evaporated and the viscous residue was treated with hexanes and passed through a SiO₂ plug, which was washed with hexanes (100 mL). Evaporation of the hexane eluent left 0.470 g of a yellowish oily mixture of carboranes that slowly crystallized, which was then short-path distilled. The first fraction (27 mg), collected up to 170 °C/0.5 mm Hg, was discarded and a second (0.260 g) was collected up to 230 °C/0.5 mm Hg. The carboranes were heated at 340 °C using Wood's metal bath under an atmosphere of dry nitrogen for 8 hrs. The resulting dark brown/black reaction mixture solidified upon cooling, was dissolved in CH₂Cl₂ and the solution filtered through a silica gel plug. Evaporation of CH₂Cl₂ gave 94 mg (4% yield) of 85% pure (by NMR) phenol **8**.

Preparation of 1-(4-heptyloxyphenyl)-*p*-carborane (9).



A suspension of 1-(4-hydroxyphenyl)-*p*-carborane (**8**, 0.719 g, 3.38 mmol), heptyl tosylate (1.10 g, 4.06 mmol), anhydrous K_2CO_3 (1.41 g, 10.22 mmol), and NBu_4Br (0.109 g, 0.338 mmol) was stirred at reflux in anhydrous CH_3CN (30 mL) overnight. Precipitation was filtered off and washed with CH_2Cl_2 . The solution was evaporated giving a light orange/red oil. The crude product was passed through a short silica gel plug (hexane, $R_f = 0.4$) giving 1.01 g (96% yield) of product **9** as a colorless oil: ^1H NMR (400 MHz, CDCl_3 , 25 °C, CHCl_3): $\delta = 1.50\text{--}3.00$ (br m, 8H), 0.88 (t, $J = 6.9$ Hz, 3H), 1.28–1.40 (m, 6H), 1.42–1.50 (m, 2H), 1.80 (quint, $J = 7.0$ Hz, 2H), 3.99 (t, $J = 6.6$ Hz, 2H), 6.81 (br s, 1H), 6.94 (d, $J = 8.8$ Hz, 2H), 7.69 (d, $J = 8.8$ Hz, 2H); ^{11}B NMR (128.4 MHz, CDCl_3 , 25 °C, $\text{B}(\text{OH})_3/\text{MeOH}$): $\delta = -12.8$ (d, $J = 168$ Hz, 4B), -10.2 (d, $J = 166$ Hz, 4B).

Preparation of 10-Vertex *p*-Carborane



The 10-vertex *p*-carborane was prepared using modified literature procedures starting from 12-vertex *ortho*-carborane (*closo*-1,2- $\text{C}_2\text{B}_{10}\text{H}_{12}$). The steps include degradation of *ortho*-carborane to [*nido*-7,8- $\text{C}_2\text{B}_9\text{H}_{12}$] $^-$ anion and its oxidation with FeCl_3 to [*nido*- $\text{C}_2\text{B}_8\text{H}_{12}$] (Plesek oxidation). Thermal disproportionation of [*nido*- $\text{C}_2\text{B}_8\text{H}_{11}$] $^- \text{Na}^+$ gives *closo*-1,2- $\text{C}_2\text{B}_8\text{H}_{10}$ and [*nido*-6,9- $\text{C}_2\text{B}_8\text{H}_{10}$] $^{2-} 2\text{Na}^+$. The latter is oxidized with anhydrous CuCl_2 to give additional amounts of $\text{C}_2\text{B}_8\text{H}_{10}$. These two batches of $\text{C}_2\text{B}_8\text{H}_{10}$ should be processed separately since the batch from CuCl_2 oxidation is significantly less

pure. Finally, the resulting *closo*-1,2-C₂B₈H₁₀ is thermally isomerized to *p*-carborane, *closo*-1,10-C₂B₈H₁₀.

Alternatively, *p*-carborane (*closo*-1,10-C₂B₈H₁₀) was prepared by thermal dehydrogenation of [*nido*-C₂B₈H₁₂] at 350 °C in a stainless steel bomb for 12 hrs (*careful! hydrogen gas is generated during reaction*). However, in our hands, yields of *closo*-1,10-C₂B₈H₁₀ were only 20% and the main product was an insoluble yellow-green material.

Preparation of K[C₂B₉H₁₂]

ortho-Carborane (C₂B₁₀H₁₂, 10.0 g, 0.069 mol) was dissolved in CH₃OH (50 mL), and KOH was added in three portions (3 x 5.0 g, 0.263 mol). The reaction was exothermic with the development of foam with bubbling. The last portion of KOH dissolved slowly and was assisted by gently refluxing overnight. The reaction was diluted with H₂O (50 mL) and CH₃OH was evaporated. The remaining viscous residue was extracted with Et₂O (3 x 30 mL). The ethereal layers were combined (yellowish color) and diluted with H₂O (75 mL). The Et₂O was removed *in vacuo* giving a slightly red solution of K[C₂B₉H₁₂] (concentration of ~ 1 M).

Oxidation of K[C₂B₉H₁₂]

A ~1 M solution of KC₂B₉H₁₂ (75 mL) water (75 mL), pentane (100 mL), and conc. HCl (15 mL) were added. The solution was cooled to 0 °C in an ice bath, and a cooled solution of anhydrous FeCl₃ (36 g, 0.22 mol) in conc. HCl (25 mL) and H₂O (75

mL) was added. The reaction was vigorously stirred for 2 hours at 0 °C. The red/orange suspension was warmed up to rt, vigorously stirred for another hour, and the pentane was removed after the reaction was poured into a separatory funnel. The aqueous layer was returned to the original reaction vessel, and fresh pentane (100 mL) was added. The separation of pentane was repeated every 30 mins for 2 additional hours at which point the red/orange suspension began to develop a greenish hue. Each individual pentane layer was washed with 2M K₂CO₃ (100 mL), producing a dark green aqueous suspension that was separated and set aside. The pentane layer was filtered, dried (MgSO₄), and filtered. The pentane layers were combined (slight yellow color) and evaporated in cold water (~20 °C) giving 4.5 g (4.3 g was obtained for a second attempt) of a yellow oily residue which was sublimed onto a cold finger at -78 °C (be sure to avoid condensation of H₂O inside finger, 70 °C, 2 mm Hg) giving 3.4 grams of pure *nido*-C₂B₈H₁₂ (40% overall yield from *ortho*-carborane) as a white slightly tacky solid. The remaining residue was a yellow crystalline film. A second attempt provided 3.0 g of *nido*-C₂B₈H₁₂ (36% overall yield from *ortho*-carborane).

Disproportionation of *nido*-C₂B₈H₁₂ to *closo*-1,2-C₂B₈H₁₀ and Na₂C₂B₈H₁₀

A solution of freshly sublimed *nido*-C₂B₈H₁₂ (3.00 g, 24.5 mmol) in Et₂O (50 mL) was treated slowly with a suspension of dry NaH (5 g, 122.5 mmol, 60 % in mineral oil, washed with pentane before use) in Et₂O (100 mL). Once bubbling of H₂ was no longer observed (used bubbler as means to detect, the suspension was stirred for an additional 10 mins and filtered through fritted glass overlaid with cotton. The resulting light yellow

solution was evaporated to dryness and dried *in vacuo* giving 4.7 g of a light yellow tacky residue. The residue was pyrolyzed (some residual ether bubbles off) at 120-200 °C under vacuum (1.5 mm Hg) with a cold finger (-78 °C) collecting 1.10 g of a white crystalline solid.

The remaining off-white solid after the pyrolysis ($\text{Na}_2\text{C}_2\text{B}_8\text{H}_{10}$) was suspended in anhydrous CH_2Cl_2 (50 mL) and freshly dehydrated (140 °C, 2 mm Hg) $\text{CuCl}_2 \cdot 2\text{H}_2\text{O}$ (5 g, 29.3 mmol) was added. The dark brown suspension was stirred overnight at rt under a N_2 atmosphere. In the morning, the white suspension was filtered through a silica gel plug eluting with CH_2Cl_2 . The CH_2Cl_2 was evaporated giving 1.5 g of a light yellow oil. The oil was heated (100 °C) under vacuum (1.5 mm Hg) with a cold finger (-78 °C) and 0.50 g of a white solid was collected via sublimation. The remaining residue was a yellow tacky solid. Total yield of carboranes $\text{C}_2\text{B}_8\text{H}_{10}$ was 1.60 g (54% yield) based on *nido*-carborane $\text{C}_2\text{B}_8\text{H}_{12}$.

Isomerization of *closo*-1,2- $\text{C}_2\text{B}_8\text{H}_{10}$ to *closo*-1,10- $\text{C}_2\text{B}_8\text{H}_{10}$

The crude *ortho*-carborane $\text{C}_2\text{B}_8\text{H}_{10}$ (1.60 g) was divided into two portions and loaded into thick-walled glass tubes. The tubes were evacuated under reduced pressure and back-filled with Ar several times before being sealed under reduced pressure (50 mm Hg). The tubes were heated at 330 °C for 20 hr. The tubes were cooled to -78 °C and carefully opened (*careful! hydrogen gas pressure can develop in some experiments!*). The product was removed with small amounts pentane; a significant amount of insoluble

yellow/green crystalline material was left in one tube, while nearly all solid in the second tube was soluble. The combined solutions were passed through a short silica gel plug (pentane). Evaporation of pentane (at 0 °C on rotovap; *careful! p-carborane is very volatile*) gave 1.00 of *p*-carborane (C₂B₈H₁₀, 59% yield combined for two tubes): ¹H NMR (400 MHz, CDCl₃, 25 °C, CHCl₃): δ 2.02 (q, *J* = 164Hz, 8H), 7.00 (br s, 2H); ¹¹B NMR (128.4 MHz, CDCl₃, 25 °C, B(OH)₃/MeOH): δ -12.5 (s).

Additional pairs of signals at 6.84 and 6.63 ppm and 6.76 and 5.65 ppm in ¹H NMR amount to about 5% of the singlet at 7.00 ppm and are ascribed to the C-H of other isomers of C₂B₈H₁₀.

Acknowledgments

Financial support for this work was received from the National Science Foundation (DMR-0907542).

References

- (1) a) Frenkel, D.; Lekkerkerker, H. N. W.; Stroobants, A. *Nature* **1988**, 332, 822-823; b) Terzis, A. F.; Poon, C. D.; Samulski, E. T.; Luz, Z.; Poupko, R.; Zimmermann, H.; Müller, K.; Toriumi, H.; Photinos, D. J. *J. Am. Chem. Soc.* **1996**, 118, 2226-2234.
- (2) For reviews see: a) Galbart, W. M. *J. Phys. Chem.* **1982**, 86, 4298-4307; b) Osipov, M. A. In *Handbook of Liquid Crystals, Vol. 1* (Eds.: Demus, D., Goodby, J. W., Gray, G. W., Spiess, H. -W., Vill, V.), Wiley-VCH, New York, 1998, pp. 40-71.
- (3) a) Blinov, L. M. In *Handbook of Liquid Crystals, Vol. 1* (Eds.: Demus, D., Goodby, J. W., Gray, G. W., Spiess, H.-W., Vill, V.), Wiley-VCH, New York, **1998**, pp.

477-534; b) Blinov, L. M., Chigrinov, V. G. *Electrooptic Effects in Liquid Crystal Materials*, Springer-Verlag, New York, **1994**.

(4) For example: a) Kirsch, P.; Bremer, M. *Angew. Chem. Int. Ed.* **2000**, *39*, 4216-4235; *Angew. Chem.* **2000**, *112*, 4384-4405; b) Sage, I. C. In *Handbook of Liquid Crystals, Vol. 1* (Eds.: Demus, D., Goodby, J. W., Gray, G. W., Spiess, H.-W., Vill, V.), Wiley-VCH, New York, 1998, pp. 731-762.

(5) a) Zannoni, C. *J. Mater. Chem.* **2001**, *11*, 2637-2646; b) Bates, M. A., Luckhurst, G. R. In *Liquid Crystals I*, (Ed.: Mingos, D. M. P.) *Struct. Bonding*, **1999**, *94*, 66-137.

(6) For example: a) Vanakaras, A. G.; Photinos, D. J. *Mol. Phys.* **1995**, *85*, 1089-1104; b) Emelyanenko, A. V.; Osipov, M. A. *Liq. Cryst.* **1999**, *26*, 187-199.

(7) For recent reviews see: a) Franco-Melgar, M.; Haslam, A. J.; Jackson, G. *Mol. Phys.* **2009**, *107*, 2329-2358; b) Varga, S.; Szalai, I.; Liszi, J.; Jackson, G. *J. Chem. Phys.* **2002**, *116*, 91079119; c) McGrother, S. C.; Gil-Villegas, A.; Jackson, G. *Mol. Phys.* **1998**, *95*, 657-673.

(8) Kaszynski, P.; Pakhomov, S.; Gurskii, M. E.; Erdyakov, S. Y.; Starikova, Z. A.; Lyssenko, K. A.; Antipin, M. Y.; Young, V. G., Jr.; Bubnov, Y. N. *J. Org. Chem.* **2009**, *74*, 1709-1720.

(9) It is assumed that the computed dipole moment values in vacuum are consistent in each series and well reflect the trend. The experimental dipole moments are solvent dependent and exact values are unimportant for present considerations.

(10) For details see the Electronic Supplementary Information.

(11) Janousek, Z.; Kaszynski, P. *Polyhedron*, **1999**, *18*, 3517-3526.

(12) Ringstrand, B.; Kaszynski, P.; Young, V. G., Jr.; Janousek, Z. *Inorg. Chem.* **2010**, *49*, 1166-1179.

(13) For example: a) Douglass, A. G.; Czuprynski, K.; Mierzwa, M.; Kaszynski, P. *Chem. Mater.* **1998**, *10*, 2399-2402; b) Januszko, A.; Kaszynski, P.; Wand, M. D.; More, K. M.; Pakhomov, S.; O'Neill, M. *J. Mater. Chem.* **2004**, *14*, 1544-1553; c) Januszko, A.; Glab, K. L.; Kaszynski, P.; Patel, K.; Lewis, R. A.; Mehl, G. H.; Wand, M. D. *J. Mater. Chem.* **2006**, *16*, 3183-3192; d) Kaszynski, P.; Januszko, A.; Ohta, K.; Nagamine, T.; Potaczek, P.; Young, V. G. Jr.; Endo, Y. *Liq. Cryst.* **2008**, *35*, 1169-1190; e) Jankowiak, A.; Kaszynski, P.; Tilford, W. R.; Ohta, K.; Januszko, A.; Nagamine, T.; Endo, Y. *Beils. J. Org. Chem.* **2009**, *5*, 83.

(14) Hansch, C.; Leo, A.; Taft, R. W. *Chem. Rev.* **1991**, *91*, 165-195.

(15) Keesom, W. H. *Physik Z.* **1921**, *22*, 129 and 643; **1922**, *23*, 225.

(16) An alternative explanation of the trend in ΔT_{NI} in series **1–5** based on dimer formation (see ref 6b) is also possible although less consistent with the data.

(17) Smith, J. W. *Electric Dipole Moments*, Butterworths, London 1955, pp 127-169.

(18) Kaszynski, P.; Kulikiewicz, K. K.; Januszko, A.; Douglass, A. G.; Tilford, R. W.; Pakhomov, S.; Patel, M. K.; Ke, Y.; Radziszewski, G. J.; Young, V. G., Jr. *J. Org. Chem.* **2008**.

(19) Kaszynski, P.; Huang, J.; Jenkins, G. S.; Bairamov, K. A.; Lipiak, D. *Mol. Cryst. Liq. Cryst.* **1995**, *260*, 315-332.

(20) Electronic polarizability α is higher by 8% and its anisotropy $\Delta\alpha$ by 23% in the

polar derivative **11b** relative to **11a**.

(21) Neal, M. P.; Parker, A. J. *Chem. Phys. Lett.* **1998**, *294*, 277-284.

(22) 2-Chloro-4-heptylphenyl 4-heptylbicyclo[2.2.2]octane-1-carboxylate.

(23) Naemura, S. In *Physical Properties of Liquid Crystals: Nematics*, (Eds.: Dunmur, D. A., Fukuda, A., and Luckhurst, G. R.) IEE, London, **2001**, pp 523-581.

(24) Ringstrand, B.; Kaszynski, P. *J. Mater. Chem.* **2010**, *20*, 90-95.

(25) Wilson, M. R. *Chem. Soc. Rev.* **2007**, *36*, 1881-1888.

High $\Delta\epsilon$ Nematic Liquid Crystals: Fluxional Zwitterions of the [*closo*-1-CB₉H₁₀]⁻ Cluster.

Reproduced with permission from Ringstrand, B.; Kaszynski, P. *J. Mater. Chem.* **2011**, *21*, 90-95.
Copyright 2011 The Royal Society of Chemistry. Available online:
<http://pubs.rsc.org/en/content/articlelanding/2011/jm/c0jm02075c>

This work describes the synthesis and characterization of sulfonium **4** zwitterionic derivatives of the [*closo*-1-CB₉H₁₀]⁻ anion, and their comparison to analogous pyridinium derivatives **3**. Compounds **4** represent the first examples of polar materials type **II**, in which the configuration at the sulfur center inverts at and above ambient temperature leading to shape-shifting molecules. The goal was to determine the solubility of the nematic zwitterions **3** and **4** in nematic hosts and their effect on the dielectric anisotropy ($\Delta\epsilon$) of the bulk material. Results demonstrated that pyridinium nematics **3** were soluble in **CI Ester** and increased $\Delta\epsilon$ of the bulk material. However, pyridinium nematics **3** were insoluble in **6-CHBT** and **ZLI-132**. Sulfonium nematics **4** were soluble in all **CI Ester**, **6-CHBT**, and **ZLI-132** and increased $\Delta\epsilon$ of the bulk material. Comparison of the data revealed that sulfonium derivatives **4** have greater solubility in nematic hosts, lower tendency to aggregate, and lower impact on host's viscosity than pyridinium nematics (**3**). This, in part, is attributed to facile epimerization at the sulfur center in **4**, which permits for the coexistence of two shapes of molecules in the bulk material: a linear

molecule, which results from the *trans* configuration of substituents on the thiane ring, and a bent molecule, which results from the *cis* configuration of substituents on the thiane ring. Compared to polar materials of type **I** (Part III, Chapter 1), polar materials type **II** display nematic behavior and are more soluble in nematic hosts.

My role in this work was the synthesis and characterization of all compounds. The methodology used to synthesize pyridinium **3** and sulfonium **4** zwitterions was developed earlier in my dissertation studies (see Part II, Chapters 1 and 3). I was also responsible for preparing the solutions of polar zwitterions **3** and **4** in the nematic hosts and performing the dielectric measurements using the Liquid Crystal Analysis System.

Dr. Piotr Kaszynski performed quantum mechanical calculations that permitted the dielectric results for **3** and **4** to be analyzed using the Maier-Meier relationship.

Abstract

A new class of nematics with high dielectric anisotropy ($\Delta\epsilon$) for display applications has been developed and characterized by thermal and dielectric methods in mixtures with 3 nematic hosts: ClEster, 6-CHBT, and ZLI-1132. The key structural element is the zwitterionic derivative of the [*closo*-1-CB₉H₁₀]⁻ anion substituted at the B(10) position with either pyridinium (**3**) or sulfonium (**4**) groups. The zwitterions increase the longitudinal molecular electric dipole moment by 8 D – 12 D and give rise to $\Delta\epsilon$ in the range of 22 – 113. The sulfonium derivatives **4** have higher solubility in

nematic hosts, lower tendency to aggregation, and lower impact on host's viscosity than pyridinium **3**. This, in part, is attributed to facile epimerization at the sulfur center in **4** and existence of the *trans/cis* equilibrium. Experimental results are augmented with DFT calculations and analyzed using the Maier-Meier relationship.

Introduction

Polar liquid crystals are key components of mixtures for liquid crystals display (LCD) technologies.^{1,2} The molecular dipole moment, its magnitude and orientation, dictates the dielectric anisotropy ($\Delta\epsilon$) of the material, which directly affects the voltage characteristic of the electro-optical switching.³ Dielectric properties of the mixture are a sum of mole fraction x_i of dielectric parameters of individual components (Equation 1). Similar additivity is often observed for the nematic-isotropic transition temperature (T_{NI}), and both of these relationships are used to formulate mixtures with desired phase range and dielectrics. Therefore, compounds that exhibit high $\Delta\epsilon$, moderate T_{NI} , and have minimal effect on material's viscosity are of particular interest for technological applications.⁴

$$\Delta\epsilon = \sum_i x_i \Delta\epsilon_i \quad (1)$$

Compounds with a moderate molecular dipole moment and $\Delta\epsilon$ in a range of 10 – 30 are designed using polar groups such as CN, F, CF₃, and OCF₃, and also dipolar rings

such pyrimidine and dioxane.^{1,4} Using a combination of these elements a handful of derivatives with $\Delta\epsilon$ above 30 have been prepared, but typically with significantly compromised stability of the nematic phase.⁴ To develop materials with higher dielectric anisotropy, we have focused on zwitterionic derivatives **A** and **B** of the [*closo*-1-CB₉H₁₀]⁻ cluster (**I**, Figure 1) as structural elements of liquid crystals. Recently, we demonstrated first such derivatives of type **A**, compounds **1** and **2** (Figure 2), as high $\Delta\epsilon$ additives to a nematic host.⁵ The compounds were effective although poorly soluble in nematic hosts due to high melting point and tendency to aggregate. The second class of compounds, derivatives of type **B** in which the onium fragment is attached to the B(10) position, are much more promising. Our preliminary results⁶ demonstrated that pyridinium derivatives **3a** and **3b** exhibit nematic phases with $T_{NI} > 100$ °C, high $\Delta\epsilon$, and good solubility in some nematics, but still unsatisfactory in 6-CHBT and ZLI mixtures, which are good models of LCD materials. A record high $\Delta\epsilon$ of about 113 was extrapolated for **3c** from dilute solutions in a nematic host, however this compound has low solubility.⁶

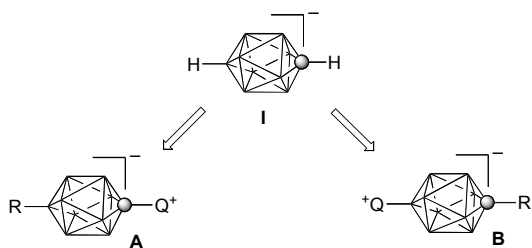


Figure 1. The structures of the [*closo*-1-CB₉H₁₀]⁻ anion (**I**) and its polar derivatives **A** and **B**. Each vertex represents a BH fragment, the sphere is a carbon atom, and Q⁺ stands for an onium group such as an ammonium, sulfonium, or pyridinium.

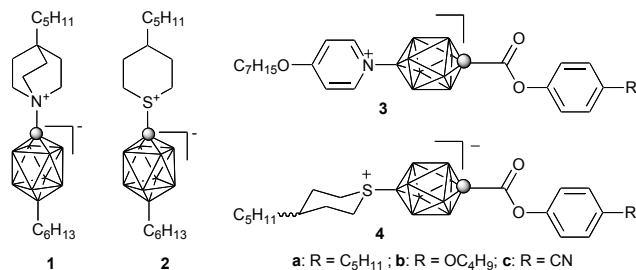


Figure 2. Structures of **1–4**.

In order to increase solubility of the polar additives, we focused on sulfonium derivatives **4** (Figure 2). Here we report a new class of highly polar mesogens exhibiting fluxional behavior that have positive effect on solubility of the additive and viscosity of the nematic mixture. The dielectric results for sulfonium **4** are contrasted with those for pyridinium **3** and analyzed using the Maier-Meier relationship with the aid of DFT calculations.

Results and Discussion

Synthesis

Colorless esters **4a** and **4b** were prepared from sulfonium acid **5** in yields >85% (Scheme 1). The acid was first converted to the corresponding acid chloride using $(\text{COCl})_2$ in the presence of a catalytic amount of DMF, and then reacted with an appropriate phenol in the presence of Et_3N . Acid **5** was obtained by alkylative cyclization of inner salt **6** with dibromide⁷ under hydrolytic conditions⁸ (Scheme 1). For comparison purposes ester **8** (Figure 3), lacking the pentyl substituent at the

thiacyclohexane ring, was obtained from appropriate carboxylic acid as previously described for its methoxy analogue.⁸ The preparation of pyridinium esters **3** is described elsewhere.⁶

Scheme 1

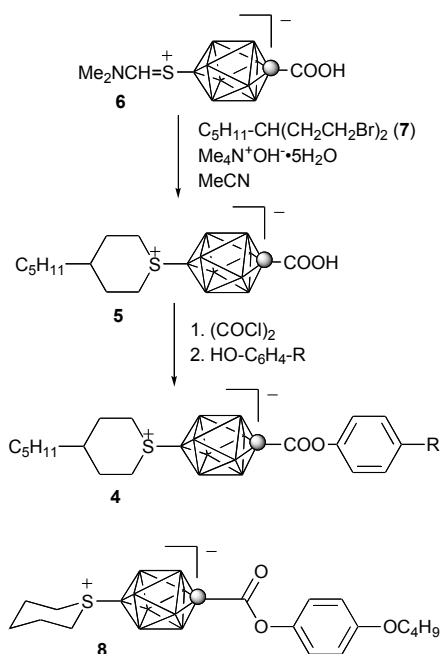


Figure 3. The structure of **8**.

Fluxional Behavior of **4**

Analysis of ^1H NMR spectra of sulfonium derivatives **4a**, **4b** and also the carboxylic acid **5** revealed a coexistence of two isomeric forms, the trans and the cis, in a ratio of about 4:1 (Figure 4). Temperature-dependent ^1H NMR studies yielded difference in enthalpy, $\Delta\text{H} = 0.83 \pm 0.04 \text{ kcal mol}^{-1}$, and entropy, $\Delta\text{S} = 0.2 \pm 0.1 \text{ cal mol}^{-1} \text{ K}^{-1}$, between **4a-cis** and **4a-trans**.⁹ NMR experiments also demonstrated that the

barrier to epimerization at the sulfur center is low and the equilibrium is established quickly within less than 10 min above ambient temperature.

Computational analysis at the B3LYP/6-31G(d,p) level of theory confirmed these results, and the energy difference between the trans and cis forms was calculated at $\Delta H = 1.28 \text{ kcal mol}^{-1}$ ($\Delta S = -3.8 \text{ cal mol}^{-1} \text{ K}^{-1}$) for both derivatives **4a** and **4b** in gas phase. For a better understanding of the fluxional character of mesogens **2** and **4**, models **9** and **10** were analyzed using the DFT and MP2 methods.

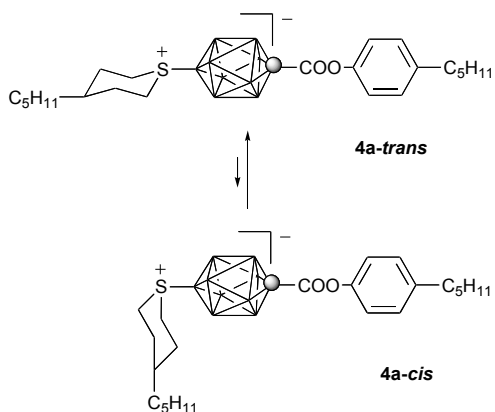
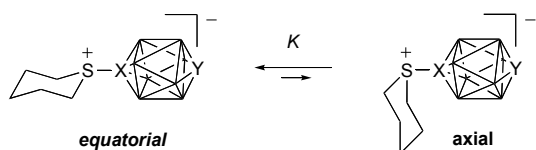


Figure 4. Interconversion of the trans and cis isomers of **4a**. Two major conformers are shown.

Results shown in Table 1 demonstrate that the epimerization process is easier for the B(10) isomer **10** than for the C(1) isomer **9** by 7 kcal mol^{-1} . The enthalpy of activation ΔH^\ddagger calculated for the former is about 24 kcal mol^{-1} , which is consistent with a relatively fast epimerization observed for **4** even at ambient temperature. In contrast, epimerization of the C(1) isomer **9** requires elevated temperatures, presumably above $100 \text{ }^\circ\text{C}$. In addition, **9** has a shorter cage–S bond by nearly 0.1 \AA , which affects the

stability of the axial epimer and, consequently, the position of the axial/equatorial equilibrium. Thus, for the B-isomer with the longer cage–S bond ($d_{S-B} = 1.854 \text{ \AA}$) the ΔG value is small and the concentration of the axial conformer is high ($K_{298} = 2$). In contrast, the steric energy for the C(1)-isomers is higher by 1.8 kcal/mol, which corresponds to a concentration of about 2% of the axial form at the equilibrium. These results are consistent with a single isomer of **2** observed by NMR spectroscopy.⁵

Table 1. Molecular parameters for **9** and **10**.^a



Compound	ΔH^\ddagger /kcal mol ⁻¹	ΔG_{298} /kcal mol ⁻¹	K_{298}	d_{S-X}^b /Å	μ^c /D
9 , X = C, Y = B	31.2	2.2	42	1.750	14.4
10 , X = B, Y = C	24.2	0.4	2	1.854	8.75

^a MP2/6-31G(d,p) level calculations with B3LYP/6-31G(d,p) thermodynamic corrections. ^b Interatomic distance between the S and the cage's C or B atoms in the equatorial epimer. ^c Dipole moment of the equatorial epimer.

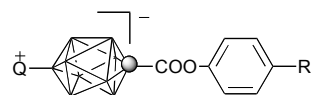
Thermal Properties

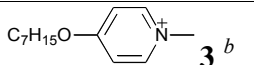
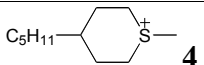
Polarized optical microscopy (POM) and differential scanning calorimetry (DSC) demonstrated that only one sulfonium derivative, ester **4b** exhibits a monotropic nematic phase with a clearing temperature of 98 °C (Table 2). A supercooled sample of ester **4a**

crystallized at 60 °C, 38 K below melting, without showing a mesophase. In contrast all three pyridine derivatives **3a–3c** exhibit a mesophase, although only one, the butoxy **3b** has an enantiotropic nematic phase. Considering that a replacement of the oxygen atom in **3b** with a CH₂ group in **3a** results in a 43 K decrease of the N-I transition temperature, a monotropic T_{NI} of about 55 °C could be expected for **4a**.

No mesophase was observed in **8** even in a sample supercooled by 20 K. A comparison of **4b** and **8** demonstrated that the pentyl chain on the thiacyclohexane ring lowers the melting point by 38 K.

Table 2. Transition temperatures (°C) for **3** and **4**.^a



Q = R	 3 ^b	 4
a , C ₅ H ₁₁	Cr 120 (N 114) I	Cr 97 I
b , OC ₄ H ₉	Cr 122 N 156 I	Cr 101 (N 97) I
c , CN	Cr 128 (N 129) I	^c

^a Cr-crystal, N-nematic, I-isotropic. Monotropic transitions in parentheses. Transition enthalpies are given in ESI. ^b Ref 6. ^c Not prepared.

Binary Mixtures

Pyridinium and sulfonium derivatives **3** and **4**, and also **11**, a carborane analogue of **3c**,⁶ were investigated as low concentration additives to three nematic hosts: ClEster, 6-CHBT, and ZLI-1132 (Figure 5). The first host with a small negative $\Delta\epsilon$ was found to

be a good solvent for zwitterions of type **A** (Figure 1).⁵ The last two hosts have significant positive $\Delta\epsilon$ (+7.6 for 6-CHBT and +11.5 for ZLI-1132) and are models for industrial LCD materials. Results for binary mixtures are shown in Table 3.

Table 3. Extrapolated parameters for selected compounds.^a

	host	$[T_{NI}]$ / $^{\circ}\text{C}$	$\epsilon_{ }$	ϵ_{\perp}	$\Delta\epsilon$	S_{app}^b	g^b
3a	ClEster	103±1	54.8±0.3	12.8±0.1	42.0±0.3	0.62	0.32
3c	ClEster	95.5±1	136.2±0.3	22.8±0.3	113.4±0.6	0.66	0.35
4a	ClEster	89±2	35.0±0.2	9.7±0.2	25.3±0.2	0.59	0.46
	6-CHBT	112±2	41.3±0.2	11.8±0.2	29.5±0.3	0.57	0.56
	ZLI-1132	36	30.7	8.6	22.1	–	–
4b	6-CHBT	133±2	47.7±0.1	12.2±0.1	35.5±0.1	0.63	0.72
11	ClEster	98±1	21.0±0.1	5.8±0.1	15.2±0.1	0.59	0.35

^a For details see SI. ^b Error ≤ 0.01

Three esters, **3a**, **4a**, and **3c** were tested in ClEster host. While the first two compounds showed good solubility to at least 15 mol %, the nitrile **3c** gave stable solutions only at or below 3 mol%, and a 5.6 mol% solution was inhomogeneous after 4 hr at rt. Despite good solubility in ClEster, the pyridinium ester **3a** did not form homogenous solutions with 6-CHBT at a concentration even as low as 2.5 mol%. In contrast, both sulfonium esters **4a** and **4b** were soluble in ClEster and 6-CHBT hosts at concentrations up to about 11 mol %, which was the highest concentration tested. In addition, sulfonium **4a** formed a stable 2.8 mol % solution in ZLI-1132.

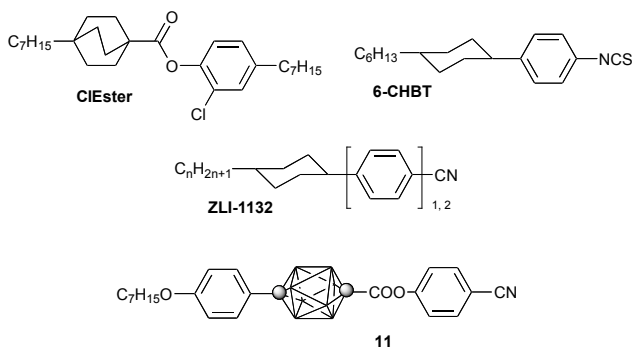


Figure 5. Structures of nematic hosts and compound 11.

Thermal analysis of the solutions revealed that the T_{NI} of a mixture increases approximately linearly with increasing concentration of the additive in ClEster and 6-CHBT (Figure 6) with the least linear behavior of **3c**. Interestingly, the $[T_{NI}]$ values (virtual T_{NI}) extrapolated for the two sulfonium esters **4a** and **4b** are significantly higher than those measured for the pure compounds, by 36 K for the latter and at least 40 K for the former in 6-CHBT. This indicates that the nematic phase in binary mixtures of **4** in 6-CHBT and ClEster is markedly expanded. Results for **4a** also demonstrate a strong dependence of the $[T_{NI}]$ on the host with a difference of about 50 K observed between ClEster and ZLI-1132 (Table 3). In contrast to sulfonium esters, the $[T_{NI}]$ values obtained for the pyridinium esters **3** are within the expectation and moderately lower than those measured for pure compounds.

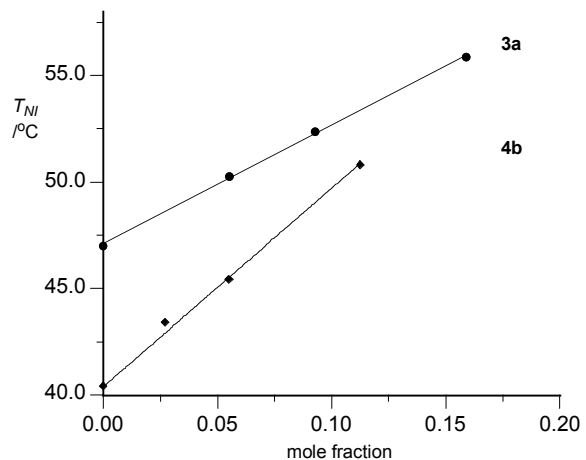


Figure 6. A plot of peak temperature of the N-I transition for binary mixtures pyridinium **3a** in ClEster (circles) and sulfonium **4b** in 6-CHBT (diamonds).

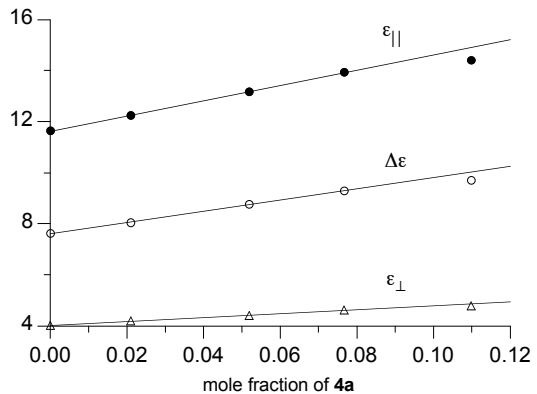
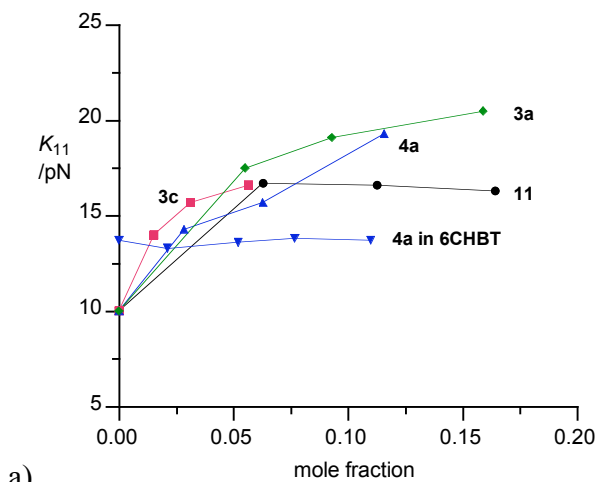
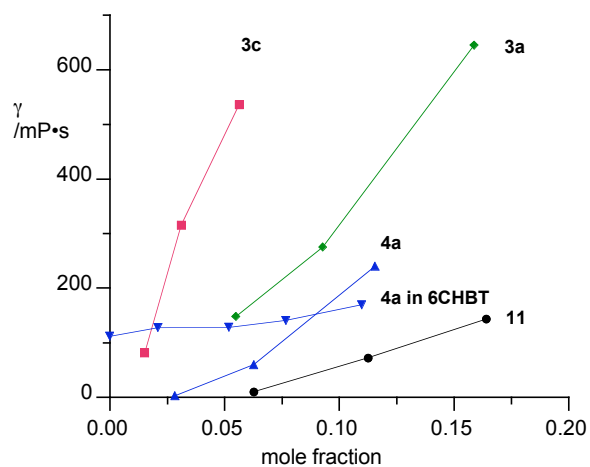


Figure 7. Dielectric parameters as a function of the mole fraction of **4a** in 6-CHBT. The last data point deviates from linearity.



a)



b)

Figure 8. Elastic constant K_{11} (a) and viscosity γ (b) of binary mixtures of pyridinium **3a** (green diamond) and **3c** (red square), sulfonium **4a** (blue triangle up), and carborane **11** (black circle) in ClEster. For comparison sulfonium **4a** in 6-CHBT is also shown (blue triangle down). Lines are guide for the eye.

Analysis of solution dielectric data shows that the permittivity of the mixtures increases approximately linearly with the increasing mole fraction of the additive (Figure 7). This indicates that none or little aggregation of the polar molecules takes place in

solution at this concentration, which is in sharp contrast with compounds of type **A**.⁵ The extrapolated dielectric parameters for pure additives **3** and **4** are impressive (Table 3), especially those obtained for the cyano derivative **3c** ($\epsilon_{||} = 136$ and $\Delta\epsilon = 113$), which are the highest ever recorded for a nematic material.⁴ A comparison with the nitrile **11**, a non-zwitterionic analogue of **3c**, shows that replacement of the C–C fragment in **11** with the isosteric polar fragment $N^+–B^-$ in **3c** results in an increase of $\Delta\epsilon$ by nearly 100! Dielectric anisotropy, $\Delta\epsilon$, extrapolated for the sulfonium ester **4a** is lower than for pyridinium analogue **3a** by about 17 in ClEster (Table 3).

Further analysis of dielectric data revealed that the pyridinium and sulfonium additives increase elastic constant K_{11} of the ClEster host by about 50%-100% (Figure 8a). In contrast the K_{11} value for solutions of sulfonium **4a** and **4b** in 6-CHBT remains approximately constant at about 14 pN.

Similar differences between the two hosts were also observed for the viscosity of the solutions. In ClEster host viscosity of the binary mixture appears to increase with increasing $\Delta\epsilon$ of the additive (Figure 8b). A comparison of solutions of sulfonium **4a** in ClEster with those in 6-CHBT demonstrates that the additive increases viscosity much less in the latter. Assuming linear increase of γ with concentration the extrapolated viscosity is 0.58 P•s for **4a** and 0.31 P•s for **4b**. For comparison, extrapolation from 3 data points gives a value of 10.8 P•s for **3c** and 1.25 P•s for the non-zwitterionic **11** in ClEster.

Unfortunately, direct comparison of pyridinium and sulfonium in 6-CHBT is not possible.

Analysis of Dielectric Data

Dielectric parameters extrapolated for pure additives were analyzed using the Maier-Meier relationship,^{10,11} which connects molecular and phase parameters. Using experimental $\epsilon_{||}$ and $\Delta\epsilon$ values and DFT-calculated parameters μ , α , and β (Table 4), Equations 2 and 3 permitted the calculation of the apparent order parameter S_{app} and the Kirkwood factor g (Equation 4) shown in Table 3. The field parameters F and h in Equations 2 and 3 were calculated using the extrapolated dielectric parameters for each additive and electronic polarizability α of the host. Full protocol for the calculations is given in the ESI.¹²

$$\Delta\epsilon = \frac{NFh}{\epsilon_0} \left\{ \Delta\alpha - \frac{F\mu_{eff}^2}{2k_B T} (1 - 3\cos^2 \beta) \right\} S \quad (2)$$

$$\epsilon_{||} = 1 + \frac{NFh}{\epsilon_0} \left\{ \bar{\alpha} + \frac{2}{3} \Delta\alpha S + \frac{F\mu_{eff}^2}{3k_B T} [1 - (1 - 3\cos^2 \beta) S] \right\} \quad (3)$$

$$\mu_{eff}^2 = g\mu^2 \quad (4)$$

Table 4. Calculated molecular parameters for selected compounds.^a

	$\mu_{ }$ /D	μ_{\perp} /D	μ /D	β ^b /°	$\Delta\alpha$ /Å ³	α_{avg} /Å ³
3a	13.99	3.31	14.38	13	51.81	61.06
3c	20.23	1.79	20.31	5	52.23	55.01
4a-trans	9.62	2.31	9.89	13	41.86	57.26
4a-cis	8.49	3.02	9.02	20	35.89	56.74
4a ^c	9.03	2.50	9.64	15	40.16	57.06
4b-trans	8.89	2.62	9.27	16	42.72	56.34
4b-cis	7.69	3.45	8.43	24	36.65	55.86
4b ^c	8.63	2.80	9.07	18	41.50	56.17
11	8.10	0.51	8.11	4	50.99	55.01

^a Vacuum dipole moments and polarizabilities Obtained at the B3LYP/6-31G(d,p) level of theory. Polarizability units were converted from a.u. to Å³ using the factor 0.1482. ^b Angle between the net dipole vector m and $m_{||}$. For details see the SI. ^c Calculated for an average molecule at the equilibrium ([cis] = 21.5 mol%).

The calculated S_{app} values are about 0.6 (Table 3), which indicates that all additives have reasonably high local order parameter and are well aligned with the nematic director of the host. A detailed comparison shows that the sulfonium derivatives **4** have slightly lower S_{app} (less aligned) than pyridinium **3** and carborane **11**, which is presumably related to the epimerization at the *S*-center and less anisometric average molecular shape.

The Kirkwood parameter g is moderate and about 0.35 for pyridinium **3**, while for

the sulfonium **4** is markedly greater reaching a value of 0.72 for **4b** in 6-CHBT. This indicates less aggregation of the polar molecules in the liquid phase, which is consistent with higher solubility of the sulfonium **4** than pyridinium **3**.

Summary and Conclusions

Sulfonium esters **4** are more soluble, have lower local order parameter S_{app} , and higher Kirkwood parameter g than the pyridinium derivatives **3**. The size of the molecular dipole moment alone cannot satisfactorily explain these observed differences. For instance, carborane **11** and sulfonium **4** have similar dipole moments, yet the g value for the former is similar to that of highly polar pyridinium **3c**. However, the observed differences in behavior of **3** and **4** are consistent with the fluxional behavior of the sulfonium and fast interconversion of the trans and cis epimers in the latter in the nematic phase.

Fast interconversion of each molecule of **4** between two forms, linear (**4-trans**) and bent (**4-cis**, Figure 4), results in an average molecule shape that is less anisometric than that for the rigid pyridinium **3**. In consequence, the more linear pyridinium exhibits better alignment with the nematic director of the host (higher S_{app}) than the shape-shifting sulfonium (Table 3). Also, fast epimerization at the S-center decreases the tendency of polar molecules to aggregate, which results in higher solubility and greater Kirkwood factor g for sulfonium than the pyridinium analogues. This fluxional shape is also a likely factor contributing to lower viscosity observed for nematic solutions of sulfonium

4 than pyridinium **3**. Such an effect of sterically demanding additives, including carborane derivatives,¹³ on phase viscosity has been observed before. Thermal and dielectric results also indicate that the additive's effect on phase properties is host-dependent, and sulfonium **4** appears to be particularly compatible with 6-CHBT: the additive expands the nematic phase and has high g factor.

In summary, sulfonium derivatives **4** represent a new concept in designing polar additives. They combine the polar zwitterionic fragment, that gives rise to a large positive $\Delta\epsilon$, and shape-shifting ability, which results in high solubility, high effective electric dipole moment μ_{eff} , and relatively low contribution to rotational viscosity γ . Further modification of polar properties and consequently $\Delta\epsilon$ of sulfonium derivatives of type **B** can be accomplished by proper substitution of the phenol part of the ester **4** as it was demonstrated for the pyridinium derivatives **3a** and **3c**.

Computational Details

Quantum-mechanical calculations were carried out using Gaussian 09 suite of programs. Geometry optimizations for unconstrained conformers of **3** and **4** with the most extended molecular shapes were undertaken at the B3LYP/6-31G(d,p) level of theory using default convergence limits. Geometry and total energy for model compounds **9** and **10** were obtained using the MP2/6-31G(d,p) method. Dipole moments and exact electronic polarizabilities for **3** and **4** for analysis with the Maier-Meier relationship were obtained using the B3LYP/6-31G(d,p) method. Dipole moment

components μ and polarizability tensors α were calculated in Gaussian standard orientation of each molecule (charge based), which is close to the principal moment of inertia coordinates (mass based).

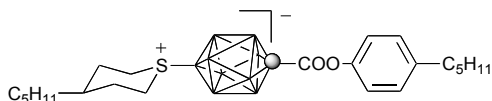
Experimental Section

Reagents and solvents were obtained commercially. NEt_3 was distilled over CaH_2 , and DMF was stored over freshly activated 4 Å molecular sieves. *N,N*-Dimethylthioformamide was distilled (80 °C, 0.25 mm Hg) prior to use. All other reagents were used as supplied. Reactions were carried out under Ar, and subsequent manipulations were conducted in air. NMR spectra were obtained at 128.4 MHz (^{11}B) and 400.1 MHz (^1H) in CD_3CN , CD_3OD , or CDCl_3 . ^1H NMR spectra were referenced to the solvent, and ^{11}B NMR chemical shifts were referenced to an external boric acid sample in CH_3OH that was set to 18.1 ppm. Thermal analysis was performed using a TA Instruments 2920 DSC. Transition temperatures (onset) and enthalpies were obtained using small samples (1-2 mg) and a heating rate of 5 K min^{-1} under a flow of nitrogen gas.

Preparation of Esters 4 and 8. General Procedure. A suspension of appropriate carboxylic acid in anhydrous CH_2Cl_2 was treated with $(\text{COCl})_2$ (1.5 equivalents) and anhydrous DMF (0.1 equivalents) at rt. The suspension began to bubble, and the reaction mixture became homogeneous. After 30 mins, the light yellow solution was evaporated to

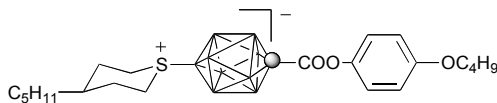
dryness, and appropriate phenol (1.5 equivalents) and freshly distilled NEt_3 (3.0 equivalents) were added. The reaction was stirred overnight at rt or monitored by TLC (CH_2Cl_2 or $\text{CH}_2\text{Cl}_2/\text{hexane}$, 1:1). The reaction mixture was evaporated to dryness, and the crude product was passed through a short silica-gel plug (CH_2Cl_2 or $\text{CH}_2\text{Cl}_2/\text{hexane}$, 1:1). The product was passed through a cotton plug, washed with hot hexane, and repeatedly recrystallized typically from combinations of cold CH_3CN , cold iso-octane/toluene mixtures, or cold aqueous EtOH.

Preparation of ester of [*closo*-1- CB_9H_8 -1-COOH-10-(1-(1-(4- C_5H_{11})- $\text{C}_5\text{H}_9\text{S}$))] and 4-pentylphenol (4a**).**



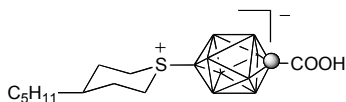
Following the General Method, ester **4a** was obtained in 93% yield as an off-white solid after chromatography. The product was recrystallized twice from cold *iso*-octane/toluene ($-20\text{ }^\circ\text{C}$) and three times from cold CH_3CN ($-40\text{ }^\circ\text{C}$) giving pure **4a** as a white powder: $R_f = 0.74$ ($\text{CH}_2\text{Cl}_2/\text{hexane}$, 1:1); mp $96.9\text{ }^\circ\text{C}$ (DSC); ^1H NMR (400.1 MHz, CDCl_3 , δ): (equatorial epimer, 78%) 0.6-2.5 (br m, 8H), 0.88-0.94 (m, 6H), 1.25-1.40 (m, 12H), 1.64-1.80 (m, 4H), 2.25-2.39 (m, 1H), 2.39 (br d, $J = 14.7\text{ Hz}$, 2H), 2.63 (t, $J = 7.7\text{ Hz}$, 2H), 3.43 (t, $J = 12.3\text{ Hz}$, 2H), 3.72 (br d, $J = 12.2\text{ Hz}$, 2H), 7.24 (s, 4H); (axial epimer, 22%, characteristic signals) δ 2.07-2.15 (m, 2H), 3.54-3.61 (m, 2H); ^{11}B NMR (128.4 MHz, CDCl_3 , δ): -19.7 (d, $J = 133\text{ Hz}$, 4B), -14.1 (d, $J = 151\text{ Hz}$, 4B), 31.6 (s, 1B); HRMS (ESI, m/z): $[\text{M}+\text{H}]^+$ calcd. for $\text{C}_{23}\text{H}_{44}\text{B}_9\text{O}_2\text{S}$, 483.3899; found, 483.3907.

Preparation of ester of [*closo*-1-CB₉H₈-1-COOH-10-(1-(1-(4-C₅H₁₁)-C₅H₉S))] and 4-butoxyphenol (4b**).**



Following the General Method, ester **4b** was obtained in 86% yield as an off-white solid after chromatography. The product was recrystallized twice from cold *iso*-octane/toluene (-20 °C) and twice from cold CH₃CN (-40 °C) giving pure ester **4b** as white leaflets: $R_f = 0.7$ (CH₂Cl₂/hexane, 1:1); mp 101.2 °C (DSC); ¹H NMR (400.1 MHz, CDCl₃, δ): (equatorial epimer, 80%) 0.6-2.5 (br m, 8H), 0.91 (t, $J = 6.9$ Hz, 3H), 0.99 (t, $J = 7.4$ Hz, 3H), 1.26-1.42 (m, 8H) 1.51 (sext, $J = 7.4$ Hz, 2H), 1.65-1.83 (m, 4H), 2.26-2.39 (m, 1H), 2.39 (br d, $J = 13.6$ Hz, 2H), 3.43 (t, $J = 12.1$ Hz, 2H), 3.72 (d, $J = 12.6$ Hz, 2H), 3.98 (t, $J = 6.5$ Hz, 2H), 6.94 (d, $J = 9.0$ Hz, 2H), 7.24 (d, $J = 9.0$ Hz, 2H); (axial epimer, 20%, characteristic signals) δ 2.07-2.16 (m, 2H), 3.53-3.63 (m, 2H); ¹¹B NMR (128.4 MHz, CDCl₃, δ): -19.6 (d, $J = 138$ Hz, 4B), -14.0 (d, $J = 163$ Hz, 4B), 31.7 (s, 1B); HRMS (ESI, m/z) [M+H]⁺ calcd. for C₂₂H₄₂B₉O₃S, 485.3692; found, 485.3707.

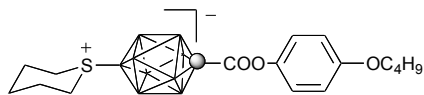
Preparation of acid [*closo*-1-CB₉H₈-1-COOH-10-(1-(4-C₅H₁₁)-C₅H₉S)] (5**).**



A solution of crude protected mercaptan [*closo*-1-CB₉H₈-1-COOH-10-SCHN(CH₃)₂] (**6**, 0.062 g, 0.25 mmol) in anhydrous CH₃CN (4 mL) was treated with a solution of NMe₄⁺OH⁻•5H₂O (0.180 g, 0.99 mmol) in anhydrous CH₃CN (6 mL) resulting in the formation of a white precipitate after mild heating with a heat gun. The suspension

was cooled to rt, and dibromide **7** (0.077 g, 0.257 mmol) was added, and the reaction mixture was stirred for 24 hrs at rt. The reaction mixture was evaporated to dryness and stirred in a methanolic solution (4 mL) of NaOH (0.01 g, 0.250 mmol) at 50 °C for 4 hrs. Solvent was removed to dryness, and 10% HCl (10 mL) was added. The suspension was stirred vigorously with Et₂O (5 mL) until the aqueous layer became homogeneous. The Et₂O layer was separated, and the aqueous layer was further extracted with Et₂O (2 x 5 mL). The Et₂O layers were combined, washed with H₂O, dried (Na₂SO₄), and evaporated leaving crude product as an orange crystalline film. The crude material was passed through a short silica gel plug (CH₃OH/CH₂Cl₂, 1:19, R_f = 0.4) and washed with hot hexane giving 0.036 g (44% yield) of acid [*closo*-1-CB₉H₈-1-COOH-10-(1-C₅H₁₁C₅H₁₀S)] (**5**) as an off-white solid. An analytical sample of **5** was prepared by passing the acid through a cotton plug and recrystallizing twice from cold CH₃CN (-20 °C), once from cold *iso*-octane/toluene (-20 °C), and dried *in vacuo* at 110 °C for 2 hr: mp 215-216 °C; ¹H NMR (400.1 MHz, CD₃OD, δ): (equatorial epimer, 75%) 0.6-2.5 (br m, 8H), 0.92 (t, *J* = 6.7 Hz, 3H), 1.28-1.42 (m, 6H) 1.63-1.80 (m, 4H), 2.17-2.29 (m, 1H), 2.37 (br d, *J* = 9.4 Hz, 2H), 3.41 (t, *J* = 12.5 Hz, 2H), 3.75 (br d, *J* = 12.7 Hz, 2H), (COOH not observed); (axial epimer, 25%, characteristic signals) 2.05-2.12 (m, 2H), 3.50 (d, *J* = 14.0 Hz, 2H), 3.61 (br t, *J* = 11.2 Hz, 2H); ¹¹B NMR (128.4 MHz, CD₃OD, δ): (equatorial epimer) -20.1 (d, *J* = 143 Hz, 4B), -14.6 (d, *J* = 166 Hz, 4B), 31.9 (s, 1B); (axial epimer, characteristic signal) 29.8 (s, 1B). Anal. Calcd for C₁₂H₂₉B₉O₂S: C, 43.06; H, 8.73; found: C, 43.13; H, 8.72.

Preparation of ester of [*closo*-1-CB₉H₈-1-COOH-10-C₅H₁₀S] and 4-butoxyphenol (**8**).



Following the General Method, ester **8** was obtained in 88% yield from acid [*closo*-1-CB₉H₈-1-COOH-10-C₅H₁₀S] as an off-white solid after chromatography. The product was recrystallized twice from cold *iso*-octane/toluene (-20 °C) and twice from cold CH₃CN (-20 °C) giving pure ester **8** as white blades: R_f = 0.55 (CH₂Cl₂); mp 138.5 °C (DSC); ¹H NMR (400.1 MHz, CDCl₃, δ): 0.6-2.5 (br m, 8H), 0.99 (t, *J* = 7.4 Hz, 3H), 1.51 (sext, *J* = 7.5 Hz, 2H) 1.63-1.76 (m, 1H), 1.78 (quint, *J* = 7.0 Hz, 2H), 2.00-2.13 (m, 3H), 2.38-2.48 (m, 2H), 3.42 (td, *J*₁ = 12.4 Hz, *J*₂ = 2.6 Hz, 2H), 3.64 (br d, *J* = 11.4 Hz, 2H), 3.98 (t, *J* = 6.5 Hz, 2H), 6.94 (d, *J* = 9.1 Hz, 2H), 7.24 (d, *J* = 9.0 Hz, 2H); ¹¹B NMR (128.4 MHz, CDCl₃, δ): -19.6 (d, *J* = 143 Hz, 4B), -14.1 (d, *J* = 161 Hz, 4B), 31.2 (s, 1B). Anal. Calcd. for C₁₇H₃₁B₉O₃S: C, 49.46; H, 7.57; found: C, 49.48; H, 7.66.

Acknowledgments

Financial support for this work was received from the National Science Foundation (DMR-0907542). We thank Prof. R. Dabrowski for the gift of ClEster.

References

- (1) Kirsch, P.; Bremer, M. *Angew. Chem. Int. Ed.* **2000**, *39*, 4216-4235.

- (2) Pauluth, D.; Tarumi, K. *J. Mater. Chem.* **2004**, *14*, 1219-1227.
- (3) a) Blinov, L. M. in *Handbook of Liquid Crystals, Vol. 1* (Eds.: Demus, D., Goodby, J. W., Gray, G. W., Spiess, H.-W., Vill, V.), Wiley-VCH, New York, **1998**, pp. 477-534; b) Blinov, L. M., Chigrinov, V. G. *Electrooptic Effects in Liquid Crystal Materials*, Springer-Verlag, New York, **1994**.
- (4) Naemura, S. in *Physical Properties of Liquid Crystals: Nematics*, (Eds.: Dunmur, D.A., Fukuda, A., and Luckhurst, G. R.) IEE, London, **2001**, pp 523-581.
- (5) Ringstrand, B.; Kaszynski, P.; Januszko, A.; Young, V. G., Jr. *J. Mater. Chem.* **2009**, *19*, 9204-9212.
- (6) Ringstrand, B.; Kaszynski, P. *J. Mater. Chem.* **2010**, *20*, 9613-9615.
- (7) J. Thomas, D. Clough *J. Pharm. Pharmacol.* 1963, **15**, 167-177. N. P. Volynskii, L. P. Shcherbakova *Bull. Acad. Sci. USSR, Div. Chem. Sci.* 1979, **28**, 1006-1009.
- (8) Ringstrand, B.; Kaszynski, P.; Young, V. G., Jr.; Janousek, Z. *Inorg. Chem.* **2010**, *49*, 1166-1179.
- (9) For details see the Electronic Supplementary Information.
- (10) Urban, S. in *Physical Properties of Liquid Crystals: Nematics*, (Eds.: Dunmur, D.A., Fukuda, A., and Luckhurst, G. R.) IEE, London, **2001**, pp 267-276.
- (11) Januszko, A.; Glab, K. L.; Kaszynski, P.; Patel, K.; Lewis, R. A.; Mehl, G. H.; Wand, M. D. *J. Mater. Chem.* **2006**, *16*, 3183-3192.

- (12) For another approach to use the Maier-Meier relationship see: D. Demus, T. Inukai *Mol. Cryst. Liq. Cryst.* **2003**, *400*, 39-58.
- (13) Piecek, W.; Glab, K. L.; Januszko, A.; Perkowski, P.; Kaszynski, P. *J. Mater. Chem.* **2009**, *19*, 1173-1182.
- (14) Dabrowski, R.; Jadzyn, J.; Dziaduszek, J.; Stolarz, Z.; Czechowski, G.; Kasprzyk, M. *Z. Naturforsch.* **1999**, *54a*, 448-452.
- (15) Baran, J. W.; Raszewski, Z.; Dabrowski, R.; Kedzierski, J.; Rutkowska, J. *Mol. Cryst. Liq. Cryst.* **1985**, *123*, 237-245.
- (16) Wu, S. T.; Coates, D.; Bartmann, E. *Liq. Cryst.* **1991**, *10*, 635-646.

Anion-Driven Mesogenicity: Ionic Liquid Crystals based on the [*closo*-1-CB₉H₁₀]⁻ Cluster.

Reproduced with permission from Ringstrand, B.; Kaszynski, P.; Monobe, H. *J. Mater. Chem.* **2009**, *19*, 4805-4812. Copyright 2009 The Royal Society of Chemistry. Available online: <http://pubs.rsc.org/en/content/articlelanding/2009/jm/b905457j>

This work describes the first examples of ionic liquid crystals derived from the [*closo*-1-CB₉H₁₀]⁻ anion. These new materials contain an anisometric rigid core anion, instead of an anisometric cation, which is the driving force for molecular arrangement into the liquid crystalline phase.

I was responsible for the preparation and characterization of two series of structurally analogous esters (**1**) and diazenes (**2**) derived from the [*closo*-1-CB₉H₁₀]⁻ anion containing 2 or 3 rings in the rigid core. Esters **1** and diazenes **2** were prepared using the chemistry developed earlier in my dissertation studies (see Part II, Chapters 1 and 2).

Dr. Hirosato Monobe from the Nanotechnology Research Institute, National Institute of Advanced Industrial Science and Technology in Japan performed powder XRD analysis on ionic liquid crystals **1d**[Pyr], **1f**[Pyr], and **2d**[Pyr] and attempted photovoltaic characterization of ester **1d**[Pyr] and diazene **2d**[Pyr]. Dr. Piotr Kaszynski performed quantum mechanical calculations to estimate the molecular length of the salts

that were analyzed by powder XRD.

Abstract

Two series of structurally analogous esters (**1**) and diazenes (**2**) derived from the [*closo*-1-CB₉H₁₀]⁻ anion and containing 2 or 3 rings in the rigid core were prepared and their liquid crystalline properties investigated. Salts containing NMe₄⁺ or NHEt₃⁺ counterion do not exhibit mesophases, whereas the ion pairs with *N*-butyl-4-heptyloxy pyridinium cation [Pyr] exhibit SmA and occasionally soft crystalline phases in the temperature range of 90 °C – 180 °C. Three representative ionic liquid crystals **1d**[Pyr], **1f**[Pyr], and **2d**[Pyr] were investigated by powder XRD. Absorption spectroscopy demonstrated that ester **1e**[Pyr] is transparent above 280 nm and the diazene **2e**[Pyr] exhibits absorption bands typical for azobenzene derivatives.

Introduction

During the past decade, research of ionic liquid crystals (ILCs) has significantly intensified and diversified.¹ Among many intriguing properties, anisotropic ion mobility exhibited by some ILCs generated considerable interest in developing ion-conductive materials²⁻⁶ for applications in batteries⁷ and dye-sensitized solar cells.⁸ It has been established that the nature of the counter anion plays a critical role in the properties.⁹ For instance, high ion-conductivity is observed for salts in which the negative charge of the anion is delocalized and has weak electrostatic interactions with the accompanying mesogenicity-driving cation.⁴ Another important aspect of ILCs is their photophysical behavior; judicious choice of the π chromophore allows to obtain photoresponsive,¹⁰

highly luminescent,¹¹ or NLO active ionic mesogens.¹² In some pyridinium ILCs containing iodide^{13,14} or bromide¹⁵ as the counter anion, charge-transfer phenomenon has been observed. This suggests potential applications for ILCs in photovoltaics, which is the driving force for the operation of solar energy conversion devices.¹⁶

The vast majority of ILCs investigated to date comprise of an organic cation, such as ammonium,^{3,17} imidazolium,^{4,6,18,19} or pyridinium,^{13,20,21} that drives mesogenicity. In general, the anion in these materials is present for charge compensation, but it can significantly affect mesophase stability and the clearing temperature of the bulk material.¹ ILCs in which the anion drives the mesogenic behavior are rare, and in which the ions are in the fully dissociated state are difficult to design. Such materials, especially lithium salts, are sought after for their potential applications as electrolytes for e.g. lithium ion batteries. The closest examples of such ILCs are alkali metal carboxylates,²² phosphates,²³ and phosphonates,²⁴ but their tight oxygen–metal interactions limit the ion conductivity in the neat phase and usefulness as an electrolyte. For this reason binary systems of non-ionic liquid crystal hosts, which contain groups capable of metal ion coordination (typically an oligoethylene oxide chain), and highly ionic metal salts are used to obtain anisotropic metal ion conductivity.²⁵

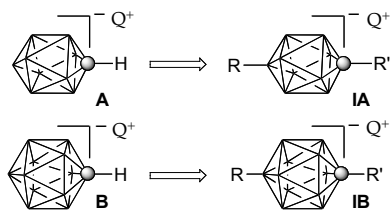


Figure 1. The structures of the $[closo-1-CB_9H_{10}]^-$ and $[closo-1-CB_{11}H_{12}]^-$ clusters (**A** and **B**), and ion pairs of their 1,10- (**IA**) and 1,12-disubstituted (**IB**) derivatives with the counterion Q^+ . Q represents a metal or an onium fragment such as ammonium or pyridinium. Each vertex represents a BH fragment and the sphere is a carbon atom.

closo-Monocarbaborates $[closo-1-CB_9H_{10}]^-$ and $[closo-1-CB_{11}H_{12}]^-$ (**A** and **B**, Figure 1) are particularly attractive structural elements for ILCs due to their electronic and geometrical features.^{26,27} In both structures, the negative charge is fully delocalized over the cage, and the clusters are among the least nucleophilic anions.²⁸ For this reason, clusters **A** and **B** and also some other *closo*-borates have been investigated as counterions in ionic liquids²⁹ and for applications as lithium-ion battery electrolytes.^{30,31} The geometry of the two *closo* clusters **A** and **B** is appropriate for the formation of calamitic liquid crystals, as can be inferred from results for their electrically neutral carborane analogues.³²⁻³⁹ As a consequence of the molecular symmetry, clearing temperatures for the 12-vertex carborane derivatives are generally higher than those for the 10-vertex analogues.^{32,34,36,38} On the other hand, the symmetry of and the energy associated with molecular orbitals allow for much more efficient electronic interactions with π substituents and consequently better control of photophysical properties of 10-vertex cluster derivatives (including those of **A**) than their 12-vertex counterparts, such as derivatives of **B**.^{36,38,40}

The unusual properties of *closo*-boranes prompted us to explore clusters **A** and **B** as structural elements of ILCs and to develop a new class of conductive mesogenic metal salts. As the first step towards this goal, we focused on two series of disubstituted derivatives of [*closo*-1-CB₉H₁₀]⁻ (**IA**), which can be accessed from the recently reported⁴¹ isomerically pure [*closo*-1-CB₉H₈-1-COOH-10-I]⁻. Here, we report the preparation of the first calamitic ILCs based on the [*closo*-1-CB₉H₁₀]⁻ cluster (**A**) and investigation of two series of compounds, esters **1** and diazenes **2**, with three different cations Q⁺ (Figure 2). We establish fundamental structure-property relationships for these ILCs using polarizing optical microscopy (POM), differential scanning calorimetry (DSC), and powder X-ray diffraction (XRD). We also briefly investigate photophysical behavior of two mesogens in solution and neat state.

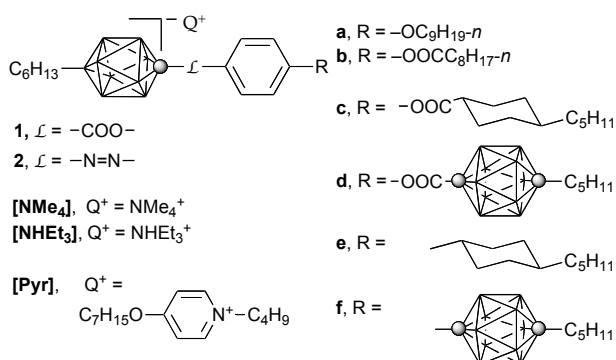


Figure 2. Structures of series **1** and **2**. Each vertex represents a BH fragment and the sphere is a carbon atom.

Results and Discussion

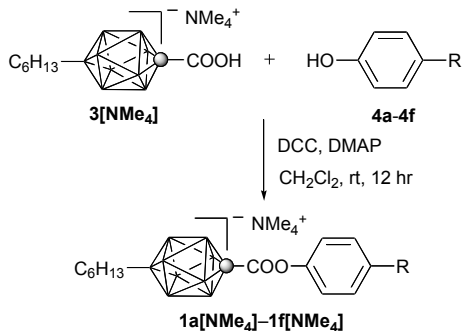
Synthesis

Esters **1a**[NMe₄]-**1f**[NMe₄] were prepared from carboxylic acid **3**[NMe₄] and phenols **4a**-**4f** using dicyclohexylcarbodiimide (DCC) and catalytic amounts of 4-dimethylaminopyridine (DMAP) in CH₂Cl₂ following a general literature procedure⁴² (Scheme 1). The preparation of phenols **4a**,³⁴ **4b**,⁴³ **4c**,³⁵ **4d**,³⁵ and **4f**³³ has been reported before.

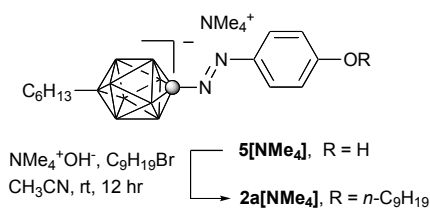
Diazenes **2a**[NMe₄] was prepared by alkylation of azophenol **5**[NMe₄] with 1-bromononane following a similar procedure that was described for the methylation of the parent azophenol⁴⁴ (Scheme 2).

Diazenes **2b**-**2d** were prepared by esterification of azophenol **5**[NMe₄] with acid chlorides **6b**-**6d** in CH₂Cl₂ in the presence of Et₃N (Scheme 3). Complete exchange of counterion NMe₄⁺ for NHEt₃⁺ was observed for diazenes **2b** and **2d** after isolation of the crude product by column chromatography. Acid chlorides **6c**⁴⁵ and **6d**³⁹ were prepared using literature protocols.

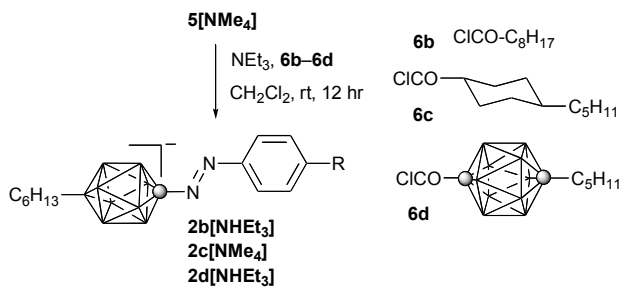
Scheme 1. Synthesis of esters 1[NMe₄]



Scheme 2. Preparation of diazene 2a[NMe₄]



Scheme 3. Synthesis of diazenes 2.

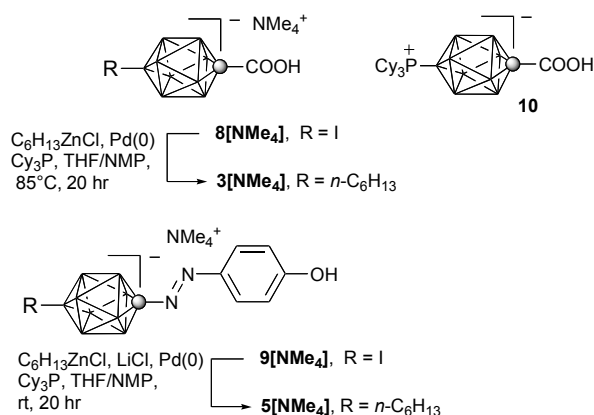


Esters **1a[Pyr]**–**1f[Pyr]** and diazenes **2a[Pyr]**–**2d[Pyr]** were prepared by exchange of the NMe₄⁺ or NHEt₃⁺ cation for *N*-butyl-4-heptyloxypyridinium using bromide **7** in a biphasic CH₂Cl₂/H₂O system.

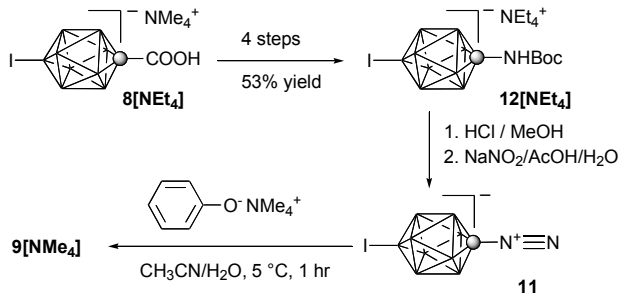
Both carboxylic acid **3[NMe₄]** and azophenol **5[NMe₄]** were prepared from iodides **8[NMe₄]**⁴¹ and **9[NMe₄]**, respectively, using the Negishi coupling^{46,47} with 12-fold excess hexylzinc chloride (Scheme 4). The electron-rich tricyclohexylphosphine

ligand, PCy₃, was conveniently generated *in situ* from air-stable [HPCy₃]BF₄. The choice of the ligand was dictated by its reported efficiency in catalysis of coupling reactions of alkylzinc reagents with a broad range of unactivated iodides, bromides, and chlorides and excellent functional group tolerance.⁴⁸ The carboxyl group of acid **8**[NMe₄] tolerated coupling reaction conditions at elevated temperatures, whereas what appeared to be reduction of the azo group as well as loss of symmetry in the {*closo*-1-CB₉} cluster were observed in azophenol **9**[NMe₄] under similar conditions. The addition of LiCl permitted the coupling reaction of **9**[NMe₄] to occur at room temperature, presumably due to increased reactivity and solubility of the organozinc reagent.⁴⁹ In reactions of **8**[NMe₄] with fewer equivalents of the organozinc reagent, the formation of phosphonium zwitterion **10** by-product was observed. For instance, with 5 equivalents of hexylzinc chloride the phosphonium by-product was isolated in about 3% yield and partially characterized.

Scheme 4. Preparation of intermediates **3**[NMe₄] and **5**[NMe₄].



Scheme 5. Preparation of dinitrogen derivatives **11**.



Azophenol **9**[NMe₄] was prepared by azocoupling of [*closo*-1-CB₉H₈-1-N₂-10-I] (**11**) and tetramethylammonium phenolate (Scheme 5). Dinitrogen species **11**⁵⁰ was prepared in 88% yield starting from carbamate **12**[NEt₄] using a procedure developed for the preparation of the parent dinitrogen derivative [*closo*-1-CB₉H₉-1-N₂].⁴⁴ The carbamate was prepared in a 4-step modified Curtius rearrangement starting from the iodo acid **8**[NEt₄] in a procedure analogous to that described for the protected parent amine [*closo*-1-CB₉H₉-1-NHBoc][NEt₄].⁴⁴ This method represents a marked improvement over our previous synthesis of the iodo amine [*closo*-1-CB₉H₈-1-NH₃-10-I].⁴¹

Liquid Crystalline Properties

Transition temperatures and associated enthalpies for compounds **1**[Pyr] and **2**[Pyr] are shown in Tables 1 and 2. Phase structures were partially assigned by comparison of POM results with published textures for reference compounds,⁵¹

established trends in thermodynamic stability,⁵² and on the basis of powder XRD results for three mesogens. The tetramethylammonium salts (**1a**[NMe₄]-**1b**[NMe₄], **2a**[NMe₄], and **2c**[NMe₄]) and the two triethylammonium salts (**2b**[NHEt₃] and **2d**[NHEt₃]) are non-mesogenic solids with melting points higher than those of the pyridinium salts.

All 3-ring pyridinium salts and 2-ring diazene **2a**[Pyr] exhibit enantiotropic SmA phases. In addition, most esters display enantiotropic crystalline and soft crystalline polymorphism. Esters **1a**[Pyr], **1b**[Pyr], and diazene **2b**[Pyr] do not form liquid crystalline phases even on cooling. For instance, the isotropic phase of diazene **2b**[Pyr] could be supercooled by 15 K before crystallization.

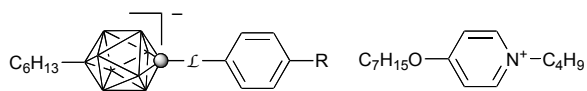
The most interesting polymorphism is displayed by esters **1e**[Pyr] and **1f**[Pyr] for which DSC analysis revealed two phases below the SmA phase. The enthalpy of the transition from the SmA is less than a half of the isotropization enthalpy in both esters, and the two lower phases are separated by a first order transition of 3.2 kJ/mol for **1e**[Pyr] (Figure 3) and 1.5 kJ/mol for **1f**[Pyr]. Optical observations of **1f**[Pyr] revealed pseudo-isotropic regions present in both soft crystalline phases, which is indicative of a non-tilted phase (Figure 4). Both phases exhibit “broken fan” textures characteristic for a crystalline E phase, with the lower temperature phase having sharper features and higher viscosity. This assignment, however, is inconsistent with the absence of weakly birefringent regions expected to form in place of homeotropic domains of SmA. After applying mechanical stress, the higher temperature soft crystalline phase quickly restores the original texture, while the lower temperature phase is more viscous and the change is

permanent. Further cooling of the sample leads to crystallization and change of the texture (Figure 4d).

Among other esters, **1d[Pyr]** exhibits noteworthy polymorphism. Its DSC appears similar to that of **1f[Pyr]** (Figure 3) with a broad high-energy transition at 97 °C followed by two transitions, X-SmA and SmA-I. The last two transitions have comparable energies (Table 1) and undergo little supercooling, while the transition at 97 °C is significantly supercooled. The texture of the unidentified phase X below the SmA phase is similar to that of an E phase (Figure 5) and significantly different from that of a crystalline phase below the X phase. Despite similarity of the textures, the X phase observed for **1d[Pyr]** and X and X' phases found in **1e[Pyr]** and **1f[Pyr]** may have different structures.

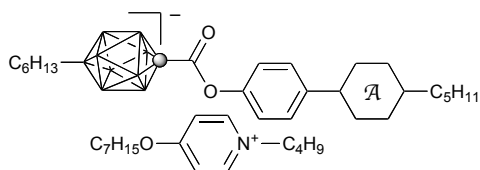
In general, the mesophase stability in both series increases with the increasing size of the substituent R and is the highest for the carborane derivatives **1f[Pyr]** and **1d[Pyr]**. A comparison of the two series demonstrates that esters **1[Pyr]** generally have higher clearing temperatures and richer polymorphism than the diazenes **2[Pyr]**. Among the two-ring mesogens, only diazene **2a[Pyr]** exhibits a SmA phase. A replacement of the CH₂ group in **2a[Pyr]** with C=O in **2b[Pyr]** results in elimination of mesogenic behavior. This is consistent with the generally observed higher mesophase stability for alkoxyazobenzenes than for their alkanoyloxy analogues.⁵³

Table 1. Transition temperatures (°C) and enthalpies (kJ/mol, in parentheses) for selected compounds.



R	L	
	-COO- (1[Pyr])	-N=N- (2[Pyr])
a	Cr ₁ 53 Cr ₂ 127 Cr ₃ 151 I (15.4) (4.5) (20.6)	Cr 93 SmA 115 I (21.9 (9.6)
b	Cr ₁ 64 Cr ₂ 101 X 107 I (9.2) (3.4) (15.1)	Cr 96 I (40.9)
c	Cr 102 SmA 164 I (43.7) (7.0)	Cr ₁ 70 Cr ₂ 106 SmA 139 I (8.8) (21.1) (6.0)
d	Cr ₁ 94 X 162 SmA 180 I (22.7) (11.0) (9.4)	Cr 136 SmA 151 I (46.9) (7.4)

Table 2. Transition temperatures (°C) and enthalpies (kJ/mol, in parentheses) for esters **1e[Pyr]** and **1f[Pyr]**



1e[Pyr] A =	1f[Pyr] A =
Cr 128 (X' 129) X 153 SmA 163 I (19.3) (3.2) (2.4) (4.5)	Cr 120 X' 145 X 166 SmA 187 I (18.1) (1.5) (4.2) (11.4)

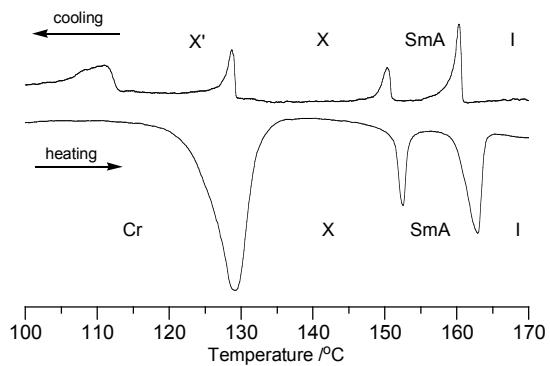
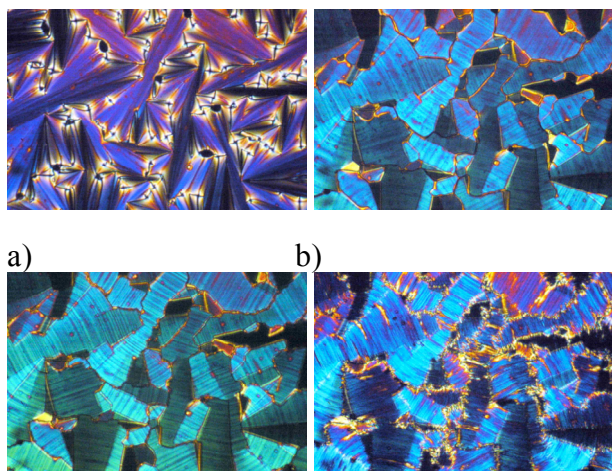


Figure 3. DSC trace of ester **1e[Pyr]**. The heating rate 5 K min^{-1} .



c) d)
 Figure 4. Optical textures of **1f[Pyr]** obtained for the same region of the sample upon cooling at (a) $173 \text{ }^\circ\text{C}$ (SmA), (b) $150 \text{ }^\circ\text{C}$ (X), (c) $125 \text{ }^\circ\text{C}$ (X'), and (d) $90 \text{ }^\circ\text{C}$ (Cr). Magnification $\times 50$.

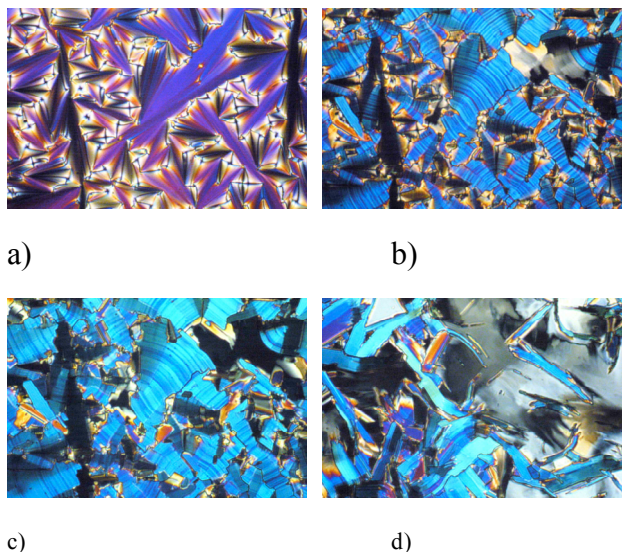


Figure 5. Optical textures of **1d[Pyr]** obtained for the same region of the sample upon cooling at (a) 170 °C (SmA), (b) 161 °C (phase X growing from SmA), (c) 150 °C (X), and (d) 80 °C (Cr). Magnification $\times 50$.

N-Butyl-4-hepyloxypyridinium bromide (**7**) is not mesogenic and melts at 34 °C to an isotropic liquid. Some 4-substituted pyridinium salts were reported to be mesogenic, but they require long alkyl chains.²¹

Powder X-ray diffraction (XRD)

Two close structural analogous, ester **1d[Pyr]** and diazene **2d[Pyr]**, and also ester **1f[Pyr]** were investigated by powder X-ray diffraction to determine their phase structures. Data were collected at several temperatures on cooling from the isotropic phase, and XRD results are shown in Figure 6 and also tabulated in the electronic supporting information.

The XRD results confirmed the SmA phase as the high temperature phase in all three compounds. The diffractograms consist of a single sharp reflection in the small angle region ($00l$) followed by up to 3 higher-order reflections ($00l$) with the reciprocal ratio of d -spacing 1:2:3:4 (Fig. 6). The wide-angle region of the high temperature phase diffractograms shows a broad halo in which two maxima can be distinguished at about $d = 5.5 \text{ \AA}$ and $d = 4.5 \text{ \AA}$ in two compounds (**1d[Pyr]** and **2d[Pyr]**, Figure 6b) and only one broad maximum at $d \approx 5.3 \text{ \AA}$ in ester **1f[Pyr]** (Figure 6a). The maximum with the lower d value can be attributed to the average alkyl chain-alkyl chain correlation distance, while the maxima with $d > 5 \text{ \AA}$ to the correlation involving larger structural units such as the boron clusters in the segregated ionic layer. Similar double halo has been observed for siloxanes ($d = 7.0$ and 4.6 \AA),^{54,55} and fluoroalkyl-containing mesogens ($d = 5.2$ and 4.6 \AA)⁵⁶ in which the large groups microsegregate.

The phases observed below the SmA phase in esters **1d[Pyr]** and **1f[Pyr]** and diazene **2d[Pyr]** have preserved the lamellar structure, as evident from sharp and more intense higher-order ($00l$) reflections. Their diffractograms also exhibit a number of additional wide-angle region reflections indicating increased order within the layers. The pattern observed for the soft crystalline phase of **1f[Pyr]** is consistent neither with an E nor a B phase. The gliding symmetry, associated with the herringbone molecular order in the E phase, precludes the observed (100) and (010) reflections, and permits the (210) reflection which is absent in the diffractogram. On the other hand, assumption of a hexagonal B phase (unit cell dimensions: $a = 10.4 \text{ \AA}$ and $c = 25.5 \text{ \AA}$) leads to the Z value

(molecule per lattice) of 1.9 (assuming density of 1.0 g cm^{-3}), while the symmetry of the phase requires $Z = 1$. Instead, the observed pattern for the upper soft crystalline phase of **1f[Py]** could be assigned to an orthogonal phase with the unit cell dimensions: $a = 9.0 \text{ \AA}$, $b = 5.2 \text{ \AA}$, $c = 25.7 \text{ \AA}$ and $Z = 0.92$ (Figure 6a). A possible structure of this phase may involve alternating ionic and hydrophobic layers with the period of 25.7 \AA , and two-dimensional rectangular lattice with the unit cell containing two molecules, the anion and the cation.

The lower temperature soft crystalline phase exhibits additional reflections, which are indicative of a more organized phase, presumably crystallization of the microsegregated ionic region of the sample. A similar pattern was observed for phase X in ester **1d[Py]** (Figure 6b) in which the number of reflections is higher than might be expected for a B-like phase, but significantly lower than that observed for a crystalline phase of diazene **2d[Py]** grown from the SmA phase.⁵⁷ Unambiguous identification of these phases and understanding of their structures will require more detailed studies of oriented samples and single crystal analysis.

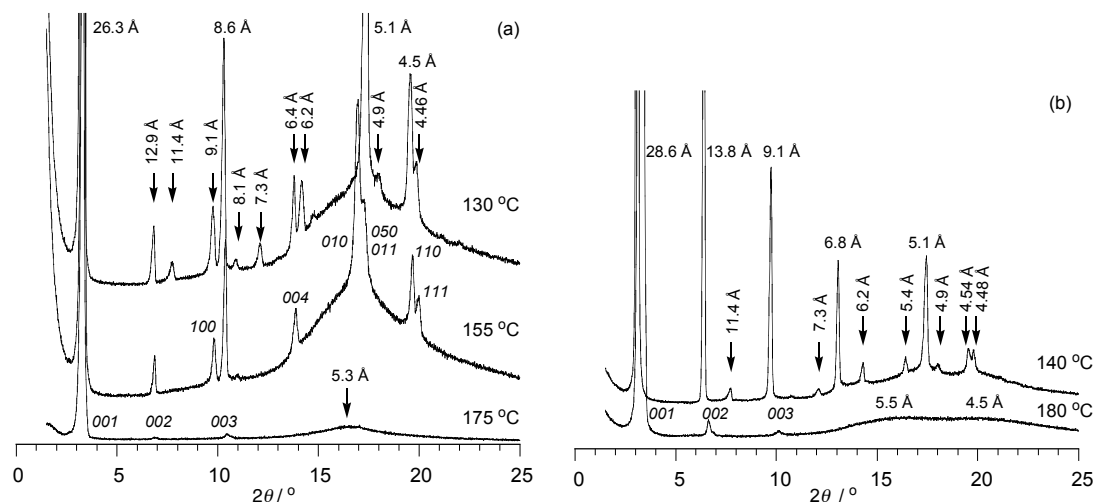


Figure 6. Stacked X-ray diffraction patterns for a) **1f[Pyr]** obtained at 175 °C (SmA, $c = 25.8$ Å), 155 °C (X, $a = 9.0$ Å, $b = 5.2$ Å, $c = 25.7$ Å), and 130 °C (X'), and b) for **1d[Pyr]** at 180 °C (SmA, $c = 26.6$ Å) and 140 °C (X).

Table 3. The molecular interdigitation in selected phases.

compd	length L^a /Å	Temperature T / °C	Phase	Interdigitation ^b $I = (L - c) / L$
1d[Pyr]	32.3	180	SmA	0.18
		140	X	0.15
2d[Pyr]	31.7	140	SmA	0.18
		100	Cr	0.21
1f[Pyr]	29.8	175	SmA	0.14
		155	X	0.14
		130	X'	0.13

^a Most extended molecular conformation optimized at the HF/6-31G(d) level of theory. See electronic supporting information. ^b The cell constant c is calculated from d_{002} .

A comparison of the layer spacing c with the molecular length L calculated for a model of the fully extended mesogen indicates that the molecules are organized in monolayers with significant interdigitation of the alkyl chains ($c < L$) in all three compounds. The calculated degree of the interdigitation, $I = (L - c) / L$, in the SmA phase was higher for **1d[Pyr]** and **2d[Pyr]** (0.18) than for ester **1f[Pyr]** (0.14). This value

decreases in the X phase of **1d[Pyr]**, increases in crystal phase of **2d[Pyr]**, and stays practically unchanged in the soft crystalline phases of **1f[Pyr]** relative to that in the SmA phase (Table 3). Incidentally, the layer spacing d is about a double of the distance between the nitrogen atom and the tip of the heptyloxy chain in the pyridinium ion.

Photophysical Properties

Electronic absorption spectra demonstrated that ester **1e[Pyr]** is transparent above 280 nm (Figure 7a). The single absorption peak at 243 nm ($\log \epsilon = 4.32$) and a large absorbance at 200 nm ($\log \epsilon = 4.65$) observed for **1e[Pyr]** in MeCN results from an overlap of high-energy absorbance of the anion **1e** (210 nm tailing to 280 nm, $\log \epsilon = 4.44$) and pyridinium chromophores (246 nm, $\log \epsilon = 4.20$). Practically identical results were obtained for **1e[Pyr]** in 1,2-dichloroethane (248 nm, $\log \epsilon = 4.30$). No evidence of intermolecular charge-transfer between the {*closo*-1-CB₉} cluster and the pyridinium was found.

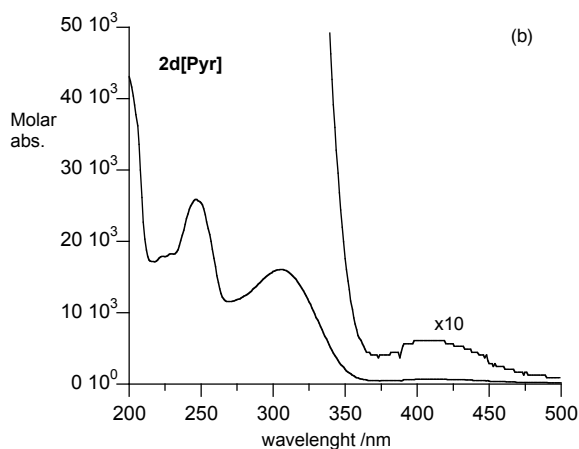


Figure 7. Electronic absorption spectra of a) ester **1e[NMe₄]** (thin line), pyridinium bromide **7** (thin line), and **1e[Pyr]** (thick line), and b) diazene **2d[Pyr]** recorded in MeCN.

The diazene **2d[Pyr]** exhibits three distinct absorption maxima (Figure 7b). The high energy maximum at 247 nm ($\log \epsilon = 4.41$) is related to the pyridinium chromophore, while the two lower energy maxima at 305 nm ($\log \epsilon = 4.20$) and 410 nm ($\log \epsilon = 2.7$) are attributed to the phenylazo group. The latter two, identified as $\pi \rightarrow \pi^*$ and $n \rightarrow \pi^*$ transitions, respectively, are similar to those observed for the parent [*closo*-1-CB₉H₉-1-(N=N-C₆H₄-OMe-4)]⁻ anion for which the analogous transitions were found at 319 nm ($\log \epsilon = 4.23$) and 407 nm ($\log \epsilon = 2.8$).⁴⁴

An attempt to induce charge separation and transfer in ester **1d[Pyr]** and in diazene **2d[Pyr]** were unsuccessful. Irradiation of the TiO₂ charge generation layer deposited on the ITO conductive layer of the electrooptical cell containing the ester or direct irradiation of the diazene sample in the electrooptical cell with 337 nm laser beam

did not result in photocurrent generation.

Summary and Conclusions

Results show that the [*closo*-1-CB₉H₁₀]⁻ anion (**A**) is an effective and unusual structural element of ionic liquid crystals in which the negative charge is fully delocalized and the anion is non-nucleophilic. This implies no specific interactions between the ions. The study of two series of mesogens, **1** and **2**, demonstrate that all 3-ring and even some two-ring (**2a**[Pyr]) compounds exhibit a partially interdigitated monolayer SmA phase when the pyridinium counterion is present. In addition, esters **1**[Pyr] exhibit a rich soft crystalline and crystalline polymorphism, which resembles behavior of typical non-ionic calamitic mesogens. Unlike in conventional calamitics, soft crystalline phases of esters **1**[Pyr] appear to adopt two mutually perpendicular layered molecular organization. Esters **1** are transparent above 280 nm, while diazenes **2** are potentially photoresponsive mesogens.

The presented work opens a possibility for further manipulation with the structure and fine-tuning of mesogenic and photophysical properties. Of particular interest are anions, which may lead to ambient temperature mesophase of their metal salts with a broad electrochemical window. Such materials are desired for devices in which cation transport is important.

Experimental Section

Synthetic Details

¹H NMR spectra were obtained at 400 MHz field for all compounds, excluding **7**, **1d**[NMe₄], **1e**[Pyr], and **2c**[Pyr] which were recorded at 300 MHz field, in acetone-*d*₆ (δ 2.04 ppm), CD₃CN (δ 1.93 ppm) or CDCl₃ (δ 7.26 ppm). ¹¹B NMR was recorded at 128 MHz field. Chemical shifts were referenced to the solvent (¹H) or to an external sample of B(OH)₃ in MeOH (¹¹B, δ = 18.1 ppm). IR spectra were recorded for microcrystalline samples using the ATR technique. Elemental analysis was provided by Atlantic Microlab, Inc.

Optical microscopy was performed using a PZO Biolar microscope equipped with an HCS402 Instec hot stage. Thermal analysis was obtained using a TA Instruments 2920 DSC. Transition temperatures (onset) and enthalpies were obtained using small samples (~0.5 mg) and a typical heating/cooling rate of 5 K min⁻¹ under a flow of nitrogen gas. UV spectra were recorded in MeCN and molar absorption was obtained from a Beer's law plot of 4-5 concentrations. XRD measurements were carried out on unoriented and uncovered samples placed on a temperature-controlled glass plate using Rigaku RINT2000 X-ray diffractometer (Cu Kα1 = 1.5405Å) and a custom-made heater. XRD patterns were collected in the range of 1.5° – 35° on cooling. Layer spacings (cell constant *c*) were determined from the (002) reflection.

Photocurrent generation was investigated in 17 μm thick electrooptical

cells using methods and setups described before.⁵⁸ The cell used for studies of ester **1d[Pyr]** had an TiO₂ layer deposited on the top of the conductive ITO layer.¹⁹

General Procedure for Preparation of **1[Pyr]** and **2[Pyr]**.

N-Butyl-4-heptyloxypyridinium bromide (**7**, 1.0 equivalent) was added to a solution of ester **1[NMe₄]** or diazene **2[NMe₄]** or **2[NHEt₃]** in CH₂Cl₂ and a white precipitate formed. Water was added, and the biphasic system was stirred vigorously until all the precipitate had dissolved. The CH₂Cl₂ layer was separated, and the aqueous layer was extracted with additional CH₂Cl₂. The CH₂Cl₂ layers were combined, dried (Na₂SO₄), and evaporated giving a white (**1[Pyr]**) or yellow (**2[Pyr]**) crystalline solid, which was recrystallized from aqueous alcohol. The crystals were dried under vacuum for several hours.

1a[Pyr]: Recrystallized from EtOH/H₂O mixtures (3x) providing 0.017 g (61% yield for cation exchange) of the pure salt as a white powder: ¹H NMR (CDCl₃) δ 0.40-2.50 (m, 8H, B-H), 0.86-0.96 (m, 12H), 1.23-1.50 (m, 26H), 1.53-1.60 (m, 2H), 1.75-1.87 (m, 6H), 1.87-1.95 (m, 2H), 1.97-2.04 (m, 2H) 3.96 (t, *J* = 6.5 Hz, 2H), 4.20 (t, *J* = 6.5 Hz, 2H), 4.26 (t, *J* = 7.5 Hz, 2H), 6.92 (d, *J* = 8.9 Hz, 2H), 7.18 (d, *J* = 8.9 Hz, 2H), 7.25 (d, *J* = 7.2 Hz, 2H), 8.30 (d, *J* = 7.2 Hz, 2H); ¹¹B NMR (acetone-*d*₆) δ -24.0 (d, *J* = 139 Hz, 4B), -16.1 (d, *J* = 150 Hz, 4B), 48.2 (s, 1B). Anal. Calcd. for C₃₉H₇₂B₉NO₄: C, 64.14; H, 9.66; N, 1.92. Found: C, 64.37; H, 9.78; N, 1.97.

1b[Pyr]: Recrystallized from cold EtOH (3x) providing 0.027 g (24% overall yield based

on acid **3**[NMe₄]) of the pure salt as a white powder: ¹H NMR (acetone-*d*₆) δ 0.40-2.50 (m, 8H, B-H), 0.83-0.93 (m, 9H), 0.94 (t, *J* = 7.3 Hz, 3H), 1.25-1.50 (m, 24H), 1.56 (quintet, *J* = 7.0 Hz, 2H), 1.73 (quintet, *J* = 7.4 Hz, 2H), 1.83-1.98 (m, 6H), 2.02-2.08 (m, 2H), 2.59 (t, *J* = 7.4 Hz, 2H), 4.45 (t, *J* = 6.5 Hz, 2H), 4.61 (t, *J* = 7.4 Hz, 2H), 7.20 (d, *J* = 8.9 Hz, 2H), 7.31 (d, *J* = 8.9 Hz, 2H), 7.65 (d, *J* = 7.3 Hz, 2H), 8.89 (d, *J* = 7.4 Hz, 2H); ¹¹B NMR (acetone-*d*₆) δ -23.9 (d, *J* = 136 Hz, 4B), -16.0 (d, *J* = 148 Hz, 4B), 48.0 (s, 1B). Anal. Calcd. for C₃₉H₇₀B₉NO₅: C, 65.39; H, 10.13; N, 1.96. Found: C, 65.19; H, 10.20; N, 2.00.

1c[Pyr]: Recrystallized from EtOH/H₂O mixtures (3x) providing 0.020 g (17% overall yield based on acid **3**[NMe₄]) of the pure salt as a white powder: ¹H NMR (acetone-*d*₆) δ 0.40-2.50 (m, 8H, B-H), 0.84-0.92 (m, 9H), 0.95 (t, *J* = 7.3 Hz, 3H), 0.98-1.10 (m, 2H), 1.20-1.44 (m, 21H), 1.45-1.60 (m, 6H), 1.83-1.97 (m, 8H), 2.01-2.08 (m, 2H), 2.10-2.20 (m, 2H), 2.52 (tt, *J*₁ = 12.2 Hz, *J*₂ = 3.5 Hz, 1H), 4.46 (t, *J* = 6.5 Hz, 2H), 4.63 (t, *J* = 7.4 Hz, 2H), 7.18 (d, *J* = 8.9 Hz, 2H), 7.31 (d, *J* = 8.9 Hz, 2H), 7.66 (d, *J* = 7.5 Hz, 2H), 8.90 (d, *J* = 7.5 Hz, 2H); ¹¹B NMR (acetone-*d*₆) δ -23.9 (d, *J* = 142 Hz, 4B), -16.0 (d, *J* = 147 Hz, 4B), 48.0 (s, 1B). Anal. Calcd. for C₄₂H₇₄B₉NO₅: C, 65.48; H, 9.68; N, 1.82. Found: C, 65.47; H, 9.70; N, 1.84.

1d[Pyr]: Recrystallized from EtOH/H₂O mixtures (3x) providing 0.041 g (20% overall yield based on acid **3**[NMe₄]) of the pure salt as white crystals: ¹H NMR (acetone-*d*₆) δ 0.40-3.50 (m, 18H, B-H), 0.83 (t, *J* = 7.2 Hz, 3H), 0.87 (t, *J* = 7.3 Hz, 3H), 0.91 (t, *J* = 7.6 Hz, 3H), 0.95 (t, *J* = 7.4 Hz, 3H), 1.10-1.43 (m, 18H), 1.45-1.52 (m, 2H), 1.53-1.60

(m, 2H), 1.67-1.75 (m, 2H), 1.83-1.97 (m, 6H), 1.98-2.07 (m, 2H), 4.47 (t, $J = 6.5$ Hz, 2H), 4.64 (t, $J = 7.5$ Hz, 2H), 7.15 (d, $J = 9.0$ Hz, 2H), 7.33 (d, $J = 9.0$ Hz, 2H), 7.68 (d, $J = 7.0$ Hz, 2H), 8.92 (d, $J = 6.7$ Hz, 2H); ^{11}B NMR (acetone- d_6) δ -23.9 (d, $J = 132$ Hz, 4B), -15.9 (d, $J = 151$ Hz, 4B), -13.2 (d, $J = 161$ Hz, 5B), -12.6 (d, $J = 154$ Hz, 5B), 48.3 (s, 1B). Anal. Calcd. for $\text{C}_{38}\text{H}_{74}\text{B}_{19}\text{NO}_5$: C, 54.96; H, 8.98; N, 1.69. Found: C, 55.17; H, 8.99; N, 1.63.

1e[Pyr]: Recrystallized from EtOH/H₂O mixtures (3x) giving 10 mg (20% overall yield based on acid **3**[NMe₄]) of the pure salt as white crystals: ^1H NMR (300 MHz, acetone- d_6) δ 0.40-2.50 (m, 8H, B-H), 0.84-0.94 (m, 9H), 0.95 (t, $J = 7.4$ Hz, 3H), 1.01-1.20 (m, 2H), 1.21-1.61 (m, 31H), 1.78-2.10 (m, 8H), 2.53 (br t, $J = 12.2$ Hz, 1H), 4.46 (d, $J = 6.5$ Hz, 2H), 4.64 (t, $J = 7.4$ Hz, 2H), 7.17 (d, $J = 8.6$ Hz, 2H), 7.30 (d, $J = 8.5$ Hz, 2H), 7.68 (d, $J = 7.5$ Hz, 2H), 8.92 (d, $J = 7.5$ Hz, 2H); ^{11}B NMR (acetone- d_6) δ -23.9 (d, $J = 131$ Hz, 4B), -16.1 (d, $J = 155$ Hz, 4B), 48.0 (s, 1B); UV (MeCN), λ_{max} 243 nm, ($\log \epsilon = 4.32$), (CH₂ClCH₂Cl), λ_{max} 248 nm, ($\log \epsilon = 4.30$). Anal. Calcd. for $\text{C}_{41}\text{H}_{74}\text{B}_9\text{NO}_3$: C, 67.80; H, 10.27; N, 1.93. Found: C, 68.04; H, 10.33; N, 1.92.

1f[Pyr]: Recrystallized from EtOH/H₂O mixtures (3x) providing 0.030 g (19% overall yield based on acid **3**[NMe₄]) of the pure salt as white crystals: ^1H NMR (acetone- d_6) δ 0.40-3.50 (m, 18H, B-H), 0.84 (t, $J = 7.2$ Hz, 3H), 0.86 (t, $J = 7.0$ Hz, 3H), 0.91 (t, $J = 7.1$ Hz, 3H), 0.95 (t, $J = 7.4$ Hz, 3H), 1.10-1.60 (m, 22H), 1.68-1.76 (m, 2H), 1.82-1.95 (m, 6H), 1.98-2.09 (m, 2H), 4.46 (t, $J = 6.5$ Hz, 2H), 4.64 (d, $J = 7.4$ Hz, 2H), 7.17 (d, $J = 8.8$ Hz, 2H), 7.34 (d, $J = 8.8$ Hz, 2H), 7.67 (d, $J = 6.2$ Hz, 2H), 8.92 (d, $J = 5.9$ Hz, 2H);

^{11}B NMR (acetone- d_6) δ -23.8 (d, J = 148 Hz, 4B), -15.9 (d, J = 153 Hz, 4B), -12.3 (d, J = 157 Hz, 10B) 47.9 (s, 1B). Anal. Calcd. for $\text{C}_{37}\text{H}_{74}\text{B}_{19}\text{NO}_3$: C, 56.51; H, 9.48; N, 1.78. Found: C, 56.55; H, 9.51; N, 1.75.

2a[Pyrr]: Recrystallized from MeOH (3x) followed by EtOH (3x) giving 0.024 g (32% overall yield based on phenol **5[NMe₄]**) of pure salt as yellow leaflets: ^1H NMR (acetone- d_6) δ 0.40-2.50 (m, 8H, B-H), 0.84-0.89 (m, 6H), 0.90 (t, J = 7.1 Hz, 3H), 0.95 (t, J = 7.3 Hz, 3H), 1.20-1.62 (m, 28H), 1.77-2.08 (m, 10H), 4.10 (t, J = 6.5 Hz, 2H), 4.46 (t, J = 6.5 Hz, 2H), 4.63 (t, J = 7.5 Hz, 2H), 7.07 (d, J = 8.9 Hz, 2H), 7.67 (d, J = 7.4 Hz, 2H), 7.84 (d, J = 8.8 Hz, 2H), 8.90 (d, J = 7.4 Hz, 2H); ^{11}B NMR (acetone- d_6) δ -24.5 (d, J = 140 Hz, 4B), -17.1 (d, J = 157 Hz, 4B), 42.5 (s, 1B). Anal. Calcd. for $\text{C}_{38}\text{H}_{72}\text{B}_9\text{N}_3\text{O}_2$: C, 65.17; H, 10.36; N, 6.00. Found: C, 65.45; H, 10.62; N, 6.03.

2b[Pyrr]: Recrystallized from MeOH (3x) followed by EtOH (2x) giving 0.052 g (72% overall yield based on phenol **5[NMe₄]**) of the pure salt as yellow leaflets: ^1H NMR (acetone- d_6) δ 0.40-2.50 (m, 8H, B-H), 0.83-0.91 (m, 6H), 0.92 (t, J = 7.1 Hz, 3H), 0.94 (t, J = 7.4 Hz, 3H), 1.25-1.51 (m, 24H), 1.58 (quintet, J = 7.1 Hz, 2H), 1.75 (quintet, J = 7.4 Hz, 2H), 1.84-1.94 (m, 6H), 1.96-2.08 (m, 2H), 2.63 (t, J = 7.4 Hz, 2H), 4.45 (t, J = 6.5 Hz, 2H), 4.62 (t, J = 7.4 Hz, 2H), 7.30 (d, J = 8.7 Hz, 2H), 7.66 (d, J = 7.4 Hz, 2H), 7.91 (d, J = 8.8 Hz, 2H), 8.90 (d, J = 7.4 Hz, 2H); ^{11}B NMR (acetone- d_6) δ -24.4 (d, J = 136 Hz, 4B), -16.9 (d, J = 149 Hz, 4B), 44.0 (s, 1B). Anal. Calcd. for $\text{C}_{38}\text{H}_{70}\text{B}_9\text{N}_3\text{O}_3$: C, 63.90; H, 9.88; N, 5.88. Found: C, 64.12; H, 10.03; N, 5.94.

2c[Pyr]: Recrystallized from MeOH (3x) followed by EtOH (2x) giving 0.043 g (38% overall yield based on phenol **5[NMe₄]**) of the pure diazene as yellow leaflets: ¹H NMR (300 MHz, acetone-*d*₆) δ 0.40-2.50 (m, 8H, B-H), 0.83-0.93 (m, 9H), 0.94 (t, *J* = 7.4 Hz, 3H), 0.98-1.13 (m, 2H), 1.20-1.64 (m, 27H), 1.80-2.01 (m, 10H), 2.10-2.22 (m, 2H), 2.55 (tt, *J*₁ = 12.2 Hz, *J*₂ = 3.6 Hz, 1H), 4.45 (t, *J* = 6.5 Hz, 2H), 4.62 (t, *J* = 7.4 Hz, 2H), 7.28 (d, *J* = 8.8 Hz, 2H), 7.66 (d, *J* = 7.5 Hz, 2H), 7.91 (d, *J* = 8.8 Hz, 2H), 8.90 (d, *J* = 7.5 Hz, 2H); ¹¹B NMR (acetone-*d*₆) δ -24.4 (d, *J* = 134 Hz, 4B), -16.9 (d, *J* = 153 Hz, 4B), 43.6 (s, 1B). Anal. Calcd. for C₄₁H₇₄B₉N₃O₃: C, 65.28; H, 9.89; N, 5.57. Found: C, 65.39; H, 9.99; N, 5.57.

2d[Pyr]: Recrystallized from MeOH (3x) followed by EtOH (2x) giving 0.073 g (71% overall yield based on phenol **5[NMe₄]**) of pure diazene as yellow needles: ¹H NMR (acetone-*d*₆) δ 0.40-3.50 (m, 18H, B-H), 0.83 (t, *J* = 7.3 Hz, 3H), 0.85-0.92 (m, 6H), 0.94 (t, *J* = 7.3 Hz, 3H), 1.08-1.44 (m, 18H), 1.45-1.52 (m, 2H), 1.57 (quintet, *J* = 7.0 Hz, 2H), 1.67-1.76 (m, 2H), 1.84-1.93 (m, 6H), 1.95-2.08 (m, 2H), 4.45 (t, *J* = 6.5 Hz, 2H), 4.62 (t, *J* = 7.4 Hz, 2H), 7.25 (d, *J* = 8.8 Hz, 2H), 7.66 (d, *J* = 7.3 Hz, 2H), 7.91 (d, *J* = 8.8 Hz, 2H), 8.90 (d, *J* = 7.3 Hz, 2H); ¹¹B NMR (acetone-*d*₆) δ -24.3 (d, *J* = 132 Hz, 4B), -16.7 (d, *J* = 141 Hz, 4B), -13.2 (d, *J* = 153 Hz, 5B), -12.6 (d, *J* = 157 Hz, 5B), 44.0 (s, 1B); UV (MeCN) λ_{max} (log ε), 247 nm (4.41), 305 nm (4.20), 410 nm (2.7). Anal. Calcd. for C₃₇H₇₄B₁₉N₃O₃: C, 54.57; H, 9.16; N, 5.16. Found: C, 54.85; H, 9.25; N, 5.16.

General Procedure for Preparation of Esters **1a**[NMe₄]-**1f**[NMe₄]

Phenol **4** (1.5 equivalents) was added to a colorless solution of [*closo*-1-CB₉H₈-1-COOH-10-C₆H₁₃]⁻NMe₄⁺ (**3**[NMe₄]), DCC (1.0 equivalent), and DMAP (0.1 equivalents) in anhydrous CH₂Cl₂. The mixture was stirred overnight at rt, and the reaction progress was monitored by TLC (R_f = 0.5, CH₃CN/CH₂Cl₂, 1:9). The solvent was removed *in vacuo*, and the crude product was isolated by column chromatography (SiO₂, CH₃CN/CH₂Cl₂, 1:9). The resulting ester was washed with hot hexane and recrystallized from EtOH/H₂O or MeOH/H₂O. Esters **1a**[NMe₄] and **1b**[NMe₄] were difficult to crystallize and were directly converted to *N*-butyl-4-heptyloxy pyridinium salts (**1**[Pyr]).

1a[NMe₄]: The crude product was washed with hot hexane giving 46 mg of ~ 85% pure salt as an oily film that slowly glassified. Attempts to recrystallize from EtOH/H₂O mixtures were unsuccessful: ¹H NMR (CDCl₃) major signals δ 0.89 (t, *J* = 6.9 Hz, 3H), 0.91 (t, *J* = 6.9 Hz, 3H), 1.56 (quintet, *J* = 6.9 Hz, 2H), 1.78 (quintet, *J* = 7.0 Hz, 2H), 3.01 (s, 12H), 3.94 (t, *J* = 6.5 Hz, 2H), 6.92 (d, *J* = 8.8 Hz, 2H), 7.15 (d, *J* = 8.8 Hz, 2H); ¹¹B {¹H} NMR (acetone-*d*₆) δ -24.1 (4B), -16.1 (4B), 48.7 (1B).

1b[NMe₄]: The crude product was washed with hot hexane giving 0.053 g of ~ 85% pure salt as a semi-crystalline paste. Attempts to recrystallize from EtOH/H₂O mixtures were unsuccessful: ¹H NMR (acetone-*d*₆) major signals δ 0.88 (t, *J* = 6.8 Hz, 3H), 0.91 (t, *J* = 7.0 Hz, 3H), 1.73 (quintet, *J* = 7.4 Hz, 2H), 2.59 (t, *J* = 7.4 Hz, 2H), 3.43 (s, 12H), 7.20 (d, *J* = 8.9 Hz, 2H), 7.31 (d, *J* = 8.9 Hz, 2H); ¹¹B NMR (acetone-*d*₆) δ -23.9 (d, *J* = 129

Hz, 4B), -16.0 (d, $J = 141$ Hz, 4B), 48.0 (s, 1B).

1c[NMe₄]: Recrystallized from EtOH/H₂O mixtures (2x) giving 0.020 g (22% yield) of the pure salt as a white crystalline powder: mp 242 °C (DSC); ¹H NMR (acetone-*d*₆) δ 0.40-2.50 (m, 8H, B-H), 0.89 (t, $J = 6.9$ Hz, 3H), 0.91 (t, $J = 7.1$ Hz, 3H), 0.95-1.10 (m, 2H), 1.15-1.45 (m, 15H), 1.48-1.62 (m, 4H), 1.80-2.00 (m, 4H), 2.14 (br d, $J = 11.2$ Hz, 2H), 2.52 (tt, $J_1 = 12.2$ Hz, $J_2 = 3.5$ Hz, 1H), 3.43 (s, 12H), 7.18 (d, $J = 8.9$ Hz, 2H), 7.31 (d, $J = 8.9$ Hz, 2H); ¹¹B NMR (acetone-*d*₆) δ -23.9 (d, $J = 139$ Hz, 4B), -16.0 (d, $J = 145$ Hz, 4B), 48.9 (s, 1B).

1d[NMe₄]: Recrystallized from EtOH/H₂O mixtures (2x) giving 0.041 g (25% yield) of pure salt as a white crystalline powder: mp 226 °C (DSC); ¹H NMR (300 MHz, acetone-*d*₆) δ 0.40-3.50 (m, 18H, B-H), 0.83 (t, $J = 7.0$ Hz, 3H), 0.91 (t, $J = 7.1$ Hz, 3H), 1.10-1.30 (m, 6H), 1.34-1.42 (m, 4H), 1.50-1.60 (m, 2H), 1.68-1.75 (m, 2H), 1.81-1.98 (m, 4H), 3.44 (s, 12H), 7.15 (d, $J = 9.0$ Hz, 2H), 7.33 (d, $J = 9.0$ Hz, 2H); ¹¹B NMR (acetone-*d*₆) δ -23.9 (d, $J = 137$ Hz, 4B), -15.9 (d, $J = 152$ Hz, 4B), -13.2 (d, $J = 160$ Hz, 5B), -12.6 (d, $J = 158$ Hz, 5B), 49.1 (s, 1B).

1e[NMe₄]: The crude product was washed with hot hexane and recrystallized from EtOH/H₂O mixtures (2x) giving 10 mg (26% yield) of the pure salt as a white crystalline powder: mp 197 °C (DSC); ¹H NMR (acetone-*d*₆) δ 0.40-2.50 (m, 8H, B-H), 0.90 (t, $J = 7.8$ Hz, 3H), 0.92 (t, $J = 7.7$ Hz, 3H), 1.05-1.17 (m, 2H), 1.22-1.45 (m, 15H), 1.45-1.62 (m, 4H), 1.85-2.01 (m, 6H), 2.54 (bt, $J = 12.1$ Hz, 1H), 3.45 (s, 12H), 7.19 (d, $J = 8.5$ Hz,

2H), 7.31 (d, $J = 8.5$ Hz, 2H); ^{11}B NMR (acetone- d_6) δ -23.9 (d, $J = 132$ Hz, 4B), -16.0 (d, $J = 152$ Hz, 4B), 48.3 (s, 1B).

1f[NMe₄]: Recrystallized from EtOH/H₂O mixtures (2x) giving 0.029 g (23% yield) of the pure salt as a white crystalline powder: mp 201 °C (DSC); ^1H NMR (acetone- d_6) δ 0.40-3.50 (m, 18H, B-H), 0.84 (t, $J = 7.2$ Hz, 3H), 0.91 (t, $J = 7.0$ Hz, 3H), 1.10-1.30 (m, 6H), 1.32-1.43 (m, 4H), 1.55 (quintet, $J = 7.0$ Hz, 2H), 1.67-1.75 (m, 2H), 1.80-1.98 (m, 4H), 3.44 (s, 12H) 7.17 (d, $J = 8.9$ Hz, 2H), 7.34 (d, $J = 8.8$ Hz, 2H); ^{11}B NMR (acetone- d_6) δ -23.9 (d, $J = 138$ Hz, 4B), -15.9 (d, $J = 151$ Hz, 4B), -12.3 (d, $J = 164$ Hz, 10B), 48.3 (s, 1B).

Preparation of [closo-1-CB₉H₈-1-(N=N-C₆H₄-OC₉H₁₉-4)-10-C₆H₁₃]⁻NMe₄⁺ (2a[NMe₄]).

A solution of 1-bromononane (0.08 mL, 0.4 mmol) in anhydrous CH₃CN (2 mL) was added to an orange solution of azophenol **5**[NMe₄] (0.042 g, 0.106 mmol, about 60% pure; contaminated with NMP) and NMe₄⁺OH⁻·5H₂O (0.06 g, 0.32 mmol) in anhydrous CH₃CN (2 mL). The solution was stirred at 50 °C for 4 hr. The reaction mixture was worked up and the product was isolated as described for esters **1**[NMe₄] and used for the preparation of **2a**[Pyr] without crystallization.

General Procedure for Preparation of Diazenes 2b[NHEt₃], 2c[NMe₄], and 2d[NHEt₃].

A solution of acid chloride **6** (4.0 equivalents) in anhydrous CH₂Cl₂ was added to an orange solution of azophenol **5**[NMe₄] (about 60% pure; contaminated with NMP) and NEt₃ (5.0 equivalents) in anhydrous CH₂Cl₂. The bright yellow solution was

stirred for 12 hrs, and reaction progress was monitored by TLC ($R_f = 0.5$ in $\text{CH}_3\text{CN}/\text{CH}_2\text{Cl}_2$, 1:9). The reaction mixture was worked up and the product was isolated as described for esters **1**[NMe₄]. Without crystallization, the resulting diazenes **2b**[NHEt₃], **2c**[NMe₄], or **2d**[NHEt₃] were converted to the pyridinium salts **2**[Pyr].

2b[NHEt₃]: Washing with hot hexane gave 0.073 g (135% yield) of crude diazene as a yellow/green viscous isotropic film, which slowly crystallized: ¹H NMR (acetone-*d*₆) major signals δ 0.89 (t, $J = 6.5$ Hz, 3H), 0.92 (t, $J = 6.9$ Hz, 3H), 1.38 (t, $J = 7.3$ Hz, 9H), 1.58 (quintet, $J = 7.1$ Hz, 2H), 1.75 (quintet, $J = 7.4$ Hz, 2H), 2.63 (t, $J = 7.4$ Hz, 2H), 3.42 (q, $J = 7.3$ Hz, 6H), 7.31 (d, $J = 8.7$ Hz, 2H), 7.92 (d, $J = 8.7$ Hz, 2H); ¹¹B NMR (acetone-*d*₆) δ -24.4 (d, $J = 137$ Hz, 4B), -16.9 (d, $J = 146$ Hz, 4B), 43.7 (s, 1B).

2c[NMe₄]: Washing with hot hexane gave 0.095 g (110% yield) of crude diazene as a yellow/green viscous isotropic film that slowly crystallized: ¹H NMR (acetone-*d*₆) major signals δ 0.89 (t, $J = 6.9$ Hz, 3H), 0.92 (t, $J = 7.0$ Hz, 3H), 2.54 (tt, $J_1 = 12.2$ Hz, $J_2 = 3.5$ Hz, 1H), 3.43 (s, 12H), 7.29 (d, $J = 8.8$ Hz, 2H), 7.91 (d, $J = 8.7$ Hz, 2H); ¹¹B {¹H} NMR (acetone-*d*₆) δ -24.4 (4B), -16.9 (4B), 43.3 (s, 1B).

2d[NHEt₃]: Washing with hot hexane gave 0.087 g (105% yield) of ~95% pure diazene as a yellow/green viscous isotropic film that slowly crystallized: mp 155 °C, ¹H NMR (acetone-*d*₆) δ 0.40-3.50 (m, 18H, B-H), 0.83 (t, $J = 7.2$ Hz, 3H), 0.91 (t, $J = 7.0$ Hz, 3H), 1.06-1.30 (m, 6H), 1.33-1.43 (m, 4H), 1.37 (t, $J = 7.3$ Hz, 9H), 1.52-1.61 (m, 2H), 1.67-1.76 (m, 2H), 1.84-2.00 (m, 4H), 3.39 (q, $J = 7.3$ Hz, 6H), 7.25 (d, $J = 8.8$ Hz, 2H), 7.91

(d, $J = 8.8$ Hz, 2H); ^{11}B NMR (acetone- d_6) δ -24.3 (d, $J = 137$ Hz, 4B), -16.7 (d, $J = 157$ Hz, 4B), -13.2 (d, $J = 151$ Hz, 5B), -12.6 (d, $J = 158$ Hz, 5B), 43.1 (s, 1B).

Preparation of [*closo*-1-CB₉H₈-1-COOH-10-C₆H₁₃]⁻NMe₄⁺ (**3**[NMe₄])

To a 100 mL three-necked flask, under inert atmosphere, equipped with a magnetic stir bar, reflux condenser, septum, and a glass stopcock was suspended solid anhydrous ZnCl₂ (2.29 g, 16.8 mmol) in anhydrous THF (16 mL). C₆H₁₃MgBr in Et₂O (9.2 mL, 16.0 mmol, 1.74 M) was added, and the exothermic reaction was stirred briefly (15 min) producing a white precipitate. Anhydrous NMP (8 mL), Pd₂dba₃ (0.061 g, 0.067 mmol), and [HPCy₃]⁺ BF₄⁻ (0.099 g, 0.268 mmol) were added, and the reaction mixture turned dark green and slowly faded to red/orange. After 5 mins, acid [*closo*-1-CB₉H₈-1-COOH-10-I]⁻ NMe₄⁺ (**8**[NMe₄], 0.482 g, 1.33 mmol) was added. The septum was replaced with an additional glass stopcock, and the reaction was stirred at 85°C overnight. After brief heating, the reaction turned from red/orange to black. Sat. NH₄Cl (50 mL) was added, excess THF was removed *in vacuo*, and the remaining aqueous layer was extracted with Et₂O (3 x 20 mL). The organic layers were combined, dried (Na₂SO₄), and removed giving a black sludge. Excess NMP and 1-hexanol were removed under vacuum (60 °C, 0.5 mm Hg) and the residue (1.13 g) was separated by column chromatography (SiO₂, CH₃CN/CH₂Cl₂, 1:4) giving 0.586 g of [*closo*-1-CB₉H₈-1-COOH-10-C₆H₁₃]⁻H₃O⁺ (**3**[H₃O]) as a yellow/orange oil, which contained remnant NMP by ^1H NMR: ^{11}B { ^1H } NMR (CD₃CN) δ -24.3 (4B), -16.6 (4B), 47.3 (1B).

The crude acid extract was redissolved in 10 % HCl (50 mL) and extracted with Et₂O (3 x 20 mL). The organic layers were combined, and H₂O (10 mL) was added. The Et₂O was removed *in vacuo*, and the aqueous layer was filtered. NMe₄⁺Cl⁻ (0.150 g, 1.37 mmol) was added to the filtrate, and a white precipitate formed, which was filtered, washed (H₂O), and dried *in vacuo* giving 0.383 g (89% yield) of pure **3**[NMe₄]: mp 135 °C dec; ¹H NMR (acetone-*d*₆) δ 0.40-2.50 (m, 8H, B-H), 0.91 (t, *J* = 7.0 Hz, 3H), 1.35-1.41 (m, 4H), 1.56 (quintet, *J* = 6.9 Hz, 2H), 1.81-1.96 (m, 4H), 3.45 (s, 12H); ¹¹B NMR (acetone-*d*₆) δ -24.1 (d, *J* = 147 Hz, 4B), -16.5 (d, *J* = 157 Hz, 4B), 46.8 (s, 1B); MS (FAB): *m/z* 244-248 (M-H, max at 247, 100%); FAB-HRMS(-): Calcd. for C₈H₂₂B₉O₂ *m/z*: 249.2460; found; 249.2464.

Preparation of [*closo*-1-CB₉H₈-1-(N=N-C₆H₄-OH-4)-10-C₆H₁₃]⁻NMe₄⁺ (**5**[NMe₄])

To a 100 mL three-necked flask, under inert atmosphere, equipped with a magnetic stir bar, septum, and two glass stopcocks was suspended solid anhydrous ZnCl₂ (1.04 g, 7.62 mmol) in anhydrous THF (5 mL). C₆H₁₃MgBr in Et₂O (9.2 mL, 16.0 mmol, 1.74 M) was added, and the exothermic reaction was stirred briefly (15 min) producing a white precipitate. Anhydrous LiCl (0.3 g, 6.93 mmol) dissolved in anhydrous THF (10 mL) was added producing a homogenous solution. Anhydrous NMP (8 mL), Pd₂dba₃ (0.019 g, 0.021 mmol), and [HPCy₃]⁺ BF₄⁻ (0.031 g, 0.084 mmol) were added subsequently, and the reaction mixture turned dark green and slowly faded to red/orange. After 5 mins, [*closo*-1-CB₉H₈-1-(N=N-C₆H₄-OH-4)-10-I]⁻NMe₄⁺ (**9**[NMe₄], 0.275 g, 0.63 mmol) was added, and the reaction was stirred at rt overnight. Sat. NH₄Cl (25 mL) was

added, THF was removed *in vacuo*, and the remaining aqueous layer was extracted with Et₂O (3 x 20 mL). The organic layers were combined, dried (Na₂SO₄), and solvents removed giving a residue as a black sludge. Excess NMP and 1-hexanol were removed under vacuum (60 °C, 0.5 mm Hg) and the resulting residue (0.740 g) was separated by column chromatography (SiO₂, CH₃CN/CH₂Cl₂, 1:4) giving 0.370 g of (**5**[H₃O]) as a yellow/orange film which solidified on standing: ¹H NMR (CD₃CN) major signals δ 0.95 (t, *J* = 7.0 Hz, 3H), 6.99 (d, *J* = 8.8 Hz, 2H), 7.79 (d, *J* = 8.8 Hz, 2H), 8.21 (s, 1H); ¹¹B NMR (CD₃CN) δ -24.8 (d, *J* = 138 Hz, 4B), -17.4 (d, *J* = 150 Hz, 4B), 42.7 (s, 1B).

The crude acid extract was redissolved in 10% HCl (50 mL) and extracted with Et₂O (3 x 20 mL). The deep red organic layers were combined, and H₂O (10 mL) was added. The Et₂O was removed *in vacuo* giving a red film deposit. H₂O was decanted, and the red film was further washed with H₂O. The water was filtered, and any insoluble matter was recombined with the red film using CH₂Cl₂ (10 mL). NMe₄⁺Cl⁻ (0.093 g, 0.85 mmol) dissolved in H₂O (10 mL) was added, and the biphasic mixture was vigorously stirred for 1 hr. The deep red organic layer slowly began to turn light orange as a result. The organic layer was separated, and the H₂O was further extracted with CH₂Cl₂. The organic layers were combined, dried (Na₂SO₄), and solvent evaporated giving 320 mg (67% yield) of ~60% pure **5**[NMe₄] (contains ~40% NMP by ¹H NMR) as a yellow/orange viscous film: ¹H NMR (CD₃CN) major signals δ 0.93 (t, *J* = 7.0 Hz, 3H), 1.57 (quintet, *J* = 7.0 Hz, 2H), 3.05 (s, 12H), 6.96 (d, *J* = 8.8 Hz, 2H), 7.77 (d, *J* = 8.8 Hz, 2H); ¹¹B NMR (CD₃CN) δ -24.8 (d, *J* = 139 Hz, 4B), -17.4 (d, *J* = 150 Hz, 4B), 42.6 (s,

1B); MS (FAB): m/z 320-327 (M-H, max at 324, 100%); FAB-HRMS(-): calcd. for $C_{13}H_{26}B_9N_2O$ m/z : 325.2883; found; 325.2877.

Preparation of *N*-Butyl-4-heptyloxy pyridinium bromide (7)

4-Heptyloxy pyridine (1.00 g, 5.2 mmol) and 1-bromobutane (1.67 mL, 15.6 mmol) dissolved in anhydrous CH_3CN (10 mL) were stirred at reflux for 6 hrs. Solvent was removed *in vacuo*, and the crude product (1.68 g) was passed through a short silica gel plug (CH_3CN/CH_2Cl_2 , 1:9) giving 1.30 g (77% yield) of the pure salt **7** as a colorless oil, which slowly crystallized: mp 34 °C; 1H NMR (300 MHz, $CDCl_3$) δ 0.85 (t, $J = 6.7$ Hz, 3H), 0.92 (t, $J = 7.4$ Hz, 3H), 1.26-1.40 (m, 10H), 1.82 (quintet, $J = 7.1$ Hz, 2H), 1.95 (quintet, $J = 7.2$ Hz, 2H), 4.24 (t, $J = 6.3$ Hz, 2H), 4.70 (t, $J = 7.3$ Hz, 2H), 7.42 (d, $J = 6.5$ Hz, 2H), 9.21 (d, $J = 6.6$ Hz, 2H); UV (MeCN) λ_{max} 246 nm ($\log \epsilon = 4.20$), (CH_2ClCH_2Cl) λ_{max} 244 nm ($\log \epsilon = 4.6$). Anal. Calcd. for $C_{16}H_{28}BrNO$: C, 58.18; H, 8.54; N, 4.24; Found: C, 56.06; H, 8.77; N, 4.40.

Preparation of [*closo*-1- CB_9H_8 -1-(N=N- C_6H_4 -OH-4)-10-I] $^-NMe_4^+$ (**9**[NMe_4])

[*closo*-1- CB_9H_8 -1- N_2 -10-I] (**11**, 0.368 g, 1.14 mmol) was slowly added to a solution of $NMe_4^+OH^- \cdot 5H_2O$ (2.5 g, 13.60 mmol) and phenol (1.27 g, 13.5 mmol) in H_2O/CH_3CN (1:4 vol/vol) at 5 °C. Upon addition of **11**, an orange solution formed. The reaction was warmed to rt, and stirring continued for 1 hr. The reaction mixture was acidified with 10 % HCl and CH_3CN was removed *in vacuo*. The aqueous solution was extracted with Et_2O (3 x 20 mL), or until the organic layer was no longer colored. The

organic layers were combined, dried (Na₂SO₄), and solvent evaporated giving 1.65 g of a crude product as a red/orange oil. The crude product was purified by column chromatography (SiO₂, CH₃CN/CH₂Cl₂, 1:6) giving 0.531 g of [*closo*-1-CB₉H₈-1-(N=N-C₆H₄-OH-4)-10-I]⁻H₃O⁺ (**9**[H₃O]) as a yellow/orange film that slowly crystallized: ¹H NMR (CD₃CN) δ 6.97 (d, *J* = 8.8 Hz, 2H); 7.80 (d, *J* = 8.8 Hz, 2H); ¹¹B {¹H} NMR (CD₃CN) δ -20.5 (4B), -16.1 (4B), 17.3 (1B).

The crude phenol was redissolved in Et₂O (10 mL), H₂O (8 mL) was added, and the Et₂O was removed *in vacuo*. The mother liquor was separated from a yellow insoluble material (0.105 g), and NMe₄⁺ Cl⁻ (0.125 g, 1.14 mmol) was added to the mother liquor. The precipitate was filtered and dried *in vacuo* giving 0.356 g of **9**[NMe₄] as a yellow solid. ¹H and ¹¹B NMR analysis demonstrated that the insoluble material from removal of Et₂O was also **9**[NMe₄]. The combined yield of **9**[NMe₄] was 0.461 g (93% yield). A small portion of the product was recrystallized from hot CH₃OH/H₂O layered with hexane, which upon cooling gave yellow crystalline leaflets for analysis: mp 100 °C dec; ¹H NMR (CD₃CN) δ 0.4-2.50 (m, 8H, B-H), 3.05 (s, 12H), 6.97 (d, *J* = 8.8 Hz, 2H), 7.45 (s, 1H), 7.80 (d, *J* = 8.4 Hz, 2H); ¹¹B NMR (CD₃CN) δ -20.5 (d, *J* = 148 Hz, 4B), -16.1 (d, *J* = 160 Hz, 4B), 17.2 (s, 1B). Anal. Calcd. for C₁₁H₂₅B₉IN₃O: C, 30.06; H, 5.73; N, 9.56. Found: C, 29.47; H, 5.95; N, 9.21.

Characterization of [*closo*-1-CB₉H₈-1-COOH-10-PCy₃] (**10**).

Phosphonium zwitterion **10** was isolated from the main fraction of acid **3**[H₃O]

separated by chromatography from the reaction mixture of iodo acid **8**[NMe₄] (0.225 g, 0.62 mmol), hexylzinc chloride (3.1 mmol), [HPCy₃]⁺BF₄⁻ (0.018 g, 0.050 mmol), and Pd₂dba₃ (0.011 g, 0.012 mmol) as described above. Thus, washing the acid fraction (0.192 g) with CH₃OH gave 10 mg (~ 3% yield) of insoluble material identified as the phosphonium zwitterion **10**: ¹H NMR (acetone-*d*₆) δ 0.40-2.50 (m, 8H, B-H), 1.30-1.48 (m, 10H), 1.74-1.76 (m, 3H), 1.81-1.91 (m, 11H), 2.22-2.25 (m, 6H), 2.66 (q, *J* = 11.9 Hz, 3H), COOH not observed; ¹¹B NMR (acetone-*d*₆) δ -19.5 (d, *J* = 125 Hz, 4B), -13.4 (d, *J* = 158 Hz, 4B), 21.7 (d, *J* = 189 Hz, 1B); MS (FAB): *m/z* 439-445 (M-H, max at 443, 100%); FAB-HRMS(+): calcd. for C₂₀H₄₂B₉O₂P *m/z*: 444.3760; found; 444.3758.

Preparation of [*closo*-1-CB₉H₈-1-N₂-10-I] (**11**).

A suspension of [*closo*-1-CB₉H₈-1-NHBoc-10-I]⁻ NEt₄⁺ (**12**[NEt₄], 1.18 g, 2.41 mmol) in a 1:3 mixture of conc. HCl and CH₃OH (50 mL) was heated gently until all solids dissolved, and stirring was continued at rt for 18 hrs. H₂O (20 mL) was added and CH₃OH was removed *in vacuo*. Conc. HCl (3 mL) was added, and the resulting solution was extracted with Et₂O (3 x 30 mL). The organic layers were combined, dried (Na₂SO₄), and solvents evaporated *in vacuo* to give 0.604 g of crude [*closo*-1-CB₉H₈-1-NH₃-10-I] as a transparent film, which slowly solidified as a light brown glass: ¹H NMR (CD₃CN) δ 8.55 (s); ¹¹B NMR (CD₃CN) δ -21.3 (d, *J* = 145 Hz, 4B), -16.3 (d, *J* = 156 Hz, 4B), 16.9 (s, 1B); IR 3185 and 3123 (N-H) cm⁻¹.

The crude product was dissolved in a 1:1 mixture of AcOH/H₂O (6 mL), and an

aqueous solution of NaNO₂ (0.183 g, 2.65 mmol) in H₂O (4 mL) was added dropwise (~1 drop/sec) at 0 °C. Immediately, a white precipitate began to form. The reaction temperature was maintained for 30 min, H₂O (2 mL) was added, and the precipitate was filtered and dried to give 0.577 g (88% yield) of **11** as a white crystalline solid: mp 106 °C dec; ¹H NMR (CD₃CN) δ 1.28 (q, *J* = 156 Hz, 4H), 2.59 (q, *J* = 170 Hz, 4H); ¹¹B NMR (CD₃CN) δ -18.3 (d, *J* = 152 Hz, 4B), -8.8 (d, *J* = 169 Hz, 4B), 34.6 (s, 1B); IR 2245 (N₂) cm⁻¹.

Preparation of [*closo*-1-CB₉H₈-1-NHBoc-10-I]⁻NEt₄⁺ (12**[NEt₄]).**

A suspension of acid [*closo*-1-CB₉H₈-1-COOH-10-I]⁻NEt₄⁺ (**8**[NMe₄], 2.94 g, 7.02 mmol) in anhydrous CH₂Cl₂ (30 mL) was treated with neat (COCl)₂ (0.65 mL, 7.72 mmol). Vigorous bubbling of CO and CO₂ gases was observed followed by the dissolution of the substrate and the formation of a clear slight yellow solution. The solution was stirred for 1 hr at rt followed by filtration to remove insoluble particulates. The mother liquor was evaporated to dryness giving 3.10 g of crude [*closo*-1-CB₉H₉-1-COCl]⁻NEt₄⁺ as a white solid: ¹¹B {¹H} NMR δ (CD₃CN) -19.3 (4B), -13.6 (4B), 23.4 (1B); IR 2582 (B-H), 1772 (C=O) cm⁻¹.

Crude [*closo*-1-CB₉H₈-1-COCl-10-I]⁻NEt₄⁺ (3.10 g, 7.02 mmol) was dissolved in anhydrous CH₂Cl₂ (10 mL) and added via syringe to solid anhydrous ZnCl₂ (0.096 g, 0.702 mmol) under N₂ atmosphere. The reaction mixture was cooled to 0 °C, and Me₃SiN₃ (1.01 mL, 7.72 mmol) was added at once. The reaction mixture was stirred at 0

°C for an additional 30 min after which it was stirred for 4 hrs at rt. The reaction mixture was poured into ice-cold H₂O (50 mL) and extracted with CH₂Cl₂ (3 x 20 mL). The organic layers were combined, dried (MgSO₄), filtered, and solvent was removed *in vacuo* giving 3.09 g of crude [*closo*-1-CB₉H₈-1-CON₃-10-I]⁻ NEt₄⁺ as a white crystalline solid: ¹¹B {¹H} NMR (CD₃CN) δ -19.7 (4B), -14.9 (4B), 21.5 (1B); IR 2570 and 2523 (B-H), 2137 (N₃), 1686 (C=O) cm⁻¹. The crude product was contaminated with about 15% of [*closo*-1-CB₉H₈-1-COOH-10-I]⁻NEt₄⁺ (**8**[NEt₄])

Crude [*closo*-1-CB₉H₈-1-CON₃-10-I]⁻ NEt₄⁺ (3.09 g, 6.96 mmol) was dissolved in anhydrous CH₃CN (30 mL) and refluxed for 1 hr. The reaction was cooled to rt, solvent removed, and the residue was dried *in vacuo* giving 2.90 g of crude [*closo*-1-CB₉H₈-1-NCO-10-I]⁻ NEt₄⁺ as a slight yellow solid: ¹¹B {¹H} NMR (CD₃CN) δ -22.0 (4B), -15.5 (4B), 13.8 (1B); IR 2564 and 2525 (B-H), 2265 (N=C=O) cm⁻¹.

A solution of anhydrous *tert*-butanol (3.33 mL, 34.85 mmol), anhydrous CH₃CN (30 mL), and crude [*closo*-1-CB₉H₈-1-NCO-10-I]⁻ NEt₄⁺ (2.90 g, 6.97 mmol) was stirred at reflux for 2 hr after which solvents were removed leaving 3.06 g of crude **12**[NEt₄] as a yellow solid. The crude solid was dissolved in CH₂Cl₂ and passed through a silica gel plug first washed with 2% NEt₃ in CH₂Cl₂. Elution with a buffered CH₃CN/CH₂Cl₂ solution (2% NEt₃, 10% CH₃CN, 88% CH₂Cl₂) afforded 1.98 g (53% yield based on starting acid [*closo*-1-CB₉H₈-1-COOH-10-I]⁻ NEt₄⁺) of pure **12**[NEt₄] as a slight yellow solid. A small portion of the product was recrystallized from aqueous EtOH for analysis: mp 156-158 °C; ¹H NMR (CD₃CN) δ 0.40-2.50 (m, 8H, B-H), 1.20 (t, *J* = 7.2 Hz, 12H),

1.48 (s, 9H), 3.15 (q, $J = 7.2$ Hz, 8H), 7.08 (s, 1H); ^{11}B NMR (CD_3CN) δ -22.1 (d, $J = 142$ Hz, 4B), -16.7 (d, $J = 155$ Hz, 4B), 13.0 (1B); IR 3305 and 3233 (N-H), 2564 and 2520 (B-H), 1679 (C=O) cm^{-1} . Anal. Calcd. for $\text{C}_{14}\text{H}_{38}\text{B}_9\text{IN}_2\text{O}_2$: C, 34.27; H, 7.81; N, 5.71. Found: C, 34.32; H, 7.79; N, 5.71.

Further elution gave 0.75 g of a 90:10 mixture of **12**[NEt₄] and stiring acid [*closo*-1-CB₉H₈-1-COOH-10-I]⁻NEt₄⁺ (**8**[NEt₄]).

Acknowledgments

Financial support for this work was received from the National Science Foundation (DMR-0606317). We thank Dr. Damian Pocięcha of Warsaw University for helpful discussions.

References

- (1) Binnemans, K. *Chem. Rev.* **2005**, *105*, 4148-4204.
- (2) Yoshio, M.; Mukai, T.; Kanie, K.; Yoshizawa, M.; Ohno, H.; Kato, T.; *Adv. Mater.* **2002**, *14*, 351-354; Yoshio, M.; Kagata, T.; Hoshino, K.; Mukai, T.; Ohno, H.; Kato, T. *J. Am. Chem. Soc.* **2006**, *128*, 5570-5577; Yoshio, M.; Mukai, T.; Ohno, H.; Kato, T. *J. Am. Chem. Soc.* **2004**, *126*, 994-995.
- (3) Ichikawa, T.; Yoshio, M.; Hamasaki, A.; Mukai, T.; Ohno, H.; Kato, T. *J. Am. Chem. Soc.* **2007**, *129*, 10662-10663.

- (4) Yazaki, S.; Kamikawa, Y.; Yoshio, M.; Hamasaki, A.; Mukai, T.; Ohno, H.; Kato, T. *Chem. Lett.* **2008**, *37*, 538-539.
- (5) Grabovskiy, Y.; Kovalchuk, A.; Grydyakina, A.; Bugaychuk, S.; Mirnaya, T.; Klimusheva, G. *Liq. Cryst.* **2007**, *34*, 599-603.
- (6) Shimura, H.; Yoshio, M.; Hoshino, K.; Mukai, T.; Ohno, H.; Kato, T. *J. Am. Chem. Soc.* **2008**, *130*, 1759-1765.
- (7) Abu-Lebdeh, Y.; Abouimrane, A.; Alarco, P.-J.; Armand, M. *J. Power Sourc.* **2006**, *154*, 255-261.
- (8) Yamanaka, N.; Kawano, R.; Kubo, W.; Kitamura, T.; Wada, Y.; Watanabe, M.; Yanagida, S. *Chem. Commun.* **2005**, 740-742; Kawano, R.; Nazeeruddin, M. K.; Sato, A.; Gratzel, M.; Watanabe, M. *Electrochem. Commun.* **2007**, *9*, 1134-1138.
- (9) Ohno, H. *Bull. Chem. Soc. Jpn.* **2006**, *79*, 1665-1680; Ohno, H. *Electrochemical Aspects of Ionic Liquids*, Wiley, Hoboken, NJ, 2005.
- (10) Antharjanam, P. K. S.; Mallia, V. A.; Das, S. *Liq. Cryst.* **2004**, *31*, 713-717.
- (11) Tanabe, K.; Yasuda, T.; Kato, T. *Chem. Lett.* **2008**, *37*, 1208-1209; Goossens, K.; Nockemann, P.; Driesen, K.; Godoris, B.; Gorller-Walrand, C.; Van Hecke, K.; Van Meervelt, L.; Pouzet, E.; Binnemans, K.; Cardinaels, T. *Chem. Mater.* **2008**, *20*, 157-168; Yang, J.; Zhang, Q.; Laiyang, Z.; Zhang, S.; Li, J.; Zhang, X.; Deng, Y. *Chem. Mater.* **2007**, *19*, 2544-2550.
- (12) Zhu, Z.-Q.; Xiang, S.; Chen, Q.-Y.; Chen, C.; Zeng, Z.; Cui, Y.-P.; Xiao, J. C. *Chem. Commun.* **2008**, 5016-5018.

- (13) Ster, D.; Baumeister, U.; Chao Lorenzo, J.; Tschierske, C.; Israel, G. *J. Mater. Chem.* **2007**, *17*, 3393-3400.
- (14) Lo Celso, F.; Pibiri, I.; Triolo, A.; Triolo, R.; Pace, A.; Buscemi, S.; Vivona, N. *J. Mater. Chem.* **2007**, *17*, 1201-1208.
- (15) Haristoy, D.; Tsiourvas, D. *Liq. Cryst.* **2004**, *31*, 697-703.
- (16) O'Regan, B.; Gratzel, M. *Nature* **1991**, *353*, 737-740.
- (17) Busico, V.; Corradini, P.; Vacatello, M. *J. Phys. Chem.* **1982**, *86*, 1033-1034; Busico, V.; Cernicchiaro, P.; Corradini, P.; Vacatello, M. *J. Phys. Chem.* **1983**, *87*, 1631-1635; Gault, J. D.; Gallardo, H. A.; Muller, H. *Mol. Cryst. Liq. Cryst.* **1985**, *130*, 163-177; Iwamoto, K.; Ohnuki, Y.; Sawada, K.; Seno, M. *Mol. Cryst. Liq. Cryst.* **1981**, *73*, 95-103; Paleos, C. M.; Arkas, M.; Skoulios, A. *Mol. Cryst. Liq. Cryst.* **1998**, *309*, 237-250.
- (18) Gordon, C. M.; Holbrey, J. D.; Kennedy, A. R.; Seddon, K. R. *J. Mater. Chem.* **1998**, *8*, 2627-2636; Holbrey, J. D.; Seddon, K. R. *J. Chem. Soc., Dalton Trans.* **1999**, 2133-2139; Kouwer, P. H. J.; Swager, T. M. *J. Am. Chem. Soc.* **2007**, *129*, 14042-14052.
- (19) Suisse, J.-M.; Douce, L.; Bellemin-Lapponnaz, S.; Maise-François, A.; Welter, R.; Miyake, Y.; Shimizu, Y. *Eur. J. Inorg. Chem.* **2007**, 3899-3905.
- (20) Tabrizian, M.; Soldera, A.; Couturier, M.; Bazuin, C. G. *Liq. Cryst.* **1995**, *18*, 475-482; Cruz, C.; Heinrich, B.; Ribeiro, A. C.; Bruce, D. W.; Guillon, D. *Liq. Cryst.* **2000**, *27*, 1625-1631; Cui, L.; Sapagovas, V.; Lattermann, G. *Liq. Cryst.* **2002**, *29*, 1121-1132.
- (21) Sudholter, E. J. R.; Engberts, J. B. F. N.; de Jeu, W. *J. Phys. Chem.* **1982**, *86*, 1908-1913; Nusselder, J. J. H.; Engberts, J. B. F. N.; Van Doren, H. A. *Liq. Cryst.* **1993**,

13, 213-225.

(22) Vorlander, D. *Ber. Dtsch. Chem. Ges.* **1910**, *43*, 3120-3135; Van Duen, R.; Ramaekers, J.; Nockemann, P.; Van Hecke, K.; Van Meervelt, L.; Binnemans, K. *Eur. J. Inorg. Chem.* **2005**, *3*, 563-571. Winsor, P. A. In *Liquid Crystals and Plastic Crystals*, Gray, G. W. and Winsor, P. A. Eds.; Horwood, New York, 1974, Vol 1, pp 225-254.

(23) Paleos, C. M.; Kardassi, D.; Tsiourvas, D.; Skoulios, A. *Liq. Cryst.* **1998**, *25*, 267-275.

(24) Gao, W.; Dickinson, L.; Morin, F. G.; Reven, L. *Chem. Mater.* **1997**, *9*, 3113-3120.

(25) Ohtake, T.; Ogasawara, M.; Ito-Akita, K.; Nishina, N.; Ujiie, S.; Ohno, H.; Kato, T. *Chem. Mater.* **2000**, *12*, 782-789; Kishimoto, K.; Suzawa, T.; Yokota, T.; Mukai, T.; Ohno, H.; Kato, T. *J. Am. Chem. Soc.* **2005**, *127*, 15618-15623.

(26) Kaszynski, P.; Douglass, A. G. *J. Organomet. Chem.* **1999**, *581*, 28-38.

(27) Korbe, S.; Schreiber, P. J.; Michl, J. *Chem. Rev.* **2006**, *106*, 5208-5249; Stibr, B. *Chem. Rev.* **1992**, *92*, 225-250; Schleyer, P. v. R.; Najafian, K. *Inorg. Chem.* **1998**, *37*, 3454-3470.

(28) Reed, C. A. *Acc. Chem. Res.* **1998**, *31*, 133-139; Strauss, S. H. *Chem. Rev.* **1993**, *93*, 927-942; Krossing, I.; Raabe, I. *Angew. Chem. Int. Ed.* **2004**, *43*, 2066-2090.

(29) Larsen, A. S.; Holbrey, J. D.; Tham, F. S.; Reed, C. A. *J. Am. Chem. Soc.* **2000**, *122*, 7264-7272; Nieuwnhuyzen, M.; Seddon, K. R.; Teixidor, F.; Puga, A. V.; Viñas, C. *Inorg. Chem.* **2009**, *48*, 889-901.

- (30) Johnson, J. W.; Brody, J. F. *J. Electrochem. Soc.* **1982**, *129*, 2213-2219.
- (31) Ivanov, S. V.; Casteel, W. J.; Bailey, W. H. *US Pat. Appl.* 2007, US 2007189946; Pez, G. P.; Ivanov, S. V.; Dantsin, G.; Casteel, W. J.; Lehmann, J. F. *Eur. Pat. Appl.* 2007, EP 1763099.
- (32) Januszko, A.; More, K. M.; Pakhomov, S.; Kaszynski, P.; O'Neill, M.; Wand, M. D. *J. Mater. Chem.* **2004**, *14*, 1544-1553; Januszko, A.; Glab, K. L.; Kaszynski, P.; Patel, K.; Lewis, R. A.; Mehl, G. H.; Wand, M. D. *J. Mater. Chem.* **2006**, *16*, 3183-3192; Jasinski, M.; Jankowiak, A.; Januszko, A.; Bremer, M.; Pauluth, D.; Kaszynski, P. *Liq. Cryst.* **2008**, *35*, 343-350.
- (33) Ohta, K.; Januszko, A.; Kaszynski, P.; Nagamine, T.; Sasnouski, G.; Endo, Y. *Liq. Cryst.* **2004**, *31*, 671-682.
- (34) Kaszynski, P.; Januszko, A.; Ohta, K.; Nagamine, T.; Potaczek, P.; Young, V. G. Jr.; Endo, Y. *Liq. Cryst.* **2008**, *35*, 1169-1190.
- (35) Januszko, A.; Kaszynski, P. *Liq. Cryst.* **2008**, *35*, 705-710.
- (36) Kaszynski, P.; Kulikiewicz, K. K.; Januszko, A.; Douglass, A. G.; Tilford, R. W.; Pakhomov, S.; Patel, M. K.; Radziszewski, G. J.; Victor G. Young, V. G., Jr., unpublished results.
- (37) For other recent publications see: Ringstrand, B.; Vroman, J.; Jensen, D.; Januszko, A.; Kaszynski, P.; Dziaduszek, J.; Drzewinski, W. *Liq. Cryst.* **2005**, *32*, 1061-1070. Januszko, A.; Glab, K. L.; Kaszynski, P. *Liq. Cryst.* **2008**, *35*, 549-553. Nagamine, T.; Januszko, A.; Ohta, K.; Kaszynski, P.; Endo, Y. *Liq. Cryst.* **2008**, *35*, 865-884.
- (38) Kaszynski, P.; Pakhomov, S.; Tesh, K. F.; Young, V. G., Jr. *Inorg. Chem.* **2001**, *40*, 6622-6631.

- (39) Douglass, A. G.; Czuprynski, K.; Mierzwa, M.; Kaszynski, P. *J. Mater. Chem.* **1998**, *8*, 2391-2398.
- (40) Kaszynski, P.; Pakhomov, S.; Young, V. G. Jr. *Collect. Czech. Chem. Commun.* **2002**, *67*, 1061-1083; Pakhomov, S.; Kaszynski, P.; Young, V. G. Jr. *Inorg. Chem.* **2000**, *39*, 2243-2245; Balinski, A.; Januszko, A.; Harvey, J. E.; Brady, E.; Kaszynski, P.; Young, V. G. Jr., unpublished results; Kaszynski, P. In *Anisotropic Organic Materials*; Glaser, R., Kaszynski, P., Eds.; ACS Symposia: Washington D.C., 2001; Vol. 798, p 68-82.
- (41) Ringstrand, B.; Balinski, A.; Franken, A.; Kaszynski, P. *Inorg. Chem.* **2005**, *44*, 9561-9566.
- (42) Neises, B.; Steglich, W. *Angew. Chem. Int. Ed.* **1978**, *17*, 522-524.
- (43) Neubert, M. E.; Wildman, P. J.; Zawaski, M. J.; Hanlon, C. A.; Benyo, T. L.; Vries, A. D. *Mol. Cryst. Liq. Cryst.* **1987**, *145*, 111-158.
- (44) Ringstrand, B.; Kaszynski, P.; Franken, A. *Inorg. Chem.* **2009**, *48*, 7313-7329.
- (45) Carr, N.; Gray, G. W.; McDonnell, D. G. *Mol. Cryst. Liq. Cryst.* **1983**, *97*, 13-28.
- (46) Erdik, E. *Tetrahedron* **1992**, *48*, 9577-9648.
- (47) Knochel, P.; Singer, R. D. *Chem. Rev.* **1993**, *93*, 2117-2188.
- (48) Zhou, J.; Fu, G. C. *J. Am. Chem. Soc.* **2003**, *125*, 12527-12530.
- (49) Krasovskiy, A.; Malakhov, V.; Gavryushin, A.; Knochel, P. *Angew. Chem. Int.*

Ed. **2006**, *45*, 6040-6044.

(50) The original synthesis and the solid-state structure of **11** is reported in Carr, M. Franken, A.; Kaszynski, P.; Kennedy, J. D., unpublished results.

(51) Demus, D.; Richter, L. *Textures of Liquid Crystals*; 2nd ed.; VEB: Leipzig, 1980. Gray, G. W.; Goodby, J. W. G. *Smectic Liquid Crystals-Textures and Structures*; Leonard Hill: Philadelphia, 1984. Dierking, I. *Textures of Liquid Crystals*; Wiley-VCH: Weinheim, 2003.

(52) Neubert, M. E. in *Liquid Crystals: Experimental Study of Physical Properties and Phase Transitions*, S. Kumar, Ed., Cambridge University Press, New York, 2001, and references therein.

(53) Steinsträsser, R.; Pohl, L. *Z. Naturforsch.* **1971**, *26b*, 577-580.

(54) Reddy, R. A.; Baumeister, U.; Keith, C.; Hahn, H.; Lang, H.; Tschierske, C. *Soft Matter* **2007**, *3*, 558-570.

(55) Keith, C.; Reddy, R. A.; Hauser, A.; Baumeister, U.; Tschierske, C. *J. Am. Chem. Soc.* **2006**, *128*, 3051–3066.

(56) Prehm, M.; Cheng, X. H.; Diele, S.; Das, M. K.; Tschierske, C. *J. Am. Chem. Soc.* **2002**, *124*, 12072–12073.

(57) See electronic supporting information.

(58) Sienkowska, M. J.; Monobe, H.; Kaszynski, P.; Shimizu, Y. *J. Mater. Chem.* **2007**, *17*, 1392-1398.

**Anion-Driven Mesogenicity: A Comparative Study of Ionic Liquid Crystals
Based on the $[closo-1-CB_9H_{10}]^-$ and $[closo-1-CB_{11}H_{12}]^-$ Clusters.**

This chapter represents a work in progress on a new series of ionic liquid crystals containing the $[closo-1-CB_{11}H_{12}]^-$ anion (**B**). The goal of the project is to compare the effect of the cage structure on the liquid crystalline properties relative to analogous derivatives of the $[closo-1-CB_9H_{10}]^-$ anion (**A**) and to develop ionic liquid crystals based on the more accessible $[closo-1-CB_{11}H_{12}]^-$ anion (**B**).

In this work, I was responsible for the preparation and characterization of two series of structurally analogous esters (**1** and **2**) derived from the $[closo-1-CB_9H_{10}]^-$ (**A**, esters **1**) and $[closo-1-CB_{11}H_{12}]^-$ (**B**, esters **2**) clusters containing up to 4 rings in the rigid core. The esters were paired with either an elongated pyridinium [**Pyr**] or cetyltrimethylammonium [**Cetyl**] cations. The chemistry used to prepare esters **1** was developed earlier in my dissertation studies (see Part II, Chapters 1 and 2), whereas the chemistry used to prepare esters **2** was developed during this work.

Ms. Lillian Johnson assisted in the synthesis and characterization of several esters **1** and **2**. Dr. Damian Pocięcha and Dr. Ewa Gorecka hosted me during a one-month stay at the University of Warsaw in Warsaw, Poland in the summer of 2010. This arrangement

was made possible through a Vanderbilt University Graduate School Dissertation Enhancement Grant. During this time, Dr. Pocięcha and Dr. Gorecka assisted me in the collection of powder XRD data for ionic liquid crystals **1f[Pyr]**, **2f[Pyr]**, **1g[Pyr]**, and **2g[Pyr]**. Dr. Piotr Kaszynski performed quantum mechanical calculations to estimate the molecular length of the salts that were analyzed by powder XRD.

Abstract

A series of structurally analogous esters derived from the [*closo*-1-CB₉H₁₀]⁻ and [*closo*-1-CB₁₁H₁₂]⁻ clusters (**A** and **B**, respectively) containing up to 4 rings in the rigid core were prepared and their liquid crystalline properties investigated by thermal, optical, and XRD methods. Salts containing *N*-butyl-4-heptyloxy pyridinium cation [**Pyr**] and cetyltrimethylammonium [**Cetyl**] exhibit SmA in the temperature range of 90 °C – 190 °C. The ionic liquid crystals derived from the [*closo*-1-CB₁₁H₁₂]⁻ cluster (**B**) generally exhibit higher melting points and moderately stabilized SmA phases but with narrower ranges, when compared to the analogous derivatives of the [*closo*-1-CB₉H₁₀]⁻ cluster (**A**). **1e[Pyr]** containing an azo group in the structure exhibited SmC below SmA. Four ionic liquid crystals **1f[Pyr]**, **2f[Pyr]**, **1g[Pyr]**, and **2g[Pyr]** were investigated by powder XRD.

Introduction

During the past decade, research of ionic liquid crystals (ILCs) has significantly

intensified and diversified, where the vast majority of ILCs investigated to date depend on an anisometric cation, such as substituted ammonium, imidazolium, or pyridinium to drive mesogenic behavior.^{1,2} Anisotropic ion mobility exhibited by some ILCs generated considerable interest in developing ion-conductive materials³⁻⁷ for applications in batteries⁸ and dye-sensitized solar cells.⁹ In general, the anion in these materials is present for charge compensation, but it can significantly affect mesophase range and stability.¹

closo-Monocarbaborates [*closo*-1-CB₉H₁₀]⁻ and [*closo*-1-CB₁₁H₁₂]⁻ (**A** and **B**, respectively, Figure 1), are weakly coordinating anions¹⁰ since their negative charge is completely delocalized over the cluster. This property and their electronic and geometrical features makes them attractive structural elements for ILCs,^{11,12} in which the anisometric anion drives the mesogenic behavior. In this context, we recently reported the first examples of such derivatives (**IA**) containing the [*closo*-1-CB₉H₁₀]⁻ cluster (**A**).¹³ These ILCs displayed SmA and soft crystalline phases when 3 rings were present in the rigid core with compensation from an elongated pyridinium cation. Esters **1a-1c** were described in this previous study.

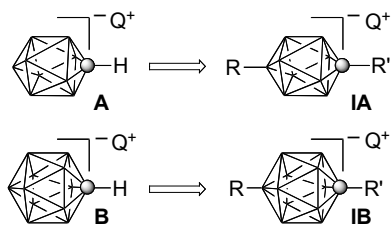


Figure 1. The structures of the [*closo*-1-CB₉H₁₀]⁻ and [*closo*-1-CB₁₁H₁₂]⁻ clusters (**A** and **B**), and ion pairs of their 1,10- (**IA**) and 1,12-disubstituted (**IB**) derivatives with the counterion Q⁺. Q represents a metal or an onium fragment such as ammonium or

pyridinium. Each vertex represents a BH fragment and the sphere is a carbon atom.

We are interested in the more accessible $[closo-1-CB_{11}H_{12}]^-$ cluster (**B**) as a structural element of ILCs (**IB**) capable of supporting anisotropic lithium ion transport. In addition, we wished to examine the effect of the cage structure of $[closo-1-CB_{11}H_{12}]^-$ cluster (**B**) on liquid crystalline behavior and to compare their properties to those already known for the $[closo-1-CB_9H_{10}]^-$ cluster (**A**). Here, we report the preparation of a series of mesogenic esters **2** as the first examples of ILCs based on the $[closo-1-CB_{11}H_{12}]^-$ cluster (**B**) and compare their properties to analogous esters **1** of the $[closo-1-CB_9H_{10}]^-$ cluster (**A**). We investigated structures with up to 4 rings in the rigid core of the anisometric anion with two different cations, an elongated pyridinium [**Pyr**] and cetyltrimethylammonium [**Cetyl**], Q^+ (Fig. 2). We establish fundamental structure-property relationships between the two series of esters **1** and **2** using polarizing optical microscopy (POM), differential scanning calorimetry (DSC), and X-ray powder diffraction (XRD).

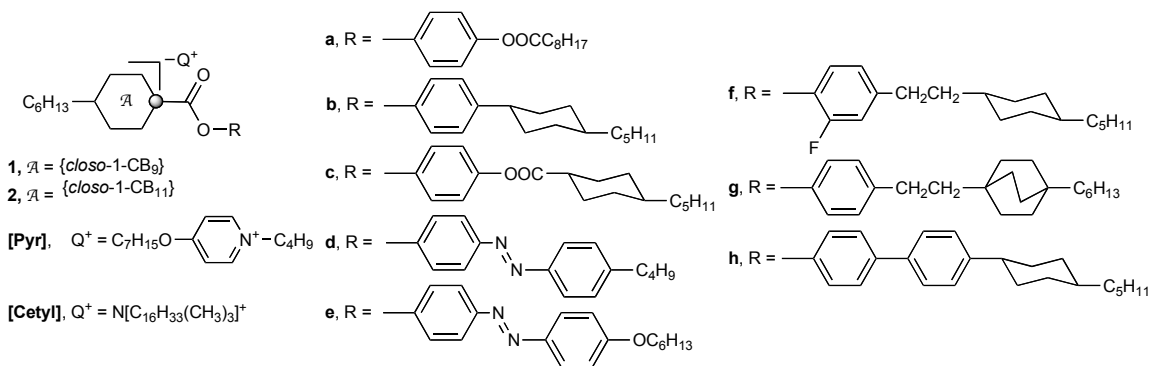


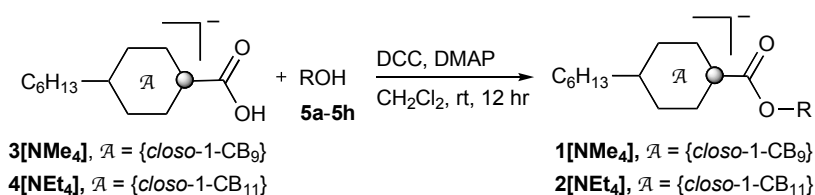
Figure 2. Structures of esters **1** and **2**.

Results and Discussion

Synthesis

Esters **1**[NMe₄] and **2**[NEt₄] were prepared from carboxylic acids, **3**[NMe₄] and **4**[NEt₄], respectively, and phenols **5a-5h** using dicyclohexylcarbodiimide (DCC) and catalytic amounts of 4-dimethylaminopyridine (DMAP) in CH₂Cl₂ following a general literature procedure¹⁴ (Scheme 1).

Scheme 1. Synthesis of esters **1**[NMe₄] and **2**[NEt₄]

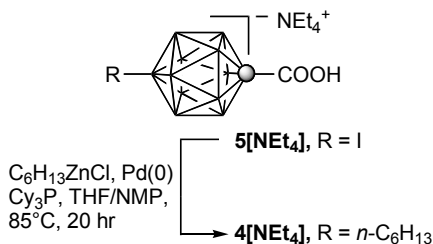


Esters **1**[Pyr] and **2**[Pyr] or **1**[Cetyl] and **2**[Cetyl] were prepared by exchange of the NMe₄⁺ or NEt₄⁺ cation for *N*-butyl-4-heptyloxy-pyridinium bromide or cetyltrimethylammonium bromide in a biphasic CH₂Cl₂/H₂O system following the procedure for the preparation of esters **1a**[Pyr]-**1c**[Pyr].¹³

The carboxylic acid [*closo-1-CB*₁₁H₁₀-1-COOH-12-C₆H₁₃]⁻ (**4**[NEt₄]) was prepared from iodide [*closo-1-CB*₁₁H₁₀-1-COOH-12-I]⁻ (**5**[NEt₄]) using the Negishi coupling^{15,16} with 12-fold excess hexylzinc chloride as was previously described for the preparation of [*closo-1-CB*₉H₈-1-COOH-10-C₆H₁₃]⁻ [NMe₄]⁺ (**3**[NMe₄]) in Scheme 4.¹⁷

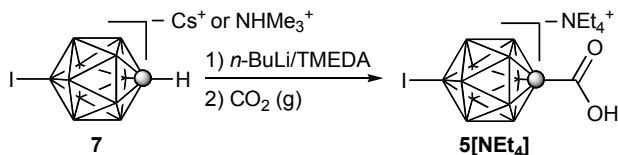
The PCy₃ ligand generated *in-situ* works equally well for both acids, and the 12-hexyl acid **4**[NEt₄] was obtained in 61 % yield.

Scheme 4. Preparation of carboxylic acid **3**[NEt₄].



Iodo acid **5**[NEt₄] was prepared in nearly quantitative yield by lithiation of iodo derivative [*closo*-1-CB₁₁H₁₁-12-I]⁻ Cs⁺ (**7**[Cs] or **7**[NHMe₃]) with *n*-BuLi in the presence of TMEDA followed by reaction with CO₂ (Scheme 5). Without TMEDA, the carboxylation of **7** was incomplete and only 20 % conversion to **5** was observed. This represents a significant improvement in the carboxylation of the {*closo*-1-CB₁₁} cluster.¹⁸ The iodo derivative **7** was prepared in 75 % yield by iodination of parent anion [*closo*-1-CB₁₁H₁₂]⁻ with I₂ in acetic acid following the literature precedence.¹⁹ Attempts to iodinate parent anion [*closo*-1-CB₁₁H₁₂]⁻ with I₂ in 5 % KOH as previously described¹⁸ only gave starting material.

Scheme 5. Preparation of carboxylic acid **5**[NEt₄]



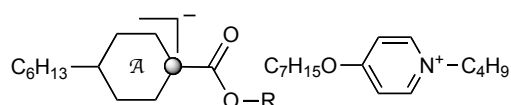
Liquid Crystalline Properties

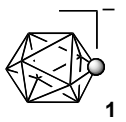
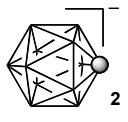
Transition temperatures and associated enthalpies for compounds **1[Pyr]**-**2[Pyr]** and **1[Cetyl]**-**2[Cetyl]** are shown in Tables 1 and 2, respectively. Phase structures were assigned by comparison of POM results with published textures for reference compounds²⁰ and established trends in thermodynamic stability.²¹ The tetramethylammonium or tetraethylammonium salts were not investigated for liquid crystalline properties based on previous results, which showed these types of cations to not support the liquid crystalline state.¹³

Two-ring (**1a[Pyr]** and **2a[Pyr]**) and three-ring (**1d[Pyr]** and **2d[Pyr]**) pyridinium salts are not liquid crystals. However, incorporation of the larger and more symmetrical {*closo*-1-CB₁₁} (**B**) cluster does increase the melting point in each pair by 10 and 24 K, respectively. While ester **1b[Pyr]** possesses an enantiotropic SmA from 153 to 163 °C and soft crystalline phases (X and X') at lower temperatures, ester **2b[Pyr]** containing the {*closo*-1-CB₁₁} cluster (**B**) displays no mesogenic behavior. Replacement of direct bond in the phenol backbone in esters **1b[Pyr]** and **2b[Pyr]** with an ester linkage in esters **1c[Pyr]** and **2c[Pyr]** induces an enantiotropic SmA phase in both materials due to increase flexibility in the anisometric anion. Despite replacement of {*closo*-1-CB₉} (**A**) with {*closo*-1-CB₁₁} (**B**), the stability of the SmA phase is essentially the same, however, the range of the phase is lower by 20 K. Replacement of a CH₂ group in ester **1d[Pyr]** for a OCH₂CH₂ group in ester **1e[Pyr]** induces the SmA phase and a SmC phase at lower temperatures. The latter was identified by the characteristic schilren

texture in polarized light. Esters **1f[Pyrr]** and **2f[Pyrr]** possessing a laterally substituted fluorine exhibit enantiotropic SmA phases of similar stability. Esters **1g[Pyrr]** and **2g[Pyrr]** exhibit both enantiotropic SmA phases, however, ester **1g[Pyrr]** displays a more rich polymorphism possessing soft crystalline phases X and X' at lower temperatures. (Table 1).

Table 1. Transition temperatures (°C) and enthalpies (kJ/mol, in parentheses) for **1[Pyrr]** and **2[Pyrr]**



R		
a	Cr ₁ 64 Cr ₂ 101 Cr ₃ 107 I (9.2) (3.4) (15.1) ^a	Cr 117 I (27.4)
b	Cr 128 (X' 129) X 153 SmA 163 I (19.3) (3.2) (2.4) (4.5) ^a	Cr ₁ 162 Cr ₂ 178 I (9.8) (24.3)
c	Cr 102 SmA 164 I (43.7) (7.0) ^a	Cr ₁ 109 Cr ₂ 119 SmA 161 I (7.7) (14.9) (6.2)
d	Cr 131 I (45.4)	Cr 155 I (46.9)
e	Cr ₁ 32 Cr ₂ 123 Sm C 132 Sm A 137 I (9.8) (43.2) (0.6) (1.3)	n/a
f	Cr 87 SmA 148 I (50.1) (10.9)	Cr 99 SmA 146 I (35.7) (8.9)

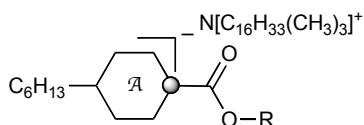
g	Cr ₁ 123 X' 129 X 132 SmA 189 I	Cr 150 SmA 182 I
	(41.3) (2.8) (3.3) (11.5)	(39.2) (13.8)

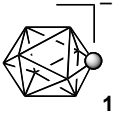
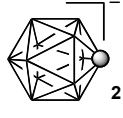
^a Previously reported.¹³

Exchange of the elongated pyridinium cation in ester **1f**[Pyr] for cetyltrimethylammonium in ester **1f**[Cetyl] demonstrated that the salt could no longer support the liquid crystalline state. The presence of the cetyltrimethylammonium cation increased the melting point by 21 K. Ester **2f**[Cetyl] was not prepared based on these results (Table 2).

Based on these results (Tables 1 and 2), it appears that salts containing a total of 4 rings are most likely to exhibit liquid crystalline properties. Thus, ester **2h**[Cetyl] was prepared to test this theory. In fact, ester **2h**[Cetyl] displays rich polymorphism possessing soft crystalline phases X and X' as well as the SmA phase. However, ester **2h**[Cetyl] decomposes upon isotropization.

Table 2. Transition temperatures (°C) and enthalpies (kJ/mol, in parentheses) for esters **1f**[Cetyl] and **2h**[Cetyl]



R		
f	Cr ₁ 64 Cr ₂ 169 I (34.4) (54.2)	n/a

h	n/a	Cr 36 X 211 X' 216 SmA 226 dec (7.6) (1.3) (12.1) (0.8)
----------	-----	--

Powder X-ray diffraction (XRD)

Esters **1f[Pyr]** and **2f[Pyr]** and **1g[Pyr]** and **2g[Pyr]** were investigated by X-ray powder diffraction to determine their phase structures. Data was collected on cooling from the isotropic phase, and XRD results are shown in Figure 3.

The XRD results confirmed the presence of SmA phase in all four compounds. The diffractograms consist of a single sharp reflection in the small angle region (*001*) (Figure 2). The wide-angle region of the diffractograms shows a broad halo with maximums that can be distinguished at about $d = 5.0 \text{ \AA}$, $d = 5.1 \text{ \AA}$, $d = 5.1 \text{ \AA}$, and $d = 5.2 \text{ \AA}$ in **1f[Pyr]**, **2f[Pyr]**, **1g[Pyr]**, and **2g[Pyr]**, respectively. These values can be attributed to the average alkyl chain-alkyl chain correlation distance or to the correlations involving larger structural units such as the boron clusters.

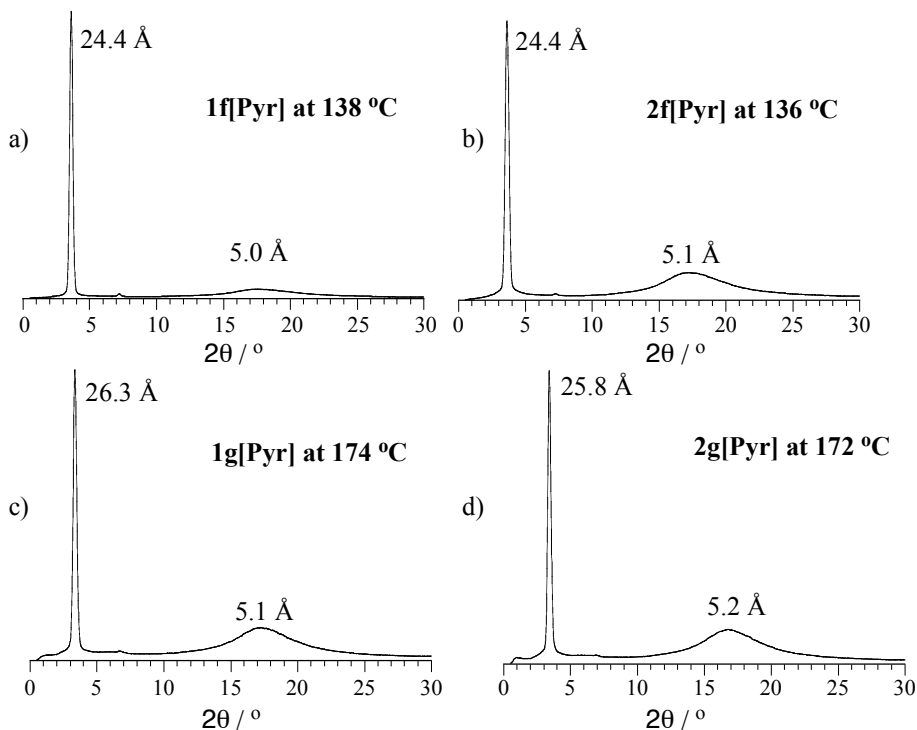


Figure 3. Stacked X-ray diffraction patterns for a) **1f[Pyr]** obtained at 138 °C (SmA, $c = 24.4$ Å); b) **2f[Pyr]** obtained at 136 °C (SmA, $c = 24.4$ Å); c) **1g[Pyr]** obtained at 174 °C (SmA, $c = 26.3$ Å); and d) **2g[Pyr]** obtained at 172 °C (SmA, $c = 25.8$ Å).

In addition, the temperature dependence of the layer thickness in the SmA phase was examined for esters **1f[Pyr]** and **2f[Pyr]** and **1g[Pyr]** and **2g[Pyr]** (Figure 4). Upon cooling, esters **2g[Pyr]**, **2f[Pyr]**, and **1f[Pyr]** undergo layer expansion with thermal expansion coefficients of 1.01 pm/K, 1.60 pm/K, and 2.45 Å/K, respectively. Ester **1g[Pyr]** surprisingly experiences layer contraction upon cooling with a thermal expansion coefficient of -0.16 pm/K.

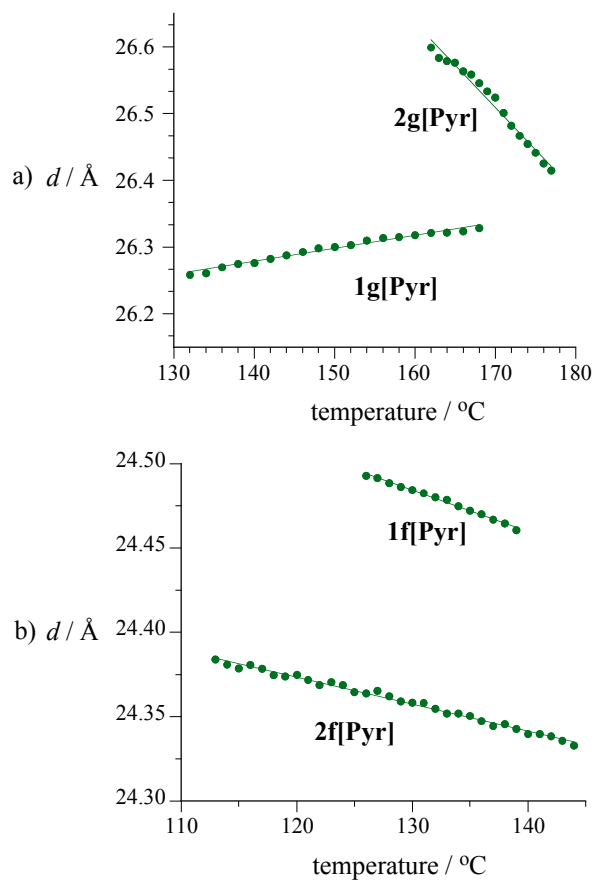


Figure 4. SmA period as a function of temperature for esters a) **2g[Pyr]** (177 to 162 °C) and **1g[Pyr]** (168 to 132 °C) and b) **2f[Pyr]** (144 to 113 °C) and **1f[Pyr]** (139 to 126 °C). Best fit line for **2g[Pyr]**: $y = 28.215 - 0.010161x$, $R = 0.98933$; **1g[Pyr]**: $y = 26.084 + 0.0015628x$, $R = 0.98894$; **2f[Pyr]**: $y = 24.565 - 0.0016x$, $R = 0.99547$; **1f[Pyr]**: $y = 24.802 - 0.024474x$, $R = 0.99707$.

Summary and Conclusions

Results show that the $[closo-1-CB_{11}H_{12}]^-$ cluster (**B**) is an effective structural element of ionic liquid crystals in which the negative charge is fully delocalized and the anion is non-nucleophilic. Similarly to esters **1** of the $[closo-1-CB_9H_{10}]^-$ cluster (**A**),

esters **2** of the [*closo*-1-CB₁₁H₁₂]⁻ cluster (**B**) exhibit a partially interdigitated monolayer SmA phase when the pyridinium counterion is present. We also demonstrated that salts containing a long aliphatic cation such as cetyltrimethylammonium are suitable for inducing the liquid crystalline state. However, such materials appear to be thermally unstable and are prone to decomposition near the isotropization point. Clearing temperatures for esters **2** are typically higher and the stability of the liquid crystalline phase is decreased when compared to esters **1**. Powder XRD of four esters **1f**[Pyr] and **2f**[Pyr] and **1g**[Pyr] and **2g**[Pyr] confirmed the presence of the SmA phase.

Experimental Section

Synthetic Details

¹H NMR spectra were obtained at 400 MHz field for all compounds in acetone-*d*₆ (δ 2.04 ppm), CD₃CN (δ 1.93 ppm) or CDCl₃ (δ 7.26 ppm). ¹¹B NMR were recorded at 128 MHz field. Chemical shifts were referenced to the solvent (¹H) or to an external sample of B(OH)₃ in MeOH (¹¹B, δ = 18.1 ppm). Elemental analysis was provided by Atlantic Microlab, Inc. The preparation and characterization details of *N*-butyl-4-heptyloxy pyridinium bromide and esters **1a**[Pyr]-**1c**[Pyr] were previously reported.¹³

Optical microscopy was performed using a PZO Biolar microscope equipped with an HCS402 Instec hot stage. Thermal analysis was obtained using a TA Instruments 2920

DSC. Transition temperatures (onset) and enthalpies were obtained using small samples (~0.5 mg) and a typical heating/cooling rate of 5 K min⁻¹ under a flow of nitrogen gas. XRD measurements were carried out on unoriented and uncovered samples placed on a temperature-controlled glass plate using GADDS X-ray diffractometer (Cu K α 1 = 1.5405Å). XRD patterns were collected in the range of 1.5° – 35° on cooling. Layer spacings (cell constant *c*) were determined from the (002) reflection.

General Procedure for Preparation of Esters 1[Pyr]-2[Pyr] and 1[Cetyl]-2[Cetyl]

Phenol **5** (1.5 equivalents) was added to a colorless solution of acid [*closo*-1-CB₉H₈-1-COOH-10-C₆H₁₃]⁻NMe₄⁺ (**3**[NMe₄]) or [*closo*-1-CB₁₁H₁₀-1-COOH-12-C₆H₁₃]⁻NEt₄⁺ (**4**[NEt₄]), DCC (1.0 equivalent), and DMAP (0.1 equivalents) in anhydrous CH₂Cl₂. The reaction mixture was stirred overnight at rt, and the reaction progress was monitored by TLC (R_f = 0.5, CH₃CN/CH₂Cl₂, 1:9). The solvent was removed *in vacuo*, and the crude product was isolated by column chromatography (SiO₂, CH₃CN/CH₂Cl₂, 1:9). The resulting ester was washed with hot hexane and used in the subsequent step for cation exchange without further purification. Typical yields for this procedure are above 80 %.

N-Butyl-4-heptyloxypyridinium bromide (1.0 equivalent) or cetyltrimethylammonium (1.0 equivalent) were added to a solution of ester **1**[NMe₄] or **2**[NEt₄] in CH₂Cl₂. Water was added, and the biphasic system was stirred vigorously until all the precipitate had dissolved. The CH₂Cl₂ layer was separated, and the aqueous

layer was extracted with additional CH₂Cl₂. The CH₂Cl₂ layers were combined, washed with H₂O, dried (Na₂SO₄), and evaporated giving **1[Pyr]**-**2[Pyr]** or **1[Cetyl]**-**2[Cetyl]** as crystalline solids, which were further purified by recrystallization from aqueous alcohol. In some cases by the pyridinium salts were further purified by column chromatography (CH₃CN/CH₂Cl₂, 1:9) and then by several recrystallizations from aqueous alcohol. The resulting crystals were dried in vacuum at ambient temperature, and typical yields range from 20%-40% based on the starting hexyl acid **3[NMe₄]** or **4[NEt₄]**.

1d[Pyr]: Recrystallized from EtOH/H₂O mixtures (1x) and MeOH/H₂O mixtures (7x) providing the pure salt as orange microcrystals: ¹H NMR (400 MHz, acetone-*d*₆) δ 0.40-2.50 (m, 8H), 0.87 (t, *J* = 6.9 Hz, 3H), 0.92 (t, *J* = 7.1 Hz, 3H); 0.94 (t, *J* = 7.4 Hz, 3H), 0.95 (t, *J* = 7.4 Hz, 3H), 1.23-1.44 (m, 16H), 1.45-1.52 (m, 2H), 1.53-1.61 (m, 2H), 1.66 (quint, *J* = 7.6 Hz, 2H), 1.85-1.92 (m, 4H), 1.95-2.04 (m, 2H), 2.73 (t, *J* = 7.7 Hz, 2H), 4.46 (t, *J* = 6.5 Hz, 2H), 4.64 (t, *J* = 7.5 Hz, 2H), 7.42 (d, *J* = 8.4 Hz, 2H), 7.51 (d, *J* = 8.8 Hz, 2H), 7.67 (d, *J* = 7.6 Hz, 2H), 7.88 (d, *J* = 8.4 Hz, 2H), 8.03 (d, *J* = 8.8 Hz, 2H), 8.92 (d, *J* = 7.6 Hz, 2H); ¹¹B {¹H} NMR (128 MHz, acetone-*d*₆) δ -23.8 (4B), -15.8 (4B), 49.4 (1B). Anal. Calcd. for C₄₀H₆₆B₉N₃O₃: C, 65.43; H, 9.06; N, 5.72. Found: C, 65.96; H, 9.02; N, 6.00.

1e[Pyr]: Recrystallized from EtOH/H₂O mixtures (4x) providing the pure salt as orange microcrystals: ¹H NMR (400 MHz, acetone-*d*₆) δ 0.40-2.50 (m, 8H), 0.88 (t, *J* = 7.0 Hz, 3H), 0.92 (t, *J* = 7.0 Hz, 3H), 0.93 (t, *J* = 6.5 Hz, 3H), 0.96 (t, *J* = 7.4 Hz, 3H), 1.27-1.32 (m, 4H), 1.33-1.45 (m, 12H), 1.46-1.62 (m, 6H), 1.80-2.09 (m, 10H), 4.14 (t, *J* = 6.5 Hz,

2H), 4.47 (t, $J = 6.5$ Hz, 2H), 4.64 (t, $J = 7.4$ Hz, 2H), 7.12 (d, $J = 9.0$ Hz, 2H), 7.50 (d, $J = 8.8$ Hz, 2H), 7.68 (d, $J = 7.4$ Hz, 2H), 7.95 (d, $J = 8.9$ Hz, 2H), 8.01 (d, $J = 8.8$ Hz, 2H), 8.92 (d, $J = 7.4$ Hz, 2H); ^{11}B NMR (128 MHz, acetone- d_6) δ -23.9 (d, $J = 143$ Hz, 4B), -15.9 (d, $J = 139$ Hz, 4B), 49.0 (s, 1B). Anal. Calcd. for $\text{C}_{42}\text{H}_{70}\text{B}_9\text{N}_3\text{O}_4$: C, 64.81; H, 9.07; N, 5.40. Found: C, 65.03; H, 9.25; N, 5.33.

1f[Pyr]: Recrystallized from MeOH/H₂O mixtures (4x) providing the pure salt as white crystals: ^1H NMR (500 MHz, acetone- d_6) δ 0.40-2.50 (m, 8H), 0.87 (t, $J = 7.0$ Hz, 6H), 0.91 (t, $J = 7.1$ Hz, 3H), 0.95 (t, $J = 7.4$ Hz, 3H), 0.96-1.03 (m, 1H), 1.15-1.20 (m, 2H), 1.21-1.33 (m, 12H), 1.34-1.44 (m, 8H), 1.45-1.51 (m, 2H), 1.52-1.59 (m, 4H), 1.77 (br d, $J = 12.3$ Hz, 2H), 1.82-1.98 (m, 9H), 1.99-2.04 (m, 4H), 2.68 (t, $J = 8.1$ Hz, 2H), 4.47 (t, $J = 6.5$ Hz, 2H), 4.64 (t, $J = 7.5$ Hz, 2H), 7.08 (d, $J = 8.2$ Hz, 1H), 7.13 (d, $J = 11.5$ Hz, 1H), 7.24 (t, $J = 8.2$ Hz, 1H), 7.68 (d, $J = 7.5$ Hz, 2H), 8.92 (d, $J = 7.5$ Hz, 2H); ^{11}B NMR (128 MHz, acetone- d_6) δ -23.9 (d, $J = 140$ Hz, 4B), -15.9 (d, $J = 150$ Hz, 4B), 49.0 (s, 1B). Anal. Calcd. for $\text{C}_{43}\text{H}_{77}\text{B}_9\text{FNO}_3$: C, 66.87; H, 10.05; N, 1.81. Found: C, 67.06; H, 10.07; N, 1.89.

1f[Cetyl]: Recrystallized from MeOH/H₂O mixtures (4x) providing the pure salt as white crystals: ^1H NMR (400 MHz, acetone- d_6) δ 0.40-2.50 (m, 8H), 0.87 (t, $J = 7.0$ Hz, 3H), 0.88 (t, $J = 6.8$ Hz, 3H), 0.92 (t, $J = 7.0$ Hz, 6H), 1.16-1.43 (m, 41H), 1.52-1.61 (m, 4H), 1.78 (br d, $J = 12.6$ Hz, 2H), 1.83-2.00 (m, 8H), 2.69 (t, $J = 8.1$ Hz, 2H), 3.37 (s, 9H), 3.54-3.60 (m, 2H), 7.09 (d, $J = 8.3$ Hz, 1H), 7.14 (dd, $J_1 = 11.5$ Hz, $J_2 = 2.0$ Hz, 1H), 7.25 (t, $J = 8.1$ Hz, 1H); ^{11}B NMR (128 MHz, acetone- d_6) δ -23.9 (d, $J = 135$ Hz, 4B), -15.9

(d, $J = 150$ Hz, 4B), 49.3 (s, 1B). Anal. Calcd. for $C_{46}H_{91}B_9FNO_2$: C, 68.50; H, 11.37; N, 1.74. Found: C, 68.92; H, 11.24; N, 1.86.

1g[Pyrr]: Recrystallized from MeOH/H₂O mixtures (4x) providing the pure salt as white crystals: ¹H NMR (500 MHz, acetone-*d*₆) δ 0.40-2.50 (m, 8H), 0.87 (t, $J = 7.0$ Hz, 6H), 0.91 (t, $J = 7.1$ Hz, 3H), 0.95 (t, $J = 7.4$ Hz, 3H), 1.06-1.10 (m, 2H), 1.18-1.51 (m, 36H), 1.56 (quint, $J = 7.2$ Hz, 2H), 1.84-1.96 (m, 6H), 1.98-2.04 (m, 2H), 2.52-2.57 (m, 2H), 4.46 (t, $J = 6.5$ Hz, 2H), 4.63 (t, $J = 7.5$ Hz, 2H), 7.15 (d, $J = 8.5$ Hz, 2H), 7.24 (d, $J = 8.5$ Hz, 2H), 7.67 (d, $J = 7.5$ Hz, 2H), 8.91 (d, $J = 7.5$ Hz, 2H); ¹¹B NMR (128 MHz, acetone-*d*₆) δ -23.9 (d, $J = 139$ Hz, 4B), -16.0 (d, $J = 152$ Hz, 4B), 49.0 (s, 1B). Anal. Calcd. for $C_{46}H_{82}B_9NO_3$: C, 69.54; H, 10.40; N, 1.76. Found: C, 69.68; H, 10.21; N, 1.87.

2a[Pyrr]: Recrystallized from MeOH/H₂O mixtures (3x) providing the pure salt as white flakes: ¹H NMR (400 MHz, acetone-*d*₆) δ 0.50-2.50 (m, 10H), 0.53-0.59 (m, 2H), 0.85 (t, $J = 7.1$ Hz, 3H), 0.87 (t, $J = 6.9$ Hz, 6H), 0.95 (t, $J = 7.4$ Hz, 3H), 1.26-1.44 (m, 26H), 1.45-1.53 (m, 2H), 1.70 (quint, $J = 7.4$ Hz, 2H), 1.89 (quint, $J = 7.0$ Hz, 2H), 1.98-2.06 (m, 2H), 2.55 (t, $J = 7.4$ Hz, 2H), 4.47 (t, $J = 6.5$ Hz, 2H), 4.64 (t, $J = 7.5$ Hz, 2H), 7.01 (d, $J = 9.0$ Hz, 2H), 7.10 (d, $J = 9.0$ Hz, 2H), 7.68 (d, $J = 7.6$ Hz, 2H), 8.92 (d, $J = 7.6$ Hz, 2H); ¹¹B NMR (128 MHz, acetone-*d*₆) δ -14.1 (d, $J = 157$ Hz, 5B), -12.0 (d, $J = 137$ Hz, 5B), 5.2 (s, 1B). Anal. Calcd. for $C_{39}H_{72}B_{11}NO_5$: C, 62.13; H, 9.63; N, 1.86. Found: C, 62.40; H, 9.63; N, 1.81.

2b[Pyrr] Recrystallized from EtOH/H₂O mixtures (3x) providing the pure salt as white

crystals: ^1H NMR (400 MHz, CDCl_3) δ 0.40-2.50 (m, 10H), 0.53-0.61 (m, 2H), 0.82 (t, $J = 7.0$ Hz, 3H), 0.87 (t, $J = 7.2$ Hz, 3H), 0.88 (t, $J = 7.0$ Hz, 3H), 0.92 (t, $J = 7.3$ Hz, 3H), 0.96-1.06 (m, 2H), 1.16-1.46 (m, 27H), 1.78-1.92 (m, 8H), 2.40 (br t, $J = 12.2$ Hz, 1H), 4.23 (t, $J = 6.5$ Hz, 2H), 4.30 (t, $J = 7.5$ Hz, 2H), 6.89 (d, $J = 8.5$ Hz, 2H), 7.11 (d, $J = 8.6$ Hz, 2H), 7.30 (d, $J = 7.1$ Hz, 2H), 8.37 (d, $J = 7.1$ Hz, 2H); ^{11}B $\{^1\text{H}\}$ NMR (128 MHz, CDCl_3) δ -14.0 (5B), -11.8 (5B), B(12) was diffused into the baseline. Anal. Calcd. for $\text{C}_{41}\text{H}_{76}\text{B}_{11}\text{NO}_3$: C, 65.66; H, 10.21; N, 1.87. Found: C, 65.46; H, 10.40; N, 1.81.

2c[Pyr]: Recrystallized from EtOH/ H_2O mixtures (3x) providing the pure salt as white crystals: ^1H NMR (400 MHz, acetone- d_6) δ 0.40-2.50 (m, 10H), 0.52-0.59 (m, 2H), 0.85 (t, $J = 7.1$ Hz, 3H), 0.87 (t, $J = 7.0$ Hz, 3H), 0.88 (t, $J = 6.8$ Hz, 3H), 0.95 (t, $J = 7.4$ Hz, 3H), 0.98-1.07 (m, 2H), 1.17-1.56 (m, 31H), 1.82-1.93 (m, 4H), 1.98-2.13 (m, 2H), 2.48 (tt, $J_1 = 12.0$ Hz, $J_2 = 3.6$ Hz, 1H), 4.47 (t, $J = 6.5$ Hz, 2H), 4.64 (t, $J = 7.5$ Hz, 2H), 7.00 (d, $J = 9.0$ Hz, 2H), 7.09 (d, $J = 9.0$ Hz, 2H), 7.68 (d, $J = 7.6$ Hz, 2H), 8.92 (d, $J = 7.5$ Hz, 2H); ^{11}B NMR (128 MHz, acetone- d_6) δ -14.1 (d, $J = 152$ Hz, 5B), -12.0 (d, $J = 140$ Hz, 5B), 5.9 (s, 1B). Anal. Calcd. for $\text{C}_{42}\text{H}_{76}\text{B}_{11}\text{NO}_5$: C, 63.53; H, 9.65; N, 1.76. Found: C, 63.79; H, 9.69; N, 1.70.

2d[Pyr] Recrystallized from an EtOH/ H_2O mixture (1x) and MeOH/ H_2O mixtures (3x) providing the pure salt as orange crystals: ^1H NMR (400 MHz, acetone- d_6) δ 0.40-2.50 (m, 10H), 0.53-0.60 (m, 2H), 0.85 (t, $J = 7.1$ Hz, 3H), 0.87 (t, $J = 7.0$ Hz, 3H), 0.93 (t, $J = 7.3$ Hz, 3H), 0.95 (t, $J = 7.3$ Hz, 3H), 1.18-1.52 (m, 18H), 1.65 (quint, $J = 7.6$ Hz, 2H), 1.89 (quint, $J = 7.0$ Hz, 2H), 1.97-2.07 (m, 2H), 2.71 (t, $J = 7.7$ Hz, 2H), 4.46 (t, $J = 6.5$

Hz, 2H), 4.64 (t, $J = 7.5$ Hz, 2H), 7.20 (d, $J = 8.9$ Hz, 2H), 7.40 (d, $J = 8.4$ Hz, 2H), 7.67 (d, $J = 7.5$ Hz, 2H), 7.84 (d, $J = 8.4$ Hz, 2H), 7.93 (d, $J = 8.9$ Hz, 2H), 8.92 (d, $J = 7.6$ Hz, 2H); ^{11}B NMR (128 MHz, acetone- d_6) δ -14.0 (d, $J = 158$ Hz, 5B), -11.9 (d, $J = 139$ Hz, 5B), 5.7 (s, 1B). Anal. Calcd. for $\text{C}_{40}\text{H}_{68}\text{B}_{11}\text{N}_3\text{O}_3$: C, 63.39; H, 9.04; N, 5.54. Found: C, 63.73; H, 9.14; N, 5.87.

2f[Pyr] Recrystallized from MeOH/H₂O mixtures (4x) providing the pure salt as white crystals: ^1H NMR (400 MHz, acetone- d_6) δ 0.40-2.50 (m, 10H), 0.52-0.58 (m, 2H), 0.85 (t, $J = 7.2$ Hz, 3H), 0.87 (t, $J = 7.0$ Hz, 3H), 0.86 (t, $J = 6.9$ Hz, 3H), 0.98-0.99 (m, 4H), 0.95 (t, $J = 7.4$ Hz, 3H), 1.12-1.52 (m, 30H), 1.74 (d, $J = 11.1$ Hz, 2H), 1.80 (d, $J = 11.8$ Hz, 2H), 1.89 (quint, $J = 7.1$ Hz, 2H), 1.98-2.08 (m, 4H), 2.61 (t, $J = 8.1$ Hz, 2H), 4.47 (t, $J = 6.5$ Hz, 2H), 4.65 (t, $J = 7.4$ Hz, 2H), 6.94 (t, $J = 7.8$ Hz, 1H), 6.98 (dd, $J_1 = 10.4$ Hz, $J_2 = 1.8$ Hz, 2H), 7.68 (d, $J = 7.5$ Hz, 2H), 8.93 (d, $J = 7.5$ Hz, 2H); ^{11}B NMR (128 MHz, acetone- d_6) δ -14.0 (d, $J = 157$ Hz, 5B), -11.9 (d, $J = 141$ Hz, 5B), 5.4 (s, 1B). Anal. Calcd. for $\text{C}_{43}\text{H}_{79}\text{B}_{11}\text{FNO}_3$: C, 64.88; H, 10.00; N, 1.76. Found: C, 65.06; H, 10.05; N, 1.82.

2g[Pyr]: Recrystallized from EtOH/H₂O mixtures (2x) and MeOH/H₂O mixtures (2x) providing the pure salt as white flakes: ^1H NMR (400 MHz, acetone- d_6) δ 0.40-2.50 (m, 10H), 0.52-0.58 (m, 2H), 0.85 (t, $J = 7.2$ Hz, 3H), 0.87 (t, $J = 7.1$ Hz, 3H), 0.88 (t, $J = 6.9$ Hz, 3H), 0.95 (t, $J = 7.4$ Hz, 3H), 1.04-1.08 (m, 2H), 1.16-1.46 (m, 38H), 1.49 (quint, $J = 7.3$ Hz, 2H), 1.89 (quint, $J = 7.1$ Hz, 2H), 1.99-2.06 (m, 2H), 2.45-2.50 (m, 2H), 4.47 (t, $J = 6.5$ Hz, 2H), 4.64 (t, $J = 7.5$ Hz, 2H), 6.85 (d, $J = 8.5$ Hz, 2H), 7.14 (d, $J = 8.5$ Hz,

2H), 7.68 (d, $J = 7.4$ Hz, 2H), 8.92 (d, $J = 7.4$ Hz, 2H); ^{11}B NMR (128 MHz, acetone- d_6) δ -14.0 (d, $J = 154$ Hz, 5B), -12.0 (d, $J = 137$ Hz, 5B), 5.1 (s, 1B). Anal. Calcd. for $\text{C}_{46}\text{H}_{84}\text{B}_{11}\text{NO}_3$: C, 67.53; H, 10.35; N, 1.71. Found: C, 67.76; H, 10.44; N, 1.88.

2h[Cetyl]: Recrystallized from MeOH (1x) and EtOH (2x) providing the pure salt as a white powder: ^1H NMR (400 MHz, acetone- d_6) δ 0.40-2.50 (m, 10H), 0.50-0.60 (m, 2H), 0.83-0.91 (m, 9H), 1.03-1.14 (m, 2H), 1.15-1.45 (m, 45H), 1.46-1.57 (m, 2H), 1.85-2.01 (m, 4H), 2.52 (br t, $J = 12.2$ Hz, 1H), 3.34-3.37 (m, 9H), 3.53-3.60 (m, 2H), 7.05 (d, $J = 8.6$ Hz, 2H), 7.30 (d, $J = 8.2$ Hz, 2H), 7.54 (d, $J = 8.2$ Hz, 2H), 7.61 (d, $J = 8.5$ Hz, 2H); ^{11}B NMR (128 MHz, acetone- d_6) δ -14.0 (d, $J = 158$ Hz, 5B), -11.9 (d, $J = 138$ Hz, 5B), 5.0 (s, 1B).

Preparation of [*closo*-1-CB₁₁H₁₀-1-COOH-12-C₆H₁₃]⁻ [NEt₄]⁺ (4[NEt₄])

A solution of anhydrous ZnCl_2 (5.84 g, 42.8 mmol) in anhydrous THF (30 mL) under Ar was treated with $\text{C}_6\text{H}_{13}\text{MgBr}$ (21.5 mL, 40.8 mmol, 1.9 M in Et_2O) at 0 °C forming a white, thick slurry which was stirred for 15 min. Anhydrous NMP (15 mL), $\text{Pd}_2(\text{dba})_3$ (0.062 g, 2 mol %), and $[\text{HPCy}_3]^+ [\text{BF}_4]^-$ (0.100 g, 8 mol %) were added and the reaction mixture turned dark green but slowly faded to red/orange. After 5 mins, [*closo*-1-CB₁₁H₁₀-1-COOH-12-I]⁻ NEt₄⁺ (**5[NEt₄]**, 1.50 g, 3.40 mmol) was added, and the reaction mixture was refluxed at 90 °C for 24 hr. ^{11}B NMR of a small aliquot (quenched in sat. $\text{NH}_4^+ \text{Cl}^-$ and extracted into ether) showed complete conversion to product. Sat. $\text{NH}_4^+ \text{Cl}^-$ (50 mL) was added, excess THF was removed, and the remaining aqueous layer

was extracted with Et₂O (3 x 20 mL). The organic layers were combined, dried (Na₂SO₄), and removed giving a black sludge. Excess NMP and 1-hexanol were removed under vacuum (60 °C, 0.5 mm Hg) and the residue was separated by column chromatography (SiO₂, CH₃CN/CH₂Cl₂, 1:9).

The crude acid extract was re-dissolved in 10 % HCl (50 mL) and extracted with Et₂O (3 x 20 mL). The organic layers were combined, and water (10 mL) was added. The Et₂O was removed *in vacuo*, and the aqueous layer was filtered. [NEt₄⁺] Br⁻ (0.790 g, 3.73 mmol) was added to the filtrate, and the resulting precipitate formed was filtered, washed (H₂O), and dried *in vacuo* giving 0.830 g (61 % yield) of **4[NEt₄]** as a light yellow crystalline solid. Further purification was achieved by recrystallization from aqueous CH₃OH: mp 122-124 °C ¹H NMR (400 MHz, CD₃CN) δ 0.40-2.50 (m, 10H), 0.46 (br t, *J* = 8.9 Hz, 2H), 0.85 (t, *J* = 7.0 Hz, 3H), 1.20 (tt, *J*₁ = 7.3 Hz, *J*₂ = 1.9 Hz, 12H), 1.07-1.29 (m, 8H), 3.15 (q, *J* = 7.3 Hz, 8H) 8.81 (br s, 1H); ¹¹B NMR (128 MHz, CD₃CN) δ -14.3 (d, *J* = 155 Hz, 5H), -12.2 (d, *J* = 137 Hz, 5B), 4.6 (s, 1H). Anal. Calcd. for C₁₆H₄₄B₁₁NO₂: C, 47.87; H, 11.05; N, 3.49. Found: C, 48.38; H, 11.32; N, 3.49.

Preparation of [*closo*-1-CB₁₁H₁₀-1-COOH-12-I]⁻ [NEt₄]⁺ (5[NEt₄]**)**

A solution of dried [*closo*-1-CB₁₁H₁₁-12-I]⁻ Cs⁺ (1.67 g, 4.15 mmol) in anhydrous THF (20 mL) in a three-necked flask at -78°C under Ar was treated with TMEDA (0.800 mL, 5.90 mmol) followed by dropwise addition of *n*-BuLi (2.90 mL, 5.80 mmol) over 30 minutes. The reaction mixture was slowly warmed to 0 °C and stirred for 1.5 hr resulting

in the formation of some precipitation (addition of extra anhydrous THF at this point is advantageous). Dry CO₂ gas was bubbled through the solution for 20 mins, and the mixture became significantly more homogeneous. Water (30 mL) was added, and the volatiles evaporated. Insoluble material was removed by filtration, the filtrate washed with Et₂O (3 x 20 mL), and the Et₂O layers set aside. The aqueous layer was acidified with 10 % HCl, extracted with Et₂O (3 x 20 mL), and the organics layers combined. Water (25 mL) was added, and the Et₂O removed. The aqueous layer was filtered, and [NEt₄⁺] Br⁻ (1.10 g, 5.23 mmol) was added producing a white precipitate. The solid was collected by filtration, washed with water, and dried giving 1.84 g (quantitative yield) of **5[NEt₄]** as a white crystalline solid. An analytical sample of **5[NEt₄]** was prepared by recrystallization from aqueous EtOH: ¹H NMR (400 MHz, acetone-*d*₆) δ 0.50-2.50 (m, 10H), 1.40 (tt, *J*₁ = 7.3 Hz, *J*₂ = 1.9 Hz, 12H), 3.50 (q, *J* = 7.3 Hz, 8H), COOH was not observed; ¹¹B NMR (128 MHz, acetone-*d*₆) δ -16.2 (s, 1B), -13.5 (d, *J* = 155 Hz, 5B), -11.3 (d, *J* = 146 Hz, 5B). Anal. Calcd. for C₁₀H₃₁B₁₁INO₂: C, 27.10; H, 7.05; N, 3.16. Found: C, 27.02; H, 7.18; N, 3.18.

Preparation of [*closo*-1-CB₁₁H₁₁-12-I]⁻ [NEt₄]⁺ (7[NEt₄])

Following the literature procedure,¹⁹ [*closo*-1-CB₁₁H₁₂]⁻Cs⁺ (2.85, 10.3 mmol) was extracted to Et₂O (3 x 20 mL) from 10 % HCl (100 mL). The ether was evaporated, and the free acid residue was dissolved in glacial acetic acid (35 mL) and treated with molecular I₂ (5.1 g, 20 mmol). The reaction was stirred at rt for 96 hrs, and the reaction progress was monitored by ¹¹B NMR. Solid Na₂SO₃ (1.0 g, 7.9 mmol) was added, and the

acetic acid removed *in vacuo*. The residue was dissolved in 10 % HCl (50 mL) and extracted to Et₂O (3 x 20 mL). The organic layers were combined and evaporated in the presence of H₂O (30 mL). The aqueous layer was filtered, and the filtrate treated with NEt₄⁺Br⁻ (2.5 g, 11.9 mmol) precipitating a white solid that was filtered and dried. Recrystallization from hot aqueous EtOH gave 3.1 g (75 % yield) of pure **7**[NEt₄]. ¹¹B NMR data was consistent with the literature.¹⁹

Acknowledgments

Financial support for this work was received from the National Science Foundation (DMR-0907542). BR would also like to thank the Vanderbilt University Graduate School for a Dissertation Enhancement Grant that permitted him to conduct the XRD measurements at the University of Warsaw.

References

- (1) Binnemans, K. *Chem. Rev.* **2005**, *105*, 4148-4204.
- (2) Axenov, K. V.; Laschat, S. *Materials* **2011**, *4*, 206-259.
- (3) Yoshio, M.; Mukai, T.; Kanie, K.; Yoshizawa, M.; Ohno, H.; Kato, T.; *Adv. Mater.* **2002**, *14*, 351-354; Yoshio, M.; Kagata, T.; Hoshino, K.; Mukai, T.; Ohno, H.; Kato, T. *J. Am. Chem. Soc.* **2006**, *128*, 5570-5577; Yoshio, M.; Mukai, T.; Ohno, H.; Kato, T. *J. Am. Chem. Soc.* **2004**, *126*, 994-995.
- (4) Ichikawa, T.; Yoshio, M.; Hamasaki, A.; Mukai, T.; Ohno, H.; Kato, T. *J. Am.*

Chem. Soc. **2007**, *129*, 10662-10663.

- (5) Yazaki, S.; Kamikawa, Y.; Yoshio, M.; Hamasaki, A.; Mukai, T.; Ohno, H.; Kato, T. *Chem. Lett.* **2008**, *37*, 538-539.
- (6) Grabovskiy, Y.; Kovalchuk, A.; Grydyakina, A.; Bugaychuk, S.; Mirnaya, T.; Klimusheva, G. *Liq. Cryst.* **2007**, *34*, 599-603.
- (7) Shimura, H.; Yoshio, M.; Hoshino, K.; Mukai, T.; Ohno, H.; Kato, T. *J. Am. Chem. Soc.* **2008**, *130*, 1759-1765.
- (8) Abu-Lebdeh, Y.; Abouimrane, A.; Alarco, P.-J.; Armand, M. *J. Power Sourc.* **2006**, *154*, 255-261.
- (9) Yamanaka, N.; Kawano, R.; Kubo, W.; Kitamura, T.; Wada, Y.; Watanabe, M.; Yanagida, S. *Chem. Commun.* **2005**, 740-742; Kawano, R.; Nazeeruddin, M. K.; Sato, A.; Gratzel, M.; Watanabe, M. *Electrochem. Commun.* **2007**, *9*, 1134-1138.
- (10) Reed, C. A. *Acc. Chem. Res.* **1998**, *31*, 133-139; Strauss, S. H. *Chem. Rev.* **1993**, *93*, 927-942; Krossing, I.; Raabe, I. *Angew. Chem. Int. Ed.* **2004**, *43*, 2066-2090.
- (11) Kaszynski, P.; Douglass, A. G. *J. Organomet. Chem.* **1999**, *581*, 28-38.
- (12) Korbe, S.; Schreiber, P. J.; Michl, J. *Chem. Rev.* **2006**, *106*, 5208-5249; Stibr, B. *Chem. Rev.* **1992**, *92*, 225-250; Schleyer, P. v. R.; Najafian, K. *Inorg. Chem.* **1998**, *37*, 3454-3470.
- (13) Ringstrand, B.; Kaszynski, P.; Monobe, H. *J. Mater. Chem.* **2009**, *19*, 4805-4812.
- (14) Neises, B.; Steglich, W. *Angew. Chem. Int. Ed.* **1978**, *17*, 522-524.

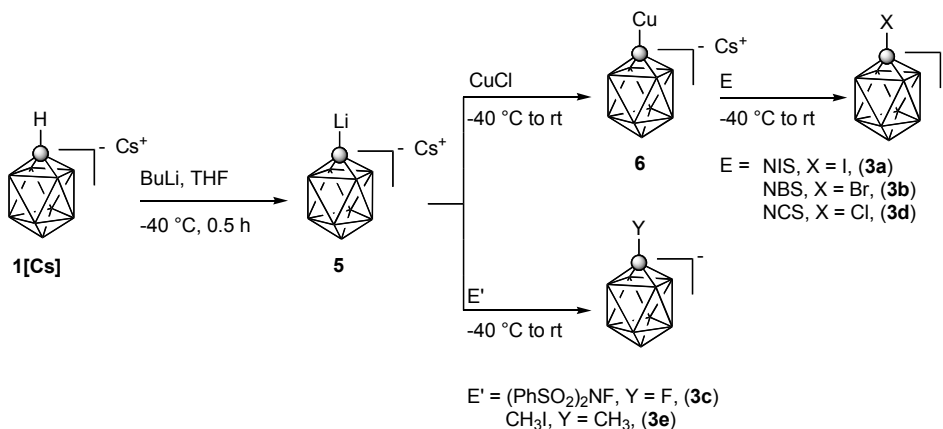
- (15) Erdik, E. *Tetrahedron* **1992**, *48*, 9577-9648.
- (16) Knochel, P.; Singer, R. D. *Chem. Rev.* **1993**, *93*, 2117-2188.
- (17) Ringstrand, B.; Balinski, A.; Franken, A.; Kaszynski, P. *Inorg. Chem.* **2005**, *44*, 9561-9566.
- (18) Jelinek, T.; Plesek, J.; Hermanek, S.; Stibr, B. *Collect. Czech. Chem. Commun.* **1986**, *51*, 819-829.
- (19) Gruner, B.; Janousek, Z.; King, B. T.; Woodford, J. N.; Wang, C. H.; Vsetcka, V.; Michl, J. *J. Am. Chem. Soc.* **1999**, *121*, 3122-3126.
- (20) Demus, D.; Richter, L. *Textures of Liquid Crystals*; 2nd ed.; VEB: Leipzig, 1980. Gray, G. W.; Goodby, J. W. G. *Smectic Liquid Crystals-Textures and Structures*; Leonard Hill: Philadelphia, 1984. Dierking, I. *Textures of Liquid Crystals*; Wiley-VCH: Weinheim, 2003.
- (21) Neubert, M. E. in *Liquid Crystals: Experimental Study of Physical Properties and Phase Transitions*, S. Kumar, Ed., Cambridge University Press, New York, 2001, and references therein.

Improved Synthesis of [*closo*-1-CB₉H₁₀]⁻ Anion and New C-Substituted Derivatives.

(Ringstrand, B.; Bateman, D.; Shoemaker, R.K.; Janousek, Z. *Collect. Czech. Chem. Commun.* **2009**, *74*, 419-431)

This work was performed at the Czech Academy of Sciences, Inorganic Chemistry Institute located in Rez, Czech Republic during the summer of 2007. The purpose of the research was to utilize the Brellocks method to gain access to the parent [*closo*-1-CB₉H₁₀]⁻ anion (**1**) and then to study substitution reactions at the C(1) vertex. The original literature report for the preparation of **1** was irreproducible; therefore, the synthesis of **1** was optimized. In addition, the unknown C-halogenated series (**3a-3d**) and the unknown C-methylated product **3e** were synthesized and NMR properties and regularities within the series were investigated. My role in this work was the synthesis and characterization of all compounds (Scheme 1).

Scheme 1.



Dr. Zbynek Janousek hosted me during my stay in the Czech Republic. Richard K. Shoemaker of the University of Colorado at Boulder performed ¹³C NMR analysis of compounds **3a-3e**. Devon Bateman assisted in the preparation of **3e**.

Part IV, Chapter 2.

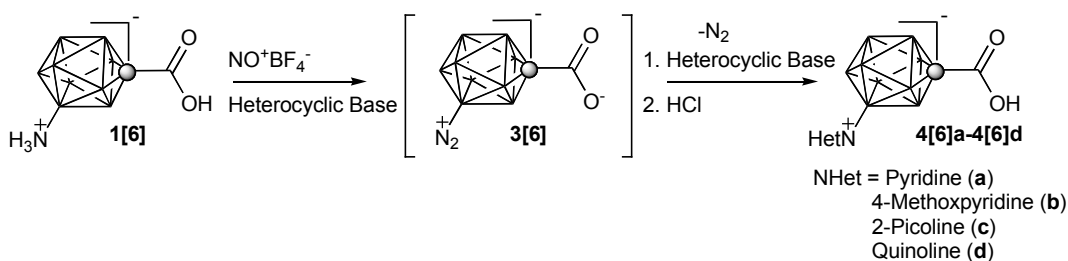
Diazotization of the Amino Acid [*closo*-1-CB₉H₈-1-COOH-6-NH₃] and Reactivity of the [*closo*-1-CB₉H₈-1-COO-6-N₂]⁻ Anion.

Reproduced with permission from Ringstrand, B.; Kaszynski, P.; Young, V. G. Jr. *Inorg. Chem.* **2011**, *50*, 2654-2660. Copyright 2011 American Chemical Society. Available online: <http://pubs.acs.org/doi/abs/10.1021/ic102557s>

In this project, we took advantage of the availability of the [*closo*-1-CB₉H₈-1-

COOH-6-NH₃] anion (**1[6]**) obtained by amination of the [*closo*-1-CB₉H₈-1-COOH-6-I]⁻ anion (see Part I, Chapter 1). The goal of this work was to understand the reactivity of the N₂⁺ group substituted on the [*closo*-1-CB₉H₁₀]⁻ anion at positions other than the C(1) (see Part II, Chapter 2) and B(10) (see Part II, Chapter 3). As a result, the [*closo*-1-CB₉H₈-1-COOH-6-NH₃] anion (**1[6]**) was diazotized in the presence of heterocyclic bases (**NHet**) such as pyridine (**4[6]a**), 4-methoxypyridine (**4[6]b**), 2-picoline (**4[6]c**), and quinoline (**4[6]d**) giving products of 6-substitution [*closo*-1-CB₉H₈-1-COOH-6-NHet] (**4[6]a-4[6]d**) (Scheme 1).

Scheme 1.



These results demonstrated that the N₂⁺ group substituted at the B(6) position in **3[6]** is far more reactive than those substituted at the C(1) (**3[1]**) or B(10) (**3[10]**) positions, and as a result, reacts *in-situ* with the solvent. The overall stability of the N₂⁺ derivatives established experimentally and aided by theoretical calculation is 3[10] > 3[1] > 3[6] and results from different contributions of π-π overlap and coulombic stabilization.

My role in this work was to synthesize and characterize all compounds. Dr. Victor G. Young, Jr. from the University of Minnesota at the Twin Cities performed single

crystal X-ray measurements on compound **4[6]a**. Dr. Piotr Kaszynski performed theoretical analysis to support the experimental results.

Part IV, Chapter 3.

The Preparation of [*closo*-1-CB₉H₈-1-COOH-10-(4-C₃H₇C₅H₉S)] as an Intermediate to Polar Liquid Crystals.

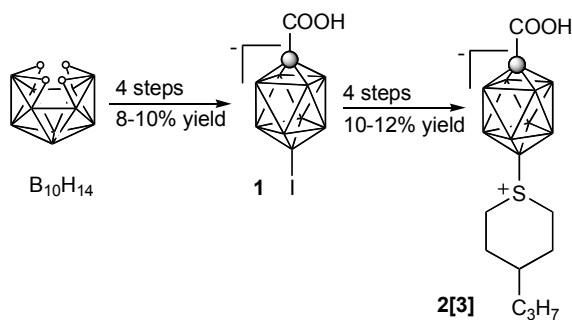
(Pecyna, J.; Denicola, R.P.; Ringstrand, B.; Jankowiak, A.; Kaszynski, P. *Polyhedron*, submitted)

This chapter represents research that was mainly performed by Mr. Jacek Pecyna and Vanderbilt undergraduate Richard P. Denicola with some contributions from Dr. Aleksandra Jankowiak. My role in this work was assist in synthesis of the desired compounds and to closely supervise and train Mr. Pecyna and Mr. Denicola during the summer of 2010 in the process of making iodo acid [*closo*-1-CB₉H₈-1-COOH-10-I]⁻ (**1**) (see Part II, Chapter 1).

The preparation of iodo acid **1** was optimized and scaled from 1 g to 40 g of B₁₀H₁₄. The synthesis of the [*arachno*-6-CB₉H₁₃-6-COOH]⁻ anion uses 4 times smaller volume, and the oxidation of [*arachno*-6-CB₉H₁₃-6-COOH]⁻ anion to [*closo*-2-CB₉H₉-2-COOH]⁻ anion requires less oxidant, 12 times smaller volume, and significantly shorter reaction time. The overall yields of the iodo acid **1** as the NMe₄⁺ salt are typically 8% –

10% (10 g – 12 g) for 40 g of $B_{10}H_{14}$. Iodo acid **1** was consequently transformed to amino acid [*closo*-1- CB_9H_8 -1-COOH-10- NH_3], followed by conversion to dinitrogen acid [*closo*-1- CB_9H_8 -1-COOH-10- N_2], and finally to sulfonium acid **2[3]** in overall yield of about 12% (Scheme 1).

Scheme 1.



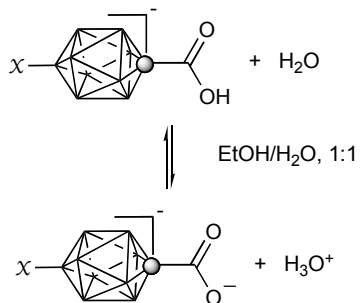
Part III, Chapter 4.

Transmission of Electronic Effects through the {*closo*-1- CB_9 } Cage: Dissociation Constants for a Series of [*closo*-1- CB_9H_8 -1-COOH-10- X]⁻ Acids.

This chapter represents a work in progress towards understanding of the extent of transmission of substituent effect through the [*closo*-1- CB_9H_{10}]⁻ cluster. For this purpose, the dissociation constants of four [*closo*-1- CB_9H_8 -1-COOH-10- X]⁻ acids ($X = H, I, N_2,$ and C_6H_{13}) were determined in aqueous EtOH (1:1) and analyzed by the Hammett methods and compared to 4-substituted benzoic acid and 4-substituted bicyclo[2.2.2]octane-1-carboxylic acid derivatives. Results of potentiometric

titration of solutions of acids are shown in Table 1 and comparison of results for benzoic acids and bicyclo[2.2.2]octane-1-carboxylic acids in Figure 1.

Table 1. Apparent Ionization constants for selected derivatives of {*closo*-1-CB₉} in 50% EtOH (v/v).



χ	pK_a
<i>n</i> -C ₆ H ₁₃ , ^a	6.76±0.02
I ^a	6.24±0.02
H ^b	6.33±0.01
N ₂	4.80±0.03

^a The NMe₄⁺ counterion. ^b The NEt₄⁺ counterion.

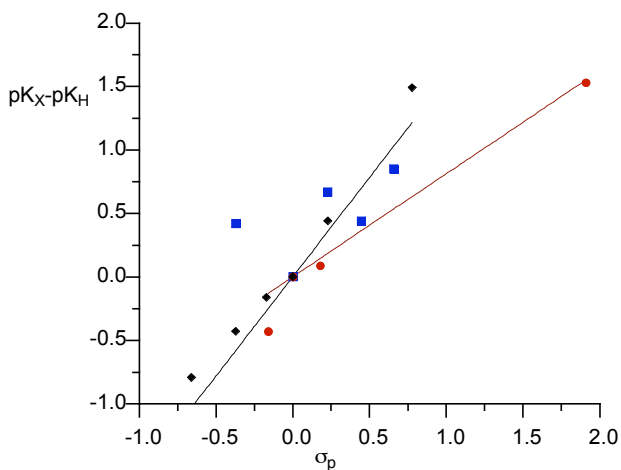


Figure 1. The Hammett plot of pK_a values for derivatives of [*closo*-1-CB₉H₉-1-COOH]⁻ (circles, $\rho = 0.8 \pm 0.1$, $r^2 = 0.96$), benzoic acid, (diamonds, $\rho = 1.6 \pm 0.16$, $r^2 = 0.95$) and

bicyclo[2.2.2]octane-1-carboxylic acid (squares) in 50% EtOH (v/v).

Inspection of Figure 1 demonstrates that the four data points for the {*closo*-1-CB₉} derivatives follow the trend for substituted benzoic acids and can be correlated with the σ_p parameters. The slope (the ρ parameter) for the {*closo*-1-CB₉} series is about half of that for benzoic acids. Data for BCO acids is shown in the graph for comparison purpose only and it is not expected to correlate with the σ_p parameters. Although, clearly more data points is needed for a detailed and accurate analysis of the electronic effects in the {*closo*-1-CB₉} derivatives, it is apparent that the cluster is more similar in its behavior to a π -aromatic system (benzene) than to a σ non-aromatic system (bicyclo[2.2.2]octane).

Part IV, Chapter 5.

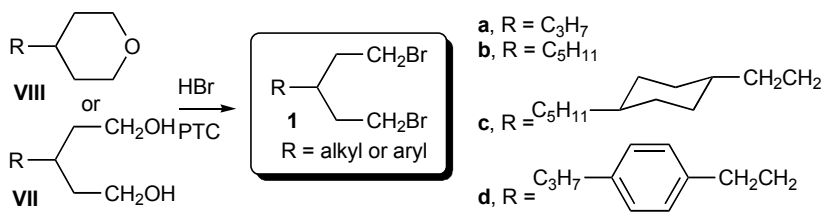
The Preparation of 3-Substituted-1,5-Dibromopentanes as Precursors to Heteracyclohexanes.

(Ringstrand, B.; Oltmanns, M.; Batt, J.; Denicola, R.P.; Jankowiak, A.; Kaszynski, P. *Beils. J. Org. Chem.* **2011**, *7*, in press)

This chapter represents work that was performed by visiting undergraduate students Jeffrey Batt and Martin Oltmanns from Augustana College and Vanderbilt

undergraduate Richard P. Denicola in the summer of 2010. I was responsible for training, supervising, troubleshooting, and designing synthetic routes to desired compounds. The purpose of this project was to investigate the preparation of various 3-substituted-1,5-dibromopentanes **1**. A total of four dibromopentanes **1a-1d** containing simple alkyl and more complex fragments at the 3-position were prepared (Scheme 1).

Scheme 1.



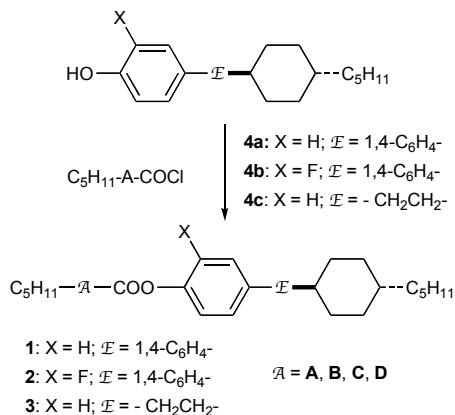
These compounds are important intermediates in the preparation of polar liquid crystals containing sulfonium fragments linked to the [*clos*o-1-CB₉H₁₀]⁻ anion (see Part II, Chapters 1 and 3). Part of this research included a literature search of previous methods for preparation of dibromopentanes **1**, 3-substituted-1,5-pentanediols **VII**, or 4-substituted-tetrahydropyrans **VIII**. Three synthetic routes to **I** were investigated. These included the Knoevenagel condensation of aldehydes with dimethyl malonate to give pentanediols **VII**, addition of Grignard to glutaconate diester to give pentanediols **VII**, and Wittig olefination of tetrahydro-4*H*-pyranone to give tetrahydropyrans **VII**. The advantages and disadvantages of each route were commented on.

Comparative Studies of Three- and Four-ring Mesogenic Esters Containing *p*-Carborane, Bicyclo[2.2.2]octane, Cyclohexane, and Benzene.

(Ringstrand, B.; Vroman, J.; Jensen, D.; Januszko, A.; Kaszynski, P.; Dziaduszek, J.; Drzewinski W. *Liq. Cryst.* **2005**, 32, 1061-1070).

This chapter represents work that was accomplished at Vanderbilt during the summer of 2004, when I was visiting as an undergraduate student from Augustana College. Twelve esters were prepared from pentyl-substituted *p*-carborane (**A**), bicyclo[2.2.2]octane (**B**), cyclohexane (**C**), and benzene (**D**) carboxylic acids and three phenols (**4a**, **4b**, and **4c**). The liquid crystalline properties of the series of esters **1-3** were examined using thermal analysis and optical microscopy (Scheme 1).

Scheme 1.



The relationships between structure and liquid crystalline properties were analyzed by comparison of the series of homostructural esters. Another undergraduate student, Jacob Vroman, and myself were responsible for the synthesis, purification, and characterization of all compounds.

Dr. Dell Jensen and Dr. Piotr Kaszynski organized the research experience for Mr. Vroman and myself. Dr. Adam Januszko assisted in identifying and characterizing the liquid crystalline materials. Dr. Jerzy Dziaduszek and Dr. Witold Drzewinski provided phenols **4a**, **4b**, and **4c**.

Part V, Chapter 2.

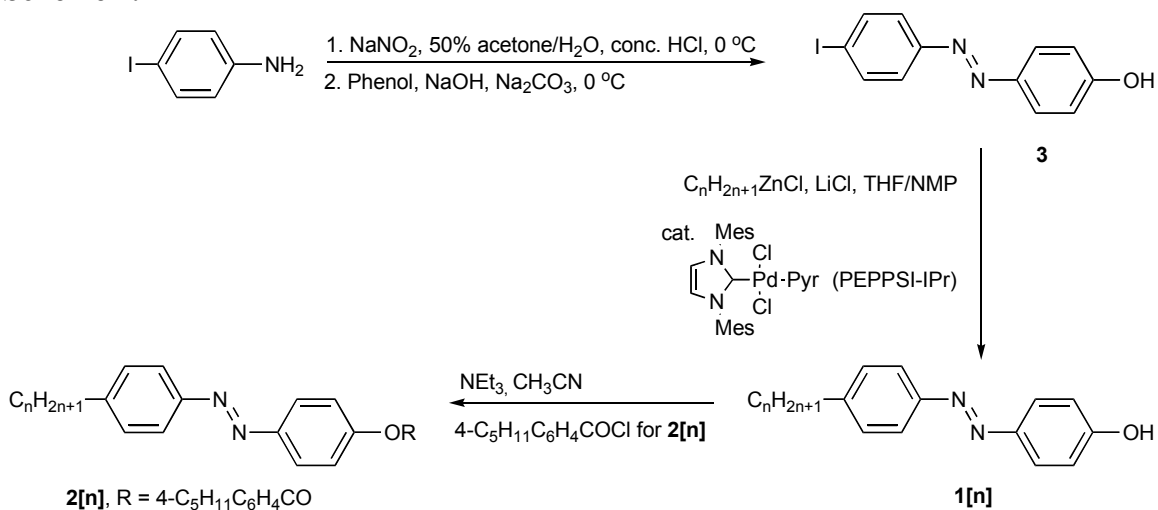
A Convenient Preparation of Long Chain 4-(4-*n*-Alkylphenylazo)phenols and their 4-Pentylbenzoate Esters.

(Johnson, L.; Ringstrand, B.; Kaszynski, P. *Liq. Cryst.* **2009**, *36*, 179-185)

This chapter represents research that was performed by Vanderbilt undergraduate Lillian Johnson in the summer of 2008. My role in this project was training, supervision, troubleshooting, designing the synthetic routes to the desired compounds, and liquid crystalline characterization. This was my first experience with directing an undergraduate student in the laboratory. The goal of this work was to prepare a series of 4-(4-

alkylphenylazo)phenols **1[n]** ($n = 2-22$, even) by Negishi coupling of alkylzinc chlorides with 4-(4-iodophenylazo)phenol (**3**). The phenols **1[n]** were then converted to the corresponding 4-pentylbenzoates **2[n]**, which exhibited enantiotropic nematic phases. (Scheme 1).

Scheme 1.



Typically, phenols **1[n]** are prepared by azo coupling of phenol with the appropriate 4-alkylaniline. The methodology presented in this chapter represents a new means of preparing such phenols **1[n]**.